STRUCTURAL INTERMODULATION INTERFERENCE IN MOBILE RADIO SYSTEMS

A Thesis Submitted for the

Degree of Doctor of Philosophy

by

Philip Shiu Wai Ho

Department of Electrical,

Electronic and Information

Engineering

City University

May 1991

TABLE OF CONTENTS

TABLE OF FIGURES

ACKNOWLEDGEMENTS

During my period of my research I have been fortunate enough to receive the support of many people and it is impossible to mention them all. However, I would like to take this opportunity to express my gratitude to a certain few who, in various but equally important ways, were extremely supportive during these years.

I would like to offer my sincere thanks to my project supervisor, Mr. W S Wilkinson, for his continuous encouragement and guidance throughout this project. Also I would like to extend my gratitude to Prof. A C C Tseung for his enthusiasm and interest in my work.

I am greatly indebted to Dr. Lyn Bevan and Mr. Laury Frampton for their patience and encouragement. Also I appreciate the time spent by Mr. M. Lunt and Mr. David Watts, Directorate of Telecommunications, Home Office, in helping me in field measurements.

I am also indebted to Mr. P. M. Tomlinson and Mr. P. Buley of the Directorate of Telecommunications, Home Office; and Prof. A C Davis of King's College, University of London.

I would like to express my gratitude to my parents for their continuous support throughout my time in higher education.

This study was supported jointly by the Science and Engineering Research Conucil, the Directorate of Telecommunication, Home Office, and the Department of Trade and Industry.

ABSTRACT

Intermodulation interference at communal base stations, with co-sited transmitting and receiving aerials, represents a major obstacle to the improvement in the utilisation of limited radio frequency spectrum available to mobile radios. An investigation has been made of the phenomenon of Structural Intermodulation Interference : its sources, generation mechanisms, and the influences of environmental factors on the interference level. Studies have also been made of the methods to reduce its effect.

It was found that corrosion products exhibit non-linear current-voltage characteristics; and they are able to generate intermodulation interference. Furthermore, it was shown that in the case of steel lattice antenna structures, metal-semiconductor rectifying contact is the underlying mechanism responsible for the observed non-linear current-voltage relationship. Experimental results also supported that corroded metallic junction is a first order factor which determines the severity of intermodulation interference effect; surface corrosion products contribute relatively little to the intermodulation interference level.

A lumped circuit model of a non-linear junction was developed, which consists of a non-linear junction resistance in parallel with a linear junction capacitance. The resultant model was used to predict the third order intermodulation level of a test sample, and the prediction was in reasonable agreement with the measured result.

The effects of weather conditions on intermodulation level were also studied in depth. It was found that wind loading on the antenna tower structure can cause large and rapid changes in the intermodulation interference level. The interference level drops significantly when it is raining. Laboratory experiments shown that the high permittivity of water is responsible for the observed large drop in the interference level when it rains, rather than its conductivity. The effect of changes in ambient temperature do not produce large changes in the interference level in short space of time.

Lastly, methods to reduce and suppress intermodulation interference were investigated. The principle is to provide an alternative linear path for the induced radio frequency current. Various techniques were tried, and metal plating was found to be the most promising. Preventive methods, including high corrosion resistant coating, were also studied and are of particular interest in the construction of new antenna towers.

SYMBOLS

PMR	Private Mobile Radio
VLSI	Very Large Scale Integration
IMP	Intermodulation Products
IMI	Intermodulation Interference
Q-factor	Quality Factor of a Resonator
f_1, f_2	Fundamental Frequencies
f_{im}	Intermodulation Frequency
dB	Decibel
VHF	Very High Frequency
UHF	Ultra High Frequency
PIMI	Passive Intermodulation Interference
SIMI	Structural Intermodulation Interference
URA	Unintended Receiving Antennas
Ohmm	Ohm-metre, measurement unit of resistivity
ε_r	Relative permittivity

Chapter 1

Introduction

1.1 Objectives of the Project

Passive structural intermodulation interference or the "Rusty Bolt" effect has been shown to be very significant in base stations where there are co-located high power transmitters and sensitive receivers. Intermodulation interference has to be reduced to a minimum to enable proper system operations. Although effective methods have been found to solve the problems of the active type by careful shielding and filtering; however, the passive type, in particular, structural intermodulation interference, remains an intractable problem.

In this dissertation, we shall investigate the sources of structural intermodulation interference and their generation mechanisms. We shall examine the effects of weather conditions on structural intermodulation interference, and

the theory behind the observed effects. Lastly, we shall also examine various ways of suppressing intermodulation interference.

1.2 Nature of the Problem

The usefulness of mobile radio communications to the public and private organizations, as well as the general public is self-evident. Some organizations, such as the police, ambulance and fire services consider their mobile radios as an essential tool for their operations. The benefits and flexibilities provided by mobile radio services, such as mobile telephones and radio pagers have so much appeal that the personal communication industry has grown enormously. Until recently, the number of licensed private mobile radios (PMR) has grown to about 400,000 (DTI 1986).

The popularity of mobile radio communications has been enhanced by significant improvements in various areas of active and passive electronic component technologies, so that it is possible to produce more compact and light weight mobile communication equipments at lower cost. Nowadays, high gain packaged modules for cellular radio applications can easily deliver 40 watt at 900 MHz. Integrated circuits can provide functions such as rf mixers, intermediate frequency amplifiers, audio frequency amplifiers, frequency synthesizers and many more.

In addition, important changes have been taking place with

the steady move towards digital communications. The motivation factors behind this trend are the availability of Very Large Scale Integration (VLSI) technology for digital signal processing, the capabilities to support transmissions and integrated services of data, text, voice and images, and the advantages of providing facilities for error-detection, error-correction and data-encryption for more reliable and secure communications. For example, the Pan-European Cellular Radio Network would demand toll quality speech at around 16 kbit/s.

Considerable amount of research and development work has been, and is being carried out to maximize the efficiency of utilizing the available frequency spectrum. The ultimate objective is to derive spectrally-efficient modulation methods and optimum channel allocation methodologies according to the system requirements.

At present, most private mobile radio systems are still employing analogue communications use amplitude or angle modulations. The frequency bandwidth of these systems are progressively reduced to 12.5 kHz per channel at the VHF band to cater for more users. Further channel bandwidth reduction might be necessary if the demand gets larger. However, there is a limit to which the channel bandwidth could shrink before interference with other radio users becomes intolerable.

The presence of non-linear elements, due to a variety of different causes, at a base station with co-located

transmitters and receivers operating at adjacent frequencies, will generate undesirable radiations known as Intermodulation Products (IMPs). Although there are many other types of radio interference present in a communication system; however, due to the multiplicity nature of transmissions and receptions, and their non-linear interactions, intermodulation interference (IMI), could well be the limiting factor on how best one could use the available frequency spectrum in a multiple-frequency transmission system.

An example showing the stringent requirements for the United Kingdom Emergency Services is given below :

The Emergency Services operate low to medium power transmitters, generally on steel lattice towers, and these feed dipoles arranged to give omni-directional or asymmetric coverage in the horizontal plane as required. Normally operating limits for receivers are as follows :-

minimum received signal	107 dBm	
protection ratio	+30 dB	
maximum level of any single unwanted signal	-137 dBm	(a)
maximum level of all unwanted signals and noise combined	-127 dBm	(b)

The intention is that any single co-channel interferer from a distant service area is not to exceed (a). Combined sources, local or distant, should not exceed (b). Planning

is based on a transmitter with effective radiated power of 50 watt.

Tests carried out by the Directorate of Telecommunication, Home Office, have shown that two signals radiated from various antennas on a steel tower can give rise to intermodulation products up to 11th order at a magnitude of 20 dB or more above the expected minimum receiver level of 107 dBm.

1.3 Mobile Radio Systems

In order to appreciate the many different origins of intermodulation interference and their mechanisms, it is useful to look at a typical mobile communication system configuration.

In this study, our main interest would be at the 150 MHz VHF band, which is allocated to the United Kingdom Emergency Services; although the findings are generally applicable to other parts of the frequency spectrum. A simplified pictorial representation of such a system is shown in figure 1.1.

An average system consists of a base station and some mobile units. Normally, such a system would employ the two-frequency simplex method for communications between base station and the mobile units. In this method, the base station transmits at frequency f_1, and receives at frequency

f_2; while the mobile units transmit at frequency f_2 and receive at frequency f_1. The base station can therefore broadcast to all mobile units, but the mobile units cannot talk to each other directly.

The two frequencies f_1 and f_2 are adequately separated by at least 5 MHz. For example, for the United Kingdom emergency services, f_1 is in the range 146 - 148 MHz, and f_2 is in the range 154 - 156 MHz respectively. Since all the neighbouring transmitters at the base station transmit at frequencies adjacent to f_2, then sufficient suppression of high level rf power at the base station receiver front-end could be achieved by using high Q-factor (over 1,000) resonators tuned to f_2. At around 5 MHz away from the centre frequency, such resonators can provide attenuation of more than 35 dB. Therefore, blocking of the receivers by the cosited transmitters is avoided. Higher attenuation can be obtained by cascading several resonators together, but at the expense of higher insertion loss. Insertion loss for each resonator is about 1 dB.

Frequency re-use is possible in the VHF and UHF band because of their line-of-sight propagation characteristics. Therefore, with good frequency planning, the limited frequency spectrum allocated to mobile radios can be used in different geographical areas. This idea also forms the basic structure of the cellular mobile radio systems. Nowadays, further developments have been extended to the 'microcellular' mobile radio systems (e.g. see Steele 1985), in which the cell size is restricted to a single street, and

the spectrum can be re-used more often to increase the network's total capacity.

Location of the base station is usually on a high building or hill top, where clear coverage of the service area is possible. The effective radiated power for private mobile radios is restricted to 25 watt in the United Kingdom, although the emergency services can radiate at 50 watt for wider coverage. At such transmitting power, the coverage areas is about 2,000 km^2 (Dryborough 1975), and this can be extended by using repeaters.

Base station antennas are usually open or folded half-wave length dipoles for omni-directional coverage. In reality, the polar radiation pattern would not be circular as predicted by simple theory. This is due to the presence of a large collection of metal rods (the supporting mast) behind the dipole, which modifies the radiation pattern significantly by reflections in many different directions. Omni-directional coverage is then only possible by placing dipoles fitted with back reflectors on each of the four faces of the mast. Fudge (1984) carried out experiments on various antenna configurations, and he found that the skeleton slot panel produces the best result.

Besides frequency separations, isolation between transmitting antennas and receiving antennas can be increased via space separations as well. At 150 MHz, vertical separation of 3 metres reduces the coupling by more than 40 dB; while for horizontal separation, the reduction

is only about 20 dB (Pannell 1979). At present, the trend is moving towards integrated site systems (e.g. see Howson et al 1975), whereby, several base station transmitters and receivers share a single antenna via a multicoupling system which provides sufficient isolation among the transmitters and receivers. This will no doubt improve the planning, control and maintenance of the base station.

Coaxial cables are normally used to connect various base station equipments together. The criteria here are low loss and high screening effectiveness. Coaxial cable type UR-67, which is single copper braided, with a loss at 100 MHz of more than 6 dB per 100 metres, has been used extensively as a compromise between cost and performance. The performance of cables with solid outer conductor is much better, but are much more expensive.

The mobile unit fixed to a vehicle is subjected to a very hostile electromagnetic environment, with wideband high frequency noise generated by contact breaking, auxiliary motors and ignition pulses (see for example Yamamoto et al 1983). Transmitter power is normally 25 watt maximum, and a quarter wave-length monopole is used to radiate and receive vertically polarized waves.

In above, a very brief introduction to the basic components of a typical mobile radio system have been given. Further details on various aspects of mobile radio systems design, including propagation characteristics, modulation techniques, area coverage techniques and frequency

assignments, can be found in the work by Parsons and Gardiner (1989),Fudge (1984), Holbeche (1985), Lee (1982), Lee (1989) and Pannell (1979).

1.4 Intermodulation Interference

1.4.1 Introduction

Intermodulation interference (IMI) is the emission of spurious frequencies (called intermodulation products, IMPs) when two or more signals mix in a device that has a non-linear characteristic. When n given unmodulated sinusoidal input frequencies at f_1, f_2, ... , f_n are incident upon a non-linear device, the output will consists of not just the input frequencies and their harmonics, but also additional frequency components of the IMPs. An IMP frequency is defined as :

$$f_{im} = a_1 f_1 + a_2 f_2 + \ldots + a_n f_n$$

where a_1, a_2, ... a_n are integers which can be either positive, negative or zero.

In addition, the order of intermodulation product is defined as :

$$\sum_{i=1}^{n} |a_i|$$

Thus with two input frequencies, the 3rd-order IMPs are :

$$\pm 2f_1 \pm f_2 \quad \text{and} \quad \pm f_1 \pm 2f_2$$

respectively.

Note that half of the frequency components are negative, which are physically unrealizable.

1.4.2 Effects on Frequency Spectrum Utilization

As expected, if the number of transmissions increases, the number of intermodulation products will increase at a prodigious rate. It has been shown that (e.g. see Watson 1980) over 1,000 IMPs up to the 5th-order will be produced by just five carriers mixed together; and over one million IMPs up to 9th-order will be generated by 20 carriers (see figure 1.2). Fudge (1984) has also shown that products up to the 11th-order and above can have adverse effects on system performance and spectrum utilization.

Figure 1.3 shows the spectral distribution for two unmodulated carriers when the non-linear characteristic consists of the square term and the cubic term as well. The figure shows the positions of various second order and third order harmonics and intermodulation products. As can be seen, the third order intermodulation frequencies, i.e. $(2f_1 - f_2)$ and $(2f_2 - f_1)$, are very close to the two fundamental frequencies. The relative amplitudes of the harmonics and

intermodulation products are shown here to indicate that the amplitudes of them decrease with order number.

The severity of the spectrum pollution depends on :

(1) degree of non-linearities
(2) amplitudes of the mixing carriers

One particular feature about intermodulation interference is that, once generated, if the IMP frequencies fall on the frequency band used by the receivers at the base station, then they cannot be removed by filtering. Until now, the only way to avoid intermodulation interference in base stations with co-sited transmitters and receivers is to produce an intermodulation-free frequency planning. In practice, third- and fifth- order compatible frequency plans are highly desirable.

Predictions of both frequencies and amplitudes of intermodulation products, due to mixing of multiple-carriers, have proved to be a good source of mathematical problems. Bennett (1933) reported using a multiple Fourier series method to compute intermodulation products; Babcock (1953) viewed the problem as a combinational problem, and produced a 3rd-order intermodulation free planning scheme for 10 operating channels. A planning table of 3rd-order and 5th-order intermodulation free, for up to seven channels with closest spacing, was given by Edwards et al (1969). Recursion formulae have been described by Mifsud (1974) and

Kotsopoulos (1983) to generate 3rd-order and 5th-order compatibility lists. These later investigations, which involved intensive number-crunching tasks, have been helped significantly by the applications of computers. Investigations into alternative frequency assignment procedures (Gardiner and Magaza 1982) based on alternative 10 and 15 kHz channelling, instead of the traditional 12.5 kHz channelling, has shown that saving in bandwidth to accommodate eight channels with 3rd-order intermodulation free, could be as high as 50%. Although there exists practical difficulties in terms of equipments compatibility.

It can be seen from above that, intermodulation interference is a major problem preventing frequency assignment planners from packing more channels in a given bandwidth. As demands on the already congested spectrum increases, the problem will deteriorate even further. Major effort should be put on reducing intermodulation interference at its sources, rather than just relying on frequency planning.

1.4.3 Types of Intermodulation Interference

Broadly speaking, there are two types of intermodulation interference. Firstly, there is active intermodulation interference due to the actions of active components in a communication system, such as transmitters and receivers; and secondly, passive intermodulation interference due to passive components in the radio system, such as cables, connectors ... etc.

1.4.3.1 Transmitter Intermodulation Interference

Intermodulation interference could be generated at the power amplifier stage of the transmitter. Normally, power amplifiers operate in the Class-C mode, which exhibits a large amplitude non-linearity.

Interfering signals could be coupled to the power amplifier stage via antenna coupling, case penetration and coaxial cables coupling. When this happens, the interfering signals would be mixed together with the carrier at the output stage, and generates intermodulation interference.

Alternatively, in a multi-coupling transmission system, a single common power amplifier stage is normally used to amplify the combined inputs. However, due to the non-linearity of the output stage, intermodulation products will be generated.

Fortunately, it is possible to eliminate transmitter related intermodulation interference by : (1) place sufficient filtering between the rf power amplifier stage and the antenna, (2) use of highly linear amplifiers, and (3) provision of adequate shielding between the component parts.

1.4.3.2 Receiver Intermodulation Interference

In this case, intermodulation interference could be generated in the rf amplifier and the mixer stage of the

receiver front-end.

Due to the limitation on the selectivity of the front-end filter, interfering signals close to the wanted signal will not be suppressed completely, and therefore, could get into the rf amplifier and the mixer as well, generating intermodulation interference.

The cure, again, is to employ high Q-factor resonators, probably in cascade, to provide sufficient attenuation to all signals except the wanted one, before they reach the receiver front-end. Sufficient shielding among equipments is essential as well.

1.4.3.3 Passive Intermodulation Interference

The provision of various measures to control spectrum pollution arising from transmitters and receivers is increasingly effective. However, there is another type of intermodulation interference termed passive intermodulation interference (PIMI), which arises due to the nature of the materials employed to construct electronic, electrical and mechanical components used in a communication system, as well as the physical states of the components. Ferromagnetic material and corrosion products have been identified as sources of passive intermodulation interference. Details on sources of PIMI will be described in Chapter 2 of this report.

One of the most troublesome sources of passive intermodulation interference has been the so-called 'rusty-bolt' effect or structural intermodulation interference. This refers to the effect that, in the presence of high rf power carriers, any metal work, fences, metal chains, antennas, and even the antenna-supporting mast can act as unintended receiving antennas (URAs) which pick up radio waves and mix them in corroded metal interfaces, then generate IMPs and re-radiate them to cause local spectrum pollution.

It has also been noted that even the weather conditions can cause large variations in the IMP levels. The difficulty here is that there are a lot of variables which are not under the control of the system planners.

1.5 Conclusion

It is obvious from the above discussion that intermodulation interference has become a significant electromagnetic compatibility problem in multi-carrier transmission systems. In particular, structural intermodulation interference poses a problem which could degrade the performance of radio systems, yet is difficult to tackle. Our objectives were to obtain a better understanding of the interference mechanisms and to evaluate possible remedies.

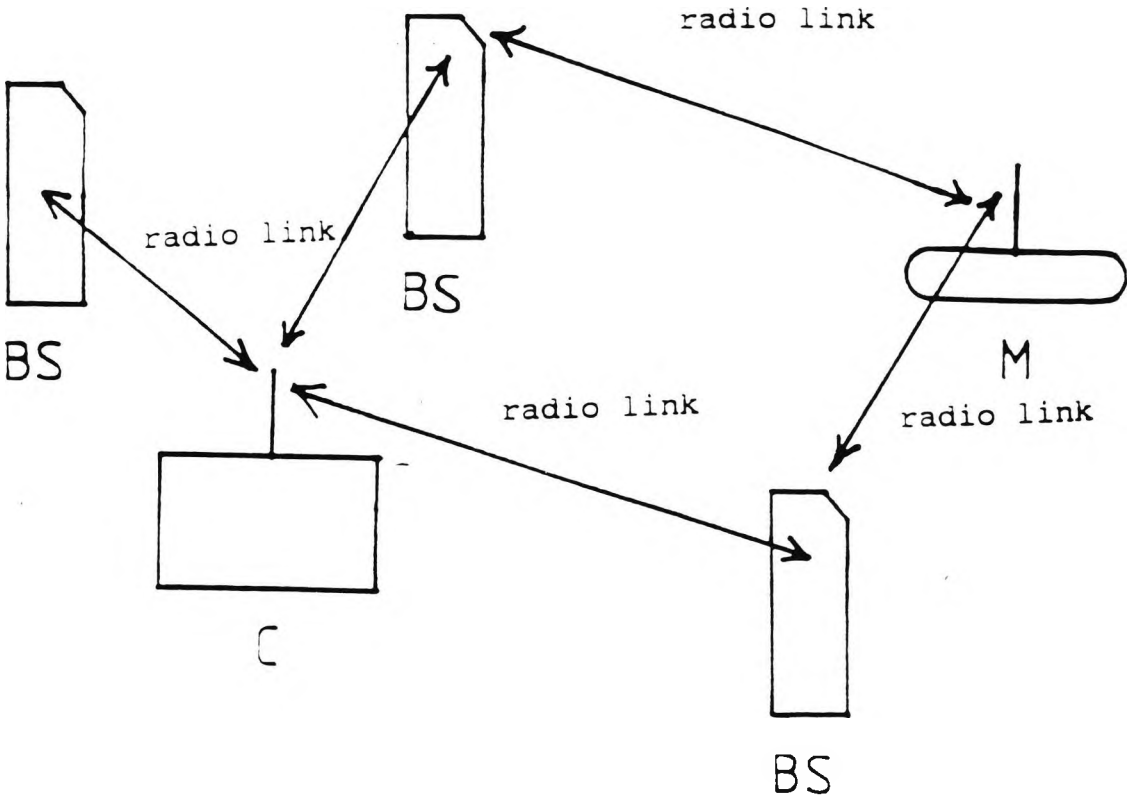

M = Mobile
C = Control
BS = Base Station

FIGURE 1.1 Basic Components of a Mobile Radio System

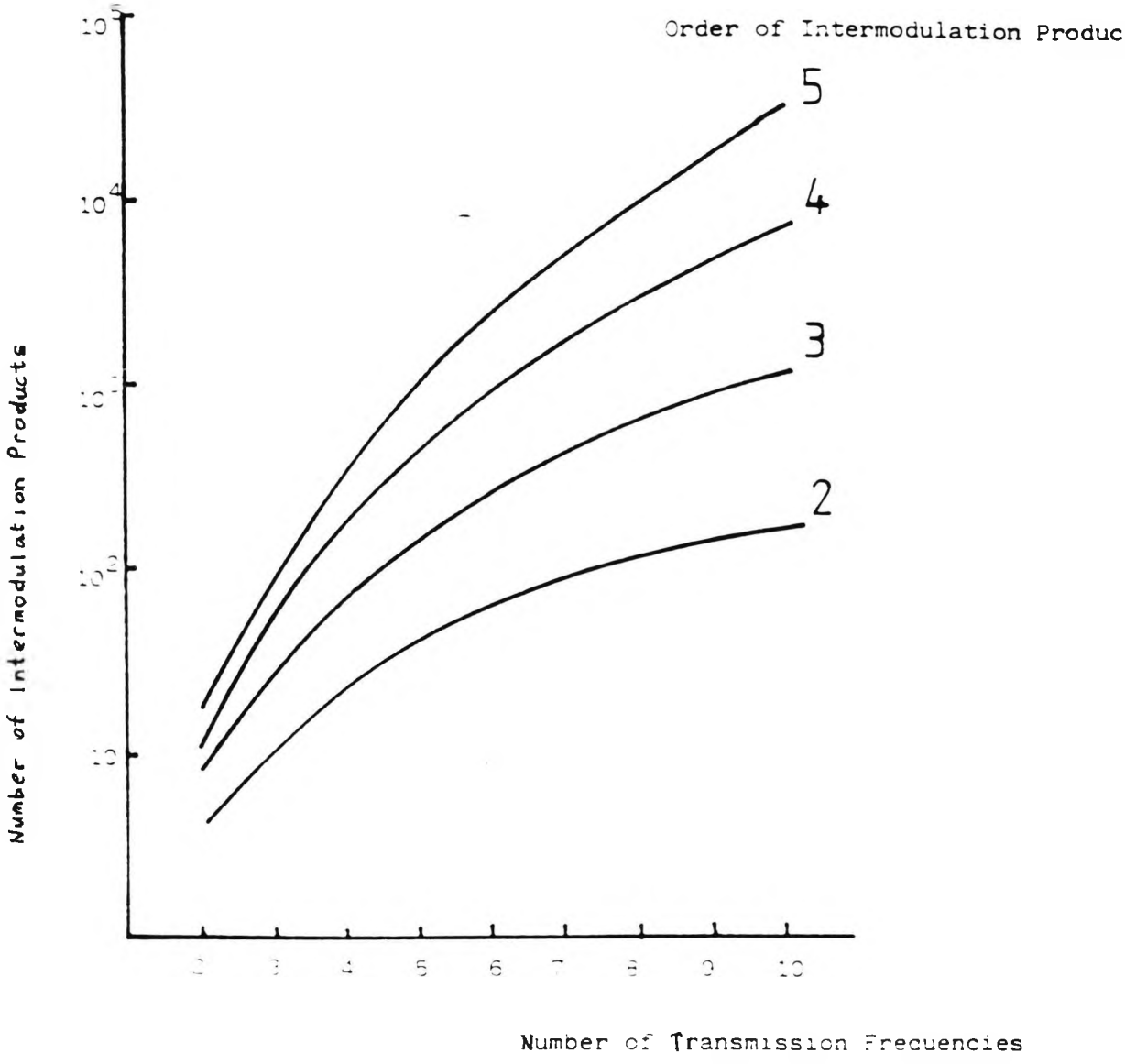

FIGURE 1.2 Relationship between Number of Intermodulation Products and Number of Transmission Frequencies

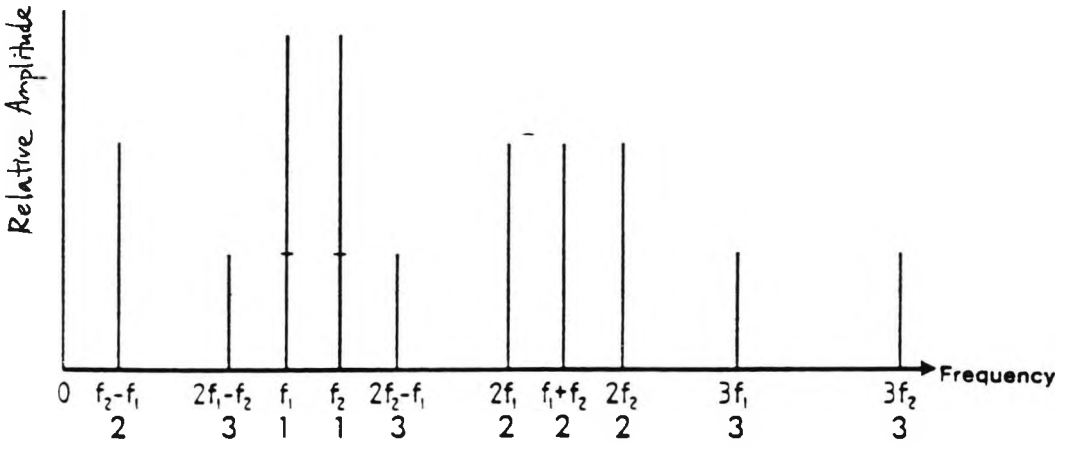

FIGURE 1.3 Spectral Distribution of the Intermodulation Products due to Two Transmission Frequencies

Chapter 2

Literature Survey on Passive Intermodulation Interference and Related Topics

2.1 A Literature Survey on Passive Intermodulation Interference

Passive intermodulation interference has been noted for a long time. The sources can be broadly divided into the following categories, namely :

(1) Cables and connectors
(2) Metallic contacts
(3) Passive rf/microwave components
(4) Non-linear materials
(5) Structures

2.1.1 Cables and Connectors

Coaxial cables are used extensively in radio communication systems. They provide a flexible way to connect antennas, filters and other terminal equipments togather easily. However, in a multiple-carrier system with shared feeders, power amplifiers and antennas, there is a real chance in generating intermodulation products within the cables due to their construction methods and ageing problems. Amin and Benson (1978) tested various coaxial cable samples at microwave frequencies 1.5, 3 and 5 GHz. They found that the three most important factors in the generation of IMPs in coaxial cables are : (1) composition of the braid materials; (2) filling factors of the braids, and (3) the pressure between the inter-braid wire contacts. Silver-plated braids were found to generate the lowest IMP levels; while braids with aluminium, nickel-plated copper and stainless steel generated strongest 3rd- and 5th- order IMPs. In addition, cables with high filling factors and high inter-wire contact pressure also produced low IMP levels.

The reason is that, the hard, thin layer of silver oxide formed on the silver surface can breakdown easily under the actions of braid contact pressure, hence reduced the non-linear contact resistance and resulted in lower IMP levels. High filling factor and high inter-wire contact pressure also help to maintain good contacts within braids.

In the area of connector hardware, Young (1976) reported that, at 250 MHz, connectors constructed from, or plated

with ferromagnetic material, such as nickel and nickel-plating; and those with Kovar-glass seals (used in hermetic seal, contains 99.7% ferromagnetic material) are serious sources of intermodulation interference to sensitive communication systems. Using two-signals tests at 45 dBm each channel, 3rd-order IMP level at90 dBm and higher was recorded. He also found that the IMP levels of Kovar devices exceeded those of stainless steel, which in turn exceeded those of nickel-plated devices.

Further work in this area has been demostrated by Shands et al (1984). In addition to supporting the previous findings, they performed experiments on cable and connector combinations as well. They pointed out that the method of construction employed in joining the cables to connectors is very important to the IMP levels. Moreover, connectors should be carefully threaded and tightened with hand tools. All equipments and interconnections should be rigidly mounted to prevent vibration.

From above, it can be seen that aged and corroded coaxial cables, which carry several rf frequency components concurrently, could be a potential source of IMI. In addition, the material used for making the components used in the communication system also has some effect. Ferromagnetic materials are stamped as sources of IMI and should be avoided in multiple carriers communication systems.

2.1.2 Metallic Contacts

It has also been recognized for a long time that metal-metal contacts in a multiple carriers sytems can cause serious problems. A paper by Cox (1970) reports measurement procedure and circuit for odd order IMPs generated in waveguide components of a 6-GHz FM diversity system. He found that loose waveguide joints produced a 3rd-order IMP at 25 dBm when using 30 dBm transmitters; and is the worst device and generator of high level intermodulation. Similar findings were reported by Nuding (1974). He tested 3rd, 5th and 7th order IMPs of a UGF 18 waveguide flange connector at 2 GHz, with input power up to 1,000 watt. He also discovered that loose contact pins, frequently used in the form of tuning screws for compensation, generated considerable IMPs when they were stimulated by external forces to vibrate; though he did not give any figures for the resultant IMP levels. Moreover, they did not indicate what were the physical states of the components under testing. The effects of loose contacts will be analysed in Chapter 5.

Further work on metal-metal contacts is demostrated by Bayrk and Benson (1975). Their work addressed the intermodulation products generated by non-linear effects at contacts between similar and dissimilar metals. They worked at 3 GHz with maximum output of about 10 watt. Both 3rd and 5th order IMPs were measured and most of the products measured falling into a range of 40 to 80 dBm. It was found that dissimilar contacts of mild steel, aluminium and stainless steel with any other metals generated high IMPs; while those with

copper, brass, beryllium copper and nickel contact generated the lowest IMPs. In addition, point contacts tend to be more susceptible to increase/decrease in contact loads than in the case of surface and spherical contacts. Point contacts produced wide variation in the IMP levels.

Martin (1978) also reported tests done on metallic contacts at HF (22 MHz) and UHF (360 MHz). He found that with output power at 30 watt each channel, aluminium, mild steel, stainless steel and nickel contacts produced higher IMPs than brass, copper, silver and gold. All samples used were new, presumably, he meant free of corrosion products.

Similar work by Arazm and Benson (1980) at 1.5 GHz again shown that electrically clean copper, brass, oxygen-free copper, oxygen-free nickel and berylium-copper produced low IMP levels; while mild steel and aluminium produced high IMP levels. In addition they compared 3rd order IMPs of various materials at 1.5, 3, and 6 GHz but could not find any relationship between IMP levels and frequency variations. In addition, it was found that the IMP levels of ferromagnetic nickel at microwave frequency band was lower than those measured at VHF band. A possible explanation is that the skin-depth of nickel at 1.5 GHz is one-third of that at 150 MHz; the volume of ferromagnetic material involved in IMP generation is therefore, about one-third of that at 150 MHz. Hence, the higher the frequency involved; the less would be the IMP level due to B/H non-linearity of materials.

Effects of oxides on the surfaces of metal samples, and of

contact pressure at junctions, on the resultant IMP levels have also been investigated by Bayrak and Benson (1975), Martin (1978) and Arazm and Benson (1980). Their results were in general similar in that oxidized samples normally produced higher IMP levels than when they were new. Martin reported that IMP of samples treated by high temperature oxidation could rise by as much as 40 - 50 dB. On the other hand, if the contact pressure at interface between two samples is increased, the corresponding IMP level decreases, though not in a linear way.

Kellar (1984) investigated IMPs generated by corroded and loose aluminium-aluminium connections at the VHF band. He used an output power of about 0.1 watt, because he was interested at cable television systems rather than high power transmission systems. He found that IMPs could be generated by corroded or loose connections with low contact pressure, and that any reasonable amount of contact pressure should prevent IMP generations.

2.1.3 Passive RF/Microwave Components

Other passive components within a communication system, such as ferromagnetic isolators, duplexers ... etc have also been examined. Young (1976) tested circulators at 250 MHz and 40 dBm input power, the 3rd order IMP was nearly 40 dBm, which is greatly inferrior to a coaxial cable load (at 30 dBm input, 3rd order IMP level is 60 dBm). However, at 6 GHz and input power at 30 dBm, Cox (1970) measured no significant

IMPs generated from isolators and circulators. In fact, he even included isolators (40 dB isolations) in his measurement setup to reduce circuit sensitivity to detuning. Nuding (1974) measured a power circulator at 2 GHz, high 3rd order IMP level of 50 dBm was obtained at an input power of nearly 59 dBm. Therefore, it seems that at microwave frequency band the effect of ferromagnetic non-linearity is significantly reduced due to skin-depth effect. Then, the use of isolators, circulators will only become a problem if very high outpower is required.

2.1.4 Non-linear Materials

Intrinsic sources of intermodulation interference can be due to non-linear resistance arising from resistive heating in conductors; and more important, due to variations in permeability in ferromagnetic components.

Betts and Ebenezer (1973) investigated the compositions of ferromagnetic steels and their effects on IMPs generations. They found that carbon steels, which is similar to a ship's steel, produced the worst (about 10 dB higher) 3rd order IMP levels, followed by alloy steels and stainless steels.

A study by Bailey and Ehrich (1979) also pointed out that nickel could produce high level IMPs, and their use in plating rf connectors should be discontinued. They also attempted to explain the intermodulation generation mechanism by considering the so-called 'magnetic domain wall

vibration' as a non-linear phenomenon.

It has also been known (for exampel, see Smithers (1980)) that carbon fibre composite material, used mainly in aircrafts for their light-weight and rigid properties, can also produce IMPs due to variation of resistance with the applied signal frequency.

2.1.5 Structures

Structures present another dimension of IMP generations. In this particular category, the major concerns are :

(i) there are numerous sources of IMI associated with a structure
(ii) the dimensions of the structure could be very effective in re-radiating IMPs
(iii) environmental effects on structural IMI are usually important.

Betts and Ebenezer (1973) investigated the effect of non-linear ferromagnetic steels on IMP generations at HF band, in the context of naval vessels, which are huge metallic structures. They found that the residual 3rd order IMP level recorded after 'cleaning-up' the ship was due to steel, which is the main building material of naval vessels. Work reported by Higa (1974) demostrates that large reflector antennas can generate IMPs by electron tunneling through the thin aluminium oxide layer formed between

antenna panels. However, Guenzer (1975) has shown doubt on Higa's procedures to establish electron tunneling as the casue of IMI.

2.2 Discussion

From above, it can be seen that intermodulation interference problems normally occur at parts of a communication system where high power multiple frequency signals share the same current path. There are two main categories of passive intermodulation interference, namely, ferromagnetic non-linearity and non-linear metal-metal contacts. Ferromagnetic materials would generate IMPs irrespective of the corrosion state of the materials; for non-ferromagnetic materials, the presence of corrosion products seems to be essential for the production of high level IMPs. However, several researchers suggested that clean loose contacts on their own could also generate high IMP levels. In the next few chapters, we will examine in details, the conditions for the generation of IMPs in non-ferromagnetic materials and their underlying mechanism.

It can be seen that a large amount of research work has been done on the IMP generations in communication hardwares. However, the aspect of structural intermodulation interference (SIMI) has received little notice. Structures, in our study, refer to any metallic objects which are not part of the communiciation system, but nevertheless, necessary in supporting and/or housing the communication

system. In this context, the antenna supporting mast, metal fence surround the base station site, steel chains and ropes ... etc, are typical examples of structures. They are normally situated in a hostile environment, where they are subjected to every possibility of corrosive attacks. Since atmospheric corrosion plays an important part in structural intermodulation interference, it is therefore appropriate to present some facts and statistics on the damaging effects of atomspheric corrosion on structures.

2.3 Atmospheric Corrosion

Corrosion is defined as the involuntary destruction of substances such as metals and mineral building materials by surrounding media, which are usually liquid corrosive agents. It usually begins at the surface and is caused by chemical and, in the case of metals, electrochemical reactions. The destruction can then spread to the interior of the material.

The economic importance of corrosion can be shown by an example : It is concluded in the Hoar Report (1971) that, in U.K., the cost of corrosion is amount to more than 10 million each year. It is therefore of utmost importance to reduce as far as possible the financial and material losses due to corrosion.

The most common forms of metallic corrosion are caused by electrochemical reactions, wherein two metallic phases

(e.g., iron and iron oxide) with different electrochemicdal potentials are connected to each other by means of an electric conductor. Electrolytes such as acids, alkalis, salt solutions, or even milder media such as rainwater, river water, or tap water need to be present. Metallic phases with different electorchemical potentials exhibit electric potential differences. Potential differences may also arise because of impurities, corrosion products, damaged protective coatings, etc. The larger the potential difference, the faster the rate of corrosion.The atmosphere consists of some chemically active components which causes the atmospheric corrosion of metals. It is therefore useful to look at these components more closely.

2.3.1 The Active Chemical Components of the Atmosphere

1. Oxygen is very important and has extensive influence on the corrosion mechanism because of its high reactivity. Atmospheric oxidation is an oxidation-reduction process, in which the metal acts an electron donor and oxygen, and other reducible species, as electron acceptors.

2. Water in its liquid form, provides a electrochemical path of the corrosion process. Water is deposited on the surface via direct precipitation and other absorption and condensation processes, which are determined jointly by the absolute humidity and the temperature as well.

3. Sulphur dioxide is the typical gas impurity found in

urban and industrial atmospheres. It is emitted to the atmosphere in large amounts during the combustion of sulphur containing fuels of all types. It dissolves easily (16.2 g SO_2 per 100 g H_2O) in water to form sulphurous (H_2SO_3) acid, which then oxidised to sulphuric acid (H_2SO_4) to promote corrosion.

4. Hydrogen sulphide has significant effects on corrosion of copper, nickel and silver.

5. Acidic gases, like chlorine and hydrogen chloride are frequently found in the air near chemical works, etc. These chemicals are extremely aggressive.

6. Chloride is a chemically active component of the atmosphere, especially in coastal areas. Its concentration falls with distance from the coast.

2.3.2 Corrosion of Galvanised Steel

Corrosion has been a major topic for research, mainly because of its economic and safety implications. Well written documentations on corrosion can be found in the works by Fontana and Greene (1967), Gabe (1978), and Barer and Peters (1970). Only a very brief account on atmospheric corrosion of metallic structures will be presented below.

Since most of the metallic structures are built with steels (its composition is mainly iron), and the steels are covered

by a layer of zinc via the hot-dip galvanisation process, it would be particular interesting to look at the corrosion of zinc and steel in atmosphere.Appreciable corrosion of steel only starts when the relative humidity of air exceeds around 65%. However, rusting is essentially an electrochemical process as described at the beginning of section 2.3. Iron is dissolved from the metallic construction material and reacts with water and oxygen to form hydrated iron oxide. This reaction product is deposited as a spot of rust or, when the reaction has proceeded further, as a layer of rust. The reaction equations are :
First, the water oxidizes the iron to Fe(II)

$$Fe + 2\,H_2O \longrightarrow Fe(OH)_2 + H_2$$

In the second step, oxygen oxidizes the iron further to Fe(III)

$$2\,Fe(OH)_2 + 1/2\,O_2 \longrightarrow 2\,FeO(OH) + H_2O$$

Rust may be considered as consisting of iron (III) oxide hydroxide with variable water content.

Impurities in air, e.g. sulphur dioxide and chlorides, can accelrate the corrosion process even at low concentrations. Oxidation causes sulphur dioxide to form sulphuric acid in the presence of suitable catalysts :

$$SO_2 + 1/2\,O_2 + H_2O \longrightarrow H_2SO_4$$

H_2SO_4 reacts with iron and oxygen to form ferrous sulphate and water.

$$Fe + H_2SO_4 + 1/2\ O_2 \text{ ------> } FeSO_4 + H_2O$$

The ferrous sulphate is then oxidized by oxygen to give ferric sulphate which is then hydrolized to produce rust and sulphuric acid :

$$2\ FeSO_4 + 1/2\ O_2 + 3\ H_2O \text{ ------> } 2\ FeO(OH) + 2\ H_2SO_4$$

It should be noted that, the end product contains apart from rust, more sulphuric acid. This can then dissolve more iron and contributes to further rust formation. Sulphuric acid can therefore convert appreciable quantities of iron into rust in a continuous cycle.

Corrosion of zinc is closely related to the amount of SO present, the relative humidity of the air, and in coastal areas, also to the salt content of the air. Zinc is particularly stable in country air and in enclosed areas. A stable protective layer is formed, consisting of zinc oxide, zinc hydroxide, and zinc hydroxycarbonate. This protective layer is self healing.

Appreciable disappearance of zinc takes place in city air and industrial air. The removal of zinc is mainly caused by the SO_2 content of the air. SO_2 reacts with water to form sulphurous or sulphuric acid. These in turn react with the protective layer on the surface of the zinc, forming zinc

sulphite or sulphate. The protective layer which is weakened in this way is then reformed by reaction of air with more metallic zinc. All this means that the zinc corrodes away. In marine air the annual removal of zinc is even higher.

A major study which attempted to determine the atmospheric corrosion rate of zinc all over Britain has been carried out by the Central Electricity Generation Board. In their study, test samples of zinc were exposed in almost every 10 Km grid square of England and Wales. Corrosive maps (e.g. see figure 2.1) are produced which show the environmental corrosion effects clearly. From figure 2.1 it can be seen that the degree of corrosion is higher near the coast due to the presence of chloride.

2.4 Conclusion

In this chapter, we have examined various sources of passive intermodulation interference in a communication system. Some of the interference sources are avoidable (e.g. use silver-plated connectors instead of nickel-plated connectors); others are not (e.g. metallic contacts; structures). By identifying these sources in a transmission system, the system designer would be in a better position to minimize the effect of intermodulation interference.

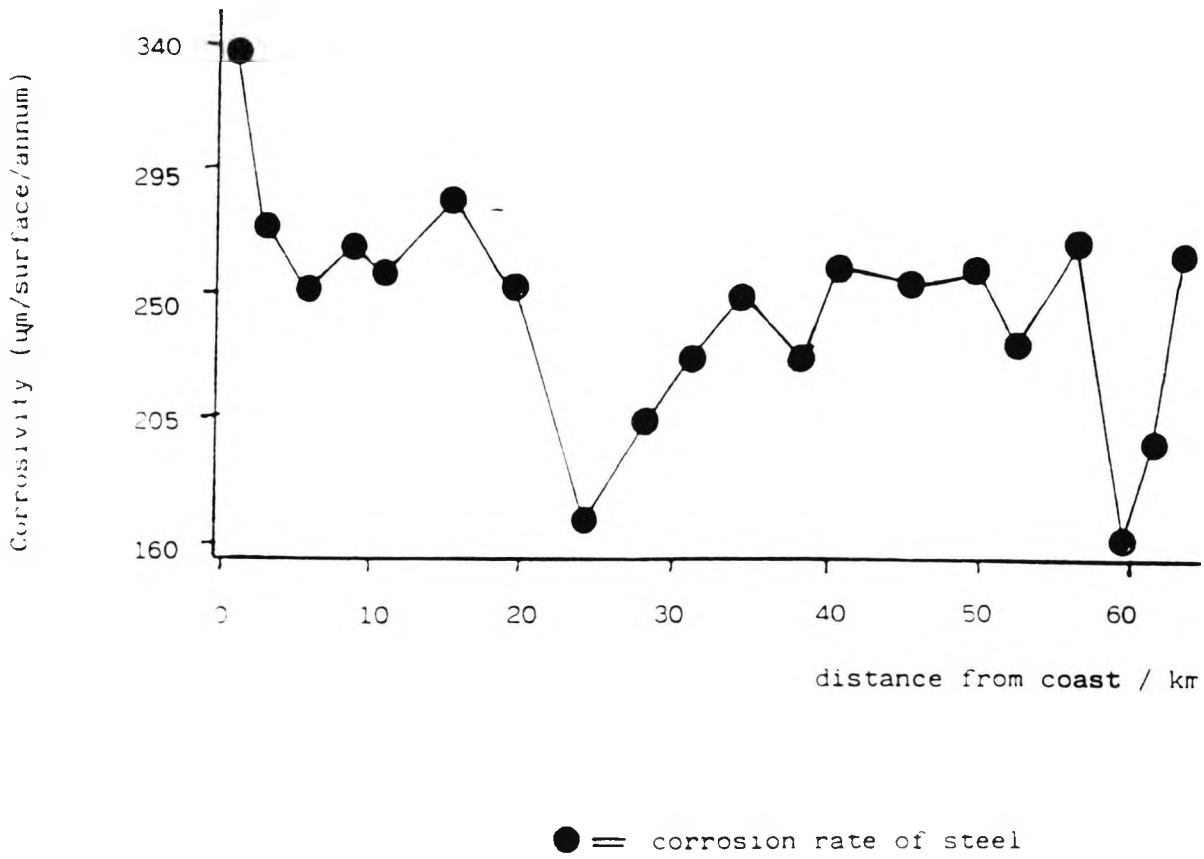

FIGURE **2.1** **Corrosivity** values obtained from 20 towers of a **transmission** route (from CEGB Research Aug 87 pp 56

Chapter 3

The Measurement of Structural Intermodulation Interference and Their Sources

3.1 Introduction

From the literature, it was found that the origin of structural intermodulation interference (SIMI) due to non-linear ferromagnetic effect has been studied. SIMI due to non-linear corroded junctions has also been investigated, although not in any great depth. In those experiments, high temperature oxidation and short-term exposure in the laboratory were the most common methods for corroding the samples. Although these dry corrosion methods could cause some deterioration in IMI levels generated from the corroded

samples, however, the natural corrosion process is mainly wet corrosion. In addition, more emphasis was placed on aluminium-aluminium contacts than other metallic contacts, and 'electron tunneling' was assumed to be the underlying mechansim responsible for the observed non-linear current-votlage characteristic of the corroded junction samples.

In this chapter, we shall investigate the major sources of SIMI and the mechanisms responsible for them. This will help us to identify possible SIMI sources in a base station and its surroundings. Moreover, it will enable us to formulate possible remedies for this effect as well.

In the following two sections, some basic theories concerning the properties and characteristics of linear and non-linear systems are described, so that an appreciation of the effects of intermodulation interference will be acquired. Some background on the physics of rectifying phenomenon is also given.

3.2 Basic Theory (I) - Linear System Theory

A linear system cannot generate new frequency components. The output of such a system will be a faithful replica of the input and will contain no new frequencies. So, in order to produce intermodulation products, the system must be non-linear. In this study, we are most interested in the non-linear relationship between input voltage and output

current, i.e. a non-linear current-voltage characteristic. Having said that, we must be aware that there are other intermodulation generation mechanisms due to non-linear dielectrics and non-linear ferromagnetic materials, for example. But their influence are normally negligible in our applications.

Boardly speaking, there are two kinds of current-voltage non-linearities, namely, small signal (see figure 3.1) and large signal non-linearities (see figure 3.2). In the small signal case, the non-linearity exists over the whole range of input levels, i.e. any input, no matter how small is its amplitude, will generate harmonics and/or intermodulation products at its output. In contrast, in the large signal case (which is also called 'piecewise linear' characteristic), if the input operates within the region A, then the system operates in its linear region, and no harmonics would be generated. However, if the input spans over the two regions A and B, then the system operates in a non-linear fashion and harmonics and intermodulation products will appear.

Mathematically, the small signal non-linearity can be represented by a power series as follows :

$$I = a_o + a_1V + a_2V^2 + a^3V^3 + \ldots \quad \text{for } V > 0$$

$$I = 0 \qquad \text{otherwise.}$$

The large signal non-linearity can be represented by the following function :

$I = 0 \qquad \text{for} \quad V = 0$

$I = c * V \qquad \text{for} \quad 0 < V$

Any one of the above two characteristics would be able to generate intermodulation products.

3.3 Basic Theory (II) - Rectification in Solids

In this section a very brief background on the theory of the rectification phenomenon will be given. The description is particularly related to our problem in hand, i.e. metal-oxide and metal-semiconductor junctions. It is reasonable to assume that other rectification systems, such as p-n junction diode and metal-insulator-semiconductor systems, are less likely to occur in the natural environment.

3.3.1 History of Metal-Oxide and Metal-Semiconductor Rectifiers

As early as in 1874, Braun and Schuster (Braun 1874) observed rectification effects when experimenting with small contacts on tarnished copper wires, which might have been covered by oxide films. They found that the resistance depended on the polarity of the applied voltage, and the

condition of the surface tarnish. They considered that rectification arises from the gas films absorbed at the surfaces of solids. After that, rectification was also observed in selenium. In 1920, when Grondahl tried to use cuprous oxide to build a photo-switch for handling large power, he discovered that cuprous oxide acted as a good rectifier. He was also aware that the phenomenon was due to a 'contact effect'. In those days, the constructions of commercial rectifiers were difficult and rectification ratio was not guaranteed to be excellent, because people did not know what sort of surface condition was responsible for the non-linear conduction effect. Main materials for making plate rectifiers were cuprous oxide, cuprous sulphide, lead sulphide, iron sulphide and selenium. Cuprous oxide was found to be a p-type semiconducting material.

From about 1905 to 1925 the point contact crystal rectifier was the primary type of detector used in radio receivers. One weakness of crystal detectors was that they had no power of amplification. Its use was soon replaced by the invention of triode vacuum tube which could be employed as a combined amplifier and detector. During the Second World War, point contact diode was used again as a frequency converter and as a low level microwave detector diode, because the crystal detector offered much lower noise operation, and was more suitable as a low level square-law detector of microwave pulses.

In 1948, Bardeen and Brattain (Bardeen and Brattain 1948) described the important discovery of carrier injection

phenomenon in point contact germanium diodes, and the next year the point contact germanium transistor was achieved. During the 1950s, the methods for fabricating p-n junction diode became available, and gradually supplanted metal-semiconductor diodes. Schottky barrier diode rose again in the 1960s, due to the invention and development of the planar process for field effect transistors, which led to a better understanding of interfaces and interface cleaning techniques.

Applications of Schottky barrier diodes in 1960s were important. In 1964, Baird patented a Schottky barrier clamp integrated with a silicon bipolar transistor. In 1966, Mead described the metal-semiconductor field effect transistor, an FET with a Schottky barrier gate. Other developements were planar Schottky varactors and varistors for microwave applications. In 1970s and beyond, when high frequency and fast switching speed devices are in demand, two major applications with Schottky diodes are : (1) saturation-preventing clamps in high speed bipolar integrated circuits for computers and other switching network; (2) discrete high frequency diodes and transistors for signal detection and amplification circuits in microwave communication systems.

3.3.2 Electrical Conductions in Oxides

In this section, it is our intention to demonstrate that transition metal oxides, such as ferrous oxide, can behave like semiconductors. However, their semiconducting property does not come from artificial doping of impurities; but by lattice defects (both interstitials and vacancies) and impurities present in the atmosphere. To facilitate a better understanding of electrical conduction mechanism in metallic oxides, we will introduce a few useful concepts in the following sections.To classify materials as metallic, semiconductors and insulators, it is useful to look at the energy band diagrams of these materials.

In a single atom, the electrons are arranged in shells of definite energy level and those nearer the nucleus require more energy to remove them from the parent atom. For a complete lattice of atoms, the electron energies are modified by the fields of adjacent atoms. The single energy levels spread out to form bands of energies. Electrons can move from one level to another within a band fairly easily by acquiring small amount of energy, but appreciable energy is required for the electron to move from one band to another, typical band structures for the three types of materials are shown in figure 3.3.

The inner energy bands where all the energy levels are completely filled, contain tightly bound electrons. Electrons in these bands have no effect on the chemical and physical properties of the material. A filled energy band is

one where there is an electron for every possible energy value within the band. The outer band, where electrons are not rigidly bound to the nucleus, is known as the conduction band. Next to this is the valence band. The difference in energy levels between the top of the valence band and the bottom of the conduction band is the fundamental explanation for the difference in behaviour of conductors, insulators and semiconductors.

From figure 3.3 it can be seen that metals always have free electrons in the conduction band responsible for their high conductivities; for intrinsic semiconductors, the energy gap is small enough that a small amount of applied energy (e.g. heat) would enable valence band electrons jump to the conduction band, thus increases the conductivity of the material; for insulators the energy gap is so large that in general it is unlikely for the valence band electrons to gain enough energy to move up to the conduction band.

In metallic oxides, the bonding between metal ions and oxygen ions is the strong ionic bond, and ionic conduction in oxides is not appreciable until very high temperature is reached. Under normal temperature and pressure, and in their pure form, they will behave as insulators because there are no free electrons available for electrical conduction. Therefore, other mechanisms must be present for electrical conduction to happen.

It is the presence of physical defects (vacancies and interstitials) which enables ionic crystals (such as

metallic oxides) to exhibit semiconducting behaviour. However, the concentration of the defects has to be large, as in transition metal oxides, before semiconduction becomes significant.

In the case of transition metal oxides, four situations could happen (see figure 3.4) :

(1) Metal excess due to anion vacanciesIn this case, the lattice loses atoms of the non-metal, however, the associated electrons are trapped in the vacancies to maintain overall electrical neutrality.

(2) Metal excess due to interstitial cations

In this case, again the lattice losses atoms of the non-metal. The excess metal ions are forced to occupy interstitial sites; and the electrons previously associated with them are trapped in the vicinity of these interstitial cations.

(3) Metal deficiency due to cation vacancies

In this case, the lattice acquires additional atoms of the non-metal which gain electrons to become anions. These electrons are obtained from the crystal as some of the metal ions are oxidised to a higher oxidation state.

(4) Metal deficiency due to interstitial anions.

In this case, the lattice acquires additional atoms of the non-metal as in (1). However, the added anions occupy interstitial positions of the lattice.

Two examples are nickel oxide and titanium dioxide (see figure 3.5). In the case of nickel oxide, there is a cation vacancy present, and electrical neutrality is maintained by two nearby nickel (II) ions, which oxidised to nickel (III) ions. Since the metal : oxygen ratio is below the stoichiometric ratio of 1 : 1, then nickel oxide is termed a metal deficiency semiconductor. In titanium dioxide, the small titanium ions can enter the interstitial sites easily, and for each titanium ion that enters, its four nearby titanium (IV) ions will be reduced to titanium (III) ions to make the lattice electrically neutral. Since the metal : oxygen ratio is above the stoichiometric ratio of 1 : 2, therefore, titanium dioxide is termed a metal-excess semiconductor.

Electrical conduction within transition metal oxides could be explained in terms of the above four conditions. In (1) and (2), the trapped electrons are not localized, and will throughout the entire lattice if there is an applied potential. The current carriers are the electrons. In (3) and (4), there are not any free electrons. So, under the influence of an applied potential, the electron in a low oxidation state metal ion will pass onto another metal ion

in a higher oxidation state. In the process, the electron donor oxidized itself to a higher oxidation state and reduced the receiver metal ion to a lower oxideation state. The movement of the electrons then contributes to the flow of current. In this case the charge carriers are the positive holes.

In terms of the energy band diagram, the presence of impuritiy ions such as nickel (III) in nickel oxide; and titanium (III) in titanium dioxide will produce additional energy levels in the band diagram, namely, the acceptor level and donor level, as shown in figure 3.6. Since the acceptor level is very close to the top of the valence band, then it is very easy to excite a valence electron in nickel (II) ion to the acceptor level, leaving positive holes in the valence band for conduction. So metal-deficiency oxides are p-type semiconductors. In contrast, the titanium (IV) ions are at the donor level, and upon excitation, the electrons will move to the conduction band, and contribute to semiconduction. Metal-excess oxides are therefore termed n-type semiconductors.

Having shown that metallic oxides could behave like semiconductors (either p-type or n-type), then the most logical rectification mechanism which could take place in a metal-metal oxide junction is metal-semiconductor rectification, which is a well-established subject (e.g. see Sze 1981, Van der Zeil 1968) .

3.4 Experimental Setup

In order to assess the dependence of the IMI level of a test sample on its physical state, it is necessary to measure various parameters, mainly electrical, of the sample. Firstly, IMI level measurement is required. Secondly, the rectification or non-linear current-voltage characteristic of the sample is needed to estimate the severity of the resultant IMI level. At high frequency, when the joint/junction capacitance becomes significant, ac impedance measurement of the sample is essential, as most of the rf current will bypass the joint resistance through the capacitive reactance.

In our studies, we have chosen to monitor the 3rd-order intermodulation product level only. This decision was taken because it is the general experience that, lower order IMPs, because they are at a higher level, produce far worse interference than higher order ones. So, the 3rd-order IMP would give us the 'worst case' interference level, and should be the value of interest to system designers and planners alike.

The measurement setup for the three different measurements are described in the following section.

3.4.1 Passive Intermodulation Products Measurement

There are mainly two different types of Passive Intermodulation Products (PIMP) measurement systems, namely, radiative and conductive testings. The building blocks for these two systems are shown in figure 3.7. The radiative testing is essential for measuring the scattering patterns and strength of IMPs and harmonics generated from a large structure, such as an automobile or a fighter aircraft. On the other hand, conductive testing is more suitable for testing components used in the communication systems, such as connectors, cables, metallic contacts, isolators ... etc.

Conductive testing method makes use of a test chamber for housing the test sample, and all rf power is terminated by a matched load (usually 50 Ohm), so that there is no rf energy radiated. This method is very popular because the test sample is placed in a controlled environment, where variations of parameter values are much easier to achieve. Radiative testing is more difficult to perform, since either a clear site or a anechoic chamber must be used, and the surrounding environment will have significant effects on the measured IMI levels.

3.4.1.1 Design Considerations

There were quite a few PIMI measurement systems developed by various groups investigating the intermodulation interference effect. In designing our own test system, there

were a few criteria which had to be satisfied. They are :

1. high accuracy
2. good repeatibility
3. low residual intermodulation interference level

and for the test jig specifically, they are :

1. easy to accomodate test samples coated with specialised materials

2. low voltage standing wave ratio (VSWR), i.e. good matching

3.4.1.2 PIMP measurement system at City University

The measurement system block diagram is shown in figure 3.8. The measurement setup consists of three major sections : (1) the Power Source Section, (2) the Power Combiner and Test Sample Section, and (3) the Load and Detector Section.

The purpose of the Power Source Section is to (1) generate the required levels of rf power at the fundamental frequencies, and (2) monitor the input power levels to the test samples.

Two Marconi 2019A synthesized signal generators are employed to provide the two fundamental frequencies at 152.0875 MHz and 155.2125 MHz respectively. The input signals are fed

into linear high power amplifiers which can deliver up to 100 watt output power each. High Q-factor (unloaded Q-factor is about 11,000) cavity resonators are used to eliminate any harmonics of the fundamental frequencies. The cavity resonators are manufactured by Aerial Facilities Limited, Model Number MB-165-2N. The centre frequency of a resonator can be tuned by adjusting a telescopic rod on the resonator. Each resonator has an insertion loas of around 1dB, and provdes an attenuation of more than 35 dB at a frequency which is 3 MHz away from the tuned frequency. Each filter branch in the Power Source Section consists of two cascaded cavity resonators. The output of the filter is connected to the Power Combiner/Test Sample Section.

A Model 43 rf THRULINE directional wattmeter is placed between the output of the linear power amplifier and the filter. The wattmeter monitors the power delivered to the test sample. The rf directional wattmeter is capable of measuring both transmitted and reflected power. It was found that because of the presence of a diode in the coupling cirucit of the wattmeter, the background intermodulation interference can increase by 10 dB. Therefore, the plug-in coupling element has to be removed, after recording the power flow.

The purpose of the Power Combiner/Test Sample Section is to (1) combine the two fundamental signals so that they can be applied to the test samples, (2) provide a flexible mechanism to house test samples.

The method of combining the two fundamental signals is to use T-pieces and half wavelength coaxial cables. This method is simple, although the length of cables used is critical to achieve maximum signal isolation. Refering to figure 3.8, the cable of length, L1, which equals to the half wavelenght of the fundamental signal f_2, acts as a half-wavelength transformer, so that the fundamental signal f_2 at port 2 sees an impedance presented by the resonators tuned to f_1, which is very large, and therefore, will not pass through them. Similarly, L2 equals to the half wavelength of the fundamental signal f_1.

The T-pieces are integral parts of the test cell. Figure 3.9a to figure 3.9k show the details of the test cell, and the way the test cell is assembled. The test cell is made of brass, and can house a test sample of about 40 mm in length and 8 mm in diameter. The test cell has two hollow sections which can house the two T-pieces (power combiners). After inserting the T-pieces, metal pieces are inserted into the slots, as shown in figure 3.9i, so that proper electromagnetic shielding is maintained. The physical dimensions of the test jig, and its associated components are shown in figure 3.10a to 3.10c.

The Load/Detector Section of the test setup is connected to the output of the test sample. The purpose of this section is to provide an appropriate termination, i.e. 50 Ohm load, for the fundamental signals, and to provide a mean of detecting the IMPs and their levels.

Filter unit 3, consists of three cascaded resonators, is tuned to the 3rd-order IMP frequency (in this case, it is $2f_2 - f_1$) which stops any fundamental signals passing through. Thus the third order intermodulation level can be measured over a wide dynamic range by the spectrum analyser. The intermodulation signal is terminated equally by a spectrum analyser and a matched load, which consists of 100 metres of RG-214 silver-plated braid cables, acting as a distributed linear dummy load. The fundamental powers are also dissipated in the linear load. Figure 3.11 shows the equipment connections and figure 3.12 is a close-up of the connections to the test cell.

The test setup was calibrated, and both accuracy and repeatibility were evaluated. The background intermodulation level, with a clean copper rod, was better than 100 dBm at an input power of 50 watts each channel. Therefore the IMP level was 147 dB below the input.

Repeatibility was tested by measuring the IMP levels of the same sample for several times over a period. It was found that variations in measurement results were normally within 5 dB. The variation might be due to changes in room temperatures or humidity etc. However, by doing sufficient number of repeated measurements with the same sample, a statistical mean level was achievable. Samples could be compared with each other for IMP performance using these mean IMP levels.

Change sample is fairly simple. One just open the lid of the

test cell, loosen the sample holder and then change the sample. Misalignment of the test sample and the sample holder of over 50% of the contact area caused an increase in measured IMI level between 1 dB (for clean copper rod) to 7 dB (for corroded steel rod). In practice, misalignment in contact area was usually less than 10%, and the measurement error due to this effect was insignificant.

The electrical matching property of the test cell with respect to the measurement system was also examined. A Hewlett Packard 8401A network analyser and a Hewlett Packard 8741A Reflection Test Unit were the main components of the test setup (see figure 3.13). By replacing the input of the normal amplified signal at the port for frequency f^1 with the output from the Reflection Test Unit (also excited with low level signal at frequency f_1), the reflection coefficient for the signal at frequency f_1 could be read off directly from the polar display of the network analyser. This procedure was repeated for f_2 and f_{1m} at the other two test cell ports. In all three cases, the reflection coefficients were less than 0.1, i.e. the VSWRs were all less than 1.23. Therefore, most of the fundament rf current would flow throgh the test sample, as required.

The comparisons of performance among different measurement systems developed by different research groups were made difficult by significant differences in parameters such as operational frequency ranges, input power, test sample size and geometry. A brief table below shows the parameters of some of the systems used in the past.

Investigator(year)		frequency band	P_i(dBm)	P_{im}(dBm)	P_i/P_{im}
Martin,	1978	HF	+14.8	-84	-99
Shands,	1984	HF	+44	-88	-132
Shands,	1983	VHF	+44	-104	-148
Ho,	1986	VHF	+17	-100	-147
Martin,	1978	UHF	+14.8	-95	-110
Cox,	1970	C Band	+1.8	-110	-112
Amin,	1978	L and C Band	+13	-117	-130

P_i is the input signal power and P_{im} is the residual third order intermodulation interference level. From the table, it can be seen that the performance of the later implementations are, in general, better than the early ones; becasue of better understanding of the problem due to ferromagnetic non-linearity effect as well as other problems. Some guildlines to reduce the measurement system residual intermodulation interference level are given below.

3.4.1.3 Background Intermodulation Interference Level Improvement Guildlines

From our experience of building and operating this test setup, and from the literature survey, the following guildlines for reducing background intermodulation interference level are of interest :

(1) Components constructed from non-linear materials, such as nickel-plated connectors should not be used in the

current paths of high power multiple carriers.

(2) Avoid using non-linear components such as circulators and isolators in the current paths of high power multiple carriers.

(3) Use semi-rigid cables wherever possible.

(4) Cable connectors should be cleaned regularly.

(5) Minimise number of metallic joints and junctions. They should be inspected regularly for loose, damages or corrosions.

(6) Sufficient shielding and isolation should be provided between high power transmissions and low level incoming signals.

(7) Joints, connectors and cables should be free from vibration.

In fact, above guildlines should be observed in any communication systems which are installed in base stations with co-located transmitters and receivers. As can be seen, careful and thorough maintenance work is one of the essential requirements for minimising passive intermodulation interference.

3.4.2 DC Current-Voltage Characteristic Measurement

This is a straight forward dc current-voltage characteristic measurement of the test samples. In these experiments, corroded joint samples were used. The test setup block diagram is shown in figure 3.14. This is a simple voltage divider circuit, and the applied voltage can be altered via the decade resistance boxes. The test rig used in IMP measuremetns is used here as well. This has the added advantage that after the dc characteristic of a test sample is measured, its IMP level can be measured immediately just by changing the connection cables without touching the sample, which might otherwise, disturb the junction characteristic. Contacts between the sample holder and the test samples are cleaned thoroughly before measurement to ensure that the measured current-voltage characteristic is solely due to the corroded joint.

3.4.2.1 Current Creeping

In our intial measurements, it was observed that on switching on the power supply to the test sample, the current tend to increase initially and then decrease quickly for a short period (exact time depends very much on individual sample), but slow down after a while. Sometimes it takes more than three minutes before the current settles down. This phenomenon, known as current creep, will be discussed in a later section 3.7.5. Our main concern here is to establish a measurement standard of when to record the

current value after switching on the power supply, so that meaningful comparisons among test samples could be made.

The procedure chosen is to record the static voltage-current relation. This involves setting various voltages in succession and recording the initial current flow in each case. The applied voltage is removed as soon as possible after recording the current. Thus the effect of heating due to power dissipation in the test sample is avoided.

3.4.3 AC Impedance Measuremet

The measurement setup is shown in figure 3.15. The heart of the system is a Hewlett Packard Model 4815A rf vector impedance meter, which has an operational frequency range between 0.5 MHz to 108 MHz. This instrument displays the impedance amplitude and phase angle directly. An adaptor is available for connection to a 50 Ohm coaxial connector. A short (10 cm) length of coaxial cable was used to connect the sample to the impedance meter. The cable contacts were soldered onto the sample to minimize capacitance effect.

Tests were carried out to check whether the short piece of cable would cause significant measurement error on the ac impedance of the sample. Measurements of the ac impedance, between 1 MHz and 100 MHz, of a 50 Ohm coaxial load shown that there was no noticeable change in the impedance value; therefore, the short piece of cable would not introduce any significant measurement error.

3.5 Preparation of Test Samples

3.5.1 Types of Samples

During this investigation, three types of samples were used, namely cylindrical, joint and large flat samples (see figure 3.16).

(1) Cylindrical Sample (see figure 3.16a)

The base material is mild carbon steel, grade En3B, of dimensions 8 mm in diameter and approximately 40 mm in length. The ends of the samples were machined flat. This type of sample was mainly used for the testing of the effect of surface corrosion products and some specialised protective coatings.

Before a sample is used in an experiment, the end surfaces of the sample are cleaned using metal cleaning liquid to remove any dirt and greasy. The sample is mounted inside the test jig by placing the sample between the two clamping bolts (see figure 3.9a); then, the clamping bolts are adjusted so that the sample is securely and tightly held between them.

(2) Joint Sample (see figure 3.16b)

This is basically a combination of two modified cylindrical samples. The overall length of the sample is about 30 mm. The overlapping area is about 8 mm by 8 mm. This type of sample was used for testing the generation of intermodulation interference from corroded joints. It is also used for testing protective coatings as well.

Each half of the sample is corroded. When a corroded joint sample is prepared, two of these halves are used, and normally, an uncorroded steel clamping bolt is used to hold them together. It is possible that the steel clamping bolt might bridge the corroded joint and produce a low resistance path for the current flow. Experiment had been performed to see the differences in the intermodulation interference level between a steel clamping bolt and a nylon clamping bolt. The result is shown in figure 6.22 and figure 6.23. It is shown that although the use of steel bolt do reduce the intermodulation level by 10 dB, it does not remove the effect of intermodulation interference. The choice of using steel bolts was taken to simulate the real life case.

Before a sample is used in an experiment, the end surfaces of the sample are cleaned using metal cleaning liquid to remove any dirt and greasy. The method to mount this type of sample is the same as the one for mounting cylindrical samples.

(3) Large Steel Flat Sample and Sample Holder (see figure 3.16c)

At the later stage of this project, an investigation was carried out to evaluate the effect of joint vibration on the intermodulation interference level. Since the above two types of samples are tightly held in position insdie the test jig, the sample is unmovable; it is, therefore, necesarry to use a different sample and sample holder for this particular investigation.

For this purpose, steel flat joint samples were used. A steel flat is about 50 cm long, 5 cm wide, and 3 cm thick. A steel flat joint sample is made up of two steel flats jointed togather by four 5 mm diameter nylon bolts. A bolt hole of diameter 1 cm was drilled at each end of the sample for electrical connection purpose. The overlapping area is about 8 cm by 5 cm.

The sample holder for steel flat joint samples and the way a sample is held is shown in figure 3.16c. The sample holder is basically a large ground plate with a 50-Ohm connector fixed to each end of it. A T-junction connector is attached to each end connector to provide two connections at each end of the sample holder, i.e. for two fundamental signals at one end, and for the linear dummy load and the detector at the other end.

The steel flat junction sample is separated from the sample holder by placing wooden blocks between them. Again, all

electrical contact parts have to be cleaned thoroughly using metal cleaning liquid.

3.5.2 Corrosion Procedure

Two different approaches to corrode samples were used. The first one was electrochemical method, and the second one was immersion in salt solution.

(1) Electrochemical Method

The corrosion setup block diagram is shown in figure 3.17. A potentiostat was used to maintain the precise corrosion potential. The anode was a piece of nickel mesh, and the cathode was the sample to be corroded. The reference electrode was just another piece of steel. The solution was saturated salt solution. A digital voltmeter was connected between the reference and common terminal to monitor the corrosion potential. An air pump was used to keep a good supply of dissolved oxygen in the solution. When all the electrical connections had been made, the corrosion potential was set at +0.6 volts. The pH value of the solution was about 8, i.e. neutral. Under these conditions a layer of Fe_2O_3 would formed on the surface of the sample, as indicated on the Pourbaix diagrams (Pourbaix 1966) for iron. Surfaces for electrical connections were protected by a layer of water insoluble grease. The sample was left in the corrosion bath for 24 hours. After that, it was dried and was ready for use in experiments.

(2) Immersion in Salt SolutionIn this method

Samples were put inside a plastic tube containing saturated salt solution. The samples were left for about ten days which then developed a relative thick layer of rust.
The corrosion products (FeO(OH)) will become loose or detached from the metal surface once they accumulated to certain thickness. When dried, they appear as reddish brown, a characteristic colour of iron (III) oxide. In general the oxide layer is firmly attached onto the base metal and will not come off easily.

3.6 Experiments

3.6.1 Introduction

In a galvanised steel tower structure, the main sources of structural intermodulaiton would come from : (a) ferromagnetic effect of steel; (b) non-linear resistance of corroded junctions and (c) corrosion products on the surface of the base material. In this section, descriptions of various experiments performed to enhance the understanding of structural intermodulation interference phenomena were given. The objectives were to :

(1) Identify the dominant source of SIMI.

(2) Investigate the current/voltage non-linearity of corrosion products of steel and galvanised steel.

(3) Investigate the relationship between dc I/V characteristics of non-linear junctions and their corresponding third order intermodulation product (IMP) level.

(4) Develop a circuit model for a non-linear junction, leading to IMP level predictions.

(5) To determine the intermodulation interference generation mechansim.

3.6.2 Experimental Procedures

Experiments were performed using both cylindrical and joint samples. In the case of corroded joint samples, the halves were corroded individually and then assembled together to form a corroded joint. The ends of all samples were cleaned throughly before each measurement was carried out to ensure good electrical contacts.

3.6.2.1 Dominant Source of Structural Intermodulation Interference

The effect of IMI due to non-linear hystersis in ferromagnetic material was demonstrated by using clean steel rod and clean steel joint samples; while the contribution from surface corrosion products was tested using corroded steel rod samples, with the end contacts remained clean, but

otherwise completely corroded over the surface. Non-linear junction effect was tested using corroded joint samples. Test results are shown in figure 3.18.

3.6.2.2 Current-Voltage Characteristics of Corrosion Products

When galvanised steel is exposed in air, the zinc layer will be attacked possibly by chemical gases, and most certainly will corrode under the effect of moisture and rain. In addition, due to protection effect, zinc would corrode in preference to iron even if the latter is exposed to air due to damage of the outer zinc layer.

In this section the current-voltage characteristics of the corrosion products of both zinc and iron were measured. Any sign of non-linearity would be a positive evidence of the ability of the corrosion products to generate intermodulation products. Typical results for corroded steel samples and corroded hot-dipped galvanised steel samples are shown in figure 3.19 to figure3.21. In addition, the alternative of using rust powder (iron (III) oxide) was also investigated, and the result is shown in figure 3.22.

The IMI levels of the samples were also measured. In Chapter 4, a circuit model of a non-linear joint making use of the measured non-linear current-voltage characteristic of the joint will be developed. IMI level prediction using that model will be performed, and compared with the measured IMI

level of a real sample, so that the accuracy of the model can be assessed.

3.6.2.3 AC Impedance of Corroded Joint Samples

It is well known that due to skin-effect at high frequency, rf current flows only on the surface of a conductor. Hence, the rf resistance of a joint test sample would be different from its resistance at dc. Other factors, such as capacitance would be very important at high frequency, which provides a shunt to the rf current. In particular, this information will be used in Chpater 4 of this report where a model of the non-linear joint is developed. In this experiment, the ac impedance of corroded joint samples, between 1 MHz and 100 MHz, were measured using a Hewlett Packard Model 4815A vector impedance meter. Measurement results are shown in figure 3.23 and figure 3.24.

3.6.2.4 Effect of Oxide Thickness on Intermodulation Interference Levels

In this experiment iron (III) oxide powder was placed at the interface of a clean joint sample in order to determine whether the thickness of oxide affects IMP levels. Oxide powder was used because naturally occurring rust is non-uniform in thickness and shows strong localised corrosion due to pitting, for example. Oxide powder does provide a more uniform contact at the interface of a oxide

and the base metal, hence a more accurate model for investigating the electronic processes at the interface between the two elements. Powder oxide thicknesses of 0.1 mm and 0.5 mm were used.

Test results are shown in figure 3.22 and figure 3.25.

3.7 Results and Discussion

3.7.1 Dominant Source of SIMI

From figure 3.18 it can be seen that clean copper has IMI level of some 15 dB below that of clean steel. It means that IMI due to ferromagnetic non-linearity of steel is quite high (with our sample geometry and input power). In case of cylindrical samples with surface corrosions only, there was an increase of mere 4 dB. The effect is therefore, less significant. By far, the highest increase in IMI level was due to corroded joints, nearly 45 dB.

It was found that even within the same group of samples, the intermodulation level of each individual sample depends largely on the state of corrosion. In general, clean samples (both joint and rod smaples) and corroded suface test samples tend to produce more consistent results within 5 dB. Corroded joint samples could have intermodulation levels between 10 dBm to 55 dBm, depending on the corrosion states of the test sample.

At first sight, it can be seen that ferromagnetic effect could be a significant structural intermodulation interference source, in view of the fact that all towers are constructed with steel. However, in real life, structural intermodulation interference due to this effect would not be too serious, because according to the British Standards BS 5493 (protective coating of iron and steel structures against corrosions) and BS 729 (hot-dipping galvanised coating on iron and steel articles), all structural steels are galvanised to a thickness of at least 0.15 mm with zinc, which is equivalent to nearly 15 skin depth for zinc at 150 MHz (skin-depth of zinc at 150 MHz is about 10 microns). Therefore more than 99% of the induced radio frequency current is carried in the zinc layer. Zinc, being non-ferromagnetic, would not produce any IMI due to that effect.

Indeed, the effects of coating non-ferrous metal over steel samples have been investigated. The results of IMP levels from copper-plated steel samples of various thicknesses are shown in figure 3.26. It is interesting to see that even with about 1m (skin-depth of copper at 150 MHz is about 5m) of coating thickness, the IMP level drops down by more than 10 dB. Larger coating thickness does reduce the IMP level further, howerver, by a lesser amount due to the exponential decay nature of the penetrating rf current.

From above, we can safely assume that provided the Bristish Standards are observed, then the effect of ferromagnetic material on the generation of structural intermodulation

interference is negligible.

Next, we found that surface corrosion products produce much lower (by at least 30 dB) IMI than corroded joints. The reason behind this could be explained by refering to figure 3.27. In the case of corroded rod, since the conductivity of corrosion products are low, then rf current would be pushed back into the bulk of the base metal due to skin effect. The equivalent circuit model has a low resistance (of base metal) in parallel with the large non-linear resistance (of the corrosion products), and more rf current would therefore flow through the linear resistance than the non-linear resistance, hence producing a smaller IMI effect.

In the corroded joint example, there is no alternative low resistance paths for the rf current and all the rf current must flow through the large non-linear resistance, and a high IMI level resulted.

From these experiments, it is found that corroded junctions are the major sources of structural intermodulation interference. Surface corrosions only contribute very little to the resultant intermodulation level due to the by-passing effect of the base metal. Ferromagnetic non-linearity will come into play only if proper procedures for coating and maintaining the strurctures are relaxed.

3.7.2 Current-Voltage Characteristics of Corrosion Products

3.7.2.1 Single-End Corroded Rod Samples

The forward and backward current and voltage characteristics of a typical corroded (one end only, i.e. only one of the two end contact surfaces of a cylindrical sample is corroded, the other one remains uncorroded) steel rod sample and corroded (one end only) galvanised steel rod sample are shown in figure 3.19 and figure 3.20. Note the scale of current flow in each case. From the figures 3.19 and 3.20, it can be seen that there are distinct regions of forward bias and reverse bias. For example, with the corroded galvanised steel sample (which is mainly zinc oxide), the forward resistance at 6 V is about 150 Ohm and at -6 V the reverse resistance is about 2,400 Ohm, sixteen times larger than the forward value. For corroded steel sample, the reverse resistance is nearly 12,000 Ohm. Reverse breakdown occuried at about -20 V for corroded galvanised steel sample; and was higher than -25 V for the corroded steel sample, because of its much higher reverse resistance. However, it cannot be overemphasised that these measurement values are specific to particular samples, and different samples would have different parameter values depending very much on their state of corrosion. But, the general characteristics of corrosion products, i.e. exhibit forward bias and reverse bias regions, are common to all samples.

It might be a suprise to find that the forward and reverse

characteristics are not symmetrical about the origin, given that the contact electrode and the base metal for the oxide are of the same material and dimensions. This might well be due to the fact that the oxide products attach more firmly onto the base metal, and therefore, make larger and better contacts between them and the base metal, thus carrying the total current over a large area, and a small contact voltage results. So, even though the contact is non-linear, the small contact voltage would ensure this contact operates in the relatively linear region of the non-linear characteristic. On the other hand, the contacts between the oxide products and the electrode is less likely to be firm, and most probably, are point contacts. As a result, the total area carrying the current is much smaller than in the previous case, and a high contact voltage results which would drive the contact into the highly non-linear high voltage range. It must be stressed that the contact between oxide products and the base metal is not 'Ohmic', but 'very low non-linear resistance'. In any event, when a series resistance is very small, the question of whether it is linear or non-linear is unimportant in most practical contexts.

Refering to section 3.3.2, the sense of forward bias and reverse bias shown in these figures, strongly indicates that the corrosion products behave like p-type semiconductors. This matches the results by Rao (1974), who found that ferrous oxide samples are of p-type semiconduction as well. The important point is that, metal-metal oxide contacts do have non-linear current-voltage characteristics, and as

such, would generate harmonics and intermodulation products when illuminated by multiple frequencies.

3.7.2.2 Corroded Joint Samples and Oxide Powder-Filled Joint Samples

From figure 3.21 to figure 3.22, it can be seen that naturally occured corrosion products of iron have a relatively large non-linear current-voltage characteristics; but chemical fine oxide powder of iron (III) oxide produces very mild non-linearity only. Overall speaking, the severity of non-linearity is not very large, especially in the low voltage range, and the non-linearity can be described as a 'weak' effect. For the corroded joint samples, mild non-linearity exists in the applied voltage range of 15 V (see figure 3.21). Above that range, non-linearity increases until oxide film breaks down, which is normally greater than 30 V for our test samples. Assuming the oxide thickness is about 0.1 mm, then the electric field strength could be as high as 300 kVm. In contrast, for iron(III) oxide powder, mild non-linearity was observed for the whole range of 30 V (see figure 3.22), and no breakdown effect was noticed. The characteristic is nearly symmetrical about the origin, and is quite different from the results for corroded rods.

When compared with the current-voltage characteristics of a semiconductor diode (see figures 3.27 and 3.28), there is no distinct ''cut-in'' voltage for the corroded (mainly iron (III) oxide) samples; while diode shows a well-defined

''cut-in'' voltage of about 0.6 V. It is interesting to note that carefully prepared thin-film aluminium-aluminium oxide-aluminium junctions do show a ''cut-in'' voltage between 0.05 V to 0.2 V (e.g. see Fisher and Glaeva 1961). Naturally occured aluminium-aluminium oxide-aluminium junctions, however, do not show such characteristics (e.g. see Higa 1975).

From the graphs, the mean resistance of iron (III) oxide powder is about 8 to 9 MOhm; for single-end corroded samples it is about 200 Ohm; for single-end corroded galvanised samples, the mean resistance is about 230 Ohm; while it is about 30 Ohm for a diode at a forward voltage of about 0.8 V.

It can be seen that non-linearities due to naturally occured metal-oxide-metal junctions are much weaker than specially fabricated devices, such as a semiconductor diode. This was further supported by a field experiment (see figure 3.22a) that in a 50 watt two-tone test, a corroded joint sample was placed across the terminal of a folded dipole and there was not any noticeable IMI level produced (test receiver floor level was set at -70 dBm). However, when a diode was connected across the terminal of the antenna, this time a very large IMI level was recorded, nearly up to 10 dBm. Therefore, a natural metal-oxide-metal junction is not a good mixer at all.

It is also interesting to note that the non-linearities shown by corroded joint samples are more symmetrical about

the origin than the single-end corroded samples. Presumably the corroded joint sample ressembles the arrangement of two back-to-back diodes in parallel; whereas the single-end corroded sample behaves like a single diode.

In this series of experiments the relationship between third order intermodulation product level and the input power is somewhere between 2 and 3 dB/dB. Therefore, the third order intermodulation product power does not increase as fast as the theory predicted. A typical relationship between the third order intermodulation interference level and the applied power is shown in figure 3.22b.

3.7.3 AC Impedance of Corroded Joint Sample

From figure 3.23, the ac impedance of a typical joint sample decreases as the applied frequency increases, showing a strong junction capacitance effect. The joint capacitance against applied frequency is shown in figure 3.24, and the capacitance value was found to vary between 18.8 pF and 23.2 pF. At higher frequencies the capacitance increases further, implying a further decrease in the capacitvie reactance. The variations of the capacitance value are between 3% to 11%, which is relatively small compared to the span of the applied frequency range from 1 MHz to 100 MHz. The capacitance variation could also originate from the contacts between the ends of the connection cable and the sample as well.

From the experimental results, it is shown that the capacitance of a corroded joint is constant over a wide frequency range, and therefore, provide a constant capacitive reactance over such wide range of frequencies. This information is used in Chapter 4 of this report to develope a model for a non-linear junction.

3.7.4 The Effect of Oxide Thickness

Figures 3.22 and 3.25 show the typical current-voltage characteristics of iron (III) oxide powder layer of thicknesses 0.1 mm and 0.5 mm respectively. The nominal resistance of the former is about 8.5 MΩ, and is around 9.5 MΩ for the latter. It can be seen that the observed non-linearity did not change (i.e. the shape of the characteristic) except that the linear resistance increased by about 1 MΩ . This shows that the non-linear current-voltage characteristic of a corroded joint sample is a 'contact' effect, rather than a 'bulk' effect within the oxide. Thus, we were able to show that, firstly, electron tunneling is not responsible for the observed current-voltage non-linearity in corroded contacts, because the oxide layer thickness (>> 100 Å) is too large for electron to tunnel through; and secondly, metal-semiconductor contact rectification is the underlying mechansim responsible for the intermodulation interference.

3.7.5 A Brief Note on Current Creep

Current creeping is used to describe the phenomenon which is observed when a constant voltage is applied to a rectifier, the current flow is not constant but is a function of time. An increase of current with time is called positive creep; and a decrease of current with time is called negative creep (see figure 3.29). Normally, both positive and negative creeps are present, but the dominance of either type of creeping depends very much on the oxide parameters, as well as the speed of the corresponding processes. In figure 3.29 the resultant curve shows an initial postive creep and then followed by a longer period of negative creep. The time for the current to settle could be as long as thirty minutes.

In section 3.3.2, it was shown that the corrosion products behave as semiconductors, and the rectification effect at a corroded joint is very similar to a metal-semiconductor rectifier. The current creep phenomenon can then be explained in terms of ionic processes at the metal-semiconductor contact. When a metal electrode and a p-type semiconductor is in contact, but without external power supply, a potential barrier will form after some re-distribution of electrons within the system. What happened is that, at the beginning, electrons move from the metal electrode towards the semiconductor and recombine with the ferrous ion centres; leaving the semiconductor with net negative charges (from oxide ions). All the time there are negative charges building up inside the semiconductor. As more electrons flood in from the metal electrode, there

comes a stage when the electric field is so strong that the incoming electrons rebound backwards to the metal electrode, and a steady state is reached. When the junction is reverse biased, i.e. metal electrode is at a negative potential with respect to the p-type semiconductor, the electric field is so strong that the positively charged ferrous ions tend to move towards the metal electrode. When this happens, they wil cause a non-uniform distribution of charges within the oxide, and the Schottky barrier width within the oxide diminishes as well; which increases the probability of electron tunneling to occur, hence, an increase in initial current flow.

3.8 Conclusion

In this chapter, we have demonstrated that the presence of corrosion products is an essential element of intermodulaiton interference generation. It was found that corrosion products exhibit non-linear current-voltage characteristics; and as such, are able to generate intermodulation products, just like a mixer. Furthermore, it was shown that in the case of steel structures, metal-semiconductor rectifying contact is the underlying mechanism responsible for the observed non-linear current-voltage relationship, rather than electron tunneling. Experimental results also supported that corroded metallic junction is a first order factor which determines the severity of intermodulation interference effect; corrosion products on a metallic surface contributes

relatively very little to the observed intermodulation interference level.

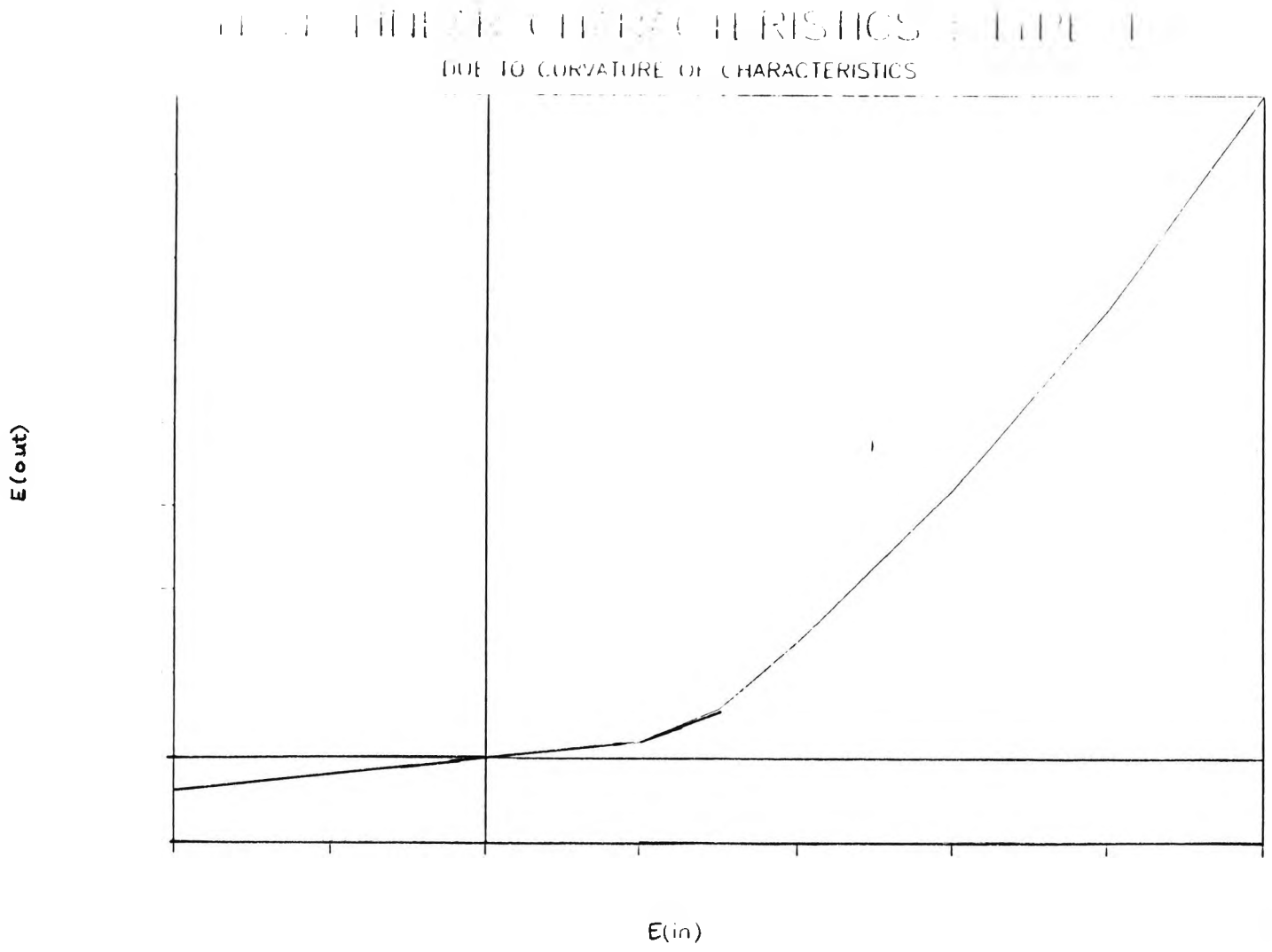

FIGURE 3.1 Small signal input/output non-linearity

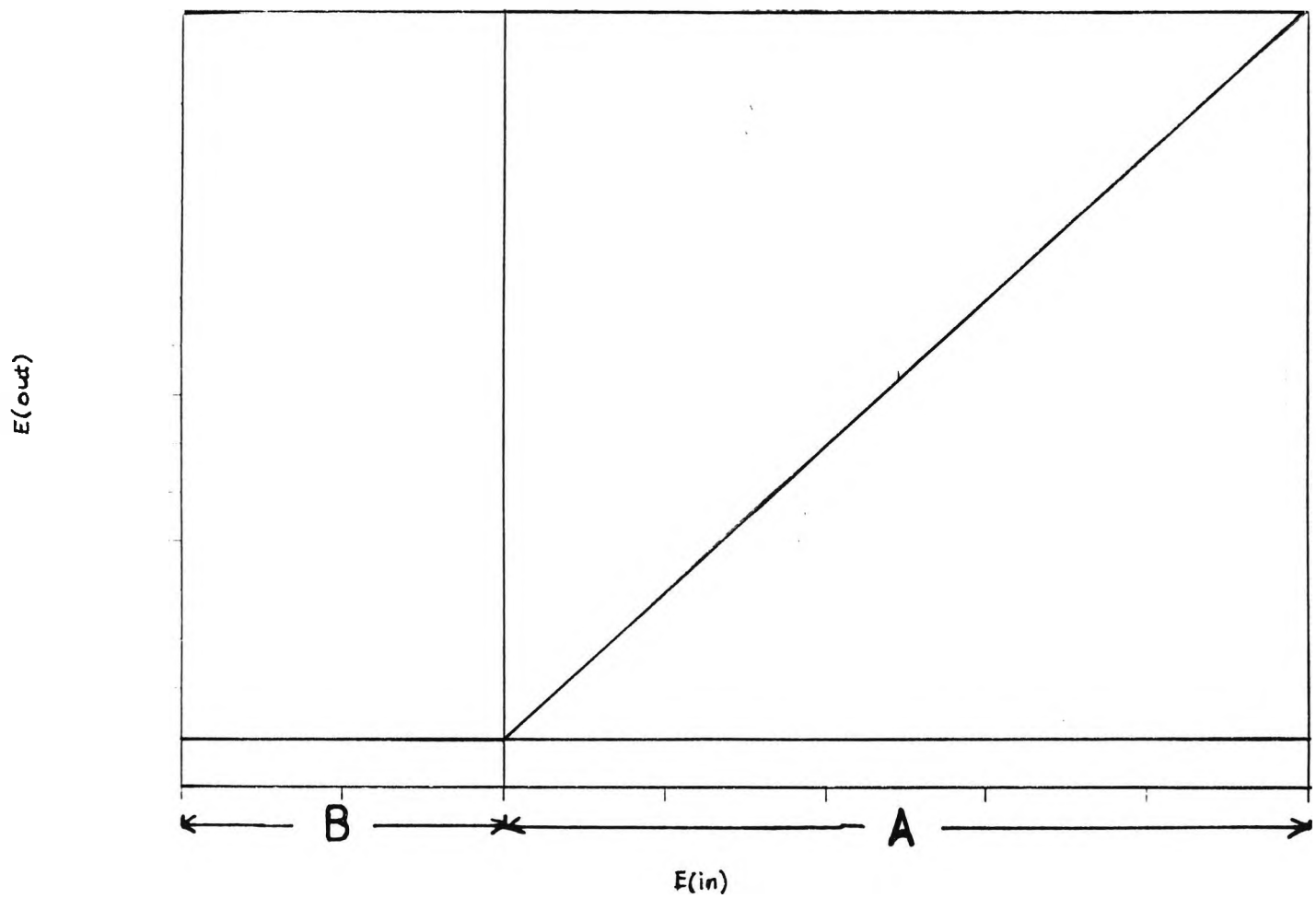

FIGURE 3.2 **Large signal input/output non-linearity**

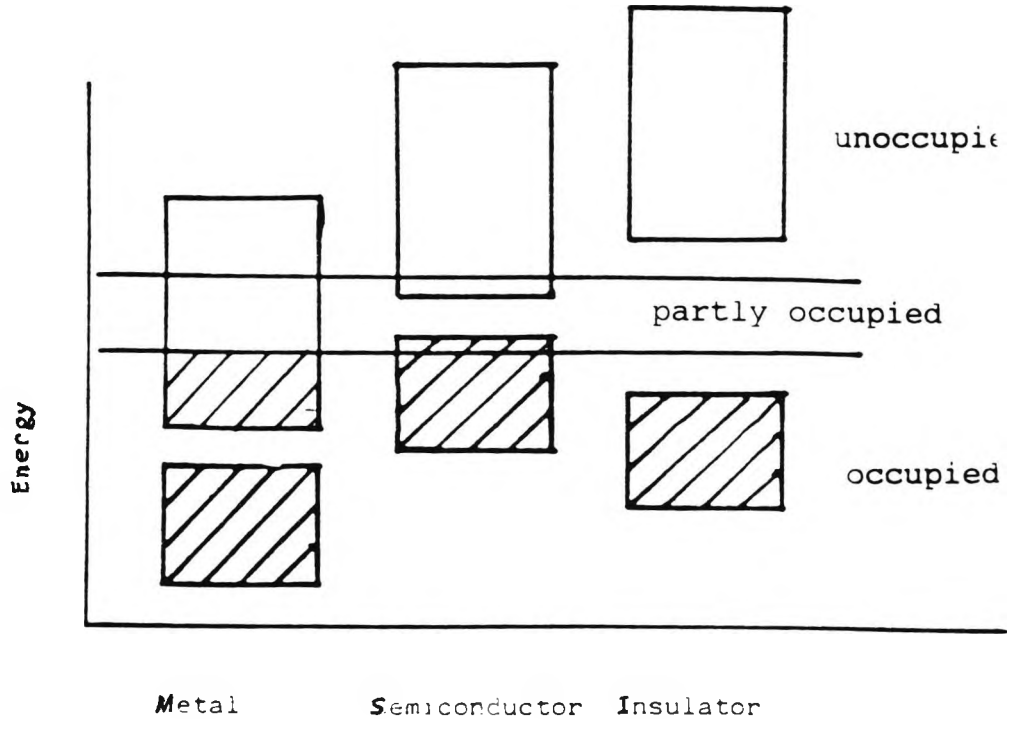

FIGURE 3.3 Energy band structures for metal, semiconductor and insulator

A = metal ion B = non-metal ion

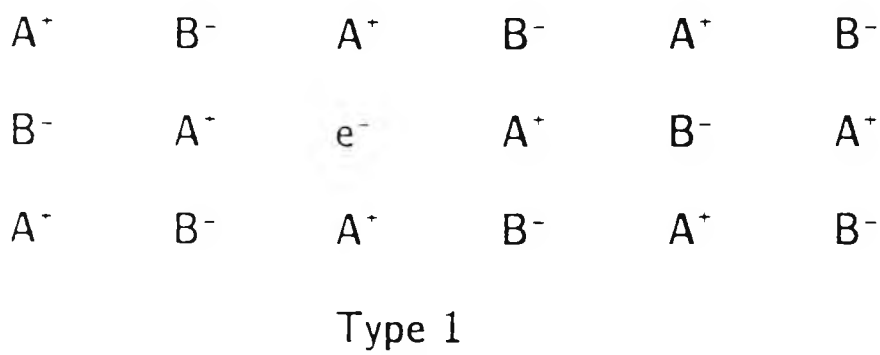

Type 1

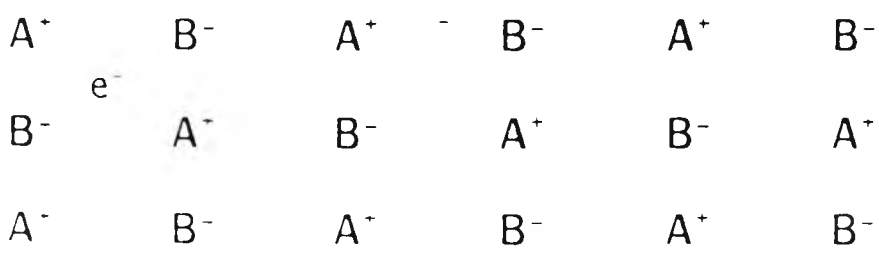

Type 2

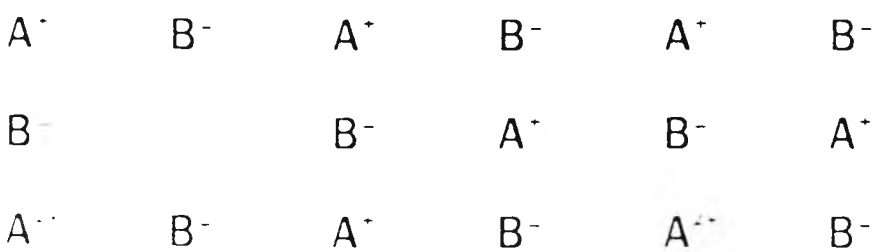

Type 3

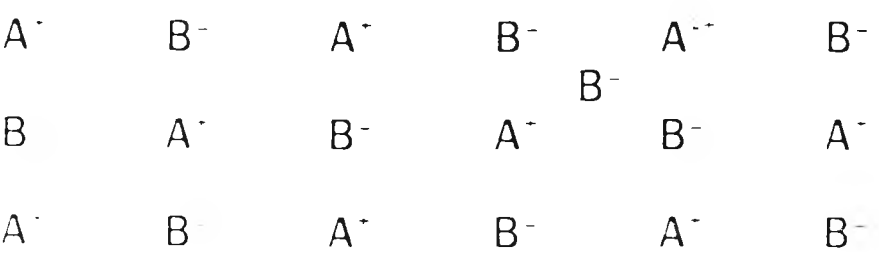

Type 4

FIGURE 3.4 Four types of physical defect in transition metal oxide

O^{2-}	Ni^{2+}	O^{2-}	Ni^{3+}
Ni^{2+}	O^{2-}		O^{2-}
O^{2-}	Ni^{3+}	O^{2-}	Ni^{2+}

Effect of a Ni vacancy in NiO

Ti^{4+}	O^{2-}	Ti^{4+}	O^{2-}
O^{2-}		O^{2-}	
Ti^{4+}	O^{2-}	Ti^{4+}	O^{2-}
O^{2-}		O^{2-}	
Ti^{4+}	O^{2-}	Ti^{4+}	O^{2-}

Effect of a Ti interstitial in TiO_2

FIGURE 3.5 NiO and TiO_2 showing crystal defects

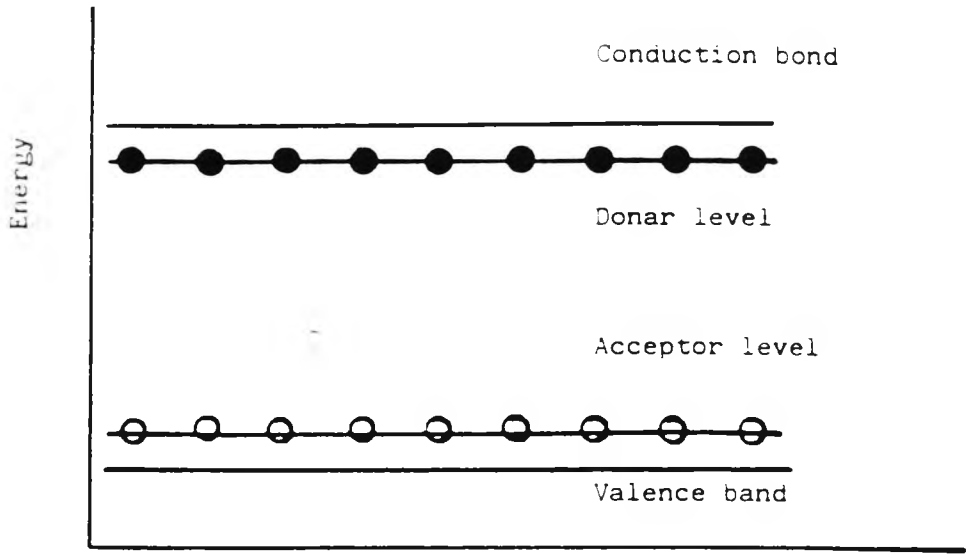

FIGURE 3.6 Band energy diagram for impure semiconductor

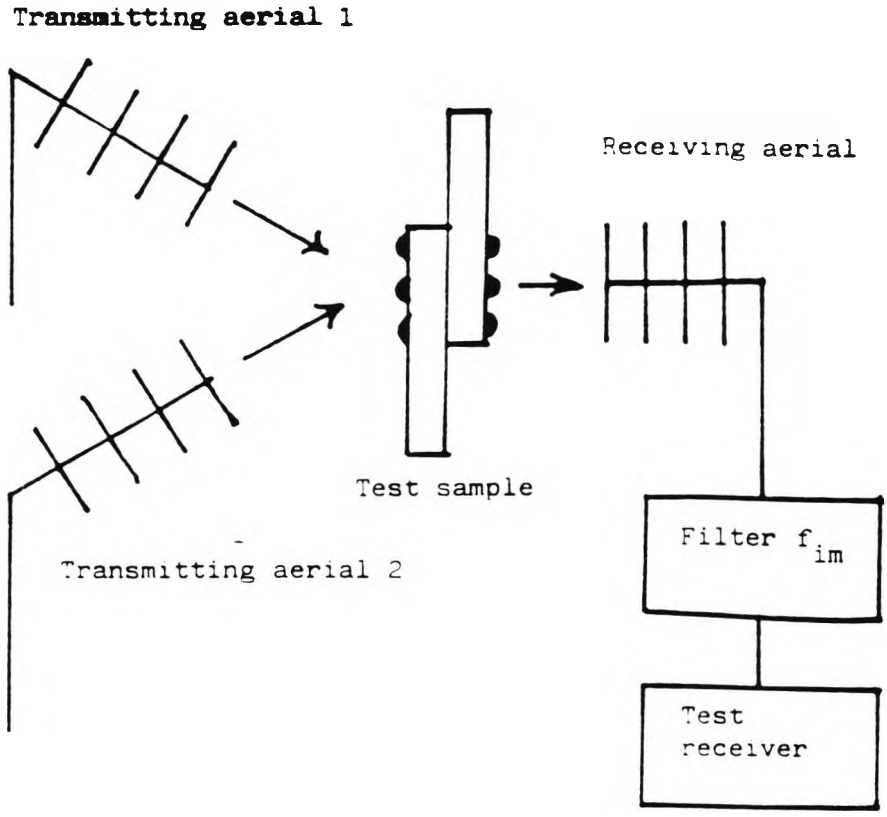

FIGURE 3.7a Radiative testing

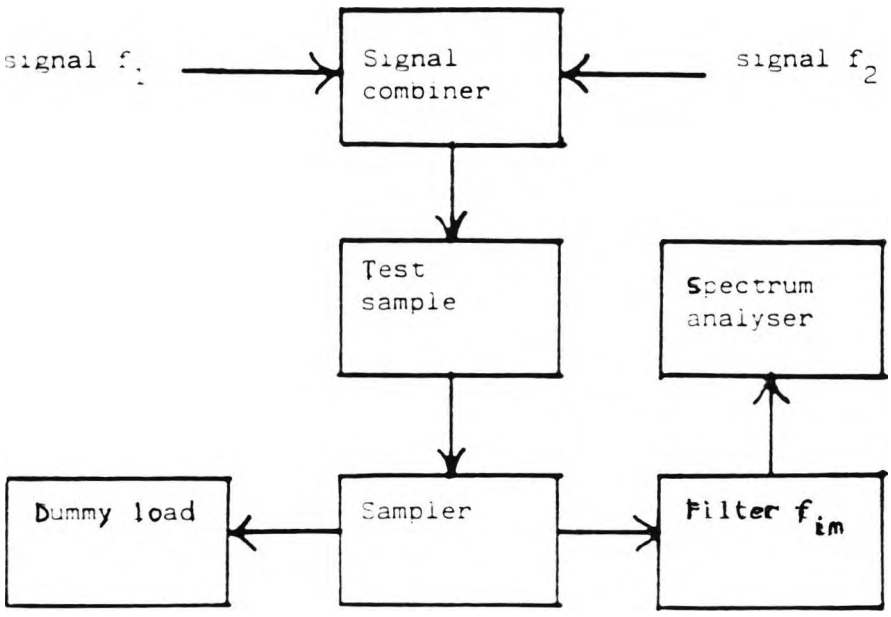

FIGURE 3.7b Conductive testing

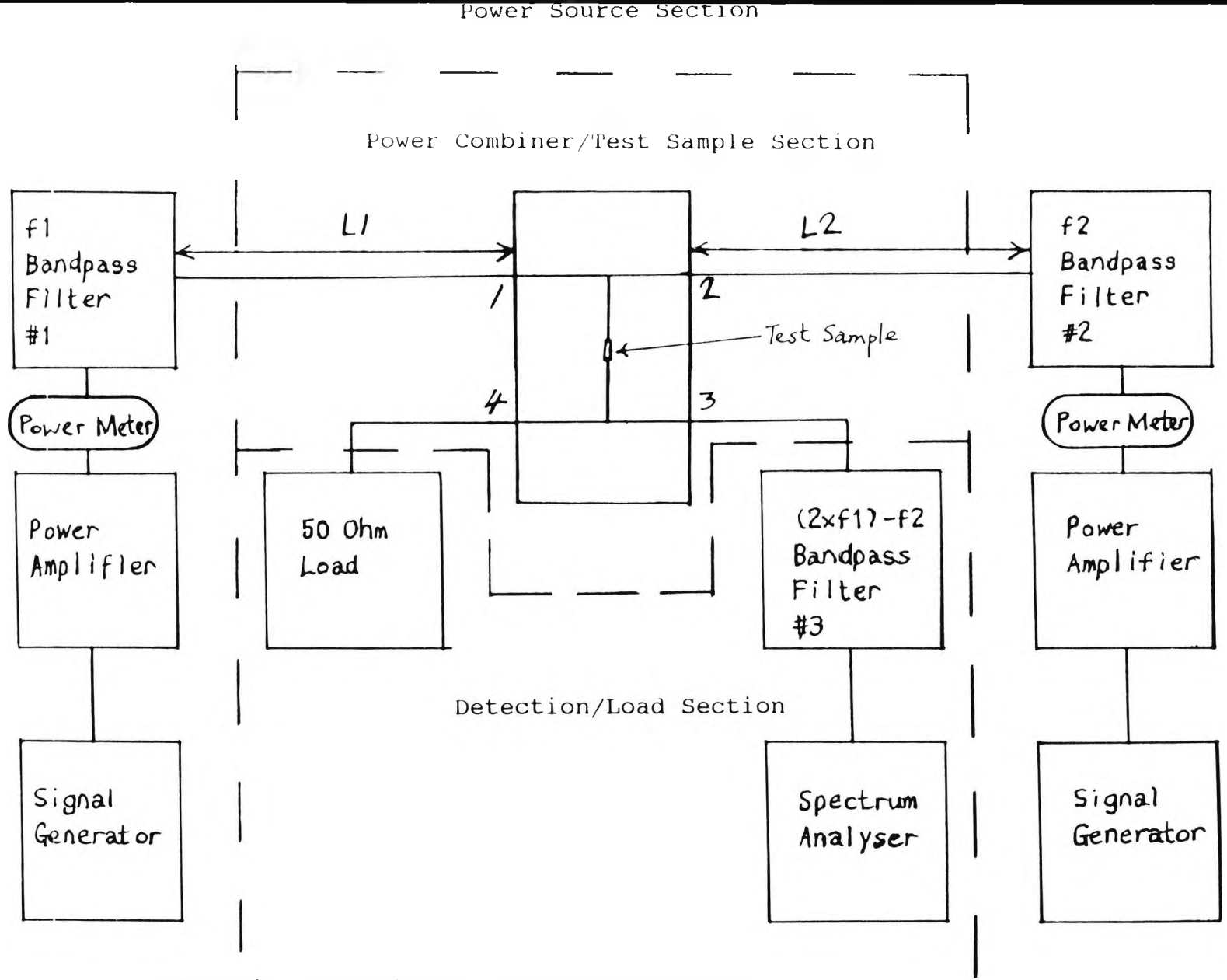

FIGURE 3.8 Block diagram of PIMP testing system

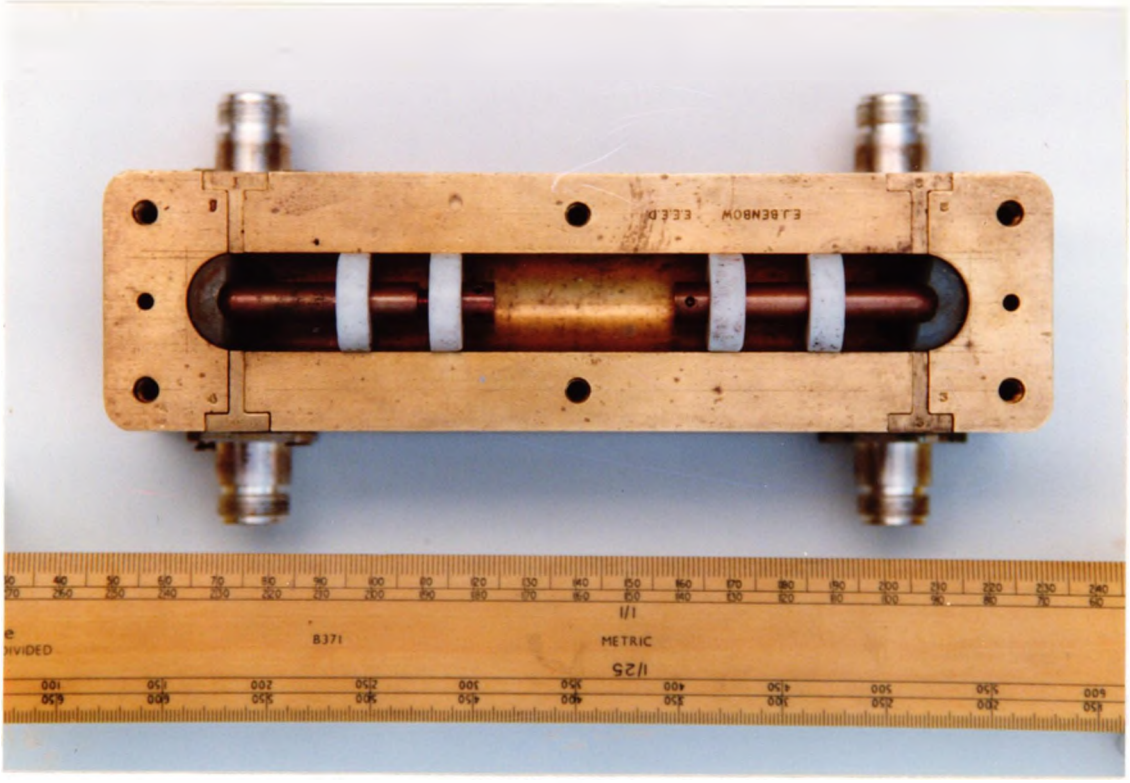

FIGURE 3.9a TOP VIEW OF THE TEST JIG

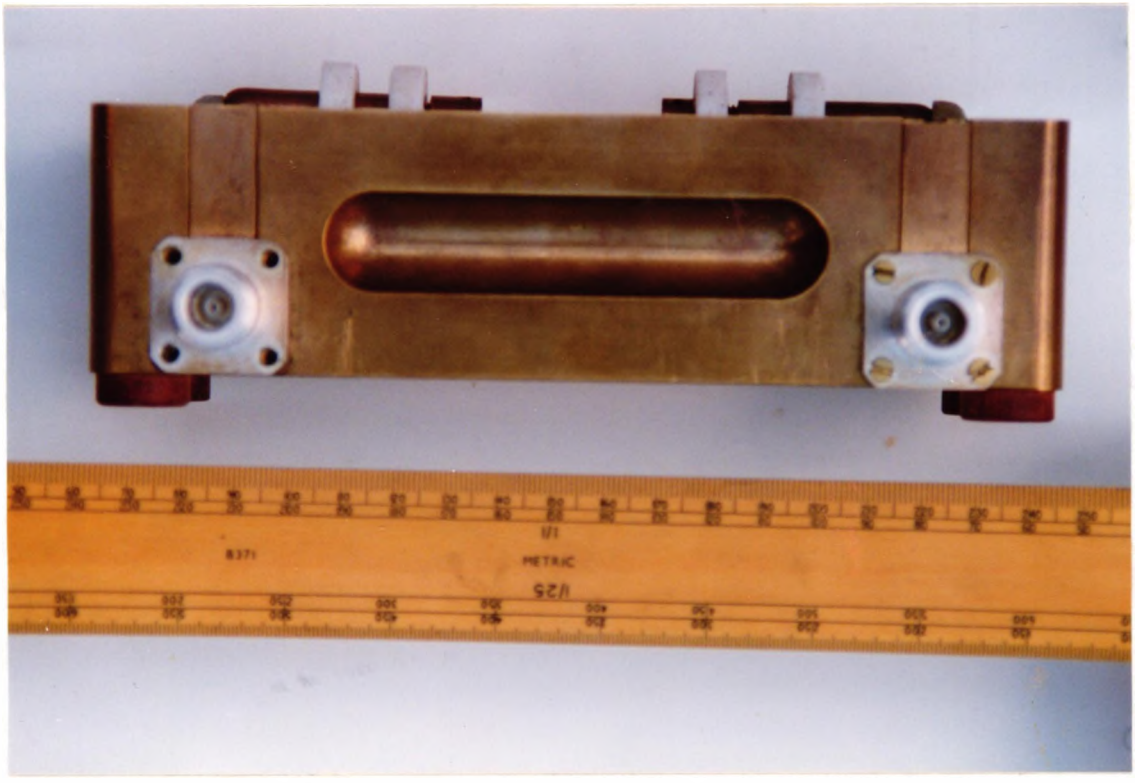

FIGURE 3.9b SIDE VIEW OF THE TEST JIG

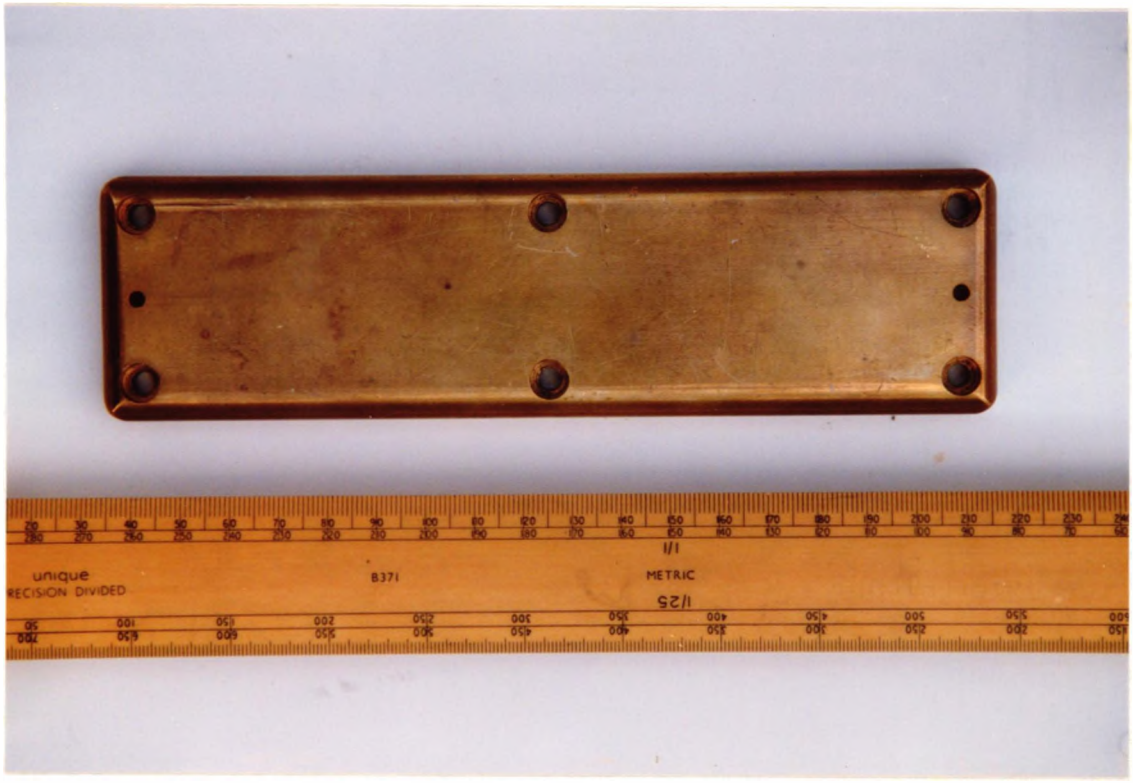

FIGURE 3.9c TOP VIEW OF THE LID OF THE TEST JIG

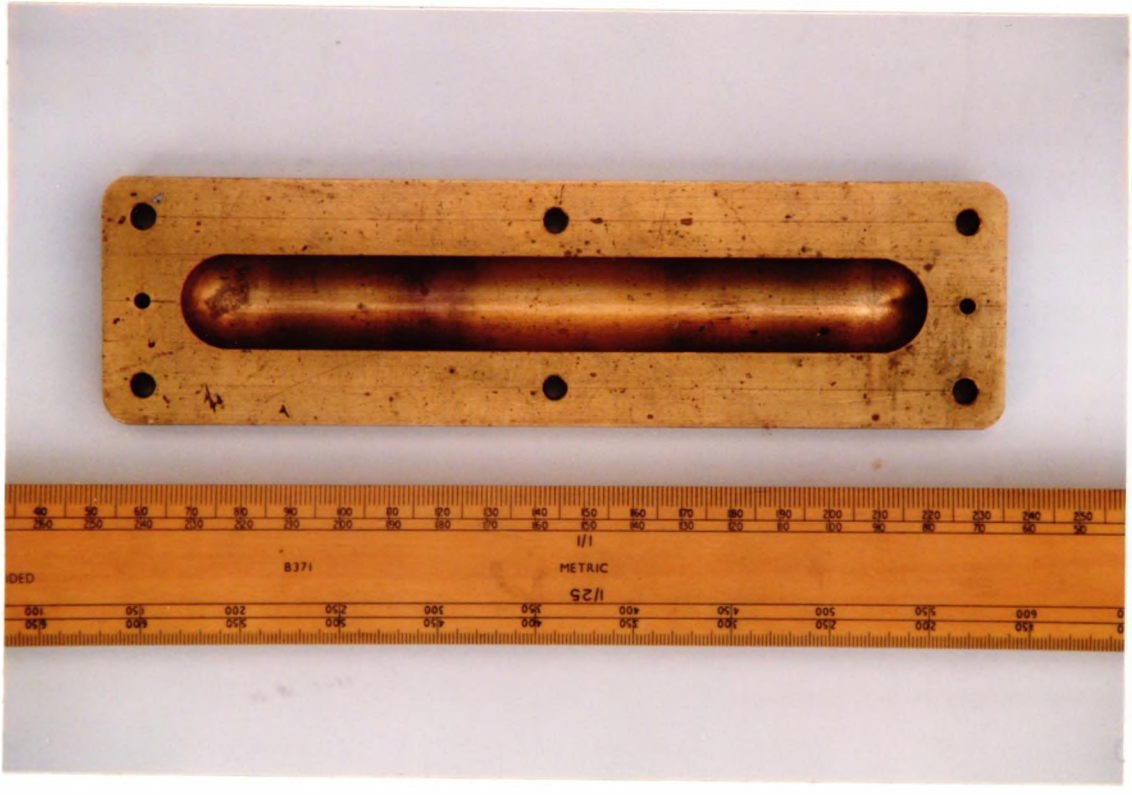

FIGURE 3.0d INSIDE VIEW OF THE LID OF THE TEST LID

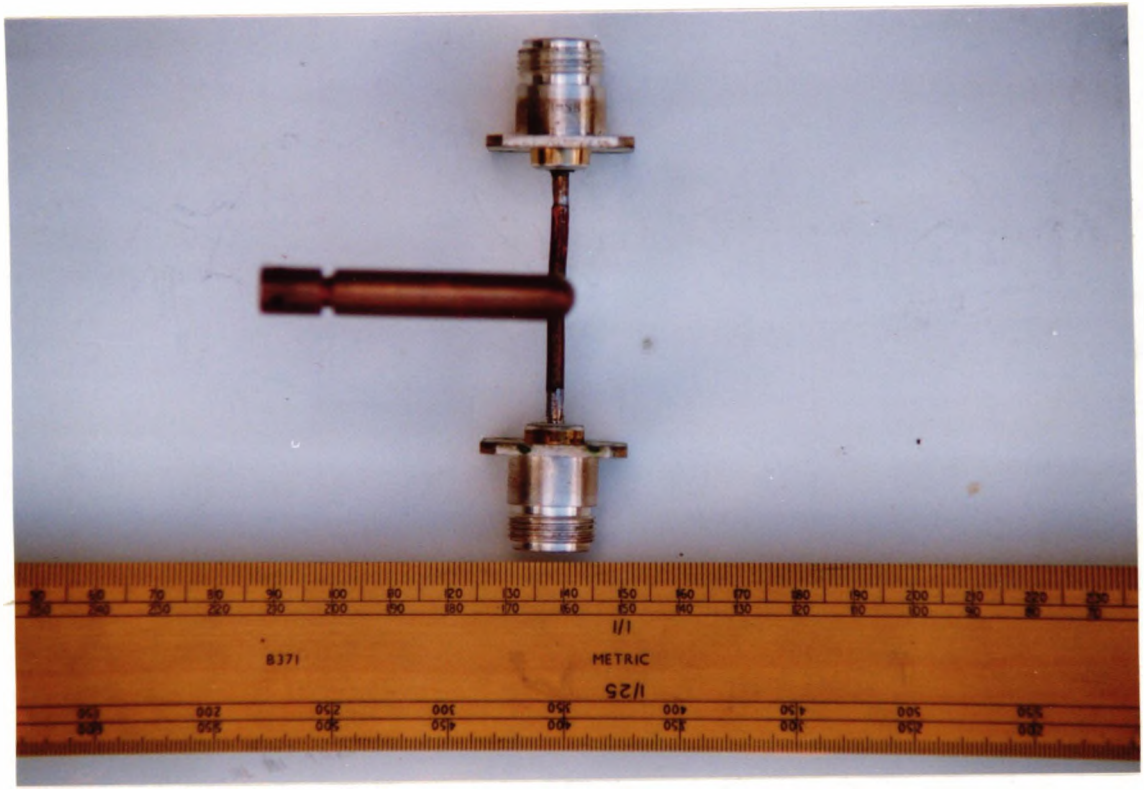

FIGURE 3.9e TOP VIEW OF A T-PIECE (POWER COMBINER)
NOTE THE N-TYPE CONNECTORS ARE SOLDERED ONTO THE T-PIECE

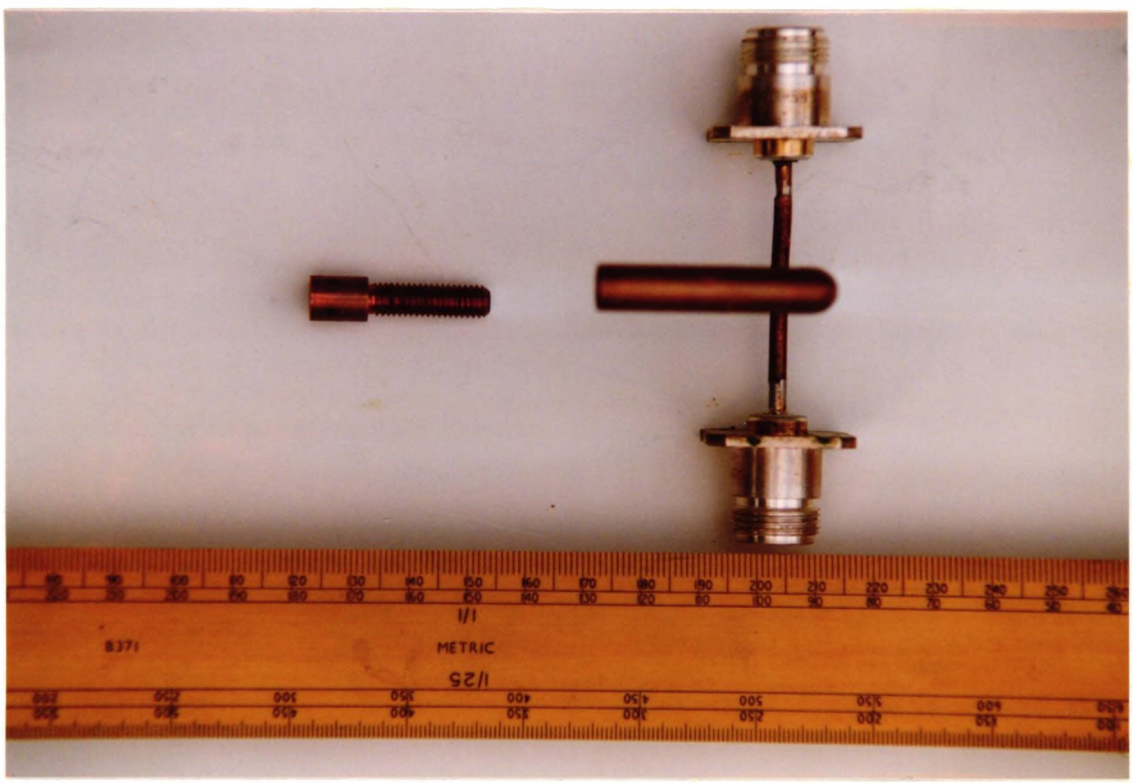

FIGURE 3.9f TOP VIEW OF THE T-PIECE (POWER COMBINER) AND THE SAMPLE CLAMPING BOLT

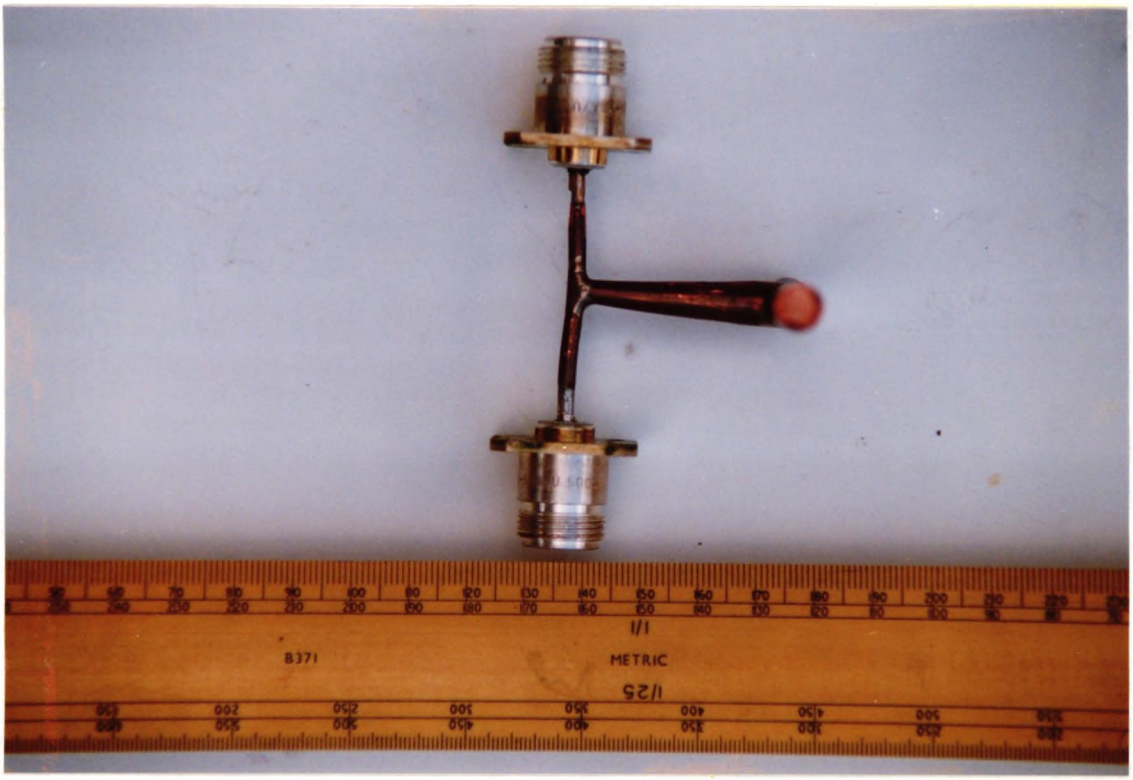

FIGURE 3.9g FRONT VIEW OF THE T-PIECE (POWER COMBINER)

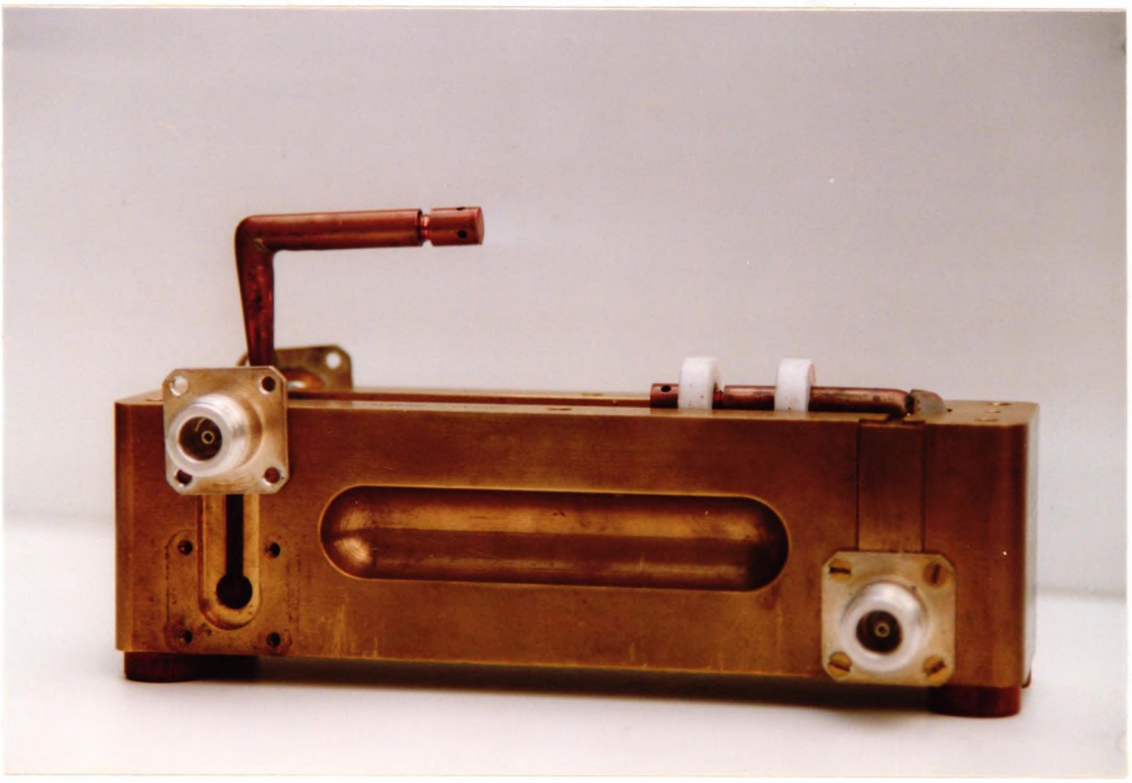

FIGURE 3.9h INSERTION OF THE T-PIECE (POWER COMBINER) INTO THE TEST JIG

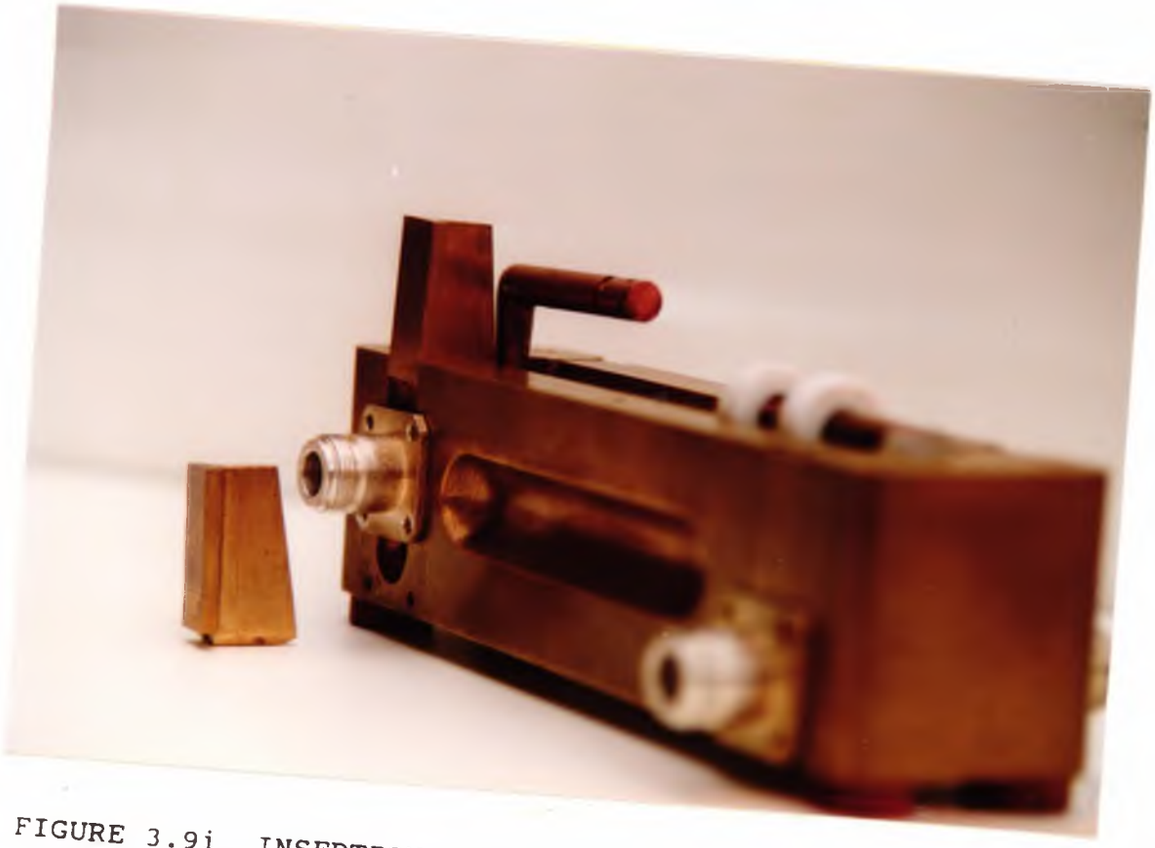

FIGURE 3.9i INSERTION OF THE METAL PIECE

FIGURE 3.9j FRONT VIEW AND SIDE VIEW OF THE METAL PIECE

FIGURE 3.9k SIDE VIEW OF THE TEST JIG WITH THE LID IN PLACE

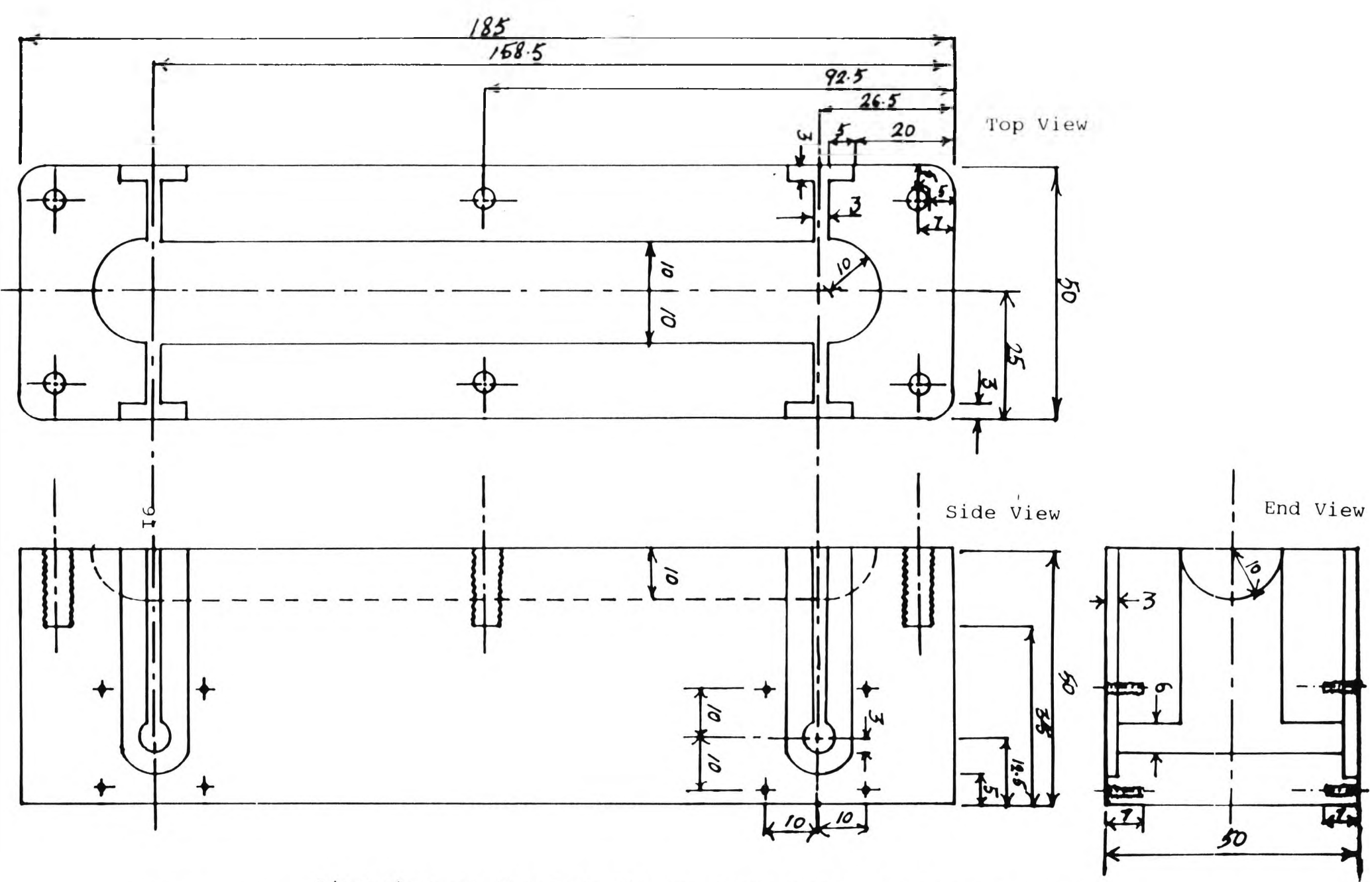

FIGURE 3.10a Dimensions of the Test Jig for Cylindrical and Joint Samples

(All Measurements are in mm)

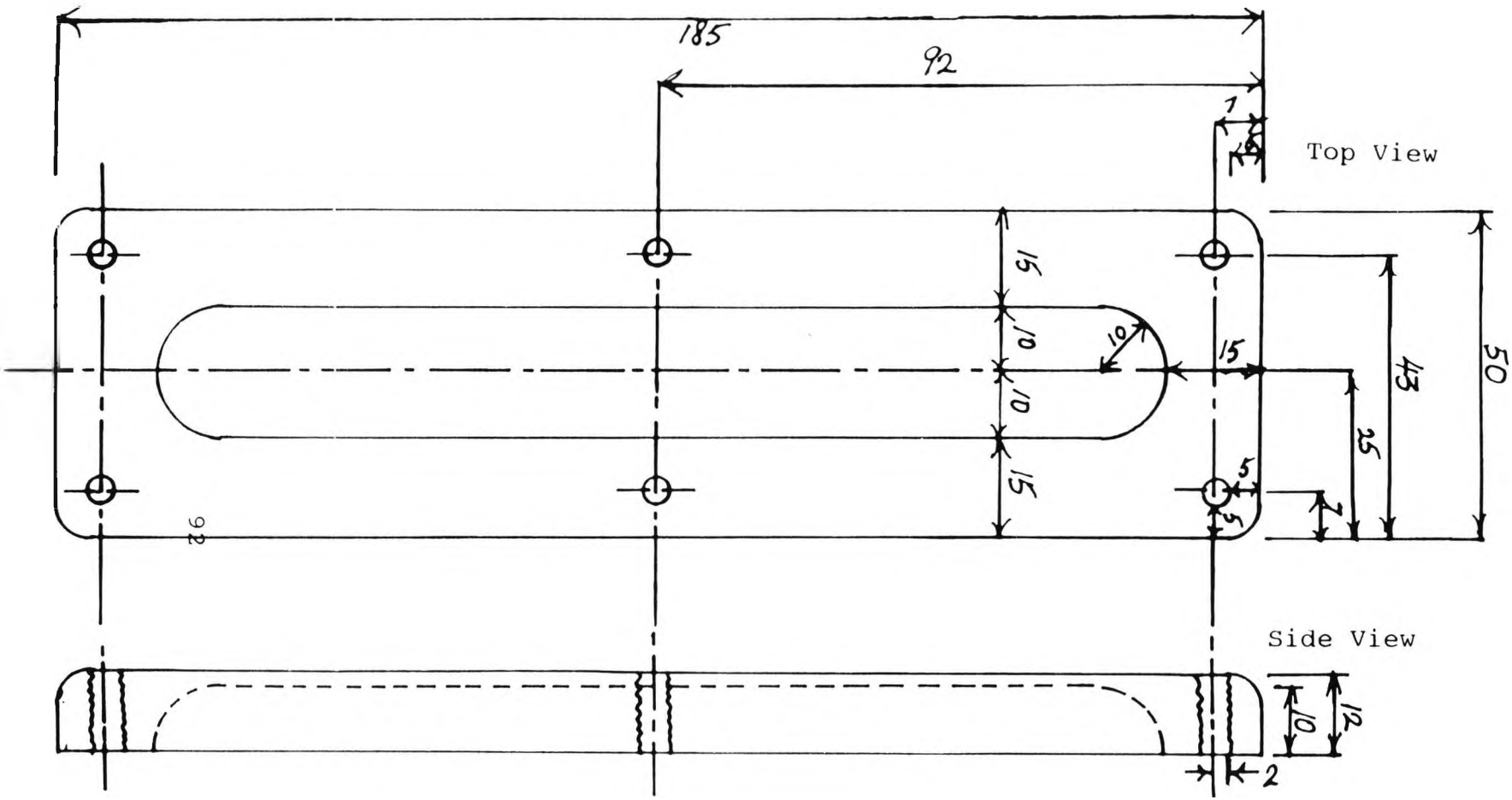

FIGURE 3.10b Dimension of the Lid of the Test Jig

(All measurements are in mm)

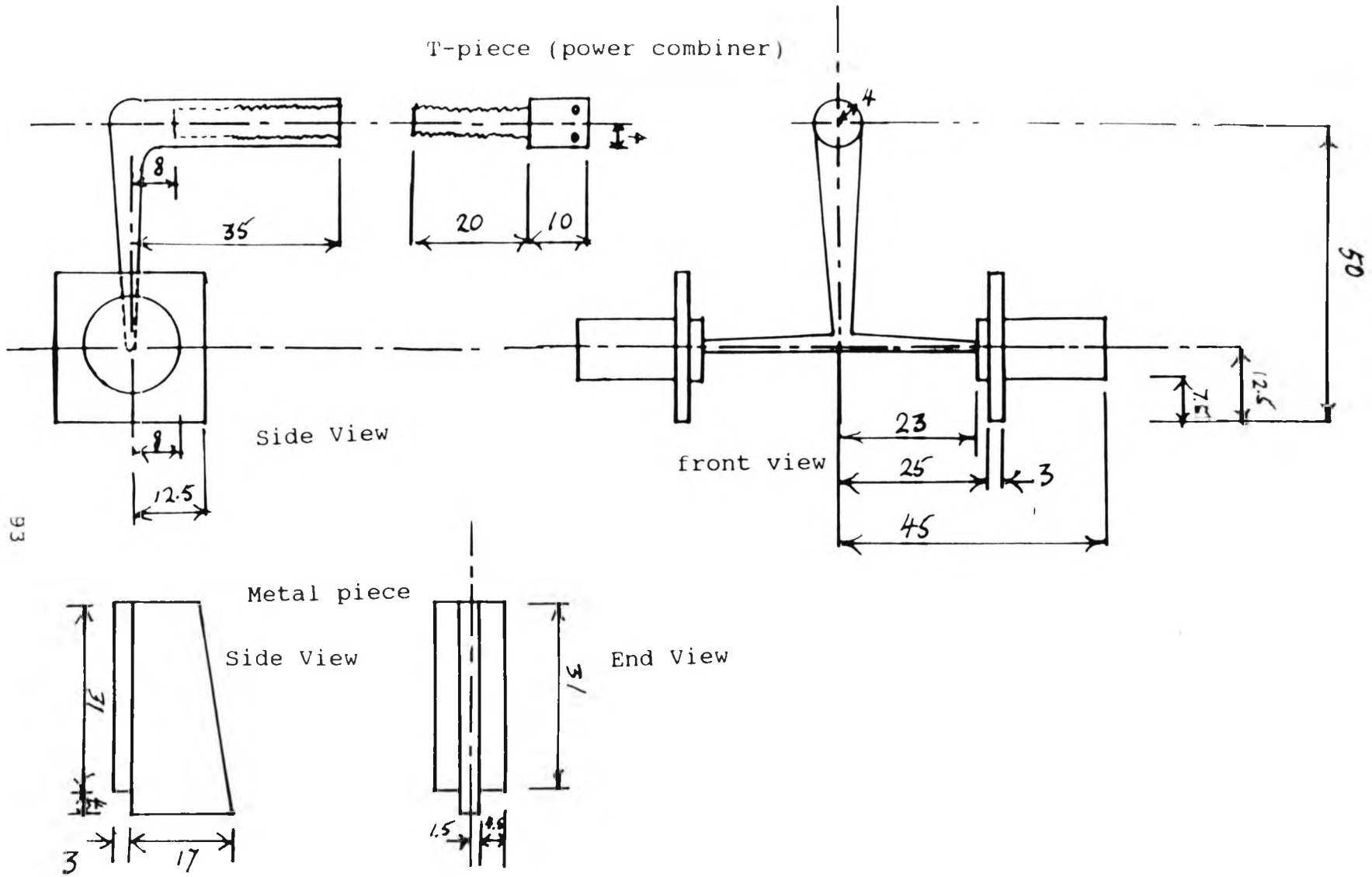

FIGURE 3.10c Dimensions of a T-piece and an associated metal piece

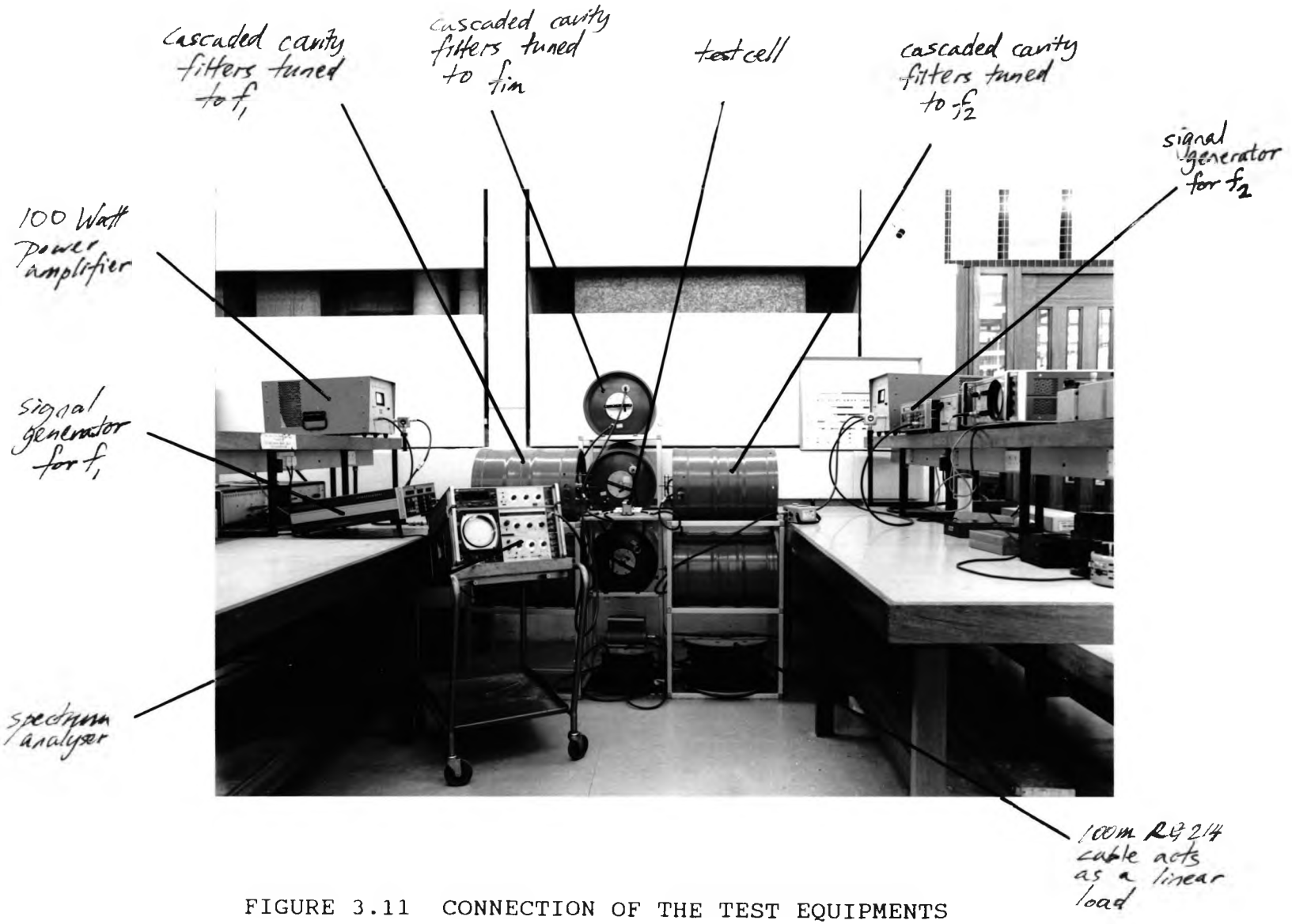

FIGURE 3.11 CONNECTION OF THE TEST EQUIPMENTS

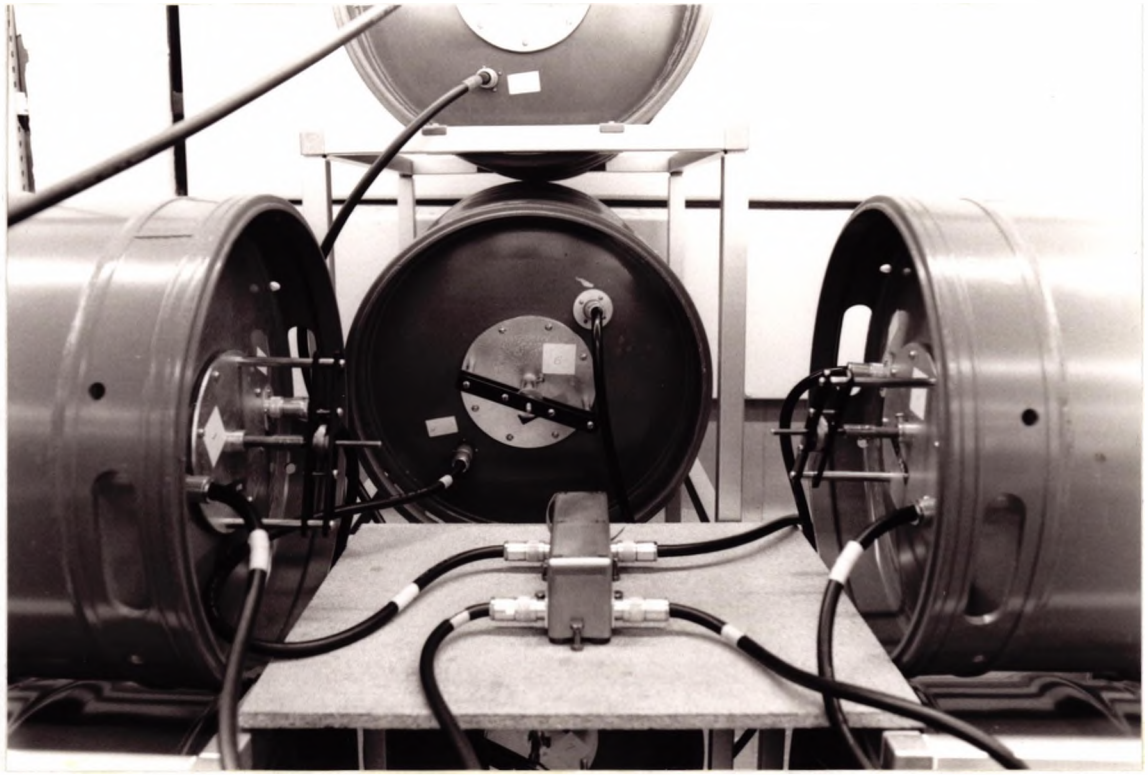

FIGURE 3.12 A CLOSE-UP VIEW OF THE TEST JIG CONNECTIONS

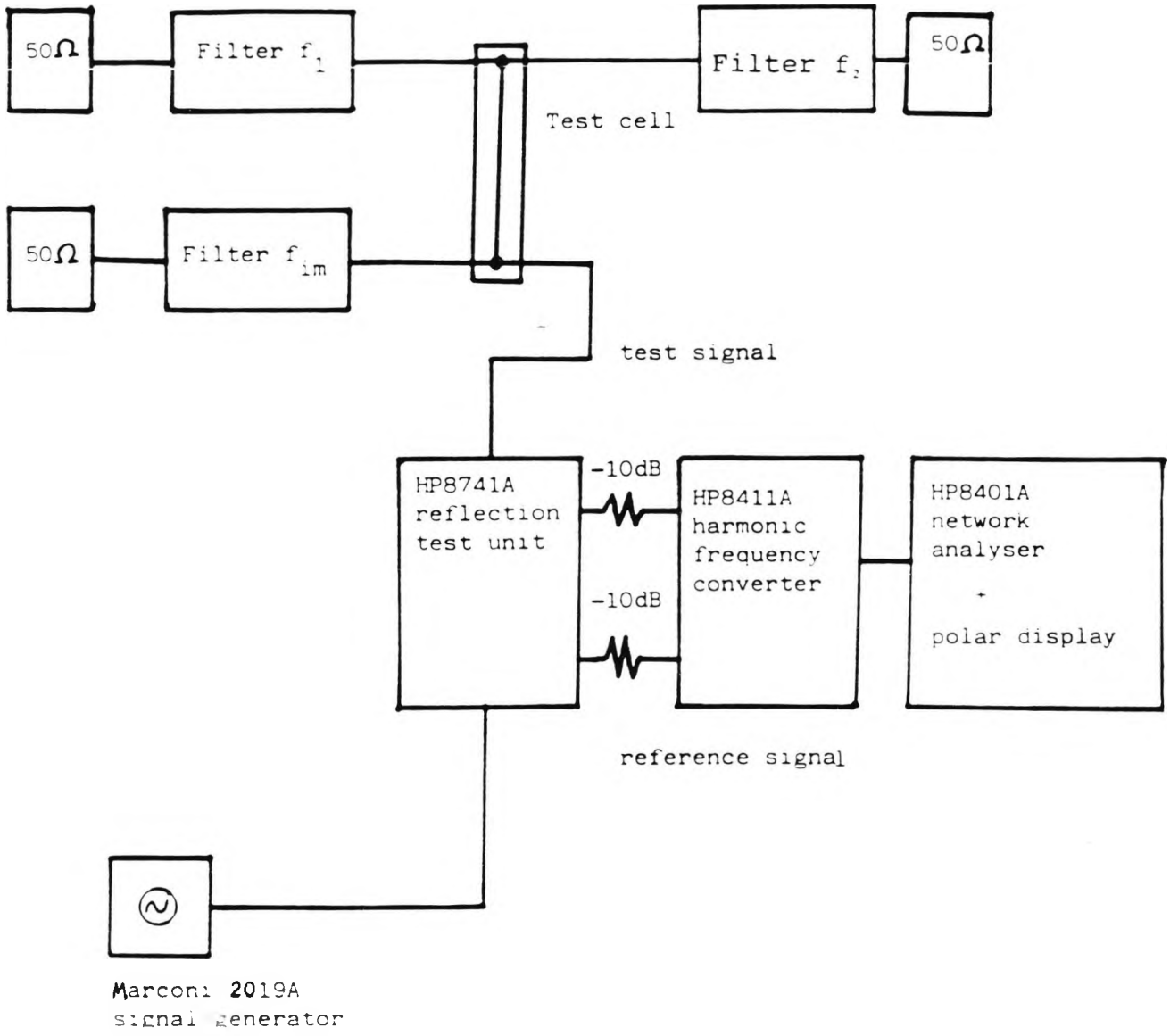

FIGURE 3.13 VSWR measurement setup for the PIMP measurement system

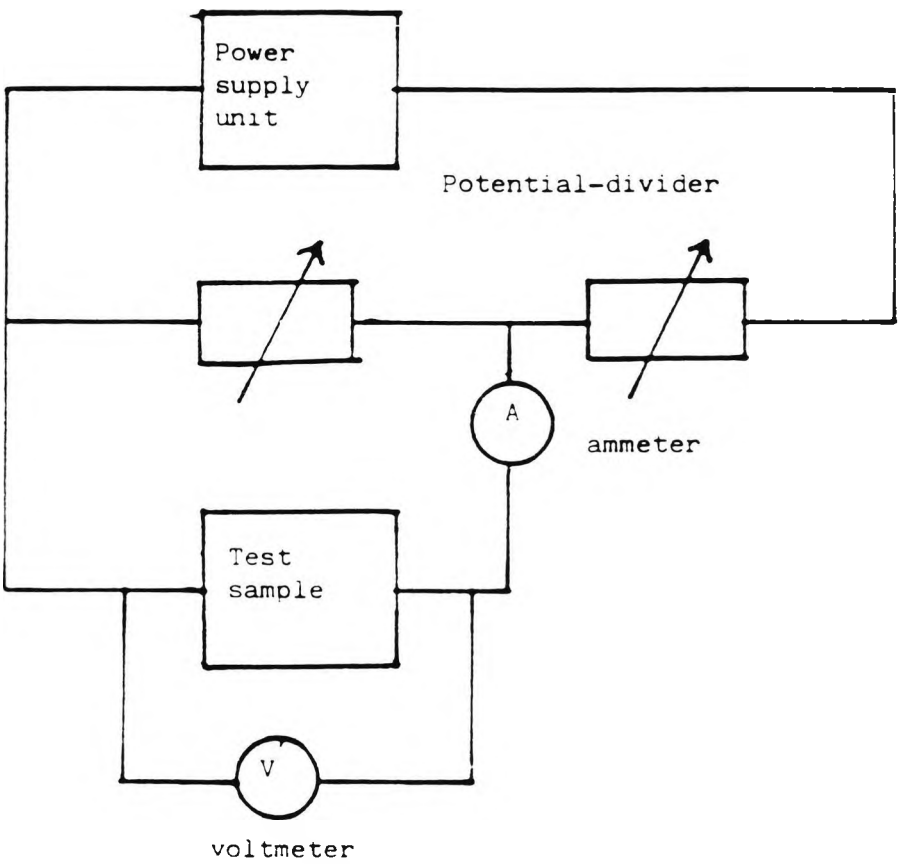

FIGURE 3.14 DC current-voltage characteristic measurement for test sample

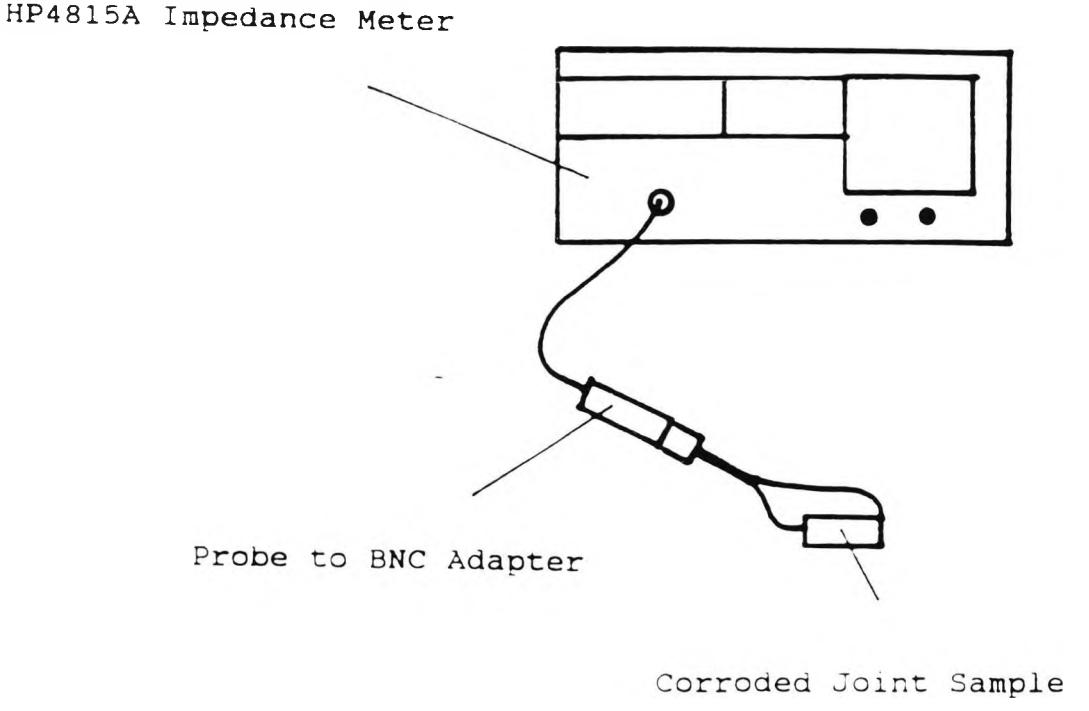

FIGURE 3.15 AC impedance measurement for test sample

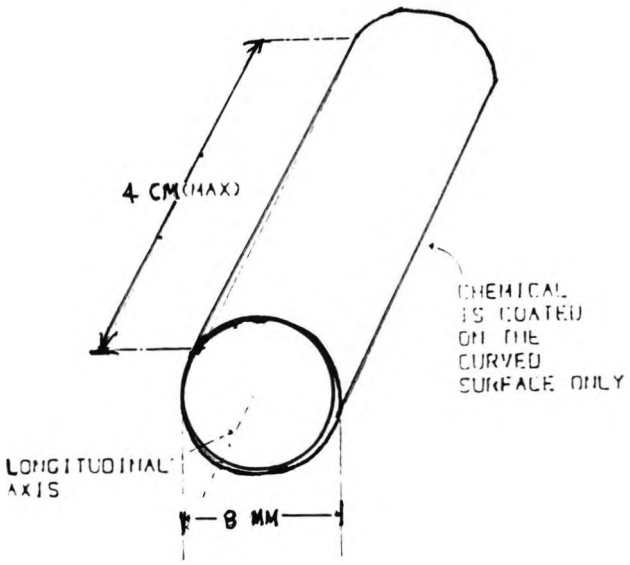

FIGURE 3.16a A cylindrical sample

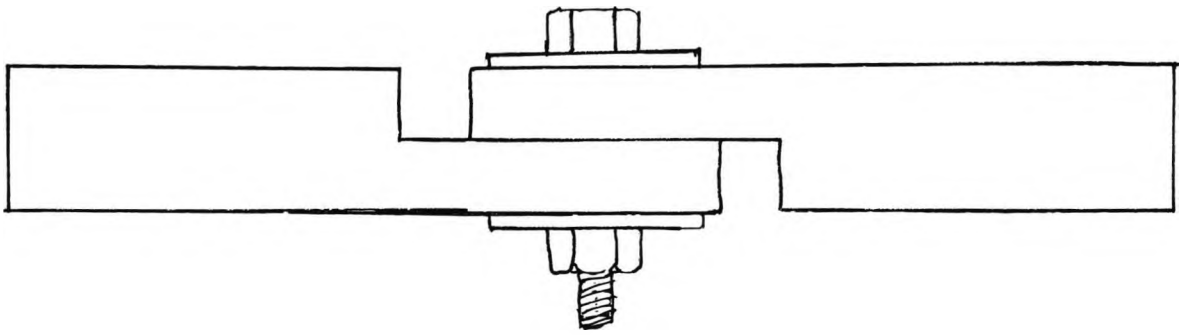

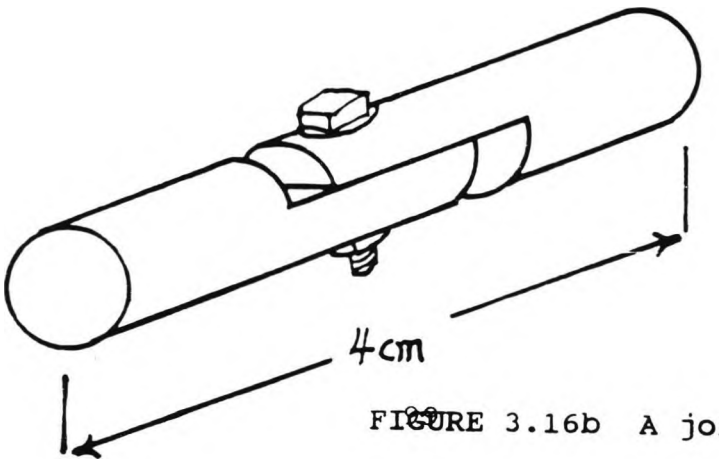

FIGURE 3.16b A joint sample

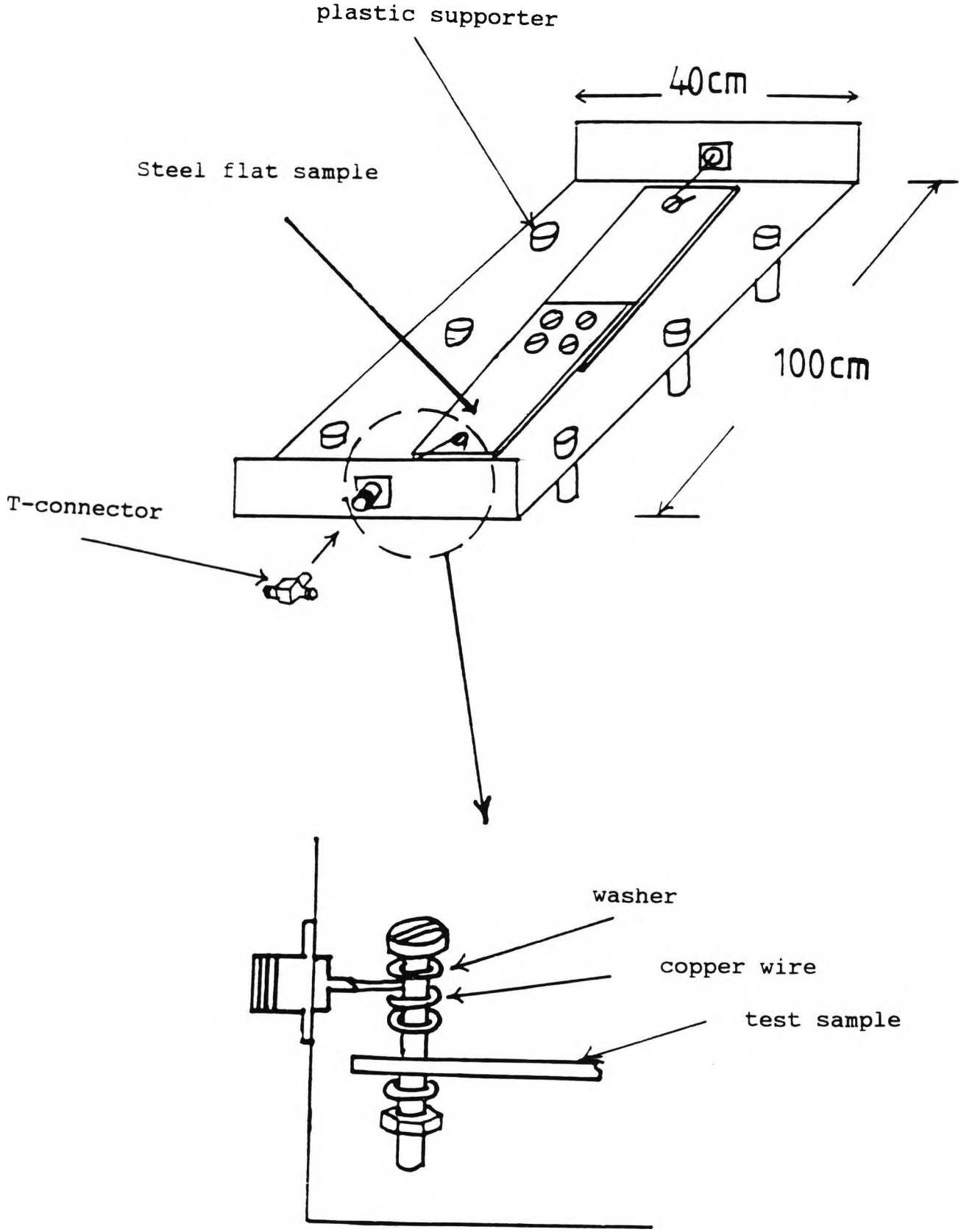

FIGURE 3.16c A steel flat sample (also shown is the sample holder)

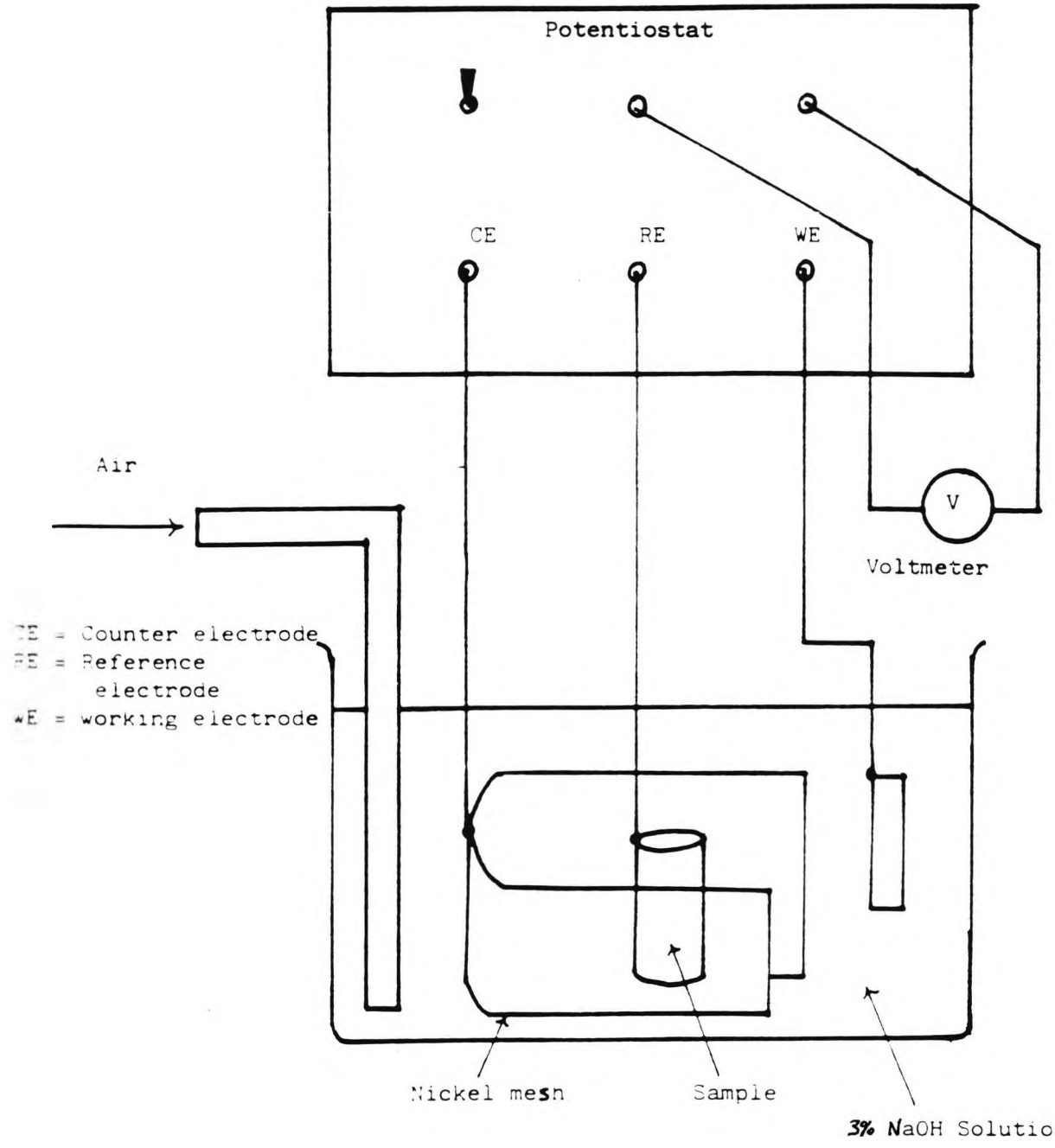

FIGURE 3.17 Corrosion setup for test sample

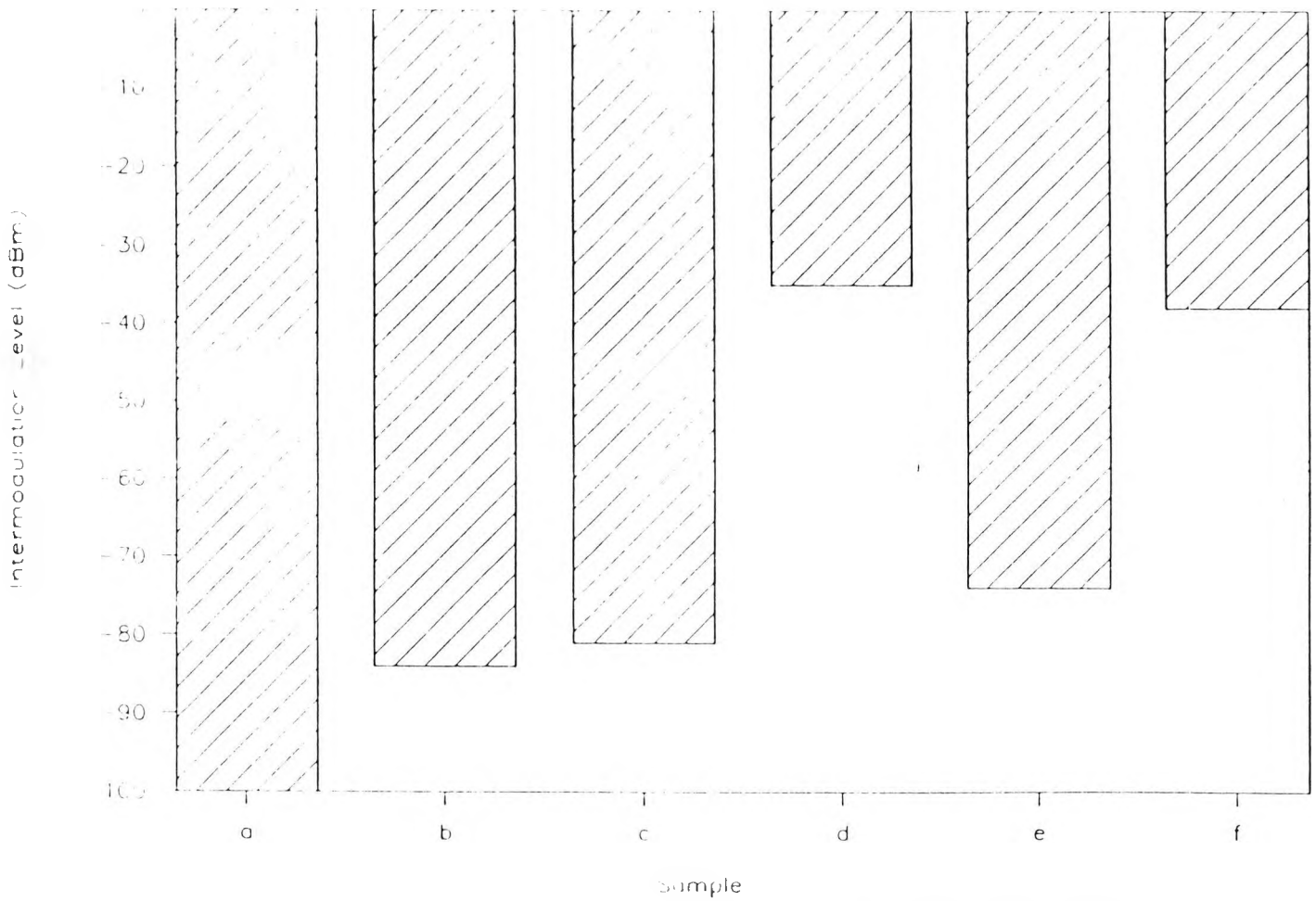

a = background b = clean steel rod c = steel rod with corroded surface
d = corroded joint sample e = clean joint sample f = corroded joint

FIGURE 3.18 Experimental results showing the dominant source of IMI

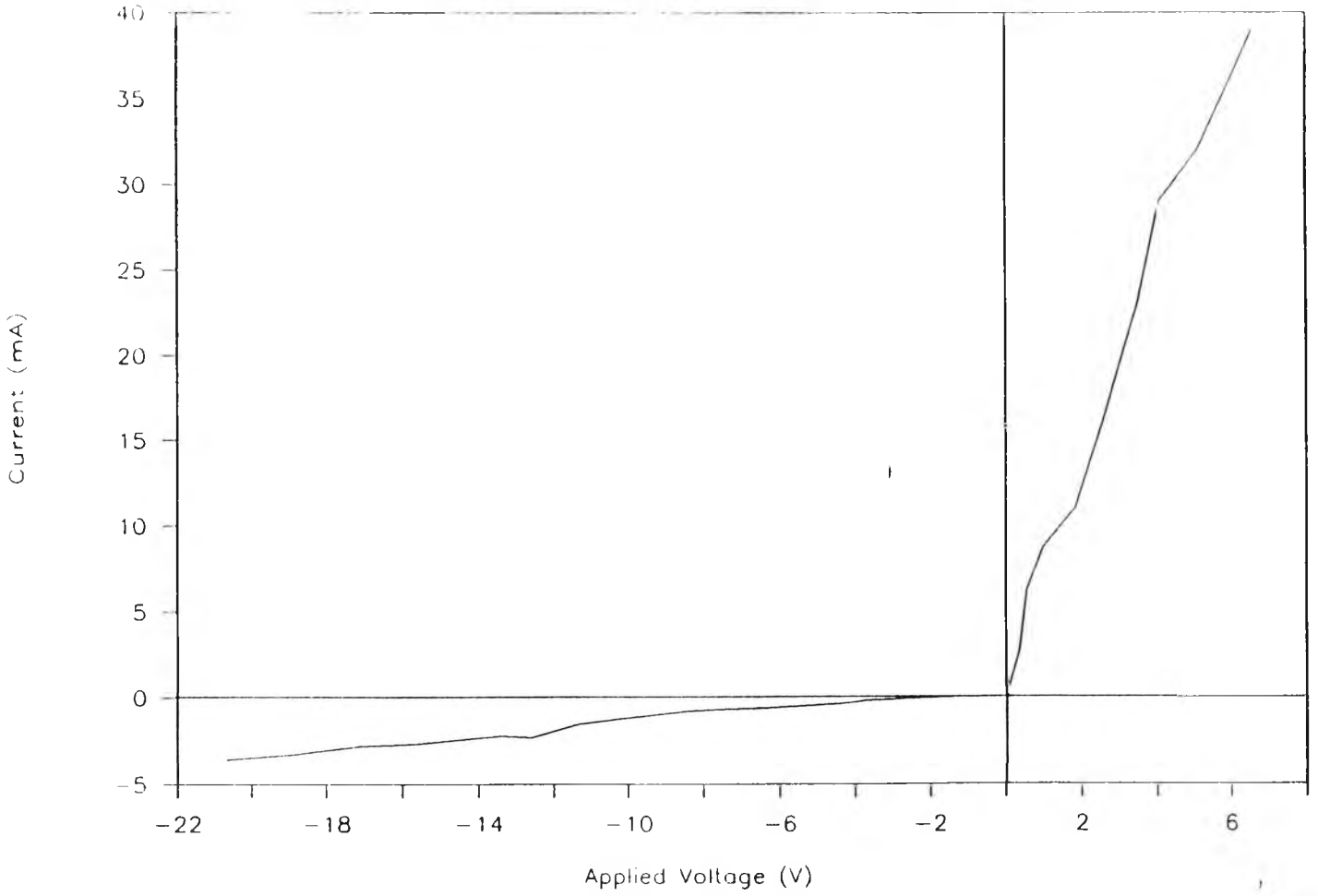

FIGURE 3.19 Current-voltage characteristic of a corroded rod sample (one end only)

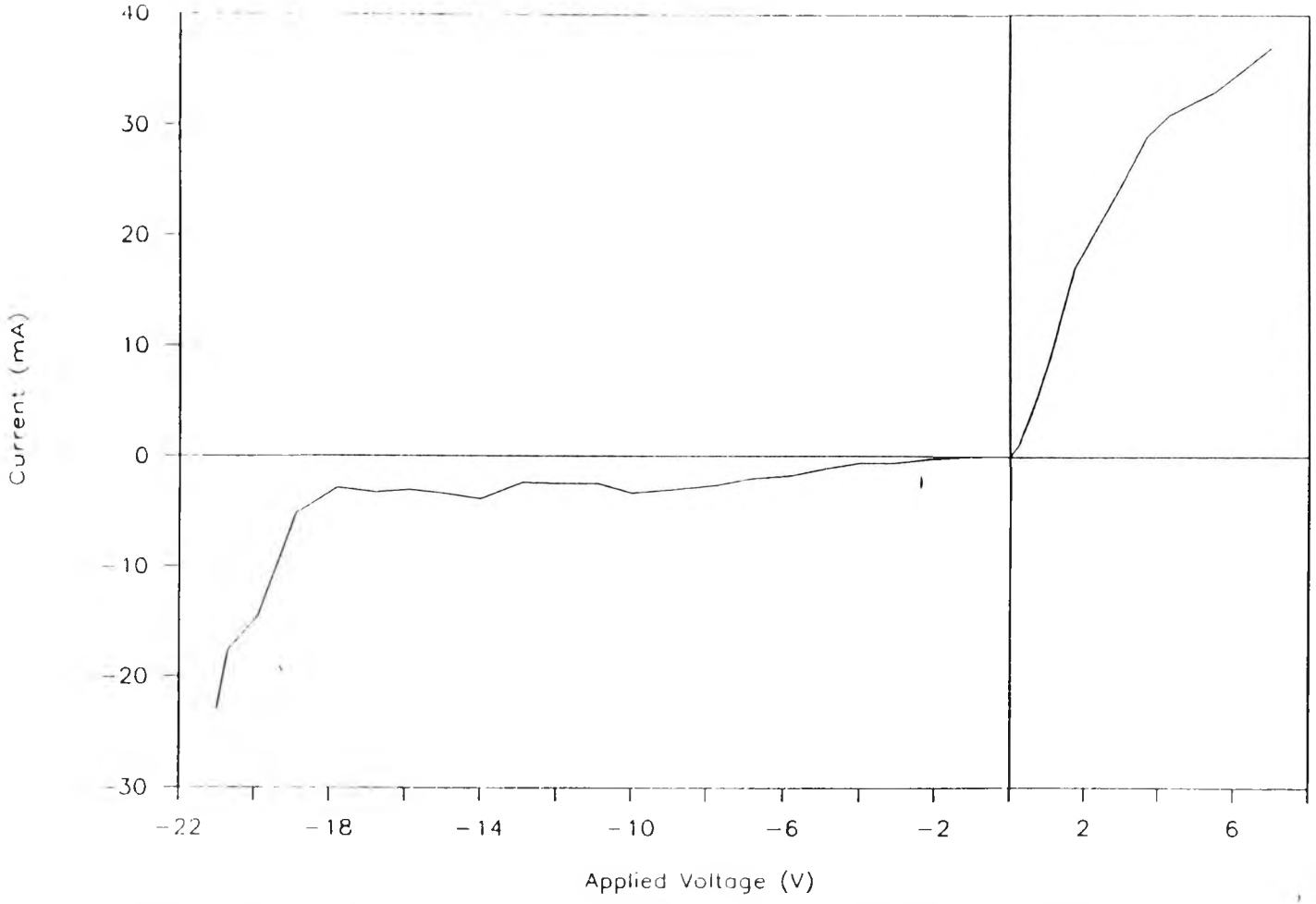

FIGURE 3.20 Current-voltage characteristic of a corroded galvanised rod (one end only)

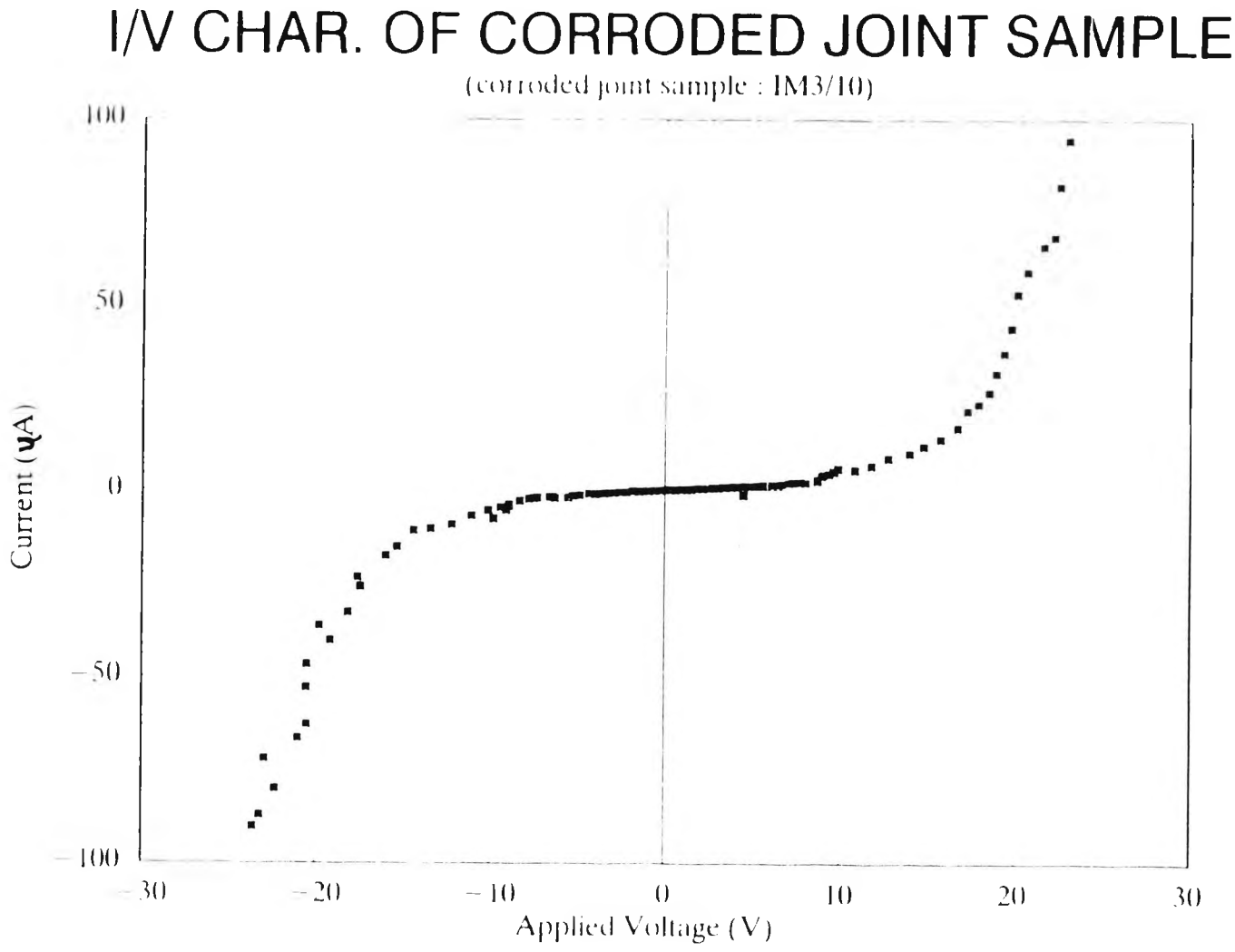

FIGURE 3.21 Current-voltage characteristic of a corroded joint sample

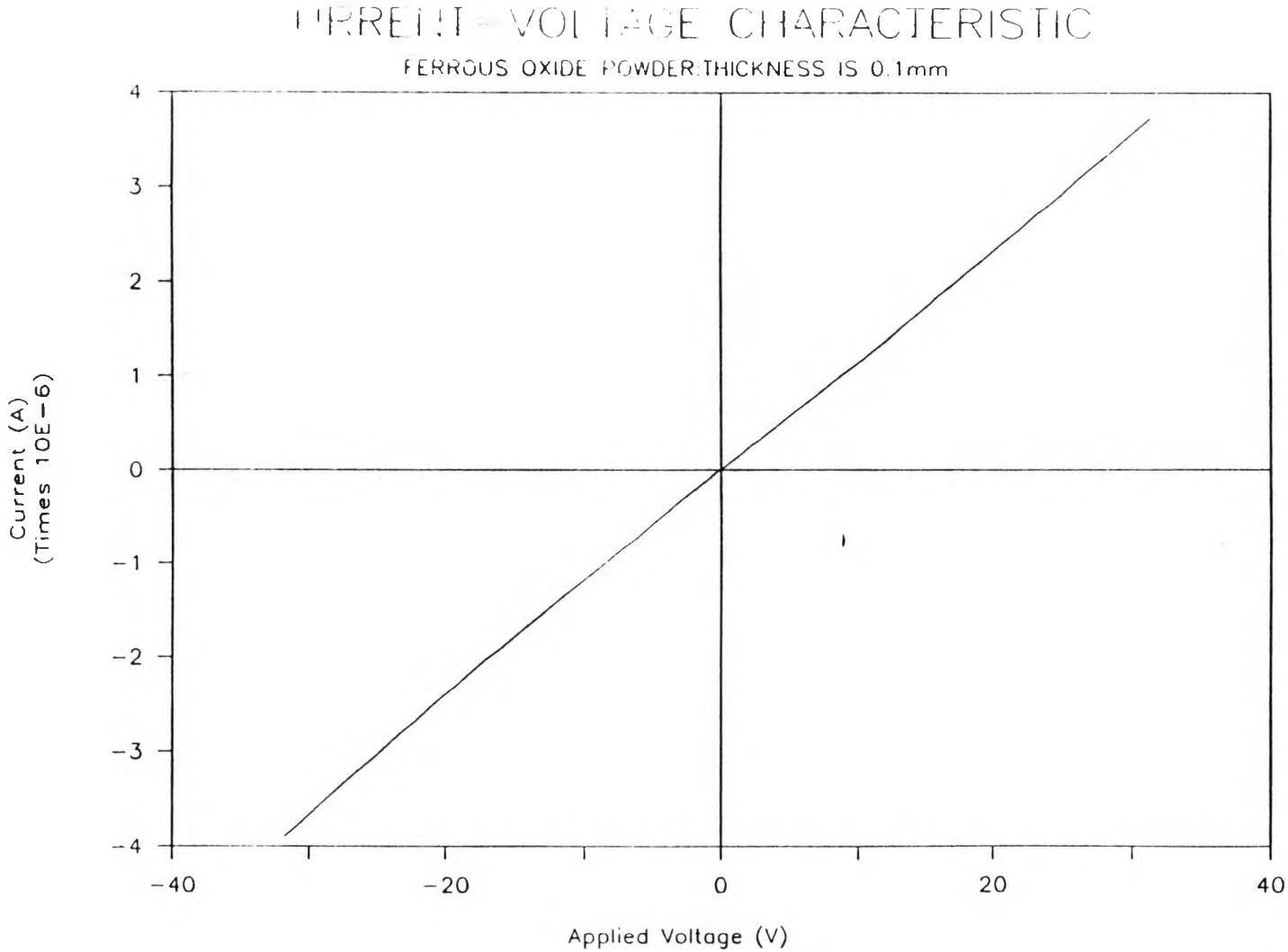

FIGURE 3.22 Current-voltage characteristic of a joint sample with 0.1mm of ferrous oxide powder

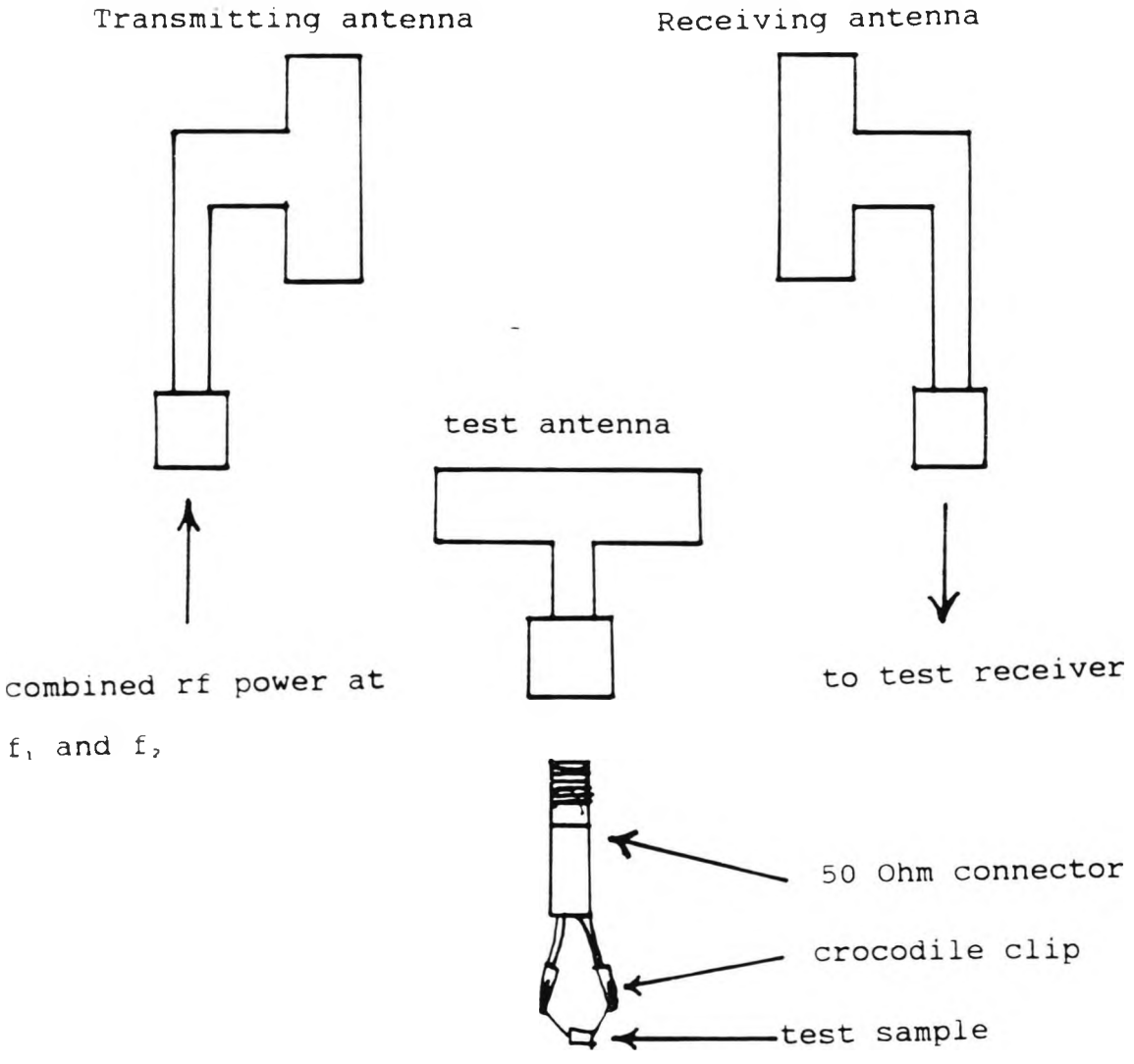

FIGURE 3.22a Test setup for investigating the effectiveness of intermodulation product generation of a corroded joint sample and a semiconductor diode

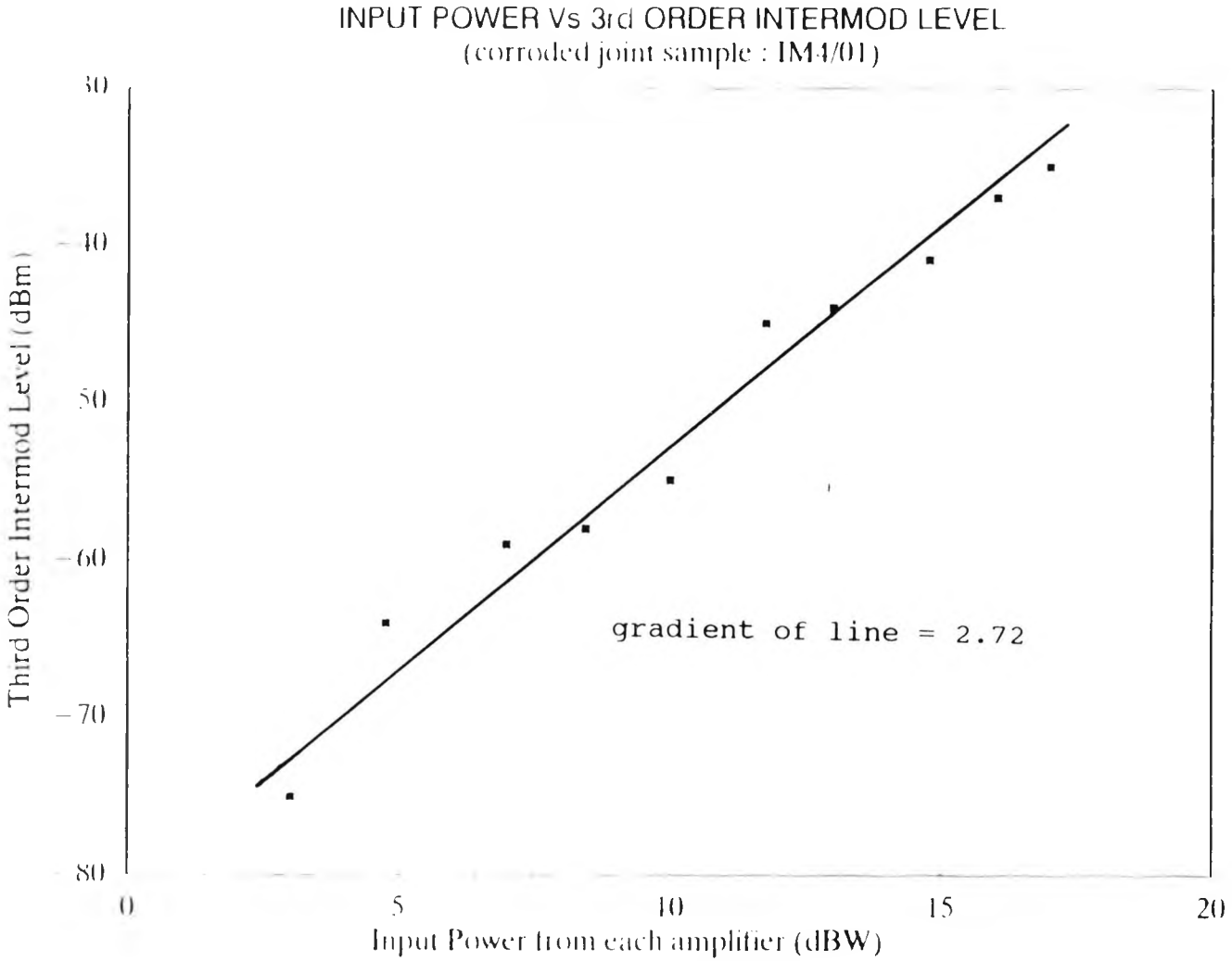

FIGURE 3.22b A typical example of the relationship between input power and the third order intermodulation interference level of a corroded joint sample

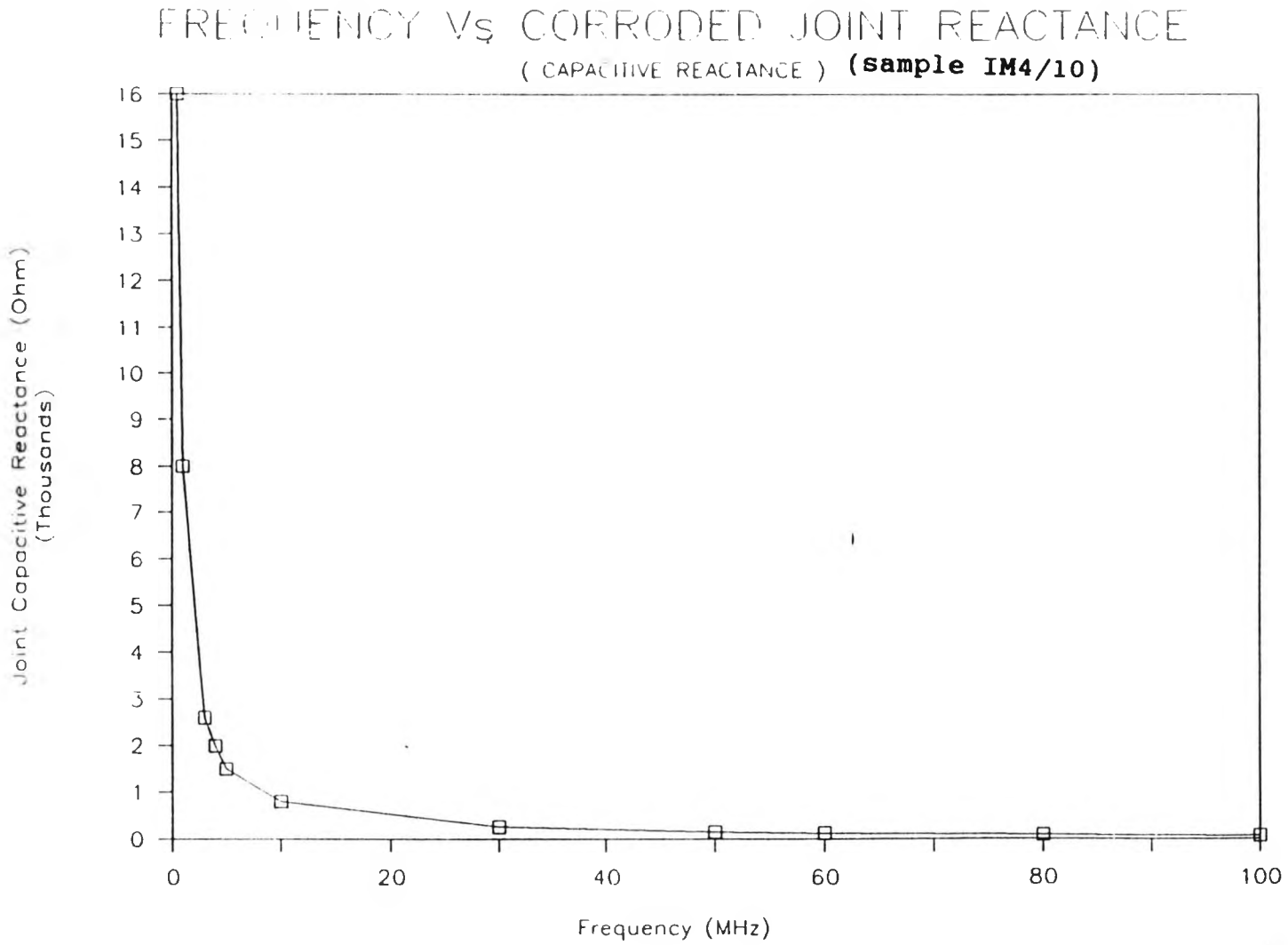

FIGURE 3.23 Relationship between corroded joint reactance and applied frequency

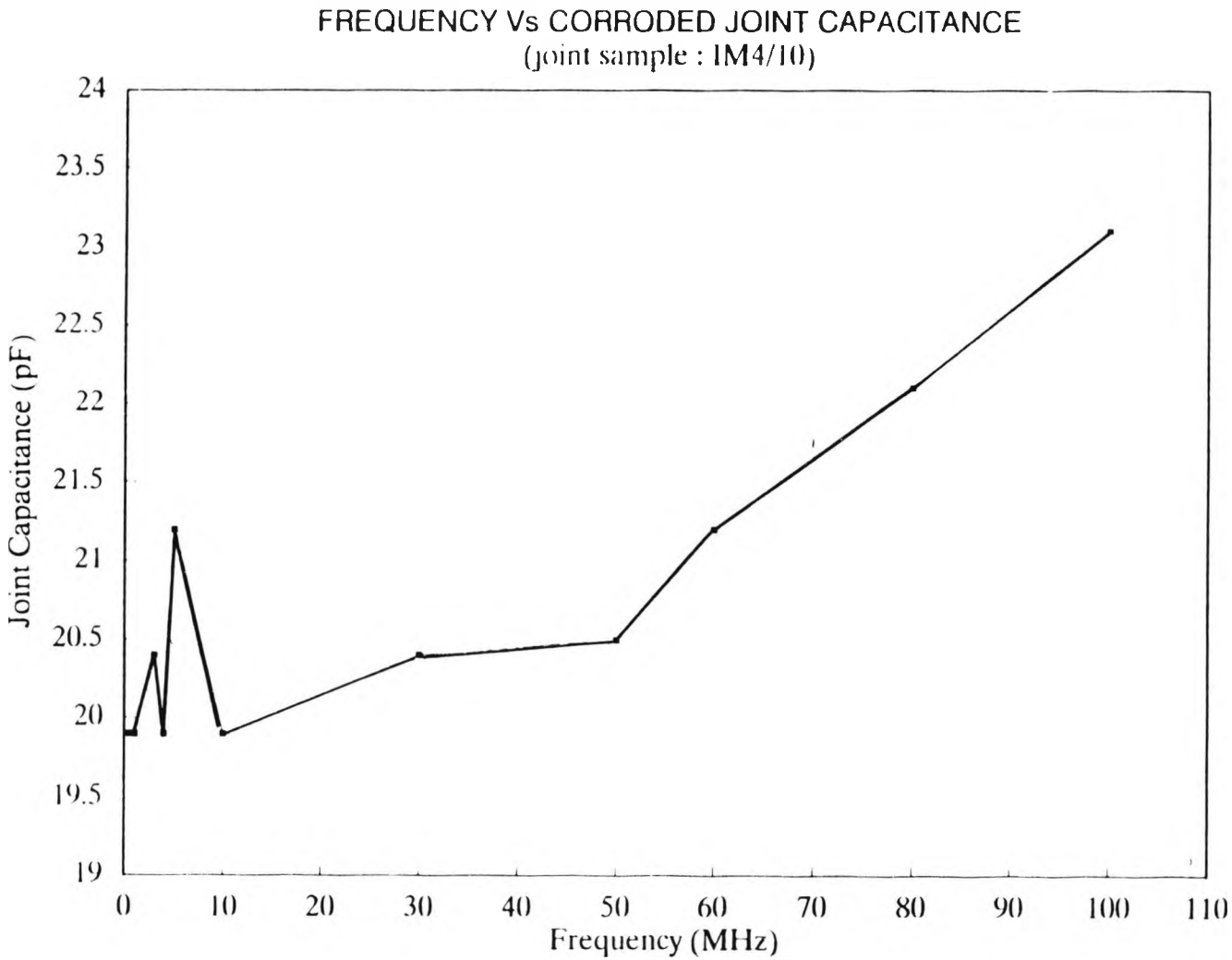

FIGURE 3.24 Relationship between corroded joint capacitance and applied frequency

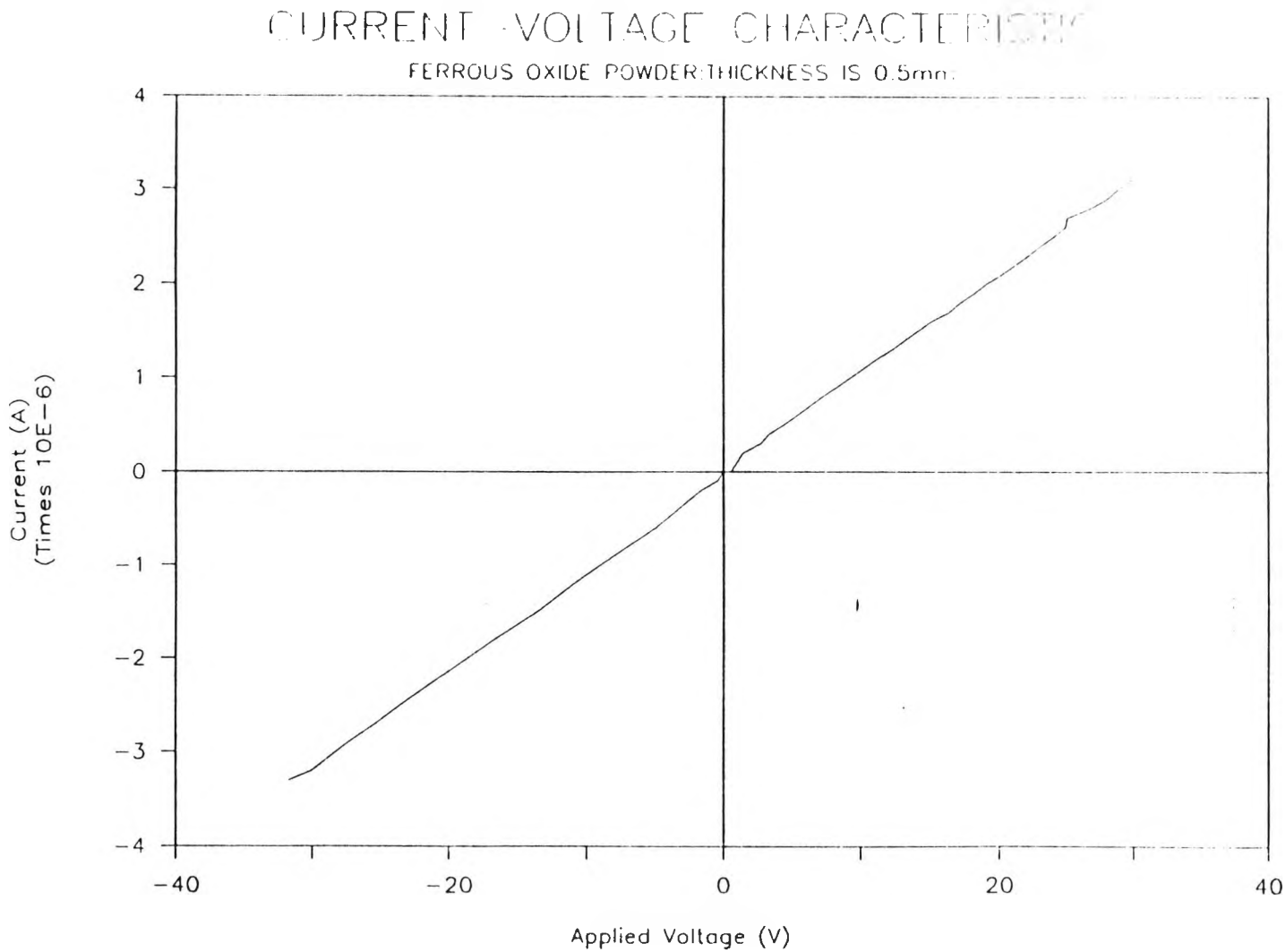

FIGURE 3.25 Current-voltage characteristic of a joint sample with 0.5 mm of ferrous oxide

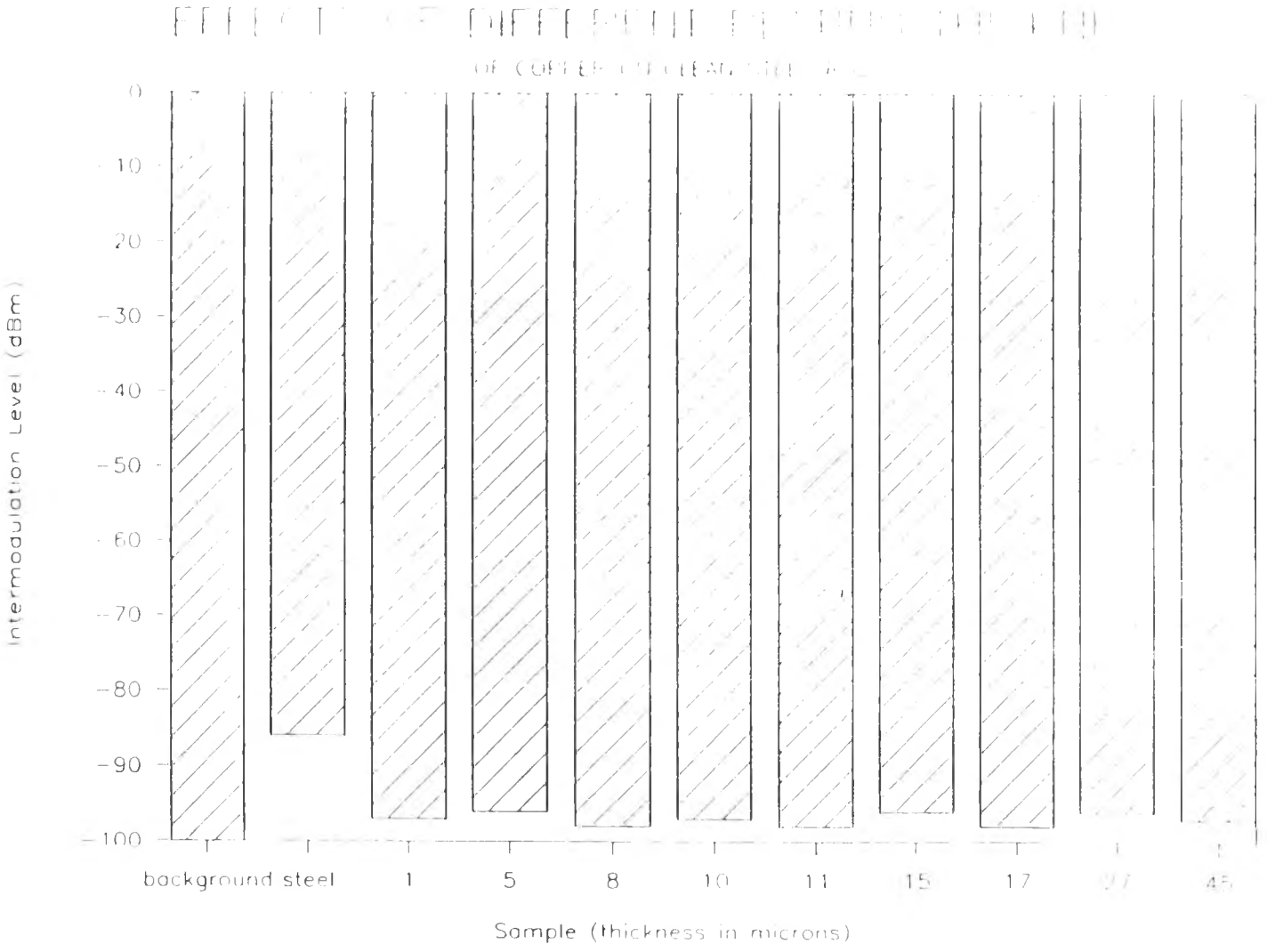

FIGURE 3.26 Effect of different copper plating thicknesses on ferromagnetic IMI

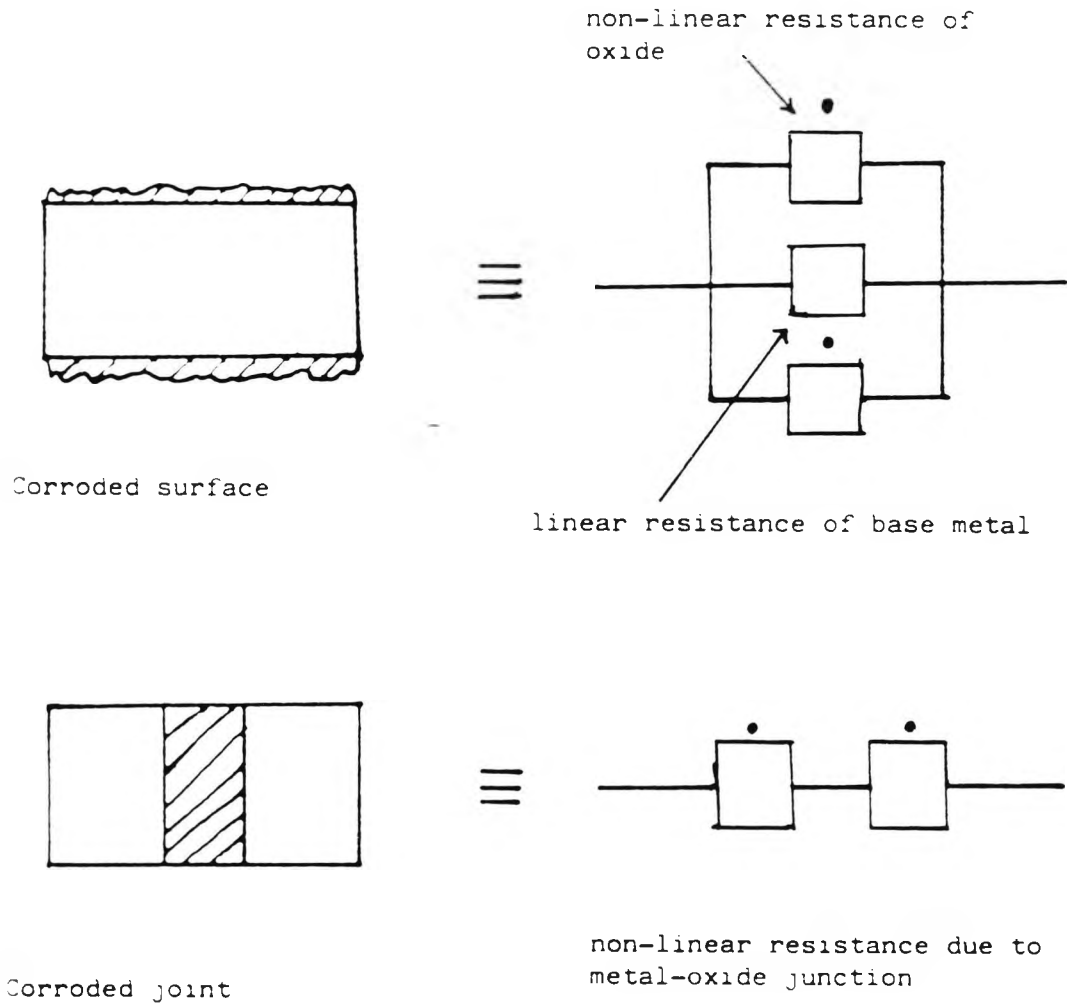

FIGURE 3.27 Circuit models of a corroded surface and a corroded joint

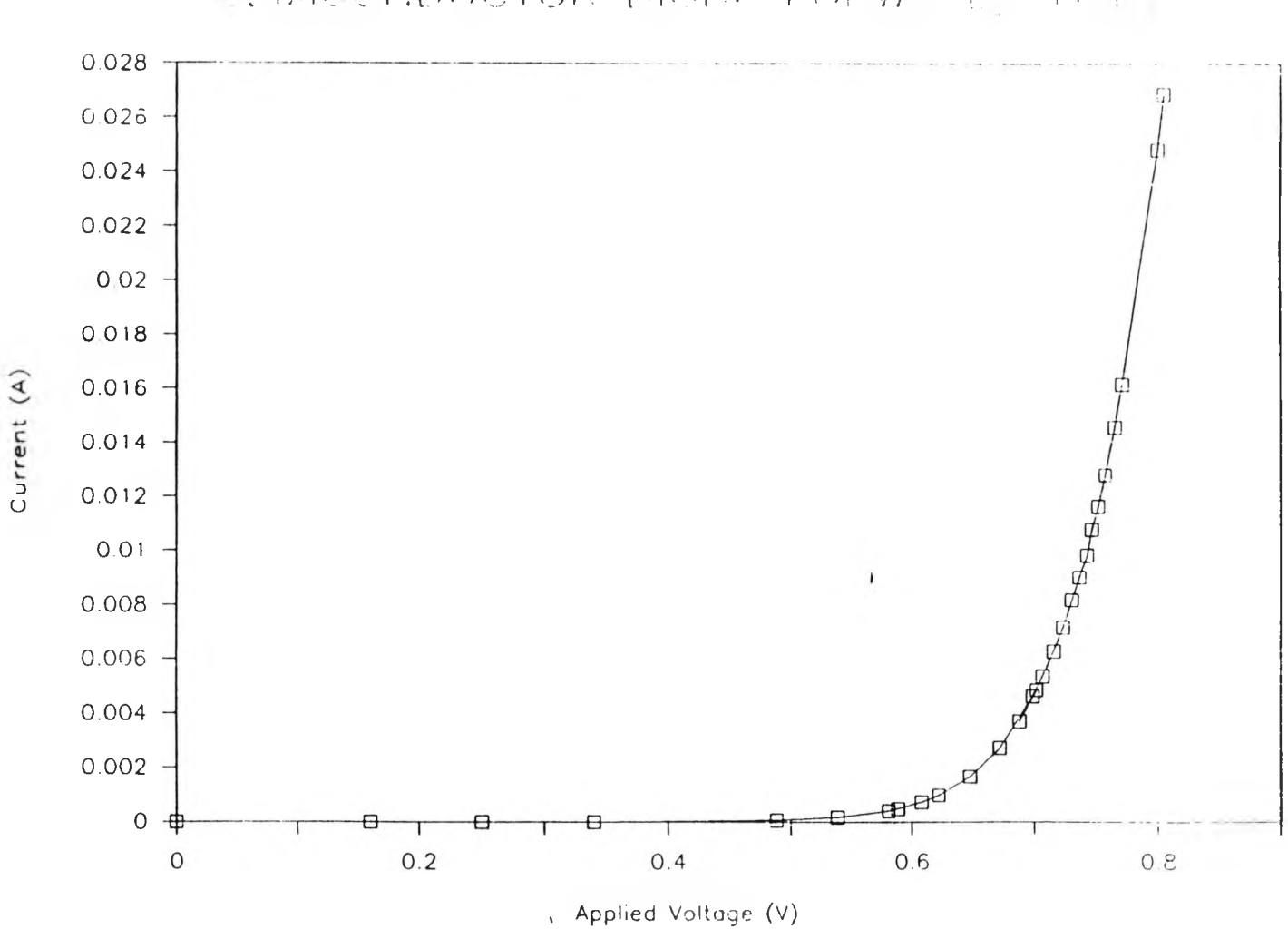

FIGURE 3.28a Current-voltage characteristic of a forward biased diode

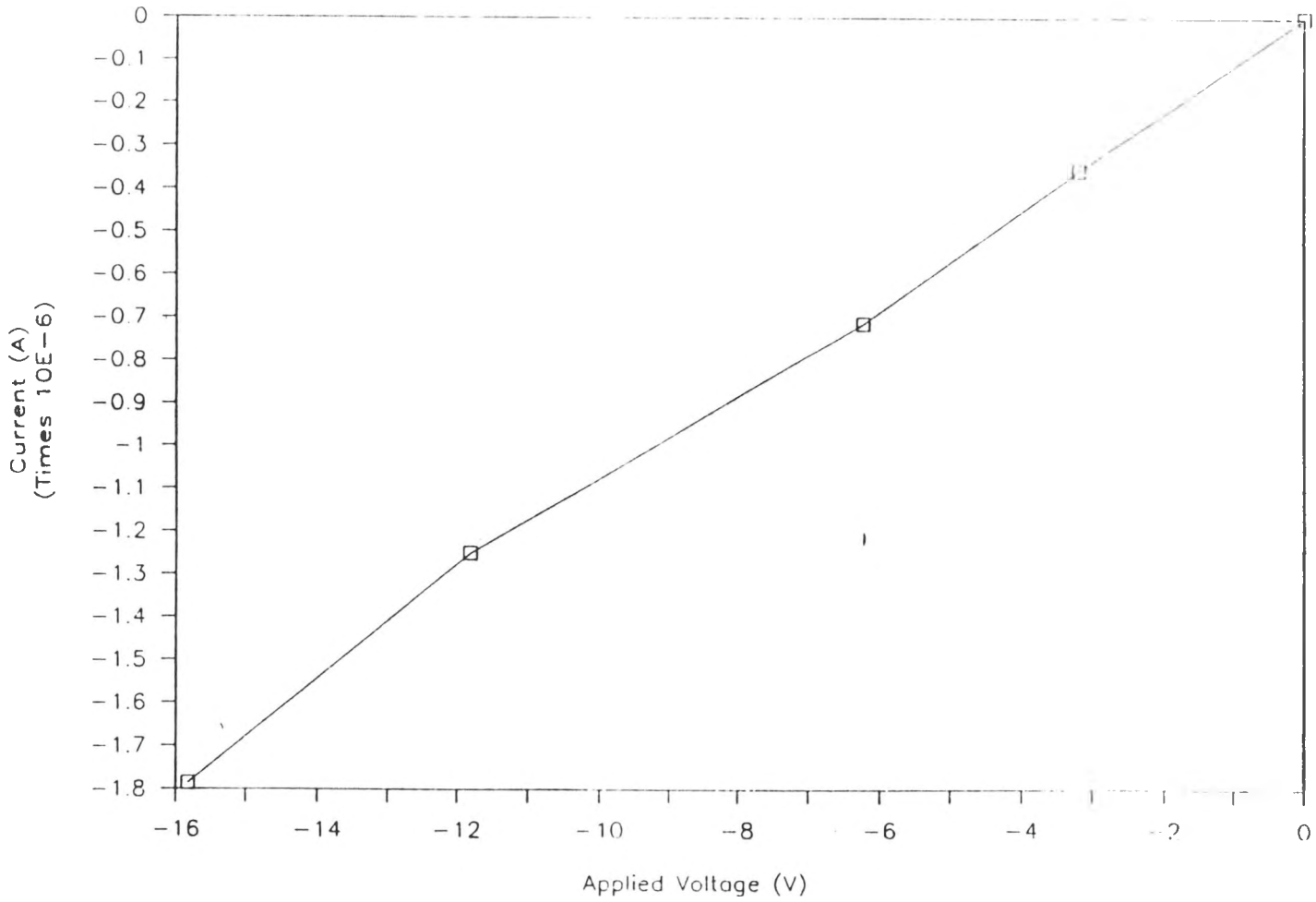

FIGURE 3.28b Current-voltage characteristic of a backward biase diode

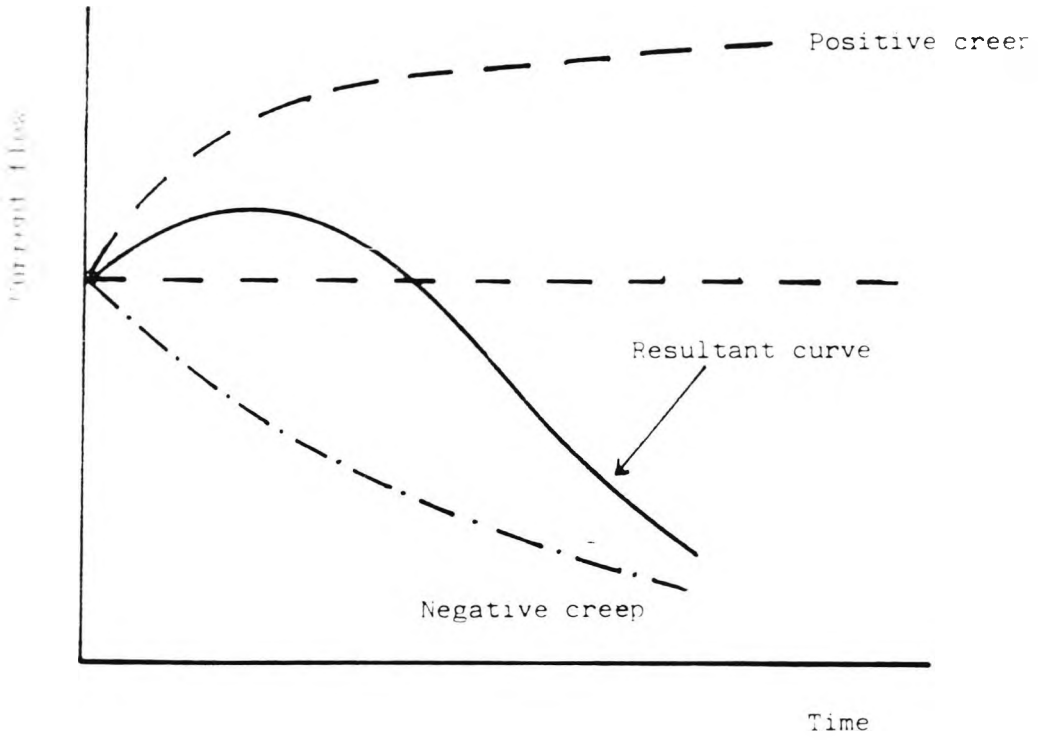

FIGURE 3.29 Current creep phenomenon

Chapter 4

Cirucit Modelling of a Non-Linear Junction

4.1 Lumped Circuit Model

A junction model is useful for describing the electrical characteristics of a corroded junction in terms of lumped circuit elements such as resistors and capacitors, which are assumed to be frequency-independant. In addition, this model could be incorporated in future simulation studies for intermodulation level predictions as well.

A typical junction can be represented by lumped circuit elements as shown in figure 4.1. In the diagram, R_0 is the non-linear junction resistance and C is the linear junction capacitance. It is assumed that any series resistance would be much smaller than the nominal resistance of the junction.

4.2 Circuit Analysis of a Non-Linear Junction Model

The current-voltage characteristics of a non-linear junction can be described by a general power series as follows :

$$I \doteq a_1 V + a_2 V^2 + a_3 V^3 + \cdots\cdots + a_n V^n \qquad (4.1)$$

where I is the current flows and V is the applied or induced voltage.

If the input voltage is composed of two frequencies, i.e.

$$V = V_1 \cos \omega_1 t + V_2 \cos \omega_2 t \qquad (4.2)$$

then the resultant current (output) would be, by equation 4.1 equals to :

$$\begin{aligned} I = {} & a_1(V_1 \cos\omega_1 t + V_2 \cos\omega_2 t) \\ & + a_2\left(V_1^2 \tfrac{1}{2}(1+\cos 2\omega_1 t) + V_2^2 \tfrac{1}{2}(1+\cos 2\omega_2 t) + V_1 V_2(\cos(\omega_1+\omega_2)t + \cos(\omega_1-\omega_2)t)\right) \\ & + a_3\left(V_1^3\{\tfrac{1}{4}(\cos 3\omega_1 t + 3\cos\omega_1 t)\}\right. \\ & \quad + 3V_1^2 V_2\{\tfrac{1}{2}(\cos\omega_2 t + \tfrac{1}{2}\{\cos(2\omega_1+\omega_2)t + \cos(2\omega_1-\omega_2)t\})\} \\ & \quad + 3V_1 V_2^2\{\tfrac{1}{2}(\cos\omega_1 t + \tfrac{1}{2}\{\cos(2\omega_2+\omega_1)t + \cos(2\omega_2-\omega_1)t\})\} \\ & \quad \left. + V_2^3\{\tfrac{1}{4}(\cos 3\omega_2 t + 3\cos\omega_2 t)\}\right) \qquad \text{---} (4.3) \end{aligned}$$

From equation 4.3, we can see immediately that the current (output) would consist of the fundamental frequencies at f_1 and f_2. In addition, there would be various harmonics and intermodulation frequencies as well.

In the case of land mobile radio systems, where the transmitting and receiving frequencies can be close, the odd

order intermodulation products are more damaging than the even order ones, since they are closer to the fundamentals and fall close the receiver's filter bandwidth; e.g. for the U.K. Emergency Services, the frequency band for the receivers is between 146 MHz to 148 MHz, and the frequency band for the transmitters is bwtween 154 MHz to 156 MHz. The third order intermodulation frequency (2 * 154 - 156 = 152 MHz) is 4 MHz from the receiver frequency, which can be a problem for the less selective receivers. The even order intermodulation products locate further away from the fundamentals and can be removed by filtering. In this report, where land mobile radio system is under consideration, then, the odd order intermodulation products are more significant than the even order products.

In this example, we would consider the third order intermodulation product cos $(2\omega_1 - \omega_2)$ t. Since odd order intermodulation products are generated from the odd power terms of the non-linear current-voltage characteristic, and lower order products are more significant than higher order products, the current-voltage characteristic which will be considered here will consist of first two odd order power terms.

Suppose

$$I = a_1 V + a_3 V^3 \qquad (4.4)$$

then, with the input as shown in equation 4.2, the resultant current would be :

$$I(t) = a_1 (V \cos \omega_1 t + V \cos \omega_2 t) + \frac{3}{4} a_3 V_1^2 V_2 \cos (2\omega_1 - \omega_2) + \ldots .$$

fundamentals — one of the 3rd order terms

(4.5)

$$= I_0(t) + I_{3im}(t) + \text{other terms}$$

where $I(t)$ is the total r.f. current

$I_0(t)$ is the primary current at frequencies f_1 and f_2 respectively

$I_{3im}(t)$ is the 3rd-order intermodulation current at $(2f_1 - f_2)$

From equation 4.5 the peak value of that particular third order intermodulation product is :

$$I_{3im.peak} = \frac{3}{4} a_3 V_1^2 V_2 \qquad (4.6)$$

Now at the frequency band we are concerned with, i.e. at 150 MHz, the non-linear resistance would be much greater than the capacitive reactance ($R_o >> X_c$). Therefore we could safely assume that :

(I) A large proportion of the transmitted current, $I_T(t) = I_1 \cos(\omega_1 t) + I_2 \cos(\omega_2 t)$, passes through the capacitance, C.

(II) All transmitted power, P_T, is dissipated in the load resistance, R_L, which is 50 Ohm.

So, the measured (transmitted) rf power is :

$$P_T = \langle I_T^2(t) \rangle R_L \qquad (4.7)$$

where the mean square current is :

$$\langle I_T^2(t) \rangle = \frac{1}{T} \int_0^T (I_1 \cos \omega_1 t + I_2 \cos \omega_2 t)^2 \, dt$$

For equal transmitter powers, then :

$$P_1 = P_2 \quad ; \quad I_1 = I_2$$

and equation 4.7 becomes

$$I_{T,peak} = \left(\frac{P_T}{R_L} \right)^{\frac{1}{2}} \qquad (4.8)$$

Since essentially all of this current passes through the capacitance, then the voltage across the capacitance C, and also across the non-linear resistance, R_o is approximately

$$V_1 = X_{c1} \left(\frac{P_T}{R_L} \right)^{\frac{1}{2}} \quad \text{and} \quad V_2 = X_{c2} \left(\frac{P_T}{R_L} \right)^{\frac{1}{2}} \qquad (4.9)$$

where V_1 and V_2 are the induced voltages across the junction due to the fundamental frequency current at frequencies f_1 and f_2 respectively.

Similarily, X_{c1} and X_{c2} are the capacitive reactance of the junction at frequencies f_1 and f_2.

Substitute these values into equation 4.6, then it becomes

$$I_{3im.peak} = \frac{3}{4} a_3 X_{c1}^2 X_{c2} \left(\frac{P_T}{R_L}\right)^{\frac{3}{2}} \qquad (4.10)$$

Thus the resultant intermodulation voltage across the capacitance is

$$V_{3im.peak} = I_{3im,peak} X_{c,im} \qquad (4.11)$$

where $X_{c,im}$ is the capacitive reactance of the joint at the intermodulation frequency.Then the intermodulation power disspated in the load, R_L, would be

$$P_{3im} = \frac{< V_{3im.peak}^2 \cos^2 (2\omega_1 - \omega_2) t >}{R_L} = \frac{1}{2} \frac{V_{3im,peak}^2}{R_L} \qquad (4.12)$$

Combining equations 4.10, 4.11 and 4.12, we arrive at the intermodulation power equation as follows :-

$$P_{3im} = \frac{9}{32} a_3^2 P_T^3 \frac{X_{c1}^4 X_{c2}^2 X_{c1m}^2}{R_L^4} \qquad (4.13)$$

From the intermodulation power equation 4.13 there are some interesting and important points to be noted. Firstly, the third order intermodulation power is proportional to the cube of the input power as expected. Secondly, the coefficient a_3, which determines how non-linear the junction characteristics would be, has a square law effect. By far, the most important term is the capacitive reactance terms.

Togather, they exhibit an eighth power law.

From above, it is obvious that capacitive reactance has a dominant effect over intemodulation interference level. However, this is not a big surprise at all. Since if the reactance gets larger, then more rf current will be forced to flow through the non-linear resistance; hence produce a larger intermodulation level. Therefore, the capacitive reactance of the non-linear junction has a strong influence on the resultant intermodulation level. However the reactance of a junction depends very much on the operational frequencies, the area of overlapping at the interface, as well as the oxide thickness. For a lattice tower, the junction formed by two structural members normally has a large overlapping area (say, 0.045 m^2) and a small saparation (1 to 3 mm), probably due to the presence of corrosion products and non-uniform contacts between rough surfaces. Due to the large overlapping area, the resultant junction capacitive reactance will tend to be low, especially in the VHF band.

Because of its geometry, it is reasonable to assume that the junction forms a parallel plate capacitor. Let the junction capacitance, C, be :

$$C = \frac{\varepsilon A}{d} \qquad (4.14)$$

where A is the overlapping area, and d is the oxide thickness, or an air gap.

From equation 4.14, we can see that the junction capacitance is directly proportional to the overlapping area and inversely proportional to the thickness of the oxide. Assuming the two fundamental frequencies are close, then their capacitive reactances would be very similar. Thus, the intermodulation power equation 4.13 will become :

$$P_{3im} = \frac{9}{32} a_3^2 P_T^3 \frac{1}{R_L^4} \left(\frac{d}{\omega \varepsilon A} \right)^8 \qquad (4.15)$$

4.3 IMP Level Prediction

In this section, we would apply the intermodulation power equation 4.15 to predict the IMP level generated from a corroded joint sample.

For our test setup and test samples, the parameters are as follow :

P_T = 20 watt

R_L = 75 Ohms

d = 0.05 mm

A = 64 mm^2

ω = $2\pi(150 * 10^6)$ Hz

ε = $15 * 8.85 * 10^{-12}$ Fm^{-1}

The output from each power amplifier is about 50 watt. The cascaded resonators has an insertion loss of around 2 dB. However, the impedance mis-match due to the presence of the

highly resistive oxide layer sample causes significant reflected power. The net result is that there is about 20 watt of total transmitted power.

From physical chemistry handbooks, it was found that at 100 MHz, cupric oxide (CuO) has a relative permittivity of 18.1; and ferrous oxide (FeO) has a value of 14.2. The relative permittivity of the corrosion products (mainly Fe_2O_3) was assumed to be 15, since normal transition metal oxides have relative permittivities between 10 and 20.

In addition, we still need to find out the value of a_g for our test sample. We could have derived a functional relationship between the current and the voltage from first principle, i.e. making use of all the physical facts, such as the transport mechanism, type of semiconductor, diffusion constant, Femi energy level, etc. However, it would be very unlikely that real corrosion products have such well-defined parameter values. Indeed, natural corrosion products are a mixture of various chemcial compounds, which would exhibit a combinations of conduction mechanisms under different conditions. It was thought that it would be more preferable if we could get the functional relationship via mathematical means for this sample. In chapter 3, we have already measured the non-linear current-voltage characteristic for this particular test sample, then it is only necessary to perform a curve-fitting using these data to get the coefficients of the power series. This was indeed the chosen method.

4.3.1 Curve-Fitting

An iterative least-squares regression technique was used to estimate the power series coefficients. Before each run, a model equation has to be supplied, as are the estimations of the coefficients. In addition, the number of iterations and tolerance of the parameters are also required. The output contains the best estimates (in the least-square sense) of the coefficients within the specified tolerances. The quality of the fit can be assessed by a parameter correlation matrix, which indicates whether there are any redundant parameters; and the standard deviations of the estimated coefficients. The quality of the model can be examined by looking at the plot of the residuals. If the form of model is correct, the residuals will show a random distribution, with no significant trends.

4.3.2 Curve-Fit for Test Sample

From figure 3.21, it can be seen that the non-linear current-voltage characteristic of this corroded joint sample is nearly symmetrical about the origin; therefore, it is only necessary to perform a curve-fit on the forward current-voltage characteristic (see figure 4.3).

At the beginning, we tried a fit for the power series :

$$I = a_1 V + a_3 V^3 + a_5 V^5$$

The results are shown below. Standard deviations are shown inside the brackets. The fitted curve, and the residual plot are shown in figure 4.2 and figure 4.3.

$a_1 = 0.395 * 10^{-6}$ $(0.888 * 10^{-7})$

$a_3 = -0.202 * 10^{-8}$ $(0.688 * 10^{-9})$

$a_5 = 0.166 * 10^{-10}$ $(0.177 * 10^{-11})$

The uncertainty percentage are 22%, 34% and 7% for a_1, a_3 and a_5 respectively. The parameter correlation matrix indicates a high degree of redundance between a_3 and a_5 (correlation coefficient between a_3 and a_5 is 0.97). Due to the much higher uncertainty in the estimation of a_3, then we discarded a_3, and carried out the estimation process again with the following model :

$$l = a_1 V + a_5 V^5 \qquad (4.16)$$

The curve-fitting results are shown below :

$a_1 = 0.168 * 10^{-6}$ $(0.470 * 10^{-7})$

$a_5 = 0.133 * 10^{-10}$ $(0.295 * 10^{-12})$

Uncertainty percentages are 28% for a_1 and 2.2% for a_5.

The fitted curve and the residual plot are shown in figure 4.4 and figure 4.5.

This is a better estimation than the first one. We followed the previous procedure (of deriving equation 4.6) to find

out the 3rd-order intermodulation power, with the non-linear current-voltage relationship shown in equation 4.16, for a two-frequency input. The resultant intermodulation power is found to be :

$$P_{3im} = \frac{25}{8} a_5^2 P_T^5 \frac{1}{R_L^6} \left(\frac{d}{\omega \epsilon A} \right)^{12} \qquad (4.17)$$

The junction capacitance of the test sample by equation 4.14 is 17 pF; and by ac impedance measurement is 20 pF. The order of magnitude agreement between the calculated and measured capacitance value, is really an assurance of the accuracy of our estimation for the relative permittivity, and other dimension measurements of the joint.

With the measured value of junction capacitance, the intermodulation power equation produced a value for the 3rd-order intermodulation level of 23 dBm. The measured IMP level is lower at 35 dBm.

4.4 Results and Discussion

In view of the large number of variables present in the intermodulation power equation, it is very encouraging to see that the measured intermodulation is relatively close (compared with experimental errors) to the estimated value, which confirmed the validity of our circuit model for a corroded junction. The discrepancy could be due to several reasons. They are :

(1) Due to skin-effect at high frequency, ac resistance of the non-linear joint is different from its dc value obtained from dc current-voltage measurement.

(2) The non-linear resistance of the joint, hence the coefficients a_1, a_3, and a_5, can also vary due to heating effect by a large rf current.

(3) Presence of series resistances, such as long cables.

In general, the quality of fit for the non-linear current-voltage characteristics is acceptable. For the above example, the correlation between a_1 and a_3 is only 0.82. The standard deviation for the estimate of a_3 is very low indeed; although for a_1 is higher. Overall speaking, both parameters are found to be statistically significant.

Referring to the residual plot, it can be seen that as the applied voltage gets larger, the residual errors get larger. However, since we are not going to use this characteristic outside its range (i.e. 25 volt), then, it would be accepted that this power series does represent a fair model of the characteristic, and that the quality of the model is adquate within this range of applied voltage.

4.5 Conclusion

In this chapter we have developed a lumped circuit model for a corroded joint. Although the model, which consisted of a

non-linear resistor in parallel with a linear capacitor, is a simplification of the real physical structure; nevertheless, it contains all the major components required for predicting the intermodulation interference generated from such a device.

It has been shown clearly that the capacitance of a junction has an important effect on the resultant intermodulation interference level : the larger the junction capacitance, the lower the interference level.

Intermodulation interference prediction using this lumped circuit representation of a corroded joint provided an estimation of the possible interference level, which is in reasonable agreement with the experimental results.

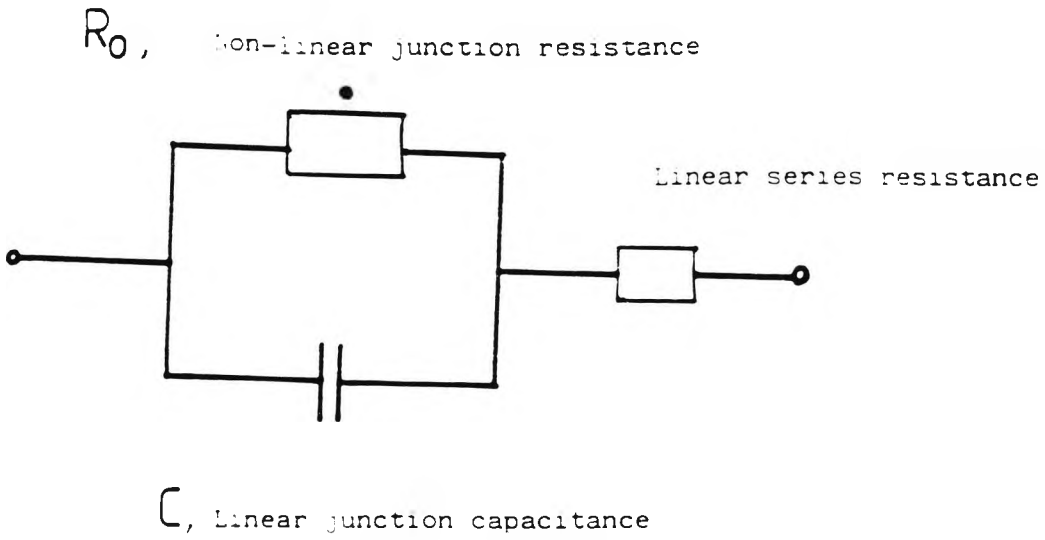

FIGURE 4.1 Circuit model of a corroded junction

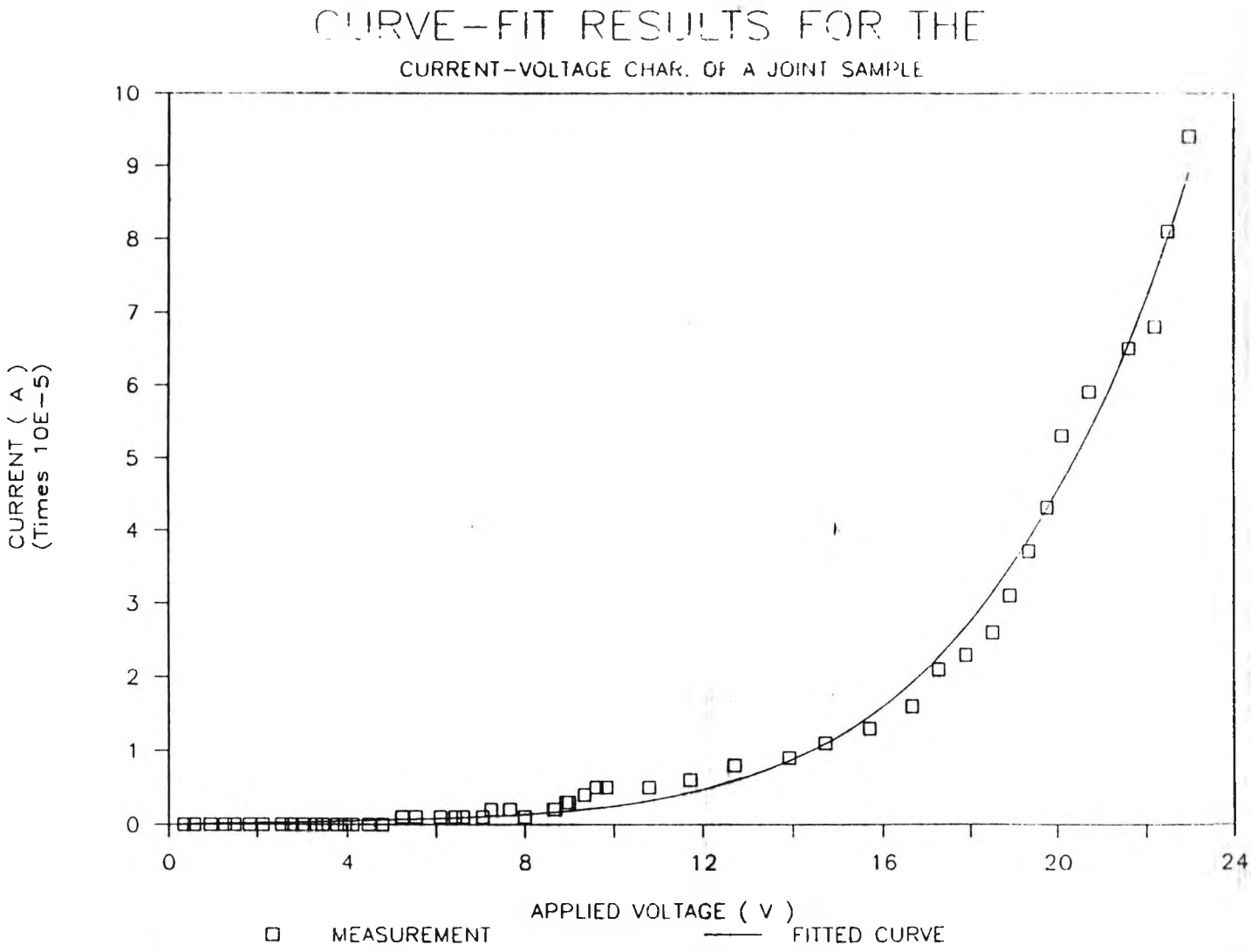

FIGURE 4.2 Curve-fit of the current-voltage characteristic of a corroded joint

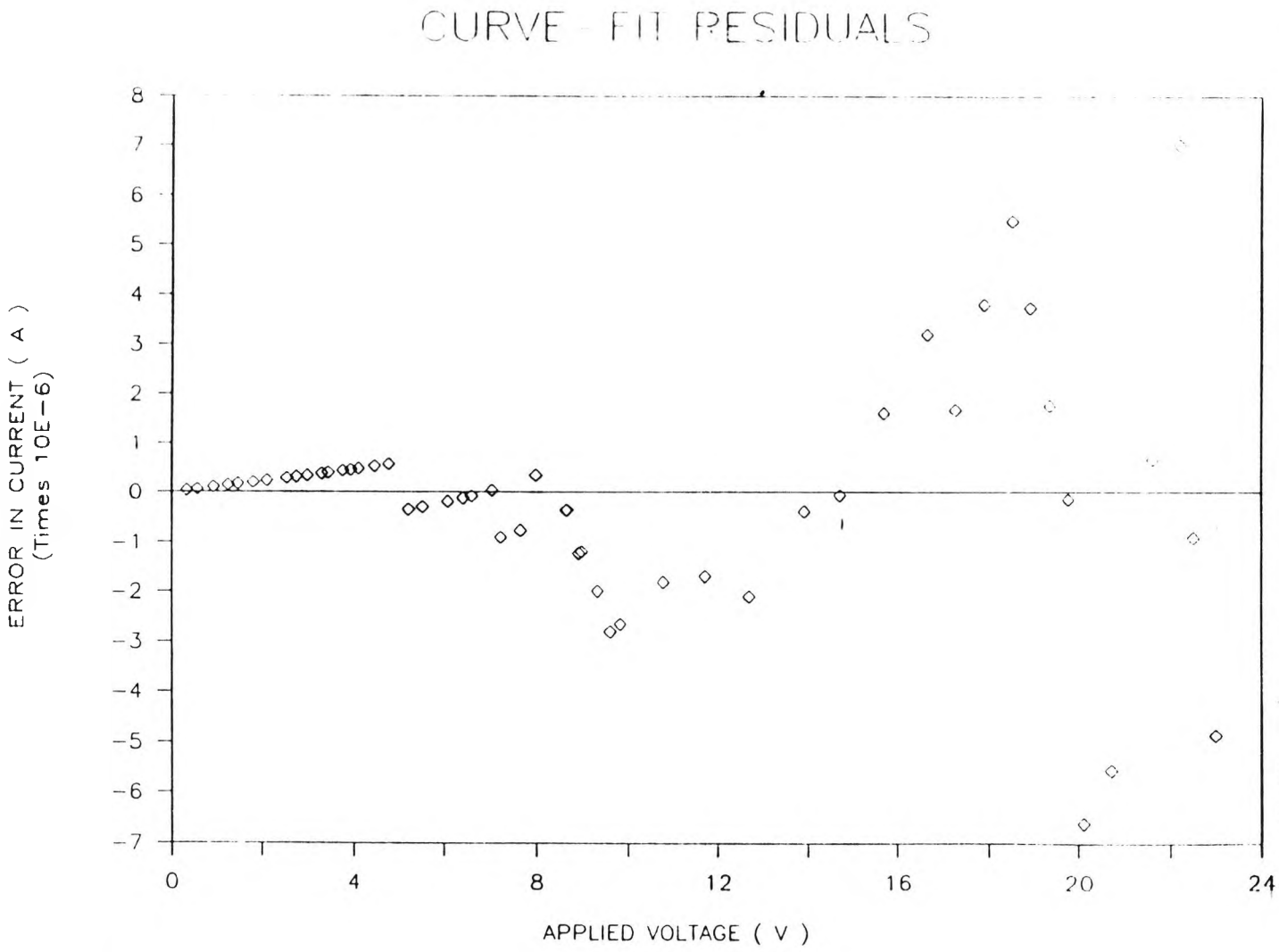

FIGURE 4.3 Curve-fit residual

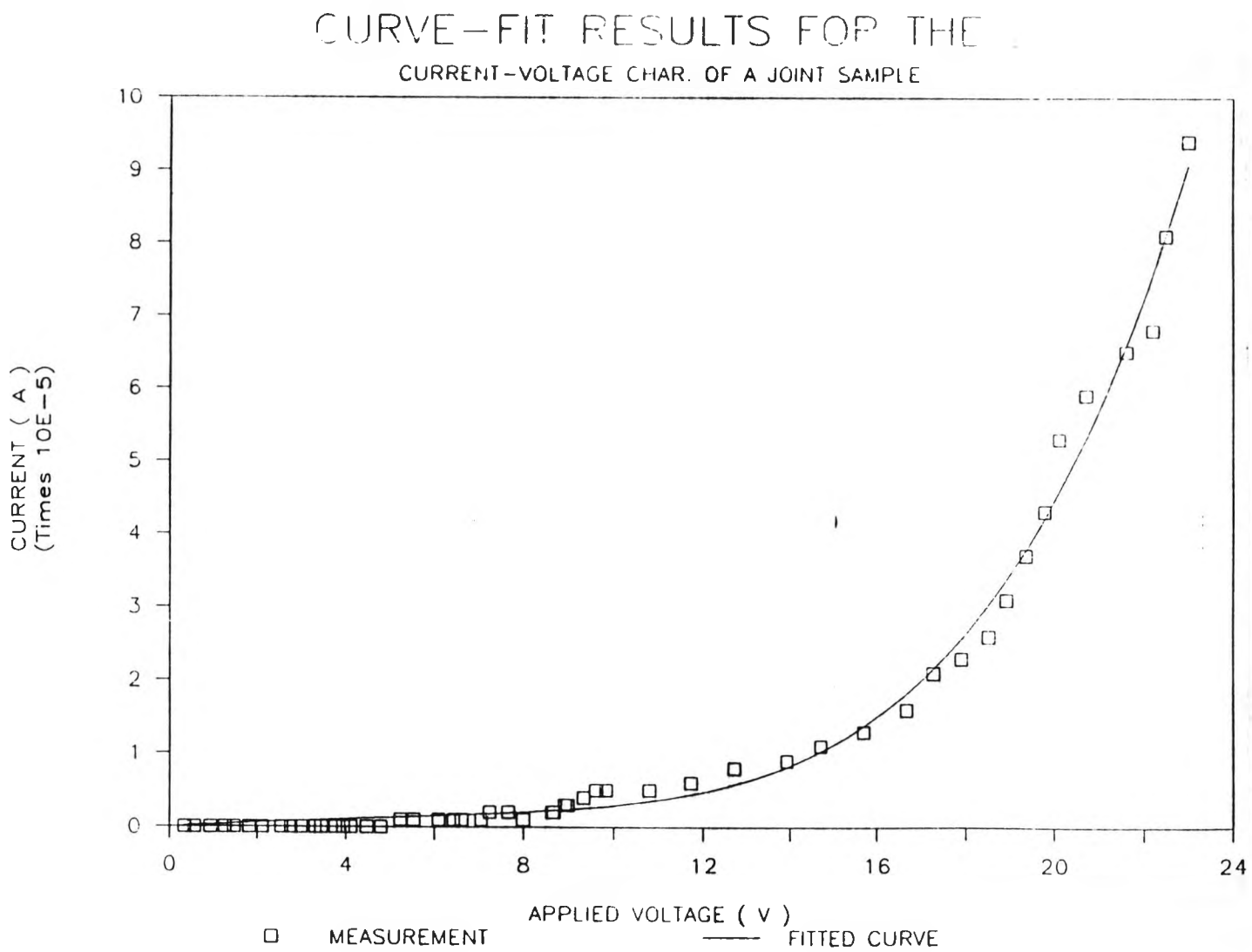

FIGURE 4.4 Curve-fit of the the current-voltage characteristic of a corroded joint

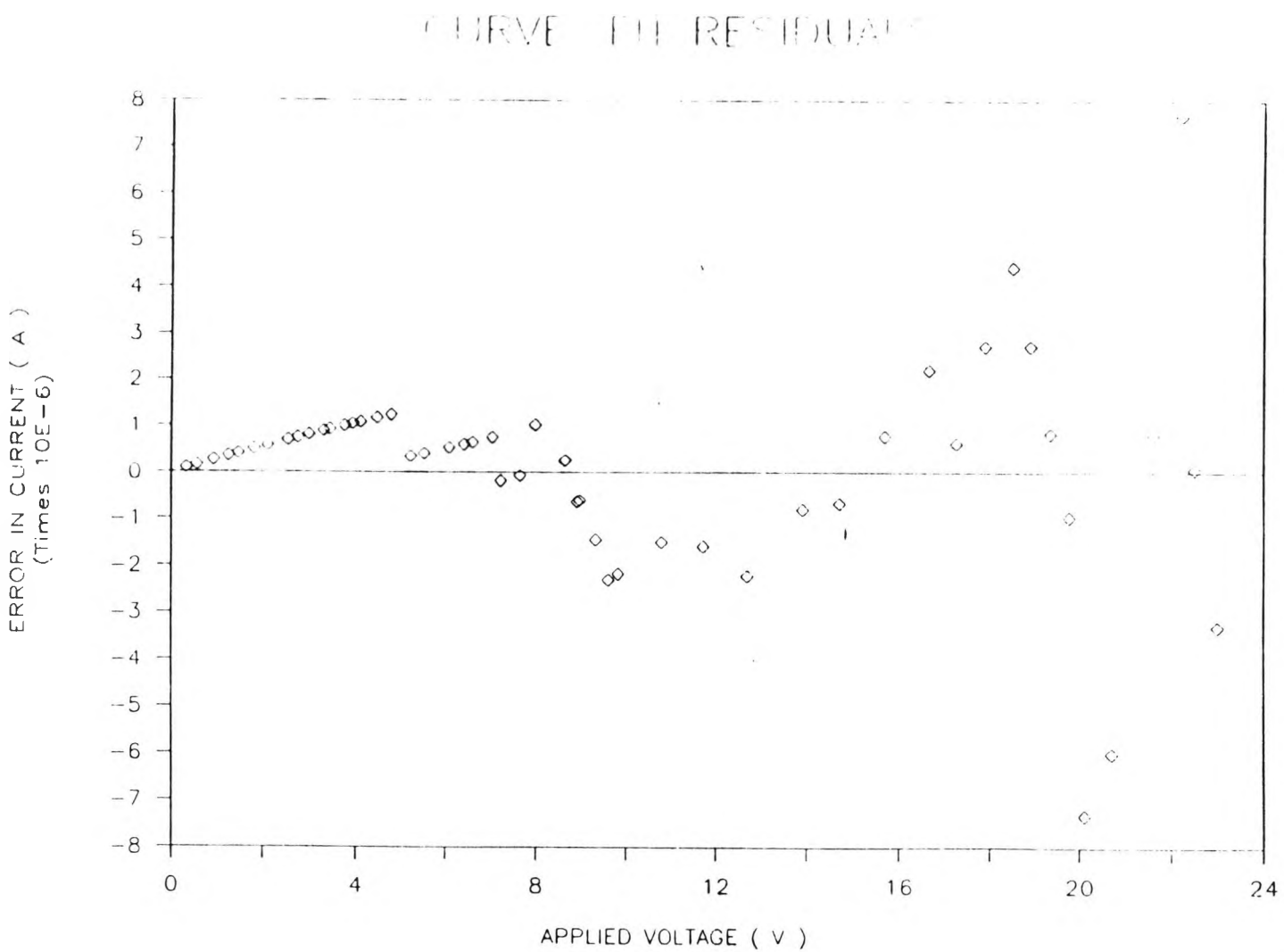

FIGURE 4.5 Curve-fit residual

Chapter 5

Effects of Environmental Conditions on Structural Intermodulation Interference

5.1 Introduction

In chapter 3, we have considered the mechanism by which intermodulation interference would appear under multiple frequencies transmission conditions. We have demonstrated that rusty joints are potential sources of intermodulation interference. In a lattice tower there are many bolted joints; all of which are potential intermodulation interference sources.

An one-off measurement was carried out by Betts and Debney (1980) on two operational lattice towers. They found that

with 30 watts two-tone test, the third order intermodulation power was about -67 dBm. Both new (one year old) and old (ten years old) towers produced similar readings.

It has been observed that intermodulation interference level could vary over 60 dB in a short space of time, and these variations were attributed to the changes in the atmospheric conditions. Until now, there have been no systematic studies on how does the climatic conditions affect the intermodulation level, as well as the mechanism of these effects.

In order to get a better understanding of the effects of environmental factors on the changes of intermodulation interference, field measurements were carried out to record long term weather data, and the corresponding intermodulation interference levels, so that possibilities of correlation among various weather parameters and intermodulation interference (IMI) level could be assessed, leading to a better understanding of the physical processes involved. In addition, laboratory experiments were also performed to determine and verify the possible causes of the observed IMI fluctuations.

5.2 Field Measurements

It is useful and necessary to conduct field trials so that long term weather and IMI data could be collected and correlated to see if there is any relationship among the

weather parameters and IMI.

5.2.1 Objectives of Field Trials

The aims of the field measurements were to :

(1) Observe the relationship among various weather parameters and IMI, qualitatively.

(2) Find out the frequency distribution of IMI level and the probability distribution function (pdf) of IMI level.

(3) Possible development of Regression Models for the IMI process.

5.2.2 Field Measurement Equipment Setup

The test site chosen, belongs to the Home Office, is at Sandridge, just outside London. This is a typical hill-top base station site with a lattice tower of height about 45 metres.

The test setup (see figure 5.1) is very similar to the laboratory test setup. It consisted of two crystal-oscillators at 152.2525 MHz and 154.0000 MHz respectively, driving two linear power amplifiers and the outputs from the power amplifiers were fed to two transmitting antennas (folded dipoles) on the mast. The

positions of the transmitting dipoles and the receiving dipole were such that there was at least 40 dB separation between each other). The receiving antenna picked up the interference level of the third order intermodulation product at 155.4705 MHz, which was displayed using a Rhode and Schwartz ESU2 Test Receiver. Readings of weather parameters, including windspeed, rainfall, and temperature, and intermodulation product levels were all recorded digitally by an IBM-compatible microcomputer via a data acquisition board. The collected data was then transferred back to the University via the public switching telephone network. The whole system was computer-controlled and required no operator intervention. A timer was built to trigger on the whole measurement system periodically.

The minimum IMI level which could be detected by the test receiver was -87 dBm with a dynamic range of about 70 dB. This setting was used because it gave the widest possible range of intermodulation interference level readings, and since the whole system was meant to be left alone, regular alterations of the settings was not desired.

From our experience, it was found that computerised remote data logging has the following advantages :

(1) A large body of data can be collected over a short period of time (the experiment can be run virtually twenty four hours a day, seven days a week).

(2) Operator intervention is not required and travelling is

minimized.

5.2.2.1 Validity of Weather Data

Windspeed : This was measured using an anemometer. It is a commercial product modified to output a pulse train, which has a pulse rate directly proportional to the windspeed. The pulse frequency was calibrated with the analogue meter provided and the accuracy is 1 knot (approximately equal to 1.93 m/s)

Rain : This was measured by a rain gauge which produces a electrical pulse for every millimetre of rainfall. In our study, the prime interest was whether the tower was wet or not.

Ambient Temperature : This was measured using an integrated circuit temperature transducer which has an accuracy of 2.5 degC over an entire range of -10 degC to 100 degC.

5.2.3 Structural Intermodulation Measurement

The field measurement was carried out over a period of three months in late 1988. During that period, both dry and wet weather was experienced.

The measurement process was triggered on by the purpose-built timer, and measurements were taken for five

minutes each hour, rather than in a continuous mode. In this way, a wider combinations of weather conditions could be accommodated without over-stretching the available computer main memory and backup storage. The sampling rate was set at one sample every ten second.

The power amplifier output was 50 watt for both fundamental frequencies in all measurements.

5.2.4 Qualitative Analysis and Discussion

In this section, both qualitative and statistical analyses were performed on the field trial data. This should prove a valuable exercise in understanding how IMI varies with weather conditions.

The collected data was divided into two groups, one group consists of dry conditions data and the other contains wet conditions data. A typical result for dry and wet weather conditions are shown in figure 5.2 and figure 5.3 respectively.

5.2.4.1 Quantitative Analysis - Dry Condition Data

g0919a (figure 5.2) : This was a continuous monitoring for 24 minutes at around mid-day. No evidence that there was any relation between windspeed and IMI, as can be seen from the two steady zones of IMI, one at the beginning, and one at

the end of the recording.

5.2.4.2 Quantitative Analysis - Wet Condition Data

g0927aa (figure 5.3) : A continuous plot of 21 minutes in the afternoon (1 pm, raining). High wind but it rained, hence the horizontal line of IMI sitting at -80 dBm.

5.2.4.3 Discussion

From these graphs, although it is not possible to put down a formula relating third order intermodulation interference level and various weather parameters, however, some comments can be made.

For dry weather,

(1) The nominal value of IMI level is about -65 dBm.

(2) Variations of IMI level could be over -40 dB.

(3) High wind does not always cause large IMI.

(4) Changes in windspeed causes IMI level to rise/fall. However this change is not in any linear fashion. In between increase/decrease in windspeed, IMI level could be quite stable.

(5) Changes in temperature cause rise/fall in IMI level. Again, not in linear fashion.

The third order intermodulation interference level was never below -90 dBm during these measurements. Bear in mind that the Home Office specification for the maximum level of all unwanted signals and noise combined must be below -127 dBm, the observed intermodulation interference level was unacceptably high, and highlighted the importance of intermodulation interference reduction procedures.

The activities of wind compress the oxide layer between the interfaces of tower beam members, and should help reducing IMI by providing possible metal to metal contacts and lower contact resistance. However, this process could also cause the formation of metal-oxide-metal contacts in other parts of the tower, hence nullify the effect of compressing oxide films at some of the junctions.

For Wet Weather,

(1) Undoubtedly, when it rained the IMI level dropped right down to the measurement system floor level. From figure 5.3, it can be seen that while the tower was wet, even high wind did not induce significant IMI.

5.2.5 Statistical Analysis and Discussion

In previous section, the general effects of wind, temperature and rain on IMI level were described. In this section, attention was paid to investigate whether there exists any functional relationship between the environmental factors and the third order intermodulation interference level.

5.2.5.1 Frequency Distribution of IMI Levels - Dry Weather

All data from the dry weather records were used to plot a frequency distribution curve, so that the trend of intermodulation level distribution could be assessed. The frequency distribution curve is shown in figure 5.4. It can be seen that the most probable IMI level is about 55 dBm. The minimum was at 85 dBm and the maximum was at 15 dBm.

The frequency distribution looks remarkably close to the Gaussian distribution curve, and a curve-fitting of a Gaussian distribution model using the available data was performed. The model takes the following form :

$$Y = \frac{P_1}{P_2} \exp\left(-\frac{(X - P_3)^2}{(P_2)^2/\pi}\right)$$

where,

Y = number of occurrence

X = intermodulation level

p_1 = a multiplication factor

p_2 = $\sqrt{2\pi}\sigma$ and σ is the standard deviation of the distribution

p_3 = mean of the distribution

The curve-fit result is shown in figure 5.5. It can be seen that the fit is reasonably compatible with our proposed model, and the parameter values are as follow :

p_1 = 6899.63 (374.382)

p_2 = 15.7187 (0.98498)

p_3 = 57.8132 (0.39291)

Standard deviations of the parameter values are shown in brackets.

The correctness of the model is demonstrated by the randomness of the residual plot shown in figure 5.6. In addition, the correlation coefficient between the parameters is 0.6 for p_1 and p_2; 0.0001 for p_1 and p_3; and 0.0001 for p_2 and p_3. Therefore, it can be seen that the model is theoretically sound, and we can assume that the mobile radio base station site IMI level follows a Gaussian distribution.

The percentage errors for p_1, p_2 and p_3 are 5.4%, 6.3% and 0.7% respectively. Since the percentage errors are very

small, the goodness of fit is excellent in this case. With these parameters, the mean value of test site intermodulation level is -57.8 dBm.

Turning to the cumulative frequency distribution graph in figure 5.7, it is observed that over 50% of the intermodulation level data points are above 60 dBm which shows the seriousness of the problem.

5.2.5.2 Frequency Distribution of IMI Levels - Wet Weather

It is a completely different story for site intermodulation interference level under wet conditions. From the frequency distribution curve in figure 5.8, it clearly shows that when it was raining, the intermodulation level dropped below 80 dBm (the measurement system floor level). Since the measurement system was preset to record IMI levels within the range between 10 dBm to 80 dBm, therefore, any data value below 80 dBm was registered as 80 dBm. It is, therefore, impossible to interpret from the curve about the type of distribution exhibited by the wet condition IMI levels. From the cumulative frequency distribution graph in figure 5.9, it can be seen that over 65% of the readings are at (or indeed below) the system measurement floor level. Under wet condition, the reduction in site intermodulation level is really very dramatic, by more than 20 dB. In a later section, the effects of water on intermodulation interference will be investigated thoroughly, to establish the responsible mechanism behind this large fall in IMI

level.

5.2.5.3 Relationship between Windspeed and Site Intermodulation Product Levels

In the qualitative analysis section, we have seen that when it rained, the intermodulation level dropped to the measurement system floor level irrespective of the values of other environmental factors, such as windspeed. Therefore, in this section, only the data from dry weather records were used.

A scatter diagram of all the data points is shown in figure 5.10. It can be seen that with a specific windspeed value, the corresponding intermodulation level values have a very wide span, of over 50 dB.

In an attempt to draw something meaningful out of the data, we have, for each windspeed, taken the average value of the recorded intermodulation levels, and attempted a linear regression with the resultant data. The result is shown in figure 5.11.

The trend of the data points indicates that when the wind gets stronger (i.e. windspeed is higher), intermodulation level increases; except for the last data point at windspeed equals to 8 knots. From the graph, it can be seen that the static wind (i.e. windspeed less than 1 knot) intermodulation interference level can be as much as 7 dB

lower than non-static wind intermodulation levels.

The regression line shows a negative gradient, indicating that an increase in windspeed will cause the intermodulation interference level to fall, which disagreed with our discussion above. However, we must be very careful in interpreting the graph. If we ignore the last data point (i.e. at windspeed equals zero), then the rest of the data points would fit equally well in a regression line with positive gradient. Indeed the error percentage of the estimated x-coefficient is over 140%; an indication of the high uncertainty of the estimation due to the wide scattering of the data.

From above, we could see that the effects of wind on the site intermodulation interference level is highly random, i.e. high windspeed could cause high IMI level at one time; and low IMI level at another time. Having said that, it is not really a big surprise. This can be explained by the fact that assuming the presence of an oxide layer between structural members is a necessary condition for the production of intermodulation interference, then under the action of wind loading, the non-linear characteristic (i.e. the coefficient values in the power series representation of the non-linear characteristic) of these oxide layers will keep on changing as well. Therefore, the same windspeed normally would not produce the same intermodulation interference level even on the same tower. All we can talk about is the long term average site intermodulation interference level.

5.2.5.4 Relationship between Temperature and Site Intermodulation Product Levels

It is a common experience that temperature changes tend to be gradual rather than abrupt, and since our record period is about five minutes per hour, therefore, temperature effect would not show up in a single record. We have displayed the relationship between site temperatures and the site intermodulation levels in the scatter diagram (see figure 5.12), using all the data from dry weather condition. It can be seen that the variations in intermodulation level for a particular temperature can be as high as 30 dB. Similar to windspeed data it would be impossible to interpret anything from the data without preprocessing them. We performed the same procedure, i.e. for each temperature value, we computed the average value of the corresponding intermodulation interference level. The resultant graph is shown in figure 5.13. A linear regression line is also shown in the same graph. It is clear from the regression line that as temperature rises, the associated intermodulation interference level increases as well. This time, the x-coefficient has a percentage error of over 25%, and the linear law should be looked at with some reservation.

Although the functional relationship between temperature and intermodulation interference level data is not exact, nevertheless, the possible mechanism due to temperature effect can be discussed. The most probable mechanism involved is that the tower is normally heated by the sun on one, and no more than two sides, therefore, differential

expansion of the tower members that are exposed to direct sunlight would cause the oxide layers to be compressed, thus changing the non-linear contact resistances by possible metal-metal contacts, and reduces/increases resultant intermodulation interference level.

5.2.6 Conclusion

It was found that environmental conditions do cause the intermodulation interference level to vary; sometimes, significantly. In general, wind is capable of producing large changes in the intermodulation level in a very short period (as short as 5 seconds); though no relationship between windspeed and intermodulation level has been established. Similarly, site ambient temperature does produce some changes in intermodulation level and differential expansion of the tower members is thought to be the mechanism responsible for it. Finally, rain was found to produce the most dramatic effect on the intermodulation level : when it rains, intermodulation interference level drops back to the measurement system floor level; a fall of at least 30 to 40 dB.

In addition, it was found that the occurrence of a particular site intermodulation interference level follows Gaussian distribution. Since each base station site has its own electrical and climatic environment, it is reasonable to assume that the mean site intermodulation interference level can differ from each other.

5.3 Laboratory Experiments (1) - Effect of Water

From the field measurement data it can be seen that when it rained, the intermodulation interference level of the third order product dropped significantly. It has been suggested that high permittivity of rain water is responsible for the observed reduction in the intermodulation interference level; while others have suggested that conductivity of water due to the presence of impurities is the main cause. In this section experiments were performed to examine which factor is the dominant one.

5.3.1 Initial Laboratory Experiments

We have performed some controlled experiments to see how water would affect the intermodulation interference levels of our corroded joints samples.

5.3.1.1 Experiments

In this experiment five corroded joint samples were used. Firstly, their initial intermodulation interference levels were measured. Secondly, their intermodulation interference levels when they were wet were noted. The method used to wet these samples was as follow:

With the sample in the test jig, a piece of plastic was placed under the sample (to content any water), then wet

cotton wool was used to cover the joint completely. The lid of the test jig was closed and the intermodulation interference level was then measured.

5.3.1.2 Results and Discussion

The measurement results are as follow:

Sample	initial IMI (dBm)	IMI when wet (dBm)
IM5-25A	-55	-74
IM5-25B	-62	-70
IM5-25C	-57	-68
IM5-25D	-46	-67
IM5-25E	-53	-71

For these measurements, the background intermodulation interference level was at -90 dBm.

It can be seen that water does have an effect on reducing intermodulation interference levels. For these samples the average reduction in the intermodulation level was about 15 dB, a significant amount.

5.3.2 Effects of Conductivity and Permittivity of Water on IMI

Having shown that water does have a role to play in reducing intermodulation interference level, we seeked to explain what causes this fall in intermodulation level ? Is it due to the high permittivity or the high conductivity of water ?

In general, electrical conductivity of pure water is very low because there is no free ions for conduction. The conductivity of water is somewhere between 10^{-7} Scm^{-1} for deionized water to 10^{-3} Scm^{-1} for tap water. Conductivity might increase due to carbon dioxide in the atmosphere dissolving into the water. In addition, in industrial areas, acidic rain (mainly due to dissolved SO_2 and CO_2 gas) and other impurities would add in the effect of increasing the ionic conductivity of rain water.

5.3.2.1 Experiments - Effects of Liquid Conductivities

In this experiment, four groups, each of three corroded rod samples were used. Different groups were treated with water of different conductivity by dipping the samples into appropriate solutions before testing. Intermodulation interference levels of these samples before and after experiments were measured, and the changes in the intermodulation levels were then calculated.

Water of different conductivities were prepared by adding different amounts of sodium chloride powder into deionized water, and mixed them well. Conductivities of the solutions were measured using a conductivity meter (Irwin Conductivity Meter Type EA 1153) which has a measurement range between $5 * 10^{-7}$ Scm^{-1} to 1 Scm^{-1} with +/-5% accuracy.

The intermodulation interference level measurement results are shown in figure 5.14.

5.3.2.2 Experiments - Effects of Liquid Permittivities

Next, the effect of permittivity on intermodulation interference level was investigated by applying liquids of lower permittivities than water to another batch of samples. In this experiment, glycol (ε_r= 45) and silicone oil (ε_r= 2.2) were used. The results are shown in figure 5.15. Other liquids, like acetone, ethyl alcohol and nitrobenzene were not used, either because of their high flammability or their high toxicity.

5.3.3 Results and Discussion

From figure 5.14, it can be seen that higher conductivity liquid did show a larger improvement in intermodulation level. Deionized water had the least improvement of about 23 dB, while concentrated salt solution had an improvement of 30 dB. However, looking at the conductivity of deionized

water (1.86 * 10^{-6} Scm^{-1}), it seems unlikely that this conductivity will be sufficient to provide any rf current bypassing effect, which could reduce intermodulation level by 23 dB. Especially when the conductivity increased by nearly 14,000 times (from deionized water to concentrated salt solution), the intermodulation level was only reduced by further 7 dB. Indeed, in a later experiment, some graphite-based coatings (resistivity of about 100ΩΩ, much lower than deionised water) were used to coat rust samples, and there was no improvement in intermodulation levels at all.

Furthermore, referring back to the copper plating experiment in Chapter 6, section 6.3, it was demonstrated that copper plating (conductivity = 5.8 * 10^{9} Scm^{-1}), which has a substantially higher conductivity than deionized water, produced only similar amount of intermodulation interference level reduction. Therefore, conductivity of water is unlikely to be responsible for the observed drop in intermodulation level. We will look at the contribution from the permittivity of water.

It has been known that water has a very high relative permittivity of 80 at zero frequency, and the variation of its relative permittivity with frequency has also been investigated. The relative permittivity versus frequency diagram is shown in figure 5.16 for water at 25 degC. From figure 5.16, it can be seen that the relative permittivity of water drops as the applied frequency goes up. However, at the VHF band (i.e. around 150 MHz), the relative

permittivity of water does not deviate from the d.c. value of about 80 by any noticeable amount. We can therefore safely assume that when there is water, the joint capacitance of our corroded test sample will increase accordingly.

We will look at the amount of intermodulation interference level reduction due to the increase in joint capacitance. The intermodulation power equation, described in Chapter 4, is repeated below for convenience. Again, assuming the two fundamental frequencies are close, then their capacitive reactance with respect to the joint, would be very similar. Thus, the intermodulation power equation (Chapter 4, equation 4.15) is applicable :

$$P_{3im} = \frac{9}{32} a_3^2 P_T^3 \frac{1}{R_L^4} \left(\frac{d}{\omega \varepsilon A}\right)^8 \qquad (4.15)$$

We have assumed that the relative permittivity of the corrosion products is about 15. Then when water is present, the relative permittivity will increase by about five times, and from equation 4.15, the resultant intermodulation level will be :

$$P_{3im}(\text{water dielectric}) = P_{3im}(\text{oxide dielectric}) \times \left(\frac{1}{5}\right)^8$$

$$= P_{3im}(\text{oxide dielectric}) - 56 \text{ dB} \qquad (5.1)$$

From equation 5.1, it can be seen that the presence of water will reduce the intermodulation level by as much as 56 dB theoretically. In practice, the reduction level that had been observed were between 10 dB to 30 dB, depending on how

well the water film distributes over the junction area.

5.3.4 Further Experiments

Further evidence to support the high permittivity theory is that, ice, though is the same compound as water, has a significantly lower relative permittivity than water (see figure 5.17). From figure 5.17, it can be seen that at 20 KHz, the relative permittivity of ice drops to about 5, and would reach a value of about 3 at even higher frequency. We would therefore expect that there would not be any reduction in intermodulation level when a wet corroded sample is frozen.

Experiments were conducted to prove this prediction. A batch of three corroded samples were covered with cotton wool soaked with tap water and the reduction in intermodulation levels were noted; then, they were placed inside a freezer until ice formed, and their intermodulation levels were re-measured immediately when they were just out of the freezer, and were also measured around five minutes later. Measurement results are shown below.

(All measurements are in dBm)

Sample	after corrosion	after dipped in tap water	after freezing	5-min after defrosted
A	-31	-74	-40 to -50	-80
B	-43	-61	-39 to -54	-76
C	-45	-65	-37 to -48	-79

From above, it can be seen easily that after dipped in tap water, the intermodulation levels of all three samples dropped. When they were frozen, the intermodulation levels of the joints rose again between 20 dB to 28 dB, as expected. When the ice melted and the joints were wet again, their intermodulation interference levels dropped to low levels, again, as expected.

From above, it can be said that, during rainy days, the observed large reduction in intermodulation interference level was due to the presence of high permittivity water film, which provides a low reactance rf current path across the corroded junctions. The conductivity of rain water, being too small, has no effects on intermodulation level reduction.

5.4 Laboratory Experiments (2) - Effects of Wind Loading

5.4.1 Introduction

The dynamic response of a structure to wind is deflection. There are two components in the deflections of a tower in the direction of wind. A mean component due to the average windspeed over an averaging period of about one hour, and a fluctuating component of random amplitude due to wind turbulence. In general a low frequency quasi-static response to the fluctuating windspeed determines the random amplitude. The low frequency quasi-static deflections have a broad spectrum peaking at about one minute. Tower deflections increase approximately as the square of the wind velocity and thus only the more severe storms are likely to cause any significant deflections. The wind mechanism responsible for rare storms in United Kingdom is normally the large cyclonic weather systems crossing from west to east, which cause the strongest winds. Depression centres of these winds usually pass north of United Kingdom and the associated winds circulate anti-clockwisely, blow more from the west.

5.4.2 General Observations

From the visits to the test site, it was found that when there was strong wind blowing, the intermodulation interference level tend to be high (since the test receiver is tuned to a particular intermodulation frequency, and with

the test receiver speaker switched on, then, the presence of that third order intermodulation product will cause the speaker to produce some noise, and the loudness of which depends on the level of the received intermodulation product). It is therefore logical to associate such jumps in the intermodulation levels with vibrations of the tower structure under wind loading.

It cannot be overemphasis that it is the vibration of the tower which causes the compression and relaxation of the corrosion product films at the tower joints, and results in the variation of intermodulation interference level.

5.4.3 Experimental

The ultimate effect of wind on any structure is to produce deflections and vibrations (either in large or small scale); so in this experiment a mean to vibrate a sample was necessary. Since the small sample was clamped between the sample holder tightly, it is virtually unmovable, and therefore, the more flexible large steel flat samples were used. The test setup was the same as that shown in block diagram 3.8, except that the sample holder was the one for the large steel flat samples, as shown in figure 3.16c.

Initially it was thought that an electromagnet would be used to vibrate the sample. However, the presence of any ferromagnetic object other than the sample was seen to be undesirable. So another approach was adopted. A piece of

string was tightened around the corroded joint of the large sample. When the signal generators and power amplifiers were switched on, the steady value of intermodulation level was noted. The string was then pulled and released at a rate of about 1 Hz approximately. It could been seen on the spectrum analyser that the intermodulation level varied up and down by more than 5 to 10 dB; and instead of a single intermodulation interference frequency f_{im}, the interference signal spreaded around f_{im}. The sideband frequency components had power level about 10 to 20 dB lower than the third order intermodulation level, and their levels were changing all the time.

5.4.4 Discussion

The variation of the intermodulation interference signal level was due to the fact that when the joint was vibrating, the oxide layer was compressed, and redistributed itself over the interface. The resultant nonlinear characteristic of the joint would be modified continuously under the action of wind-loading, hence the varying intermodulation interference levels resulted.

The mechanism responsible for the spreading of the intermodulation interference signal is due to the fact that when the joint is flexing, it modulates the fundamental signals mechanically, hence, produces a low level wideband noise.

5.5 The Role of Oxide in Intermodulation Interference Generation

5.5.1 Oxides or No Oxides ?

It has been observed by several researchers, notably Watson (1980) and Kellar (1984), that loose connections and contacts could generate a high level of intermodulation interference; and securely tightened connections always have lower intermodulation interference levels. The effects of increasing applied pressure at metallic contacts on intermodulation interference level have been investigated by Bayrak and Benson (1975) and Martin (1978). However, there has been no explicit study on whether the presence of an oxide layer is essential for the production of intermodulation interference. In chapter 3, we have demonstrated that (galvanised) structural steel-corrosion products junctions are non-linear; but the oxides themselves could have linear resistance characteristics. In the following sections, investigations were carried out to look at the possibilities of interference generation by clean (free of any corrosion products) joints, as well as Ohmic metal-metal oxide junctions.

5.5.2 Experimental

In this section, we are interested at the effects of contact resistance variations for a 'clean' contact and a 'corroded' contact. In general, metal surfaces are not completely flat;

especially with hot-dipped galvanised steel, the surface is rough. Therefore, the contact area between the structural members would be much smaller than the overlapping area, and the contact resistance would be large. The contact resistance would increase and decrease under the action of wind loading. Therefore a model of a flexing Ohmic (linear) joint could be as shown in figure 5.18, which composed of a variable resistance, whose value is a function of the tower vibration. Similarly, a model of the flexing non-linear joint could be as shown in figure 5.19 where changes in the non-linear joint characteristic is represented by the addition and removal of a diode-pair.

5.5.2.1 Laboratory Experiments

In order to test the ideas about varying joint resistance, the two models for linear and non-linear joint were implemented using appropriate components, and the test setup is shown in figure 5.20. The switching action was performed by a small electromechanical relay controlled by an external oscillator, whose oscillating frequency was set at about 10 Hz. Input fundamental powers of 0.02 watts (13 dBm) at f_1 and f_2 were directly from two synthesised signal generators.

As a control experiment, the effect of a contact on its own (see figure 5.21) was also tested, which could give a figure for the background intermodulation level.

The effects of both changing linear and non-linear

resistance were evaluated by turning on the oscillator, and the intermodulation interference level was observed on the spectrum analyser.

5.5.2.2 Results and Discussion

The interference/intermodulation levels at the third order intermodulation product frequency, under 'static' condition (i.e. the relay was not switching) are shown below for the two configurations :

circuit (figure)	contact closed	contact opened
5.18	-85	-87
5.19	-40	-30
5.21	-85	-95 (background level of test system)

For the configuration in figure 5.21, the third order intermodulation product level of 85 dBm can be regarded as the background third order intermodulation interference level for this particular test setup, i.e. intermodulation interference due to external non-linear elements, such as connections and cables. From the results, it can be seen that, under static conditions, for a non-linear joint, an additional non-linear resistance increased the intermodulation level, by 10 dB. This increase in intermodulation level is clearly due to the added

non-linearity. In contrast, adding a resistance in series with a linear resistor reduced the resultant interference level. The added resistance reduced the current flow in the circuit, i.e. less current flew through the external non-linear elements; hence, a smaller intermodulation interference level.

When the relay was driven by an oscillator running at about 10 Hz, it was observed on the spectrum analyser that for the circuits in figure 5.18 and figure 5.19, the intermodulation levels moved up and down between the values shown above. No significant wideband noise was observed. However, with the circuit in figure 5.21, wideband noise was observed, with very low level at about -90 dBm; and the spectrum varying all the time; although the level was the highest for the third order intermodulation frequency component (about -85 dBm), due to the contribution from the residual third order intermodulation level from the external non-linear elements.

In the first two situations, the addition of extra resistance (either linear or non-linear) in series with the load resistance could result in a current too smaller to produce detectable wideband noise; however, in the later case (as modelled in figure 5.21), it represents an extreme case whereby there is momentary disruption and total reflection of the rf current flow, which is unlikely to happen in real life situation. Direct switching of the rf current (similar to modulation) resulted in a higher wideband noise level, which could be observed on the spectrum analyser.

From above, it can be seen that :

(1) Variations in non-linear joint resistance will change the intermodulation level by changing the non-linear characteristic of the joint.

(2) Variations in linear joint resistance will cause variations in the current amplitude; and if there is any external non-linear elements present, will increase or decrease the rf current flow into the non-linear elements, thereby, increase or decrease the observed intermodulation interference level (due to the external non-linear elements).

(3) From (1) and (2), it can be said that variations in pure linear resistance would not generate appreciable intermodulation interference; and the presence of non-linear element is necessary for producing significant intermodulation interference levels.

As far as the experimental evidence is concerned, if the structure is absolutely clean without a trace of oxide, then vibration of the tower would produce extremely low level of intermodulation interference. However, normal hot-dipped galvanized steel would produce a layer of zinc oxide on its surface when it comes off the plating bath, because the bath temperature is well over 400 degC, and the formation of oxide layer is unavoidable. Therefore, a clean new tower structure does not mean it is free of oxide. In Chapter 3, we have demonstrated that zinc oxide/metal junction is also

non-linear and produces intermodulation interference.

5.6 Conclusion

It was found that environmental conditions do cause the intermodulation interference level to vary; sometimes, significantly. In general, wind is capable of producing large changes in the intermodulation level in a very short period (as short as 5 seconds). Similarly, site ambient temperature does produce some changes in intermodulation level. Finally, rain was found to produce the most dramatic effect on the intermodulation level : when it rains, intermodulation interference level drops back to the measurement system floor level; a fall of at least 30 to 40 dB.

It was also found that the site intermodulation interference level follows Gaussian distribution.

Laboratory experiments were performed to investigate the mechanisms responsible for the observed environmental influence on site intermodulation interference level.

From the experimental results, it was shown clearly that water does reduce intermodulation level by a large amount. Furthermore, it was found that the high permittivity of water, rather than its conductivity, is responsible for the observed immediate reduction in intermodulation level.

Considerations were also given to the effect of joint vibration on the intermodulation level. In the experimental section, lumped circuit model of a joint was built and the mechanical switching action was performed by a relay. The experimental results confirmed that vibrating clean joint is able to generate low level wideband noise; and the presence of any non-linear components increase the effect of intermodulation interference.

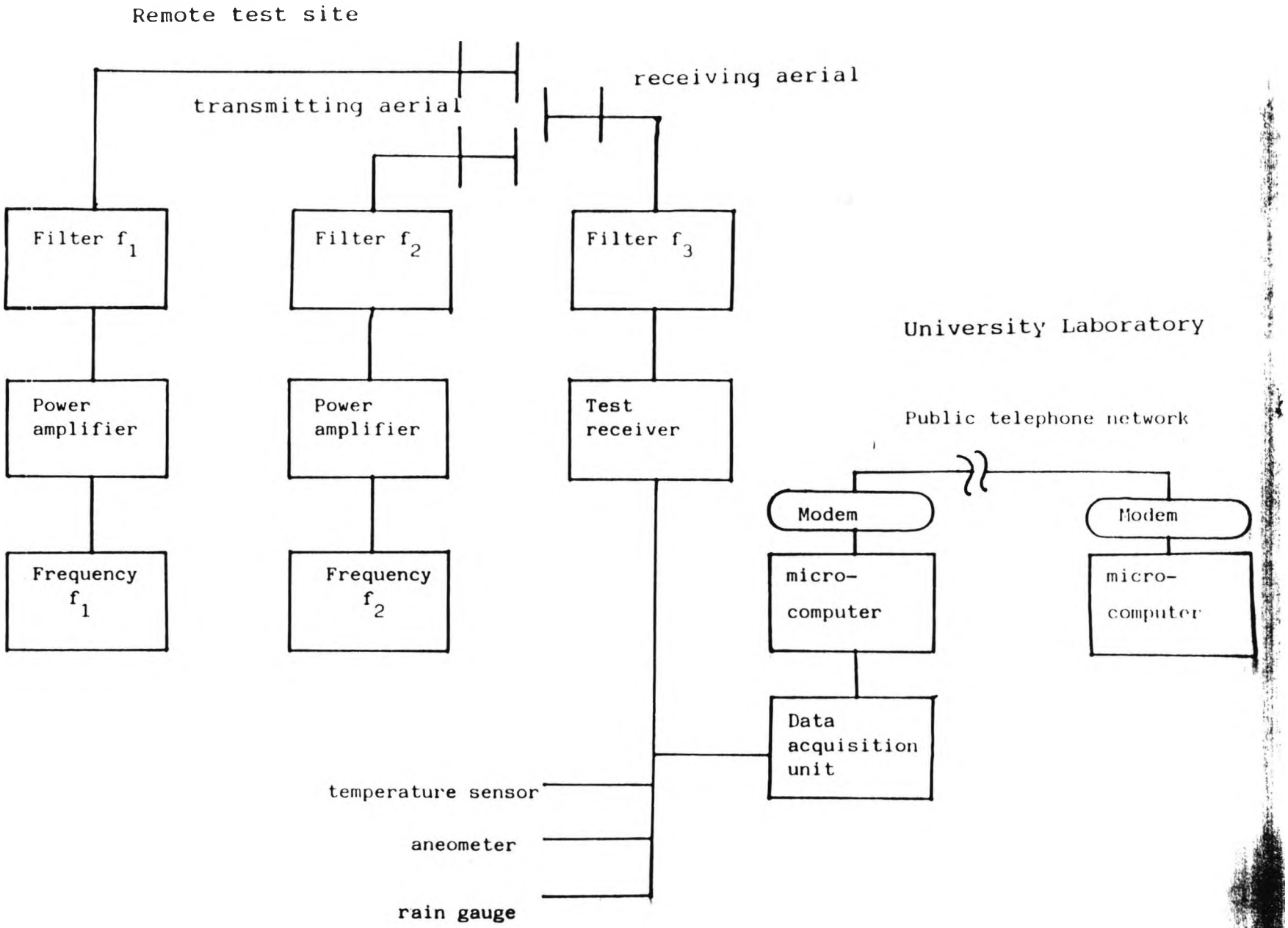

FIGURE 5.1 Field measurement setup

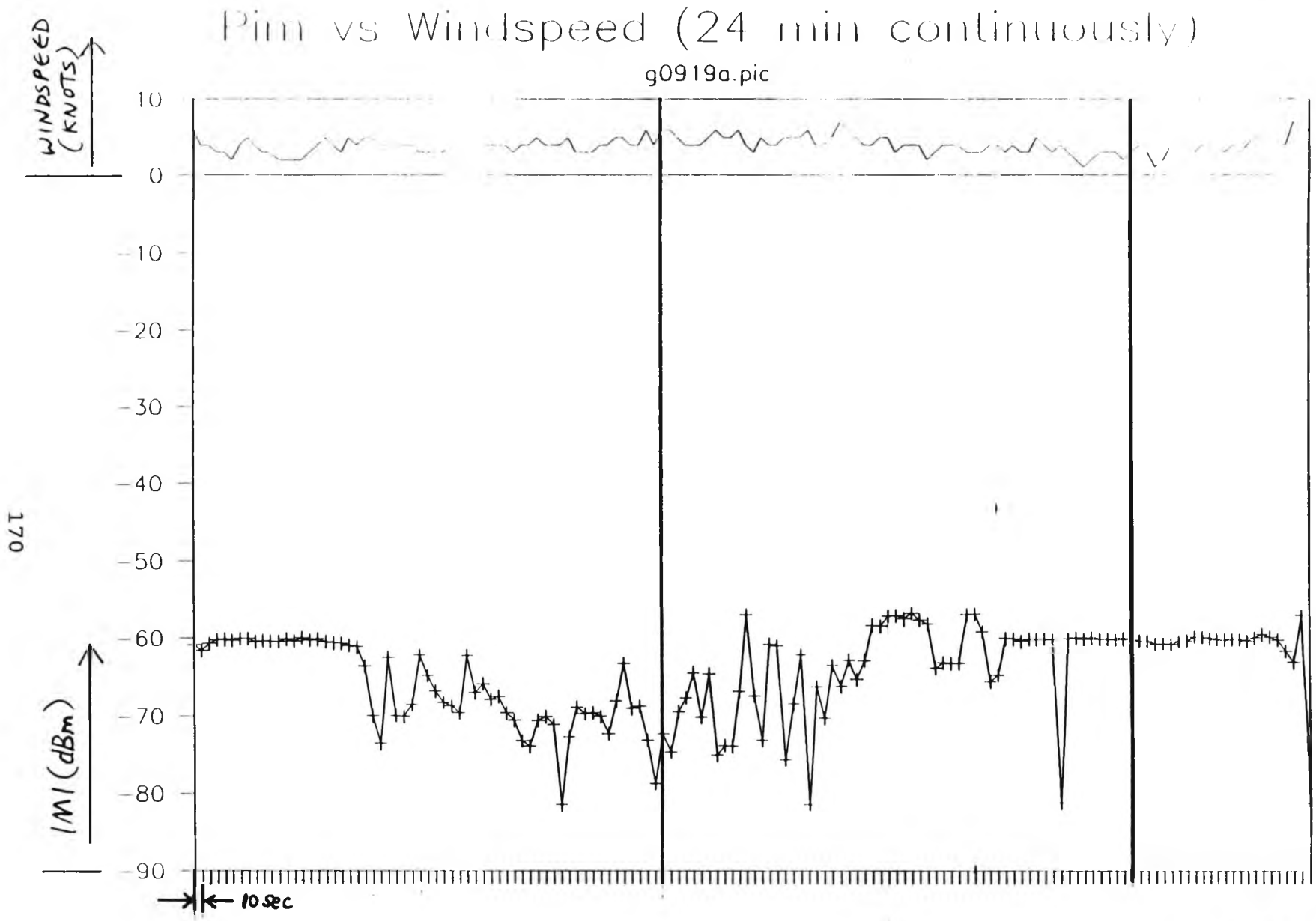

FIGURE 5.2 Weather data graph (dry condition)

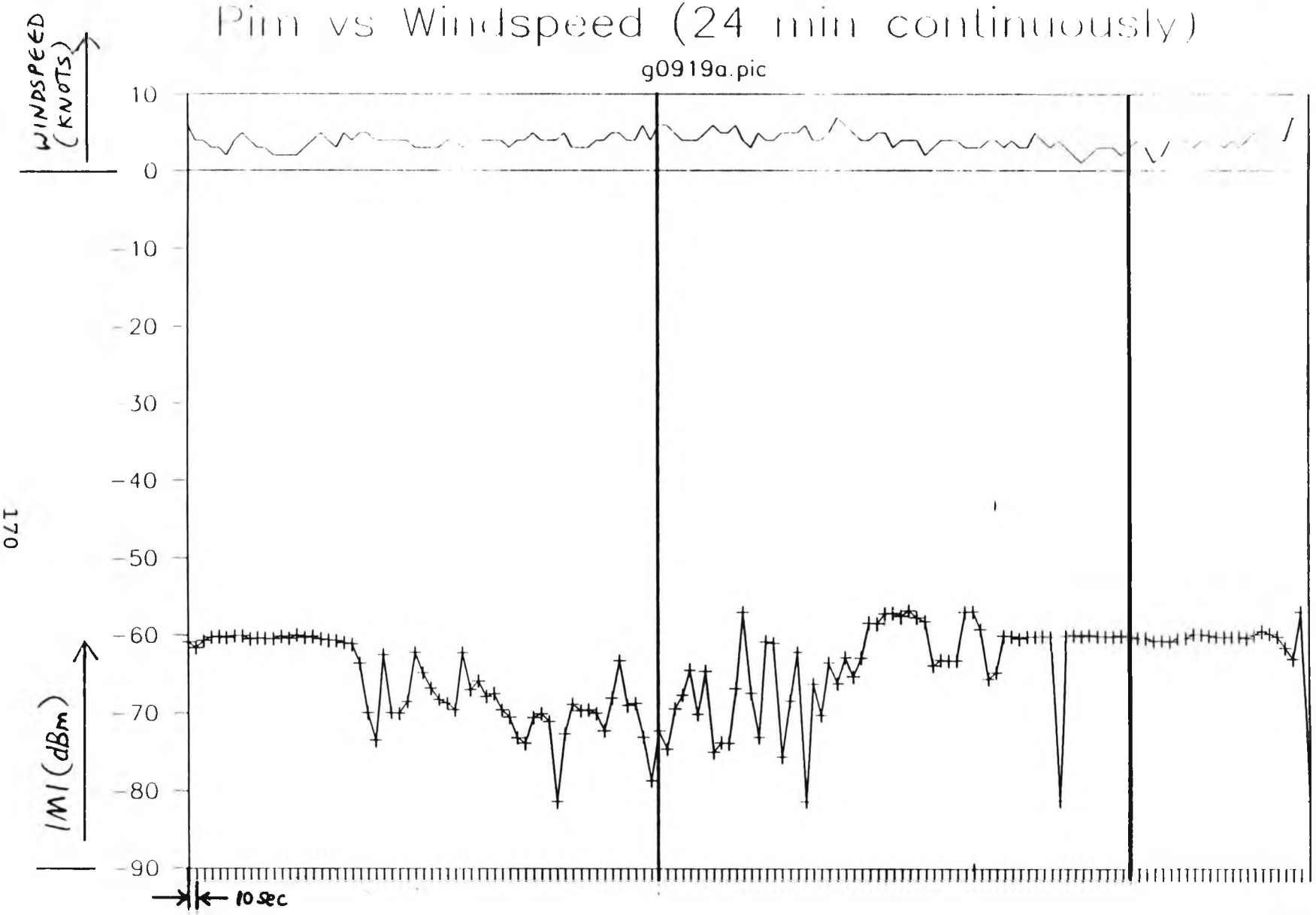

FIGURE 5.2 Weather data graph (dry condition)

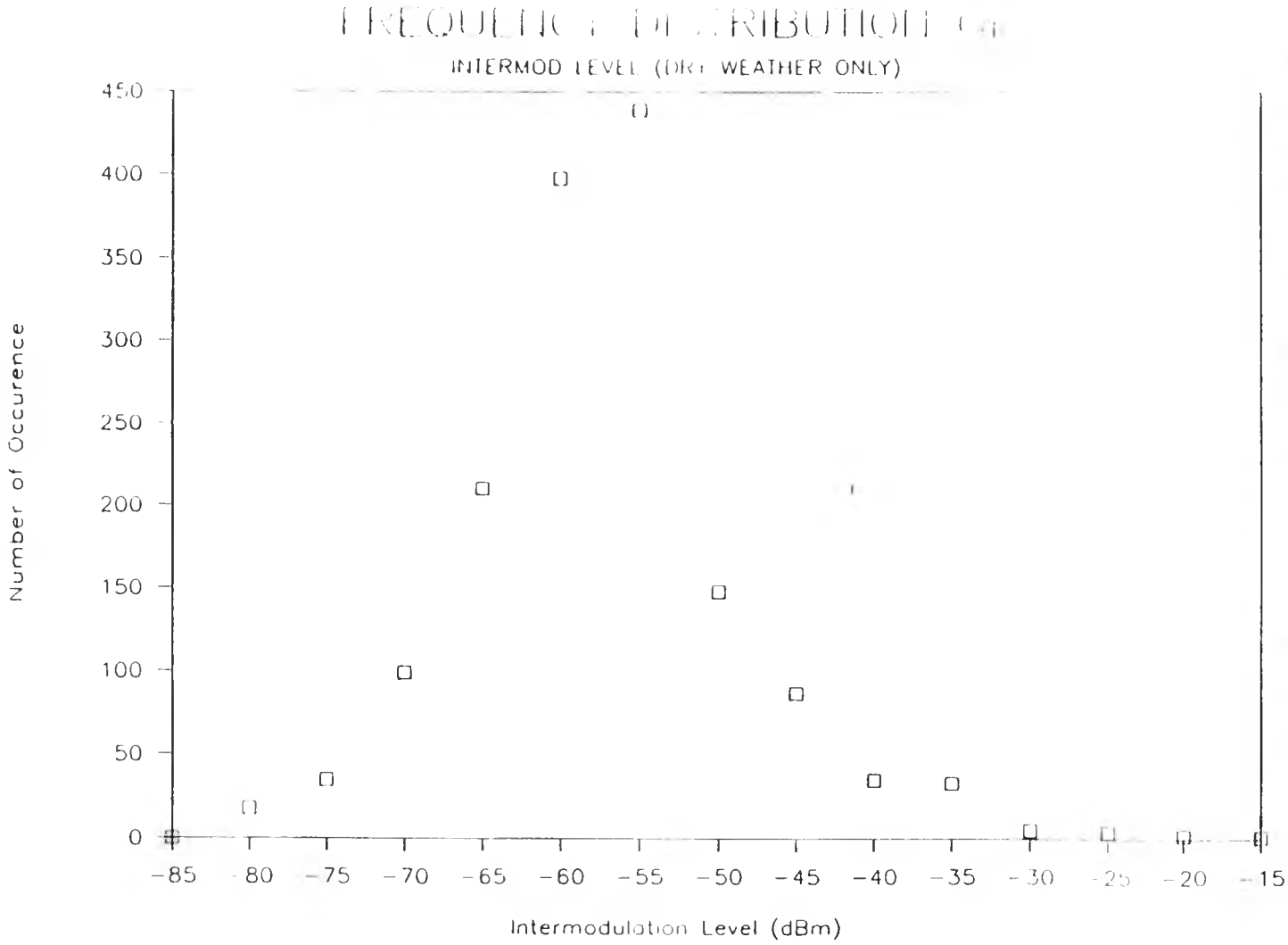

FIGURE 5. 4 Frequency distribution of IMI (dry weather data only)

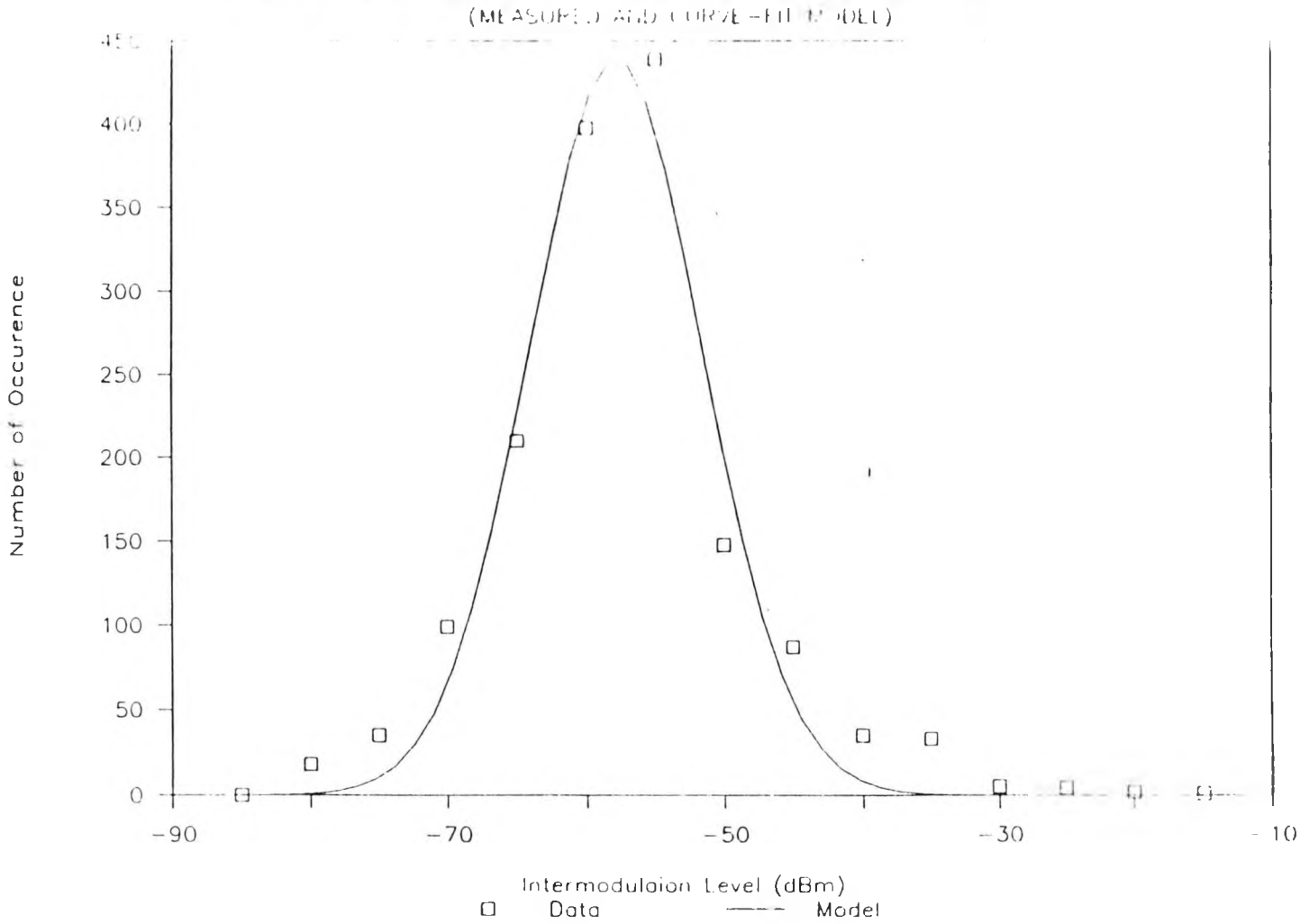

FIGURE 5. 5 Curve-fit (Gaussian) of the IMI frequency distribution

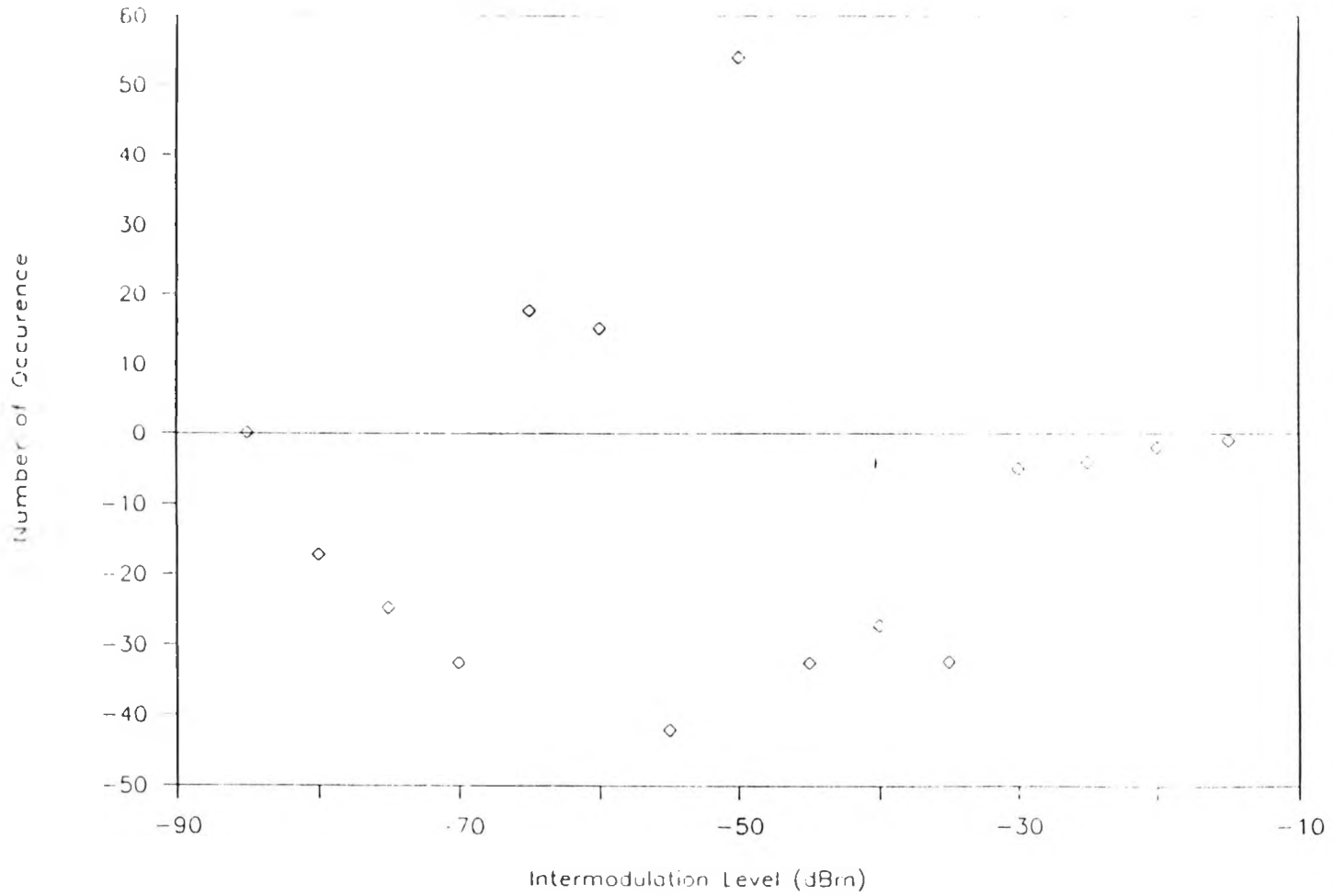

FIGURE 5. 6 Curve-fit residual

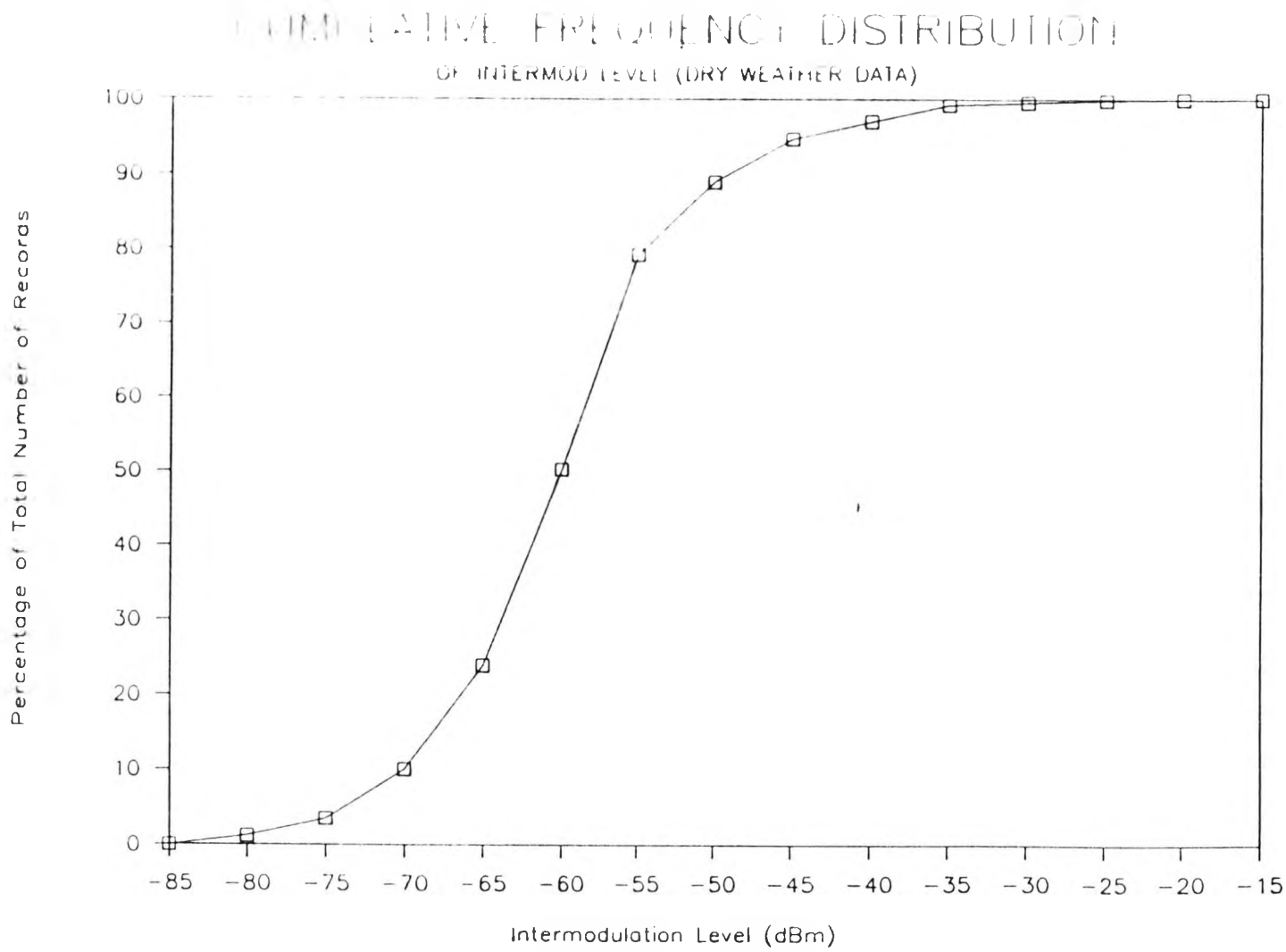

FIGURE 5. 7 Cumulative frequency distribution of IMI (dry weather data)

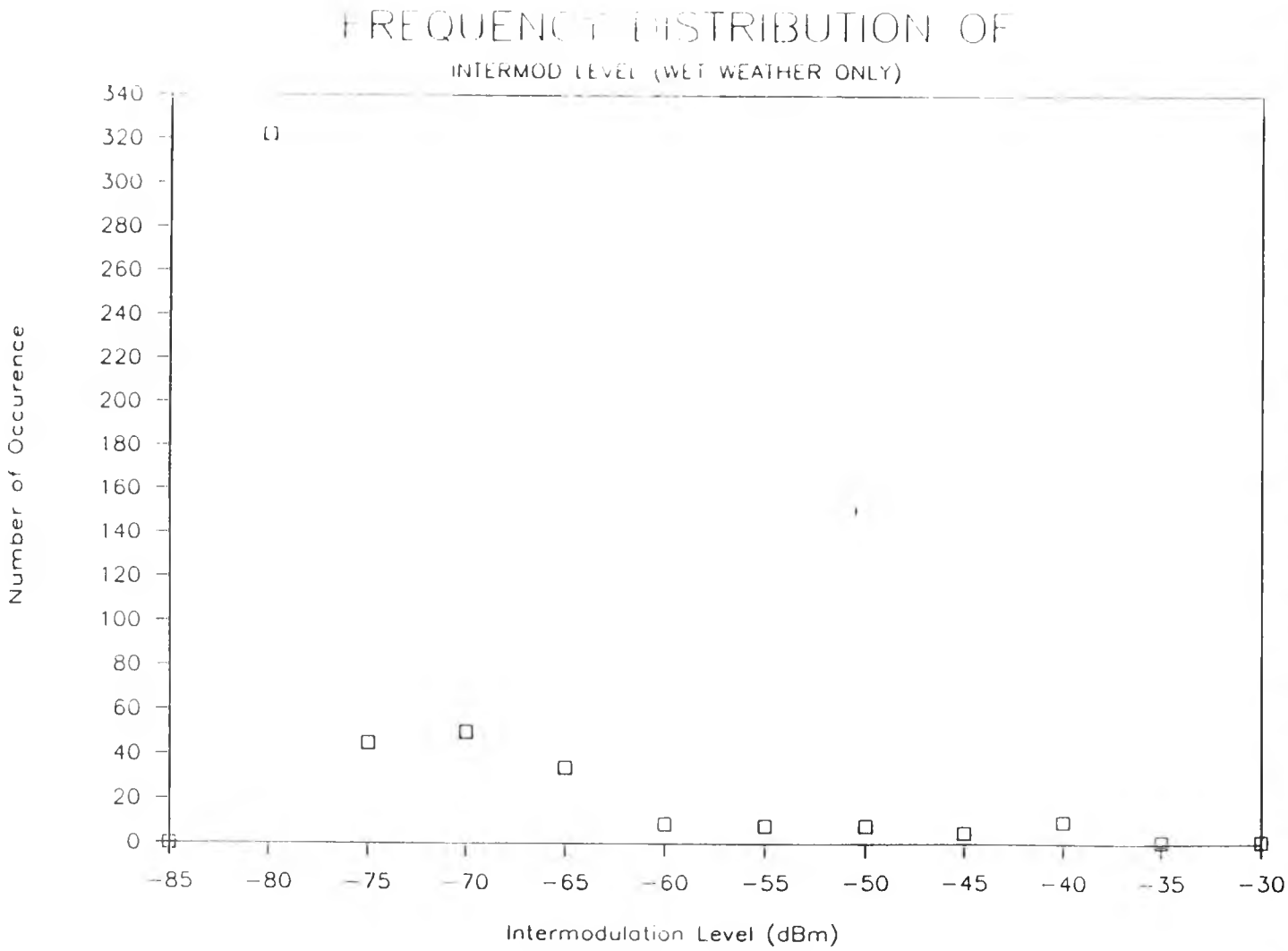

FIGURE 5. 8 Frequency distribution of IMI (wet weather data)

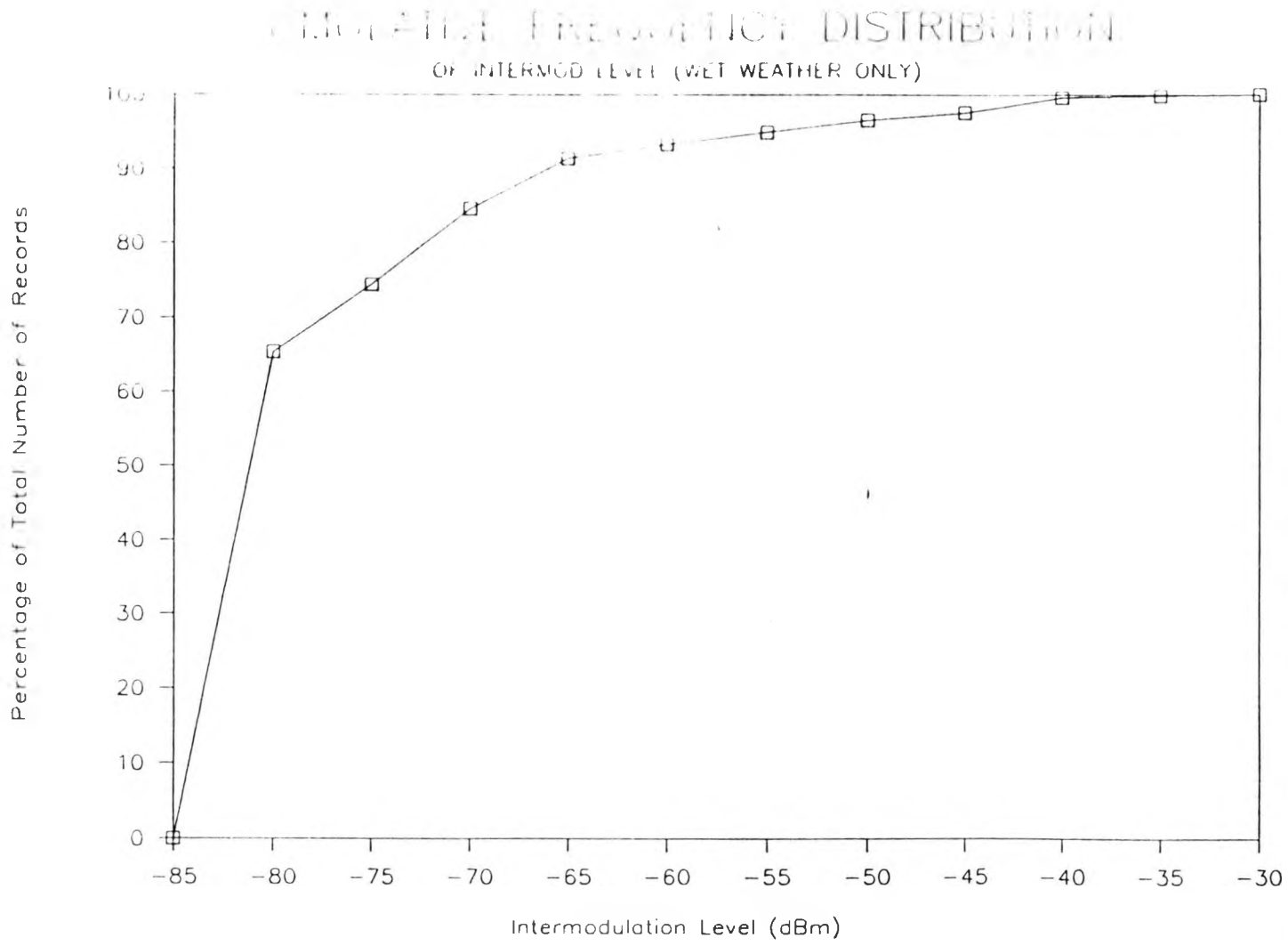

FIGURE 5. 9 Cumulative frequency distribution of IMI (wet weather data)

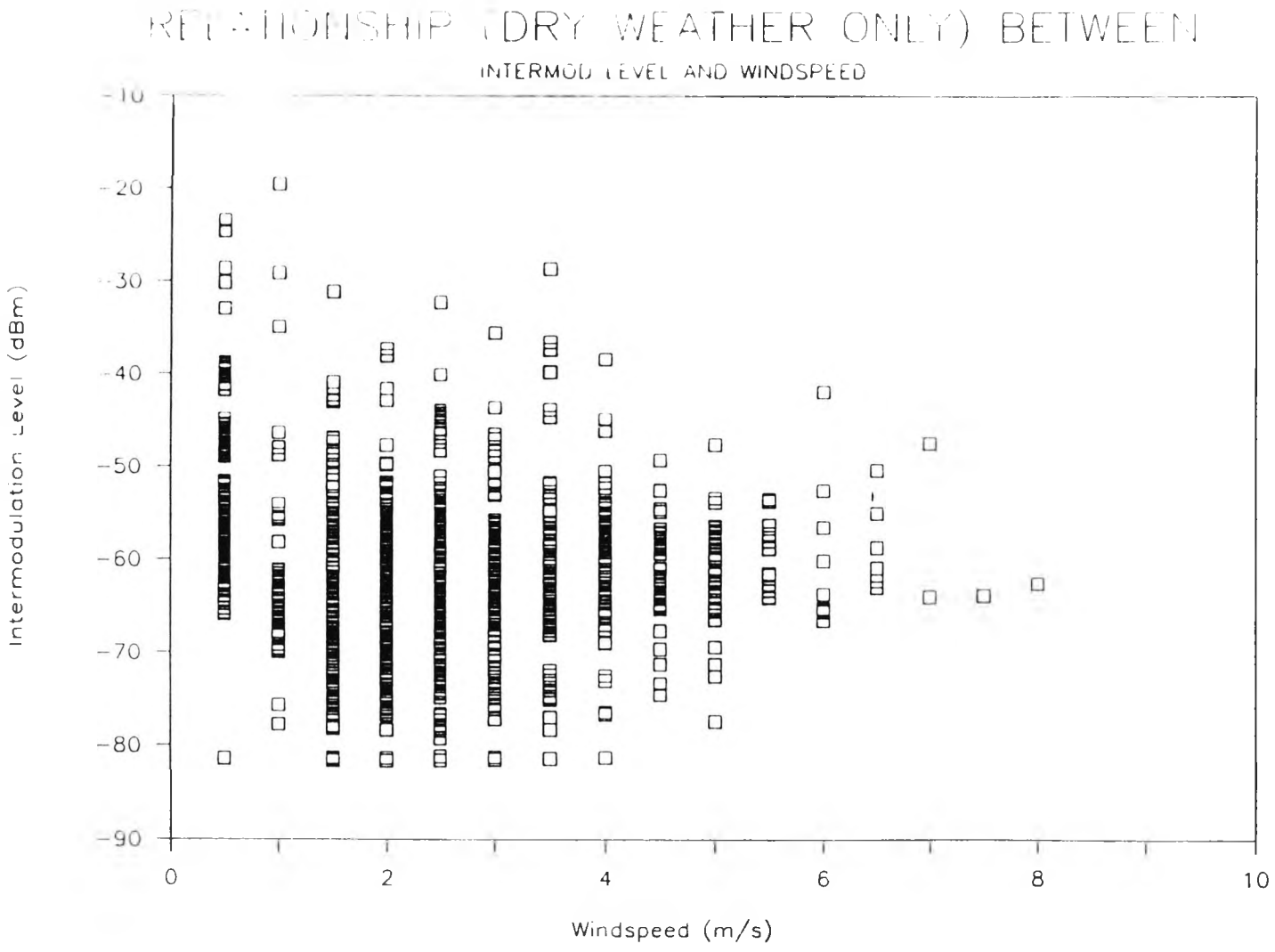

FIGURE 5.10 Scatter diagram of IMI and windspeed

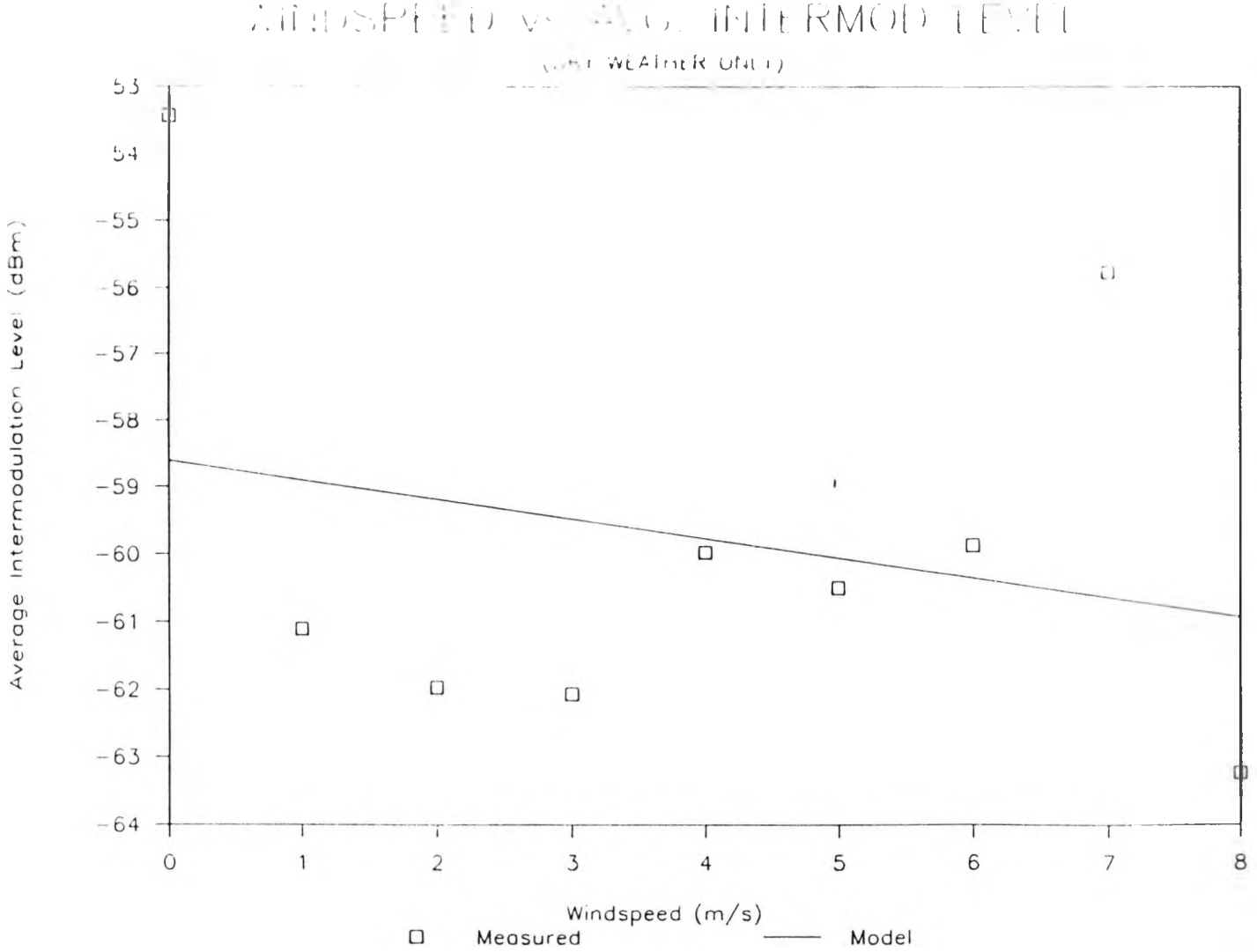

FIGURE 5.11 Regression of IMI and average IMI vs. windspeed

FIGURE 5.12 Scattering diagram of IMI vs. site temperature (dry weather data)

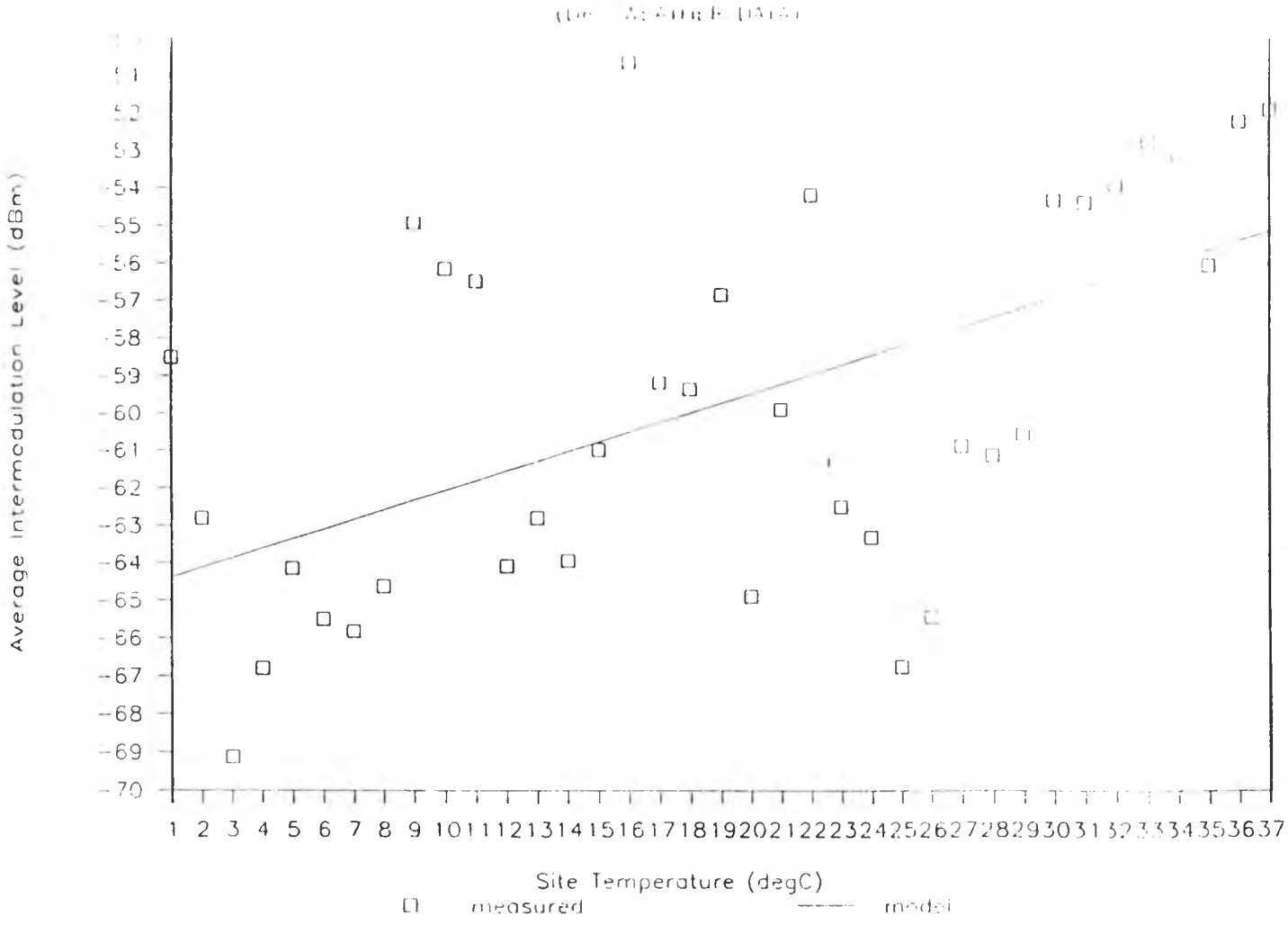

FIGURE 5.13 Regression of IMI and average IMI vs. site temperature

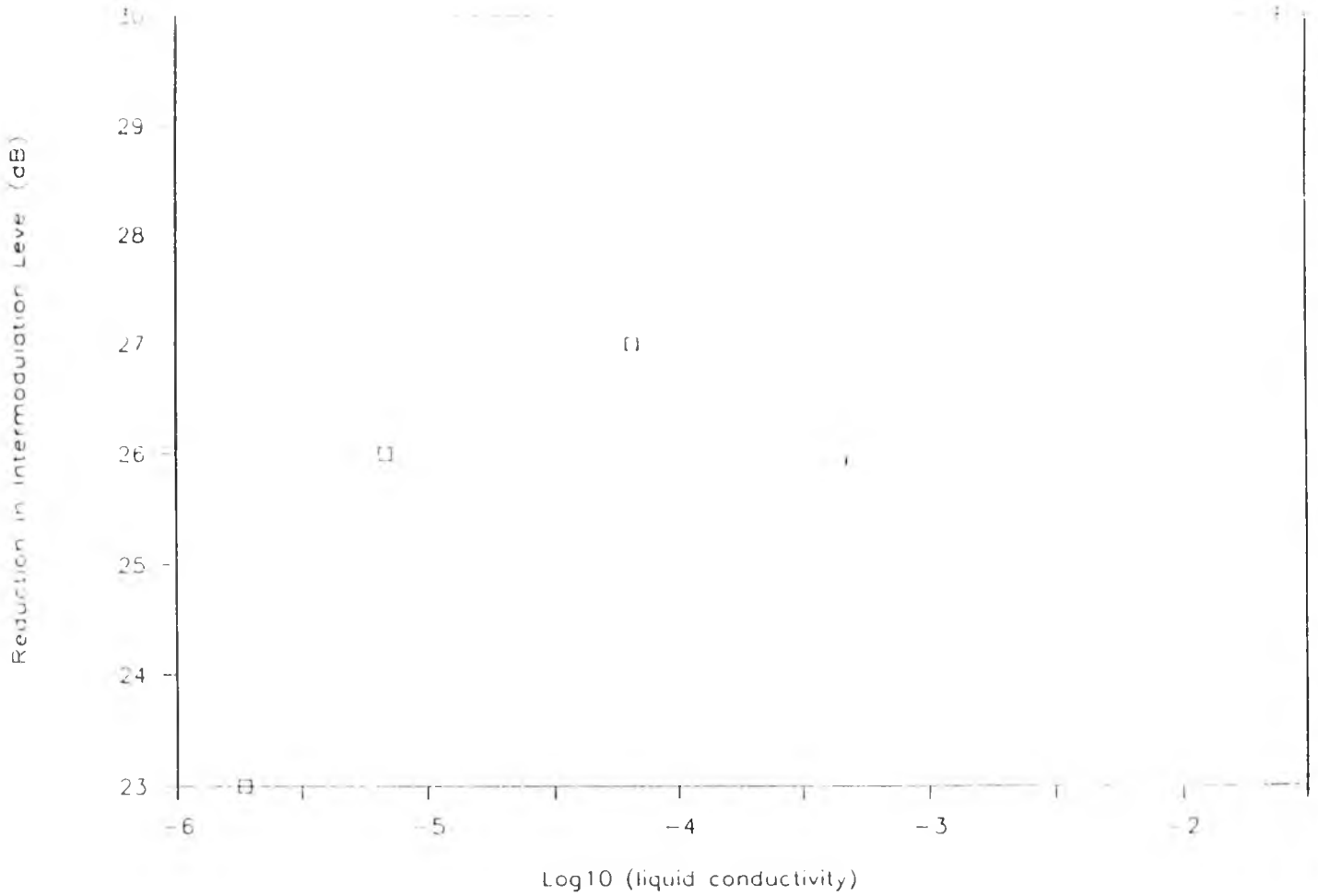

FIGURE 5.14 Relationship between IMI and liquid conductivity (note the Log_{10} scale)

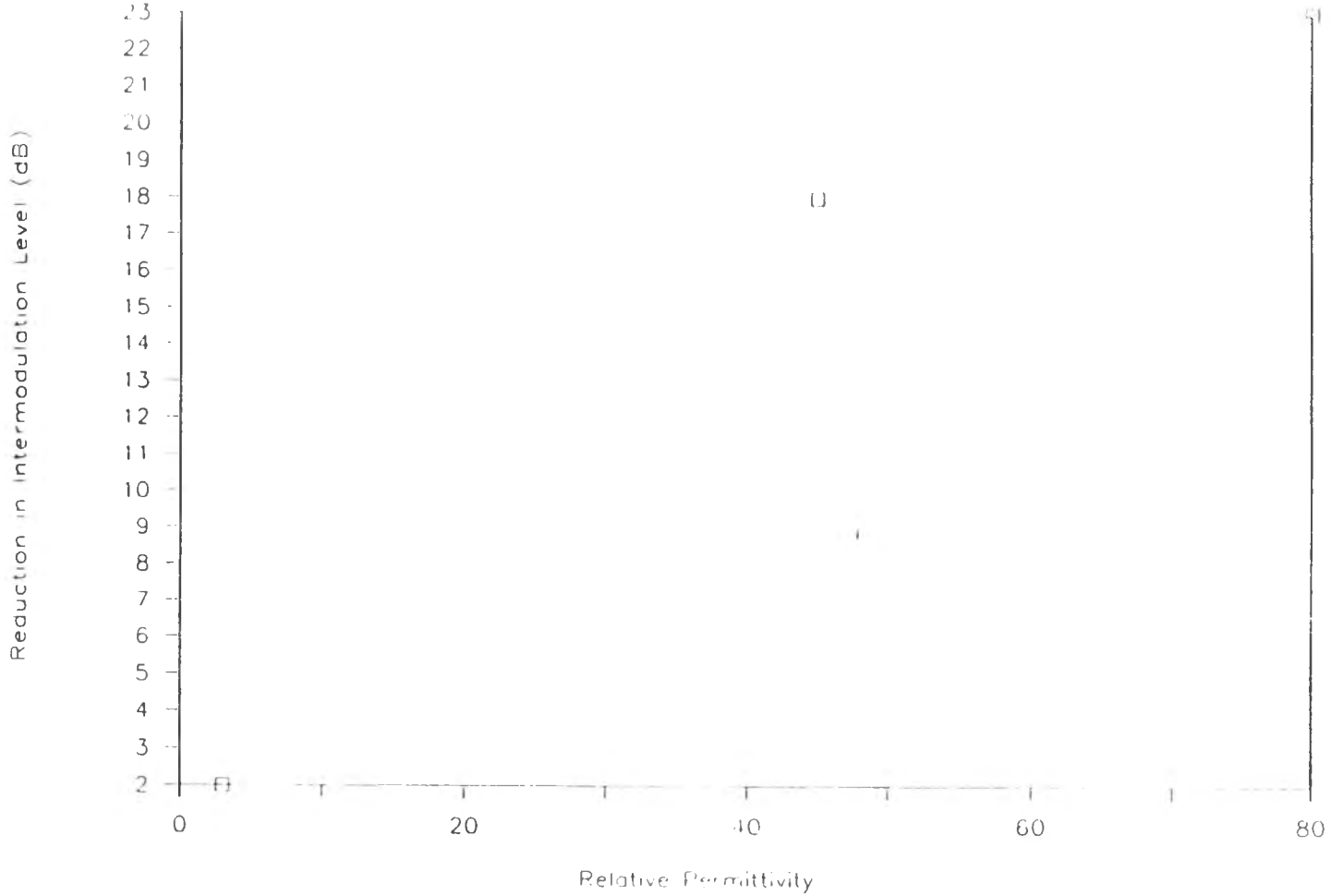

FIGURE 5.15 Relationship between IMI and liquid permittivity

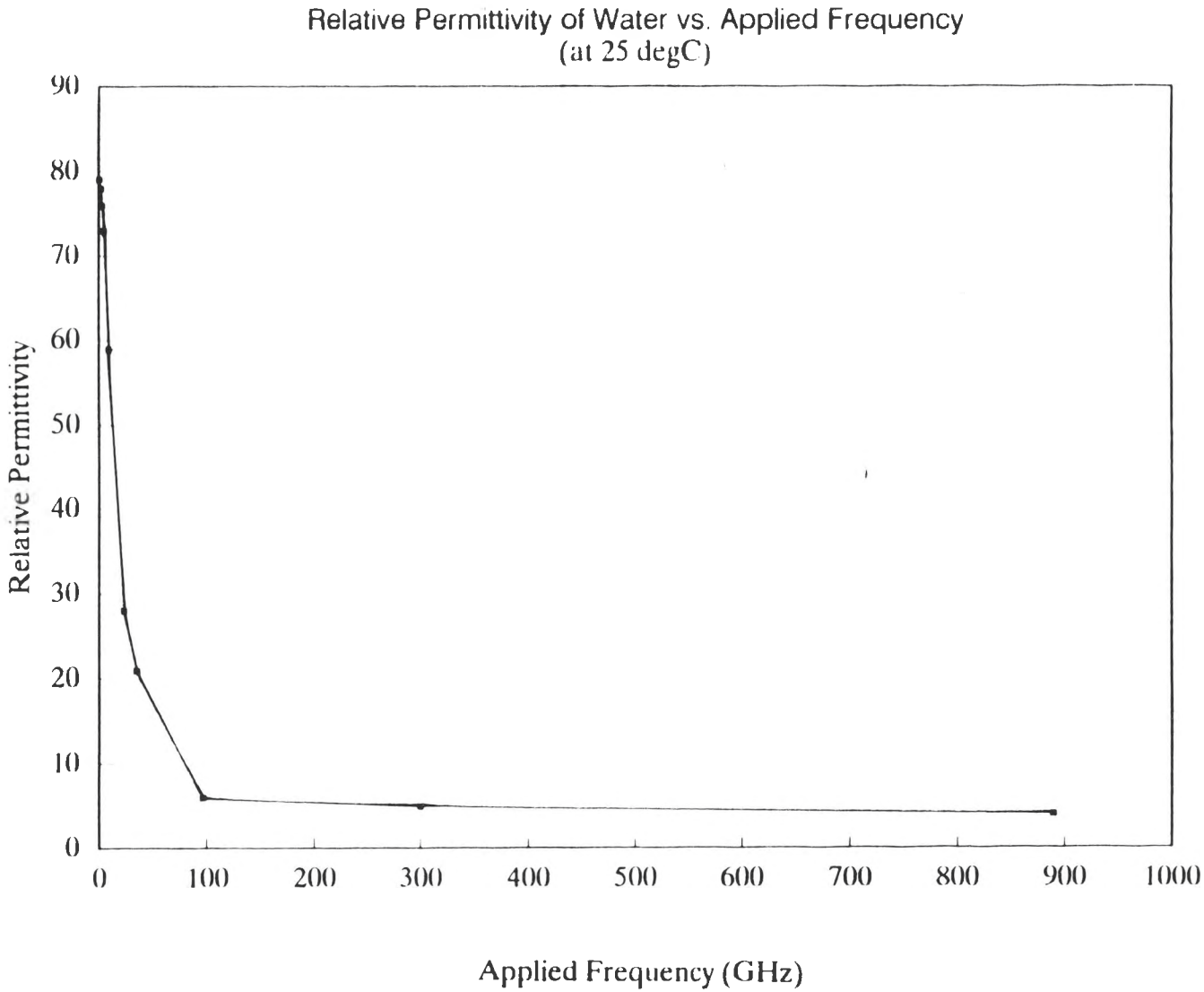

FIGURE 5.16 Relative permittivity of water at 25 degC vs. applied frequency

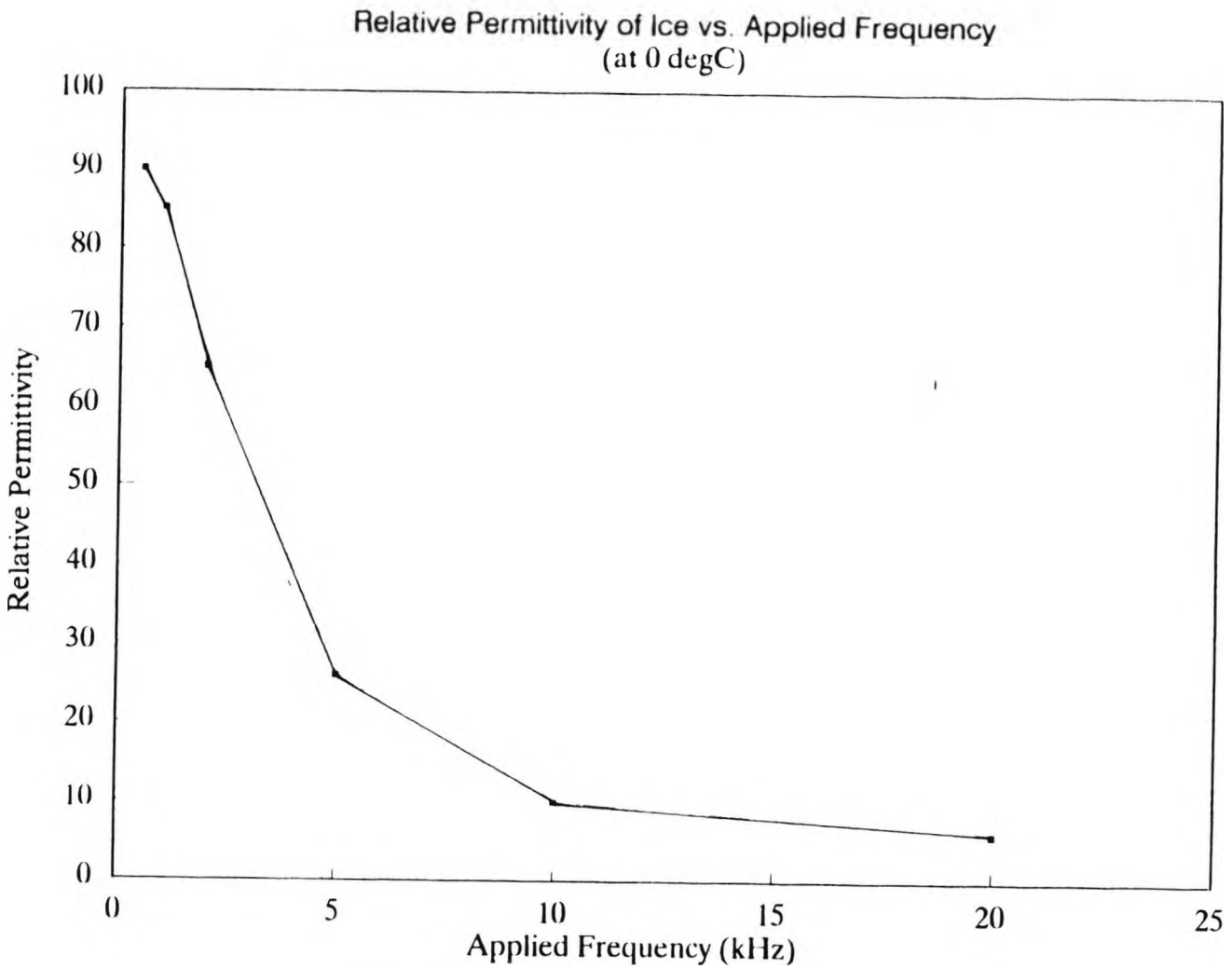

FIGURE 5.17 Relative permittivity of ice at 0 degC vs. applied frequency

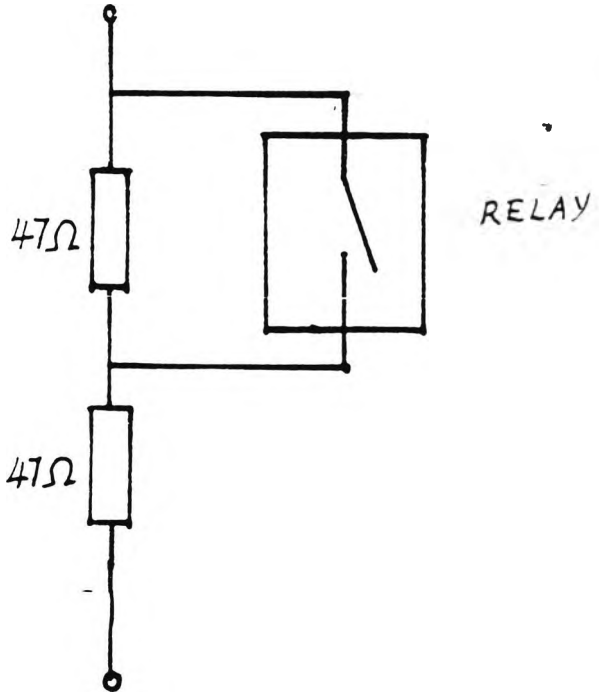

FIGURE 5.18 Circuit model of a flexing linear joint

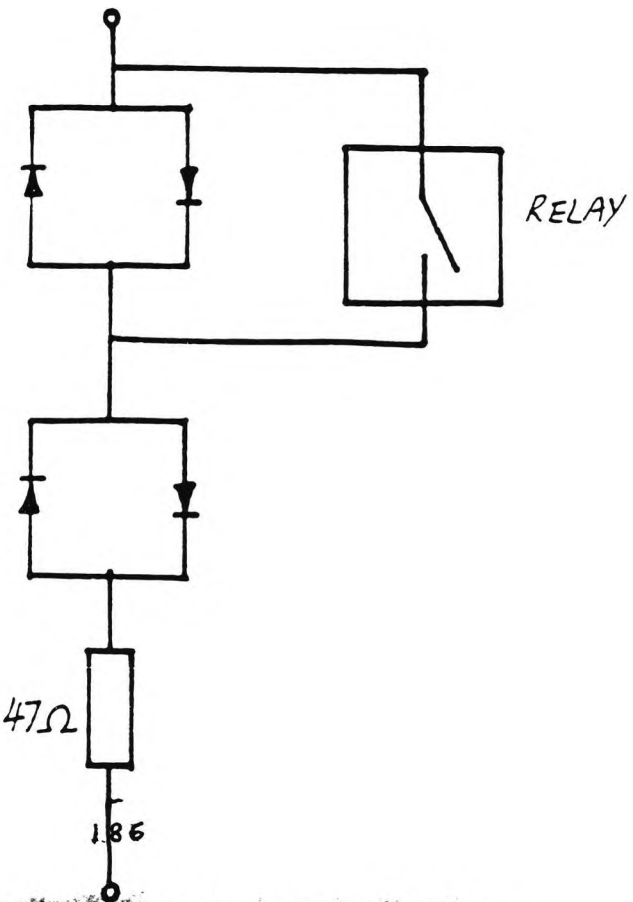

FIGURE 5.19 Circuit model of a flexing non-linear joint

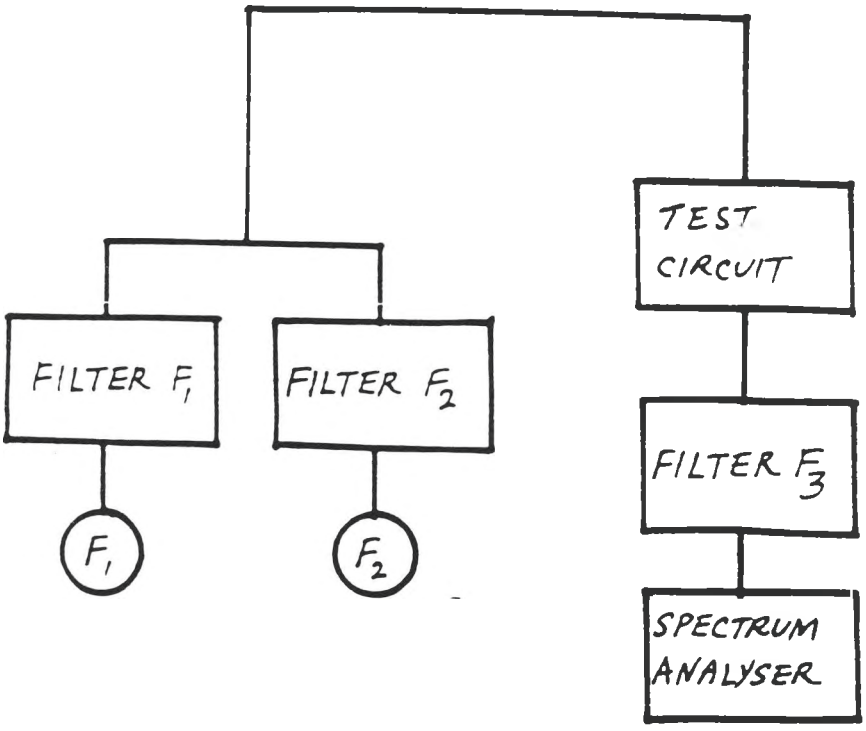

FIGURE 5.20 Test setup for the flexing joint circuits

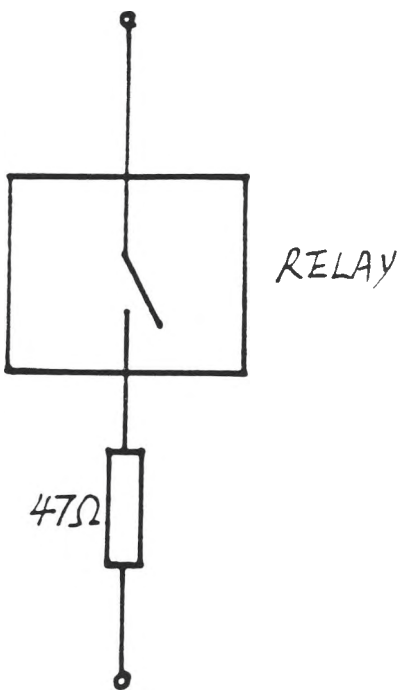

FIGURE 5.21 Circuit model of the contact (mechanical relay) on its own

Chapter 6

Investigations of Methods to reduce Structural Intermodulation Interference

6.1 Introduction

Chapter 1 highlighted the possible damaging effects of intermodulation interference on the reception quality of mobile radio communications and the efficient use of available frequency spectrum. It is therefore of great importance to find effective methods to eliminate, or at least, to reduce the intermodulation interference level at the base station. Although incidents of electrical interference due to electrical appliances, electrical motors, power lines ... etc have been reported in the

literature for many years, however, the effects of intermodulation interference did not cause a big concern at that time, mainly because the frequency spectrum was not as congested as today; therefore, there has not been any extensive investigations on methods to reduce intermodulation interference.

Recently, studies on the phenomenon of intermodulation interference in the sea-borne environment have been carried out by the United States Naval Research Laboratory (e.g. Cooper 1984). They have experienced problems on intermodulation interference due to co-located high power transmitters, radars and receivers. Although the Mil. Std. 1310C recommends the bonding of all metal-to-metal joints on ships by flexible welded metal straps, so that the corroded (non-linear) joints would be bypassed; in practice, this method is only effective when the metal strap length is short (say, no longer than one-tenth of the wavelength) compared to the wavelengths of the transmission frequencies. At the HF band (3 to 30 MHz) where the wavelength is between 10 to 100 metres, this method is more effective. However, at the VHF band, say, at 150 MHz, the wavelength is only 2 metres; any strap of this length will act as a relatively efficient dipole, which re-radiates the intermodulation products and worsen the interference.

In this chapter, various methods to suppress structural intermodulation interference are investigated.

6.2 Principles of Structural Intermodulation Interference Reduction

In Chapter 3, it was demonstrated that under static conditions, the presence of corrosion products (i.e. rust) is essential for the production of intermodulation interference; and in Chapter 5, it was found that under dynamic condition, even clean joints could generate low level, wideband high frequency noise due to the modulation effect of tower vibration. It is clear that in both cases, some sort of continuous conducting medium is required : in the former case, to bypass the rusty joint; and in the latter case, to provide a constant low resistance current path between structural members due to tower vibration.

Various techniques have been proposed to overcome the intermodulation interference problem. They all employed the principle of providing an alternative radio frequency path to the rusty junction (see figure 6.1). There were particular interests in the chemical approach (e.g. see Cooper 1984; Watson 1980), using high dielectric constant materials. The argument for that approach is based on modelling the non-linear junction as two back-to-back diodes. Putting high dielectric constant coating on the joint provides a shunt capacitance across it, and at high frequency, this capacitance bypasses most of the induced radio frequency current and generates less interference, as described in Chapter 4. Their results have shown that some short term useful improvements had been achieved. However,

over a longer term, their coating deteriorates and tends to dry off.

In next section, an account of experiments performed, in their chronological order, is given; so that they reflect the investigation approaches taking into account the emerging experimental evidences.

6.3 Experimental

6.3.1 Measurement Setup and Procedures

The intermodulation interference measurement setup and test procedures, and the sample preparation methods were the same as described in Chapter 3, except where stated otherwise. Repeatability of the results were generally good, and we are confident that the measurement results gave fair comparisons among different intermodulation interference reduction techniques.

6.3.2 The Chemical Approach

One method of dealing with the problem of intermodulation in the past has been to identify the troublesome components and electrically bypass them using straps or plates. Another approach is to treat the exposed metal parts at the time of installation with a protective film, but clearly this is no solution for existing structures.

6.3.2.1 Experiments, Results and Discussion

The chemical approach which was adopted has been along two paths :

(1) The oxidation process (corrosion) on the surface of the metal could be reversed by suitable chemical treatment. This involves the application of a film containing a chemical reducing agent capable of reconverting the oxidised species back to the metallic state, usually in a dispersed form, which has the added benefit of restoring surface conductivity. Although possible for metal such as iron, metals such as zinc or aluminum are not amenable to this treatment as chemical means alone are incapable of achieving the reduction.

A range of these preparations has been examined. Mild and strong organic acid reducing agents are combined in varying proportions with liquid urethane elastomers or with polyvinylpyrrolidone (PVP) which has the ability to "mop up" metal ions such as iron (II) and iron (III) and facilitate their reduction to metallic iron. The chelating agent was ethylenediamine tetra-acetic acid (EDTA) or its sodium salt which has also been used for similar purposes. In order to achieve control over the necessary viscosity change during application, ethylene glycol, acetone, water and ethanol were used as solvents in the preparations.

Originally, attempts were made to reproduce the results obtained for similar tests carried out by Cooper, Panayappan

and Steele (1984) in the USA; but, as mentioned before, it proved difficult, often impossible, to obtain a satisfactory adherent film on the sample using the prescribed proportions of constituents and the approach was considerably modified and augmented in the light of practical experience with the materials. However, the experimental results obtained from these agents were in general poor.

(2) An alternative conducting path can be offered which is impervious to atmospheric degradation, and which would reproduce the advantageous properties of a noble metal. Experiments with foils of noble metals, such as gold; platinum and other material such as copper, were carried out to investigate their increases in intermodulation levels when they were left in open air for two weeks. The experiment results are shown in figure 6.2. From the results, it was noticed that the original intermodulation levels of inert materials show very little difference from the background intermodulation levels. However steel and corroded steel show an appreciable amount of intermodulation product generation. After exposure to air outside the laboratory for two weeks, it can be seen that the inert materials' intermodulation levels remained close to their previous values, but steel oxidized significantly and its level increased by about 20 dB. Clearly, to construct antenna and tower components from such materials, or even just electroplated the components, whilst technically possible, would be economically prohibitive; but an equivalent situation could be contrived using the more traditional construction materials in a number of ways. The

Essex University's Chemical Energy Research Centre (then at City University) has extensive experience in developing a wide range of novel conducting and semiconducting compounds, fabrication techniques, and the applications of coatings. A number of inexpensive conducting coatings have been formulated and applied to the surface of steel test samples. The chemical coatings were based essentially on a combination of carbon, teflon binder, a conducting polymer and mild chemical reducing agent. The compositions of various coatings are shown in appendix A.

Out of the long list of chemical coatings prepared, the coating C3 (refer to the list in Appendix A) has shown to give a coating which was easily applied by brush and could be cured with a hot air gun to give an even coverage, which was very adherent and resistant to scratching. This coating contains a high proportion of high surface area carbon black, which is conductive; and is the primary medium for bypassing radio frequency current. Moreover, it has the desired property of not forming solid oxide products on exposure to atmosphere.

Experiments were carried out using rod samples, to test the effects of this coating on clean samples, and samples with corroded surface. The experiment results are shown in figure 6.3.

It can be seen that the presence of the coating on top of a clean sample did not change its residual intermodulation level, which was due to the ferromagnetic effect of steel

itself. For samples with corroded surface, the coating had an effect of reducing the intermodulation level; though by a very small amount.

It was apparent that the conductivity of the coating C3 was not high enough to bypass all the rf current, and significant amount still flowed through the corrosion products. Conductivity measurements revealed that the coating had a conductivity of around 0.1 Scm^{-1}, which is too low to stop rf current from penetrating into the non-linear junctions.

It is useful to establish the requirement of the coating conductivity, so that any candidates with this magnitude of conductivity could be considered. We wanted to find a coating such that a thickness of about 0.5 mm would reduce the rf current at the corrosion product to 5% of its surface value.

With the usual notations, the rf current at a distance x below the surface of an object will be given by the following equation :

$$I(x) = I_o * \exp (- x/\delta) \qquad (6.1)$$

and

$$\delta = 1 / \sqrt{\pi f \mu \sigma} \qquad (6.2)$$

where

I_o is the value of the rf current on the surface of the object

I(x) is the value of the rf current at a distance x below the surface is the skin depth

σ is the conductivity of the material

f is the applied frequency of the rf current

μ is the permeability of the material

With our criterion, then :

$$\exp (- 0.0005 / \delta) = 0.05$$

$$0.0005 / \delta = 3$$

$$\sqrt{\pi f \sigma \mu} = 6000$$

At 150 MHz, the relative permeability is approximately one, and we found that the required conductivity is at least $6 * 10^4$ Sm^{-1}. The conductivity of graphite-based coatings are therefore, not high enough for our applications. It is clear that to satisfy the conductivity requirement, the coating must be metallic in nature; since only metals have such high conductivities, and chemical coatings on their own would never achieve such high conductivity values.

It was also found that metal-based paints would not work because the bulk conductivity of the paint is much less than the metal. An experiment was carried out using silver-based paint with a quoted resistivity equal to 10^{-5} Ohmm. In this case, the intermodulation level of a corroded joint sample

dropped from -50 dBm to -65 dBm. Although the absolute value of -65 dBm was still high, but an improvement of 15 dB is a convincing argument for intermodulation interference reduction by covering the rusty joints and surfaces with a continuous layer of high conductivity material, i.e. metal.

After suspending the work on the graphite-based coating, we turned our attention to various metal plating. In order to establish the thickness requirements of metal plating, a range of twelve copper-plated steel samples were prepared with carefully-controlled amounts of copper, from 1 micron thickness to 50 microns thickness of copper deposited on rod samples by electro-plating. The thicknesses were selected to provide copper layers of greater than, equal to, and less than the calculated skin-depth of about 5 microns under the prevailing test conditions. Measurements (see figure 6.4) show that the reduction in measured intermodulation interference level is essentially the same in all samples, confirming that substantial improvements could be achieved with only a modest layer of copper on the surface.

The electro-plating setup is very similar to the electrochemical corrosion setup shown in figure 3.17, except that the anode is the sample to be plated, and the cathode is a nickel mesh. A smooth layer of metal plating can be obtained by carefully control the applied plating potential. With too high a potential, the metal plated surface would be rough and lumps of metal accumulated, especially at the edges; with too low a potential, the metal plating process would take a long time. However, with care, smooth plated

surfaces could be obtained. A circular cathode (nickel mesh) was useful in providing a uniform electric field around the sample, and plating thickness was found to be even over the sample. The thickness of the plated sample was measured either using a calliper with an accuracy of 0.02 mm, or by weight measurements.

After establishing the thickness requirement of the plating, further investigations were carried out to examine different metal plating for their deterioration in intermodulation interference levels when exposed to the atmosphere. In particular, copper, zinc and silver were looked at because of their general uses in plating. Initially, the method of electro-plating described above was used to plate metal onto the surface of clean rod samples. Obviously, in real life situation, other more practical methods had to be found to apply the plating process.

The electrolyte for different metal plating are as follow :

metal	electrolyte
copper	copper sulphate
zinc	zinc chloride
silver	silver nitrate

Various systems involved both single-layer and multiple-layer plating were looked at, including copper/steel, zinc/steel, silver/steel, copper/zinc/steel and silver/zinc/steel. The intermodulation interference levels of these samples, before and after being treated with

concentrated hydrogen sulphide gas (to simulate an industrial environment) are shown in figure 6.5 and figure 6.6.

From figure 6.5 and figure 6.6, it is clear that after plating a layer of non-ferromagnetic material on the sample surface, the residual intermodulation interference level dropped by at least 10 dB (from -74 dBm); and can be as much as 20 dB. After treatments in a very corrosive environment of concentrated hydrogen sulphide gas, the intermodulation interference increased by 5 dB to more than 10 dB; which is not very different from the deterioration of unprotected plain clean steel rod sample treated in a similar environment. From the experimental results, it can be seen that all oxides of the plating metals are non-linear and generate intermodulation interference. Obviously, if a corroded joint is by-passed via a layer of plated metal, its intermodulation level could drop by some 40 dB, as shown in Chapter 3. Since the deterioration in intermodulation level due to surface corrosion of the plated metal would be around 10 dB; then, there is a big gain in reducing intermodulation interference by coating a linear metal over a corroded joint, despite subsequent surface corrosion of the plated metal.

Having established that multi-layer metal plating did not help to generate lower intermodulation interference, it is reasonable to assume that a layer of zinc coating is just as good as other metallic coating in protecting the steel

structural members from atmospheric corrosion. Therefore, we seeked to find a way to bypass the rusty joint by a single layer of metallic coating.

At first, we have tried various methods to plate silver onto corroded joint samples, mainly because of the availability of several silver plating methods, including silver-plating solution, silver-based microballs and silver-loaded paint.

The silver-plating solution is a proprietary product, and is a kind of electroless-plating method which plates a layer of silver on the surface of a metal by dipping it in the solution. The appearance of the plated-silver was black, indicating that the plating was not as fine as that done by electro-plating. In addition, the corroded joint sample must be cleaned by brushing off the rust around the joint using a wire-brush; otherwise, silver would not deposit onto the surface.

Silver-based microballs are glass balls coated with a layer of silver for electrical conduction. They are applied in the form of a paint; and has been used for electromagnetic shielding in plastic cases containing sensitive electronic circuits. In addition, some ferromagnetic material is also coated on the glass balls, so that the glass balls are attracted to each other to form a continuous layer of metal.

We have already described the silver-loaded paint in previous section, and its relatively low bulk conductivity is not sufficient in our applications.

The intermodulation interference levels of some corroded joint samples before and after applying the above mentioned plating methods are shown in figure 6.7.

It can be seen from figure 6.7 that none of the above methods provide sufficient reduction in intermodulation interference level. The main difficulty with these methods is that they do not provide a continuous highly conductive medium covering the rusty joint to bypass rf current. At zero frequency, they do provide a good dc current path. Furthermore, silver-based microballs have an undesirable property that they are ferromagnetic.

After experimenting with silver-based methods, we turned our attention to copper-based methods. In this case, we concentrated on plating solution methods; since they were more likely to produce a continuous layer of plating than other methods.

Steel can be readily coated with copper in a number of ways :

(a) by electroplating
(b) by simple galvanic replacement reaction
(c) by electroless deposition
(d) by flame-spraying

The plating of clean steel is therefore no problem and we have already shown that a substantial reduction in intermodulation is possible in uncorroded steel, with a

coating as low as 1 micron (one-fifth of the estimated skin-depth).

With a corroded sample of steel, however, attempts to electroplate were futile - deposits are blistered, adhesion poor, control difficult. Considerable effort was made to produce an electroless bath which could operate at ambient temperature, as the chemical reduction (electroless deposition) was found to be less discriminating with regard to the nature and condition of surface. In addition, since no power source is required for plating, it is more preferable in real life applications.

One aspect which is very important in electroless plating is the ambient temperature. It is known that the higher the temperature; the faster will be the plating rate. Experiments were carried out to investigate the effect of ambient temperature on the plating rate. In essence, two batches of uncorroded rod samples were immersed in two beakers of plating solution; with one beaker placed in a hot water bath maintained at 26 degC and the other in a bath at 33 degC. The results of plating thickness versus plating time is shown in figure 6.8.

From the graph, it is clear that at higher ambient temperature, the rate of plating is faster. At 26 degC, the plating rate is about 0.7 microns/hour; and at 33degC, the plating rate is doubled at 1.5 microns/hour. No doubt the temperature requirement limits the practicality of electroless plating in our applications, and its use would

be a problem in real situations.

Bearing in mind the conditions under which the treatment will be applied, one can discount anything involving elevated temperatures (electroless plating). Also, normal electroplating will require a power input, and a means of containing the electrolyte around a specified area of the structure, which could be impractical. Establishing a copper surface on steel could of course be carried out by simple electrochemical replacement from a solution containing cupric ions. This spontaneous process however only continues smoothly for a few monolayers before breaking down into a rough deposit with poor adherence, after the iron surface becomes increasingly shielded. Using this simple technique, the intermodulation levels were always poor, showing no improvement on the levels of the rusted samples.

In above, we have highlighted the main difficulties of various copper-plating method : electroplating requires power source; electroless plating requires elevated temperature; and simple replacement reaction only plates a monolayer of copper. A further approach, in which copper deposition can be accelerated and sustained, makes use of a sacrificial zinc (or aluminum) electrode; the effect is the same as electroplating (with a fixed potential difference governed by the wet corrosion voltages of the two metals), but no external power source is required. Also the electrolyte can be made up in the form of a gel which is simple to apply by paintbrush to unenclosed structures. A gel has been developed with a conducting polymer base from

which any thickness of copper can be deposited, limited only by the amount of sacrificial anode used, the latter being strapped or otherwise attached to the steel, and the whole painted with the gel. This process is relatively simple to apply, requiring no skilled operatives, and no external power source.

The sacrificial zinc/copper gel plating setup is shown in figure 6.9. The corroded joint sample was brushed using a wirebrush to remove any loose rust around the joint. The sample was immersed in a beaker of gel, and it was then connected to a piece of zinc by a short length of wire. Initial intermodulation interference level measurements with corroded joint samples shown that improvements of around 35 dB was achieved using this treatment. The experimental results are shown in figure 6.10. Further experiments were conducted with new plating gel formula, which was more viscous, and would be more practical in real life situation. However, the experimental results (see figure 6.11) were not as promising as before. The drawback can be explained by the fact that with a more viscous gel, it became more difficult for the metal ions to diffuse onto the base metal surface; and both the plating rate and the plated surface were not satisfactory. The intermodulation level measurement results for these samples were therefore very poor.

From above, it is clear that a mean has to be found to contain the plating solution without the use of a thick gel. Sponge had been tried as a possible alternative. The experimental results are shown in figure 6.12. They show an

improvement of between 20 dB to 30 dB.

6.4 Discussion

The principle of providing an alternative rf current path by plating technique is sound. However, one of the major difficulties is to contain the plating solution in practical situations (high on the tower; possibly strong wind; rain ... etc). It was unfortunate that the plating gel was not able to fulfill the requirements; which would otherwise provide an ideal solution. Other techniques, such as electroless plating also suffer from the same problem. The sponge method tried did show some useful improvement was achievable. Further development could be in the areas of refining the material used for retaining the plating solution, as well as the application technique.

6.5 Alternative Approach (1) - Zinc Spraying

Although the copper plating technique mentioned above has produced some good results; however, the application technique has to be improved in practical situations for easy use. Another possible problem is that the plating thickness by this method is relatively small, and there is a real chance that the coating could be torn apart when the tower moves under severe weather conditions. A mean of coating a rusty joint with a thick layer of conductive coating is therefore highly desirable. In fact, there exists

a well-established technique, zinc spraying, for protecting metal against corrosion. Zinc is usually sprayed onto the metal surface in atomized form of adherent scales. Intermodulation level measurements on zinc-sprayed corroded joint samples were performed, and their values before and after spraying are shown in figure 6.13. The samples were all covered with a continuous thick layer of zinc particles.

The experimental results in figure 6.13 show that the improvements of all the corroded samples were more than 30 dB; however, they were not quite down to the system background level (i.e. -100 dBm) as expected. This can be explained by the fact that flame sprayed zinc particles are very hot (zinc melts at around 400 degC), and they oxidize before landing on the corroded sample surface. The zinc particles are surrounded by a thin layer of oxide and the zinc coating is not as continuous as a electrodeposited zinc coating (see figure 6.14), hence the deteriorated intermodulation level from the ideal situation.

The zinc-spraying method has one distinct advantage over the plating method, in that the pre-cleaning of the corroded sample, i.e. removing rust around the corroded joint, is not too critical; since the success of the flame spraying method does not depend on any electrochemical reaction with the base metal, but purely on the impact force of the zinc particles.

The effectiveness of flamed sprayed zinc is good. The coating can be as thick as required, and is firmly attached

on the base metal surface. However, the major drawback, is again, the practicality. The flame spraying setup usually involves gas cylinders and spray-gun, which is not very convenient to use at 100 metres above ground ! In addition, there are safe hazards to the rigger who performs the spraying. For example, there could be sudden strong wind blows the sprayed zinc back to the rigger, which would be very dangerous indeed. Prevention by wearing special safety clothes and mask would restrict the movement of the rigger, which again is not desirable.

6.6 Alternative Approach (2) - Corrosion Protection

This method is applicable to newly assembled towers only, and does not help any existing corroded towers.

Since we have identified that corroded joints are the major sources of intermodulation interference, then there is a big advantage of preventing any corrosion products from forming in the first place. It is clear that to achieve this aim, any joint should be free of both rain water and moisture. Traditionally, varnish is used to protect yachts and other outdoor objects. Varnish provides a water impermeable layer which shields the coated object from the atmosphere and thus protects any metallic object from getting corroded. Application of this technique is relatively simpler than other techniques (e.g. spraying) with the use of a paint-brush. From our experience, the thickness of a varnish coat, with two layers of paint, is between 0.2 mm and 0.3

mm. Under normal circumstances, this layer of coating should provide an adequate protection for two years. Degradation in corrosion resistance performance of the varnish coating is mainly due to long term exposure under ultra-violet light. Obviously, with so many joints in each tower, there is a great incentive to prolong the life of the coating, so that interval between re-painting could be extended and maintenance costs reduced.

A novel coating, code-named Celcote (Tseung et al 1990), was developed at the Chemical Energy Research Centre, and has been tested extensively for its corrosion resistance property, which is many times better than any commercial varnishes. Celcote is a paint-like material, thicker than varnish, and can be applied by a paint-brush easily. Two layers of this coating on a clean rod sample has a thickness between 0.2 mm and 0.4 mm. We have tested and compared the effectiveness of both varnish and Celcote under accelerated corrosion environment. The test setup is shown in figure 6.15. The measured current is used as an indication of the degree of corrosion. It is evident that when the sample is completely protected by the coating (either varnish or Celcote), then the sample is insulated from the electrolyte and there would not be any current flow at all. However, as the layer is kept under attack, there comes a stage when the layer is broken and current will start flowing, and the sample gets corroded. The test results for varnish coated samples and Celcote-coated samples are shown in figure 6.16.

From the test results, it is clear that Celcote-coated

samples were still protected after nearly 24 hours under accelerated corrosion test; but the varnish-coated samples corroded. Corrosion was observed near edges of a sample where the coating tends to be thinner than that over the sample (see figure 6.17). These samples were also tested for their intermodulation interference level, and the results are shown in figure 6.18. As expected, the corroded samples produced significantly higher intermodulation levels; which were essentially unchanged for Celcote-coated samples.

Other tests performed by the Chemical Energy Research Centre on ultra-violet degradation, water absorption, water vapour absorption and oxygen diffusion also produced very promising results (Tseung 1990). Thus, a very high performance corrosion resistance paint is available for coating the joints of a newly assembled lattice tower which could prevent the formation of rusty joints, and will therefore, minimize the problem of intermodulation interference at its source ! Of course, in our application, the strength of the material has to be evaluated as well.

6.7 Alternative Approach (3) - Composite Materials

So far, we have demonstrated that for a galvanised lattice tower, the possible sources of intermodulation interference are :

(1) Corroded joints

(2) Surface corrosion products

(3) **Mechanical switching action of flexing structural members**

Corroded joints have been shown to be major sources of intermodulation interference; much more significant than that produced by surface corrosion products. In Chapter 5, it was also shown that flexing structural members could generate wideband interference. The applicability of various methods described above for the suppression and prevention of intermodulation interference are summarised below :

Interference Source	Effective For				
	(1)	(2)	(3)	New Tower	Old Tower
Metal-plating	X		X	X	X
Metal-spraying	X	X	X	X	X
Corrosion prevention	X	X		X	

Under ideal situation, both metal-plating and metal-spraying could provide the necessary protection against all sources of intermodulation interference for both existing and new towers. In reality, however, non-ideal situations render the applicability and the results of these methods less than satisfactory. In this section, investigations of the possibility of using alternative building material to tackle the intermodulation problem are carried out.

If we could build a tower with any new material which would

not produce any intermodulation interference at all, then the two most useful properties of the building material would be :

(1) it would not corrode, or it would not form any solid oxides

(2) it would not conduct

The first property would eliminate the interference due to "Rusty-bolt" effect and surface corrosion products; and the second property would solve the problem of "mechanical switching effect of flexing structural members". Which material has these desirable properties ? One obvious answer is Carbon Fibre Reinforced Plastic (CFRP). Being non-metallic, the corrosion resistance of CFRP is excellent. The radio frequency resistivity of carbon fibre composites had been reported by Smithers (1980). Smithers found that the resistivity increased as the applied signal frequency went up; and it has a value of about $2 * 10^{-4}$ Ohmm at 150 MHz, which is 10,000 times higher than copper. Since the resistivity is much higher in this case, then the resultant rf current flowing over the structural members would be much smaller (10,000 times less); hence the flexing joint would become an insignificant source of wideband noise interference due to the excitation current becomes very small.

From above, it is clear that CFRP could be a possible candidate as a new material to build antenna towers for

intermodulation reduction; however, other aspects, such as mechanical properties and costs, have to be considered as well.

One of the most important material parameter is the Young's modulus. A small modulus implies a floppy material; and a large value implies a stiff material. Normal structural mild steel has a Young's modulus of around 200 GNm^{-2}; and CFRP can have a value of around 200 GNm^{-2} as well (Ashby and Jones 1980). The tensile strength of CFRP is 670 MNm^{-2}, and is far higher than mild steel which is about 430 MNm^{-2} only. Therefore the strength of CFRP is as good as steel, and one would expect antenna supporting structure built with CFRP would exhibit mechanical strength similar to that of steel. Indeed, modern fighter aircraft wings are built with carbon fibre composite materials for their strength and light weight.

Furthermore, to build a tower structure using CFRP with the same mechanical strength as a steel tower, the amount of CFRP required would be less than that of steel, because of the lower density of CFRP (CFRPs' density is around 1.5 Mgm^{-3} ; mild steel's density is around 7.8 Mgm^{-3}). Referring to figure 6.19, if block A was built with steel, then the force on the block B would be the weight of block A, say, F. Now, if block A was built with CFRP, then the force on block B would be one-fifth of F; since the density of CFRP is one-fifth that of steel. Therefore, the cross-sectional area of block B could be reduced to one-fifth of its original value, and still provide the same support. From this

argument, it is clear that if one replace a steel structural member by a CFRP structural member with the same strength, the volume of material required would be one-fifth of its original volume.

We would proceed to calculate an estimate of the cost of building a CFRP antenna tower which would suppress the generation of intermodulation interference. Obviously, to build an antenna tower completely with CFRP would be very expensive and is not required anyway. In real life situation, nearly all the antennas (both transmitting and receiving antennas) are located close to the top sections of the tower; therefore, one only need to replace those sections with CFRP material only. The antenna tower plan diagram is shown in figure 6.20. The top three sections represented a total length of around 60 feet, i.e. around 18 metres. If we just consider the four main legs, and assumed that the members are 2.5 inches in diameter on average, i.e 6.25 cm. The total volume of CFRP required is :

$$\text{Volume} = \pi * (0.03125)^2 * 18 * 4 \quad m^3$$

$$= 0.22 \quad m^3$$

Since the density of CFRP is around 1.5 Mgm^{-3}, then the mass of this volume of CFRP is :

$$\text{Mass} = 0.22 * 1.5 * 10^3 \quad kg$$

= 330 kg

Now, the cost of CFRP is around 90,000 Sterling pounds per tonne (see Ashby and Jones 1980), i.e. approximately 90,000 Sterling pounds per 1,000 kg. Therefore 330 kg of CFRP would cost :

Cost = (330 * 90000) / 1000

= 29,700 Sterling pounds

approximately 30,000 Sterling pounds

The cost of a lattice tower, built with galvanised steel, would be around 50,000 Sterling pounds. Therefore, the cost of a tower with CFRP sections would cost around 60% higher. With some conservation, then the cost would be nearly doubled.

In above, we have established the suitability of carbon fibre composite materials as possible alternatives for building antenna supporting towers. The intermodulation suppression properties, the mechanical properties and the costs of such alternative were evaluated. At first glance, the cost could be a big obstacle for adopting this approach. However, since using carbon fibre composite materials for building large structures has never been attempted before, then there is a good chance that new design disciplines could be developed which would reduce the manufacturing cost

substantially. For instance, there would be more savings in maintenance cost because of the better corrosion resistance of CFRP; lighter weight could save transportation and assembling costs etc.. It is certain that when more people turn to carbon fibre composites as alternative building materials, the cost of them will come down to be very competitive with other conventional building materials.

Another way of using alternative materials is to build a special socket with a highly insulating, high strength material to connect two steel structural members together. This idea could be seen in figure 6.21. The steel members are insulated from each other, and there would not be any rf current flow at all; hence no intermodulation interference would occur. The insulator, as with most non-metal, would not form any oxides when exposed to atmosphere. This idea was tested with some corroded joint samples. The corroded halves of a joint sample was separated from each other by a layer of silicone rubber. Nylon bolts and nuts were also used to provide insulation (see figure 6.22). All samples were corroded under the same condition.

The intermodulation interference measurement results are shown in figure 6.23. It is beyond doubt that by insulating all the component parts, and there would be no intermodulation interference due to corroded joints. The result of -70 dBm for the completely insulated corroded joint was due to the ferromagnetic effect of steel itself. Although no rf current could flow through the joint, rf current still flew over the sample surface and was totally

reflected at the joint, and therefore, generated interference via the ferromagnetic effect. In fact this value is similar to the intermodulation interference level generated by clean joint samples, which proved our explanation.

Also from figure 6.23, it can be seen that the usual joint sample configuration (i.e. metal bolt and no insulation at the junction) produced an intermodulation level of -42 dBm; while the joint configuration with metal bolt, and with insulation at the junction also produced similar intermodulation level. It is clear that the metal bolt provided an alternative current path for the rf current. Since the interface between the metal bolt and the corroded joint sample also constituted a non-linear junction, therefore, the benefit of having an insulated joint interface was removed by the presence of an alternative metal/metal oxide junction.

The worst intermodulation interference level was recorded for the joint configuration with nylon bolt, and without insulation at the junction. In this case, the interference level was higher because all rf current was forced to flow through the severely corroded junction interface; whilst in the above two cases, part of the rf current could flow through the less non-linear corroded sample/metal bolt interface.

For this intermodulation interference reduction technique, we need a material which is highly insulative. Although the

conductivity of carbon fibre composites are much lower than metal, they are far from non-conducting; and as such, are not suitable in this application. Non-conductive polymers meet this electrical criterion; however, their mechanical properties (e.g. Young's modulus of Alkyds is only 20 GNm^{-2}) is too weak for our application. In addition, because of their thermal property, they are also not suitable for long term outdoor usages. It seems that more material science research is required to syntheses such material.

6.8 Conclusion

In this Chapter, experiments on various methods to deal with intermodulation interference are reported. In general, two approaches are found to be useful : firstly, preventive methods, such as corrosion resistant coatings, as well as non-corrodible building materials; secondly, corrective methods, such as by-passing a corroded joint via another linear rf current path; and some surface treatment techniques, such as rust removing agents.

It was found that any type of coating for by-passing the rusty junctions must have a very high conductivity for it to work and metal was found to be the only choice; other non-metallic conductors, such as graphite, do not possess the high conductivity required.

In general, metallic plating is the most suitable technique which could provide a continuous metal film if the base

metal is very clean. Other techniques, such as metal-loaded paint, are less than satisfactory because of their low bulk conductivities. Among all the metallic plating techniques that were attempted, it was found that sacrificial zinc/copper gel (solution) provides a better plating result than other means, such as electroless plating. In addition, three other alternative methods were also investigated, namely, zinc spraying, high performance corrosion resistant coating, and new materials for construction. Zinc spraying is good for both new and existing towers; however, its applicability is seriously hindered by the operational difficulty that it has to be used high above ground (about 150 metres) with continuously changing wind profile. The high performance corrosion resistant coating - Celcote promises a method to reduce intermodulation interference at its source by preventing the joints from getting corroded in the first place. Alternative building materials, such as CFRP, which would not corrode under normal atmospheric conditions and need less maintenance, are also of great interest.

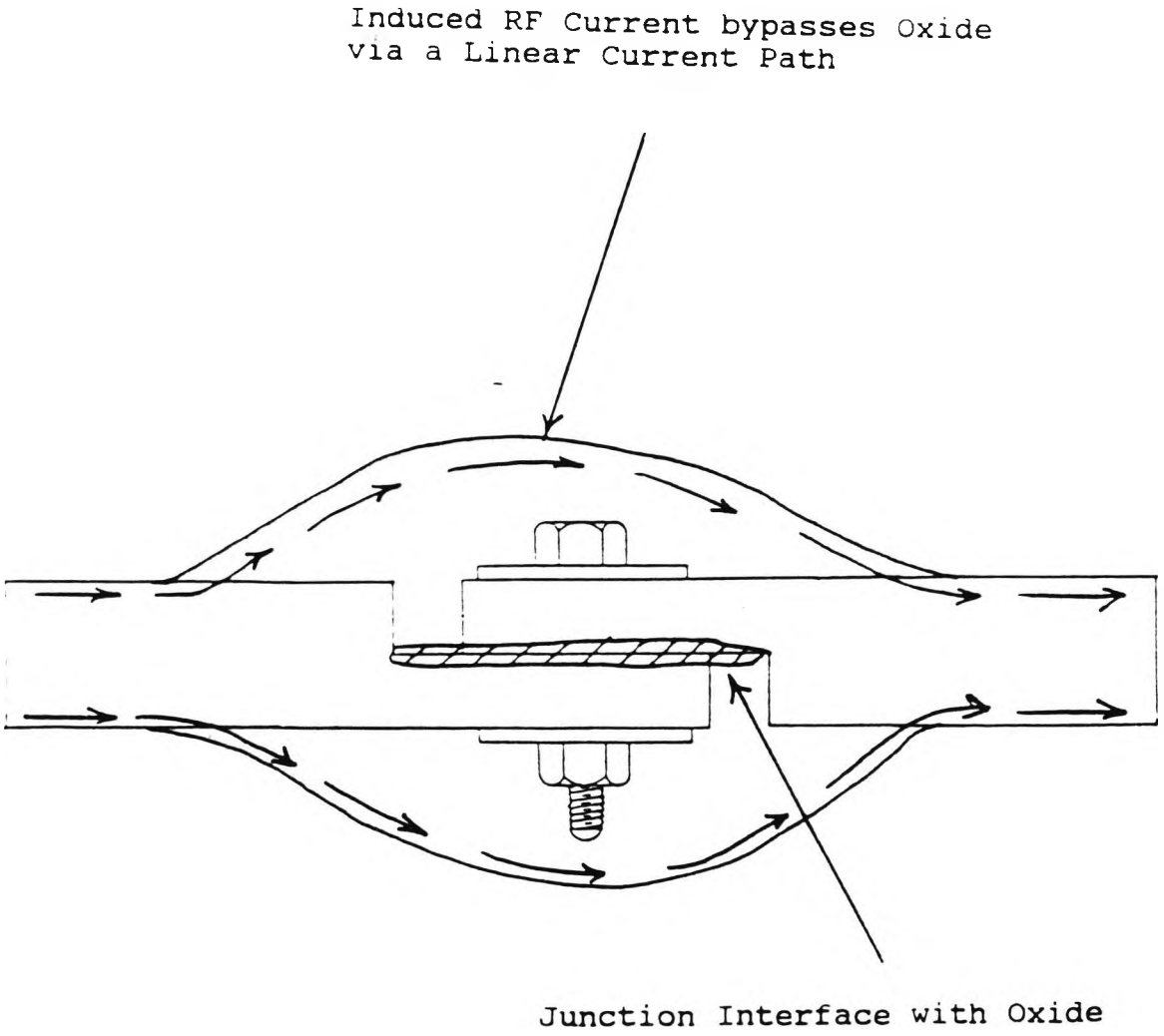

FIGURE 6.1 **Alternative linear electrical path for the induced radio frequency current**

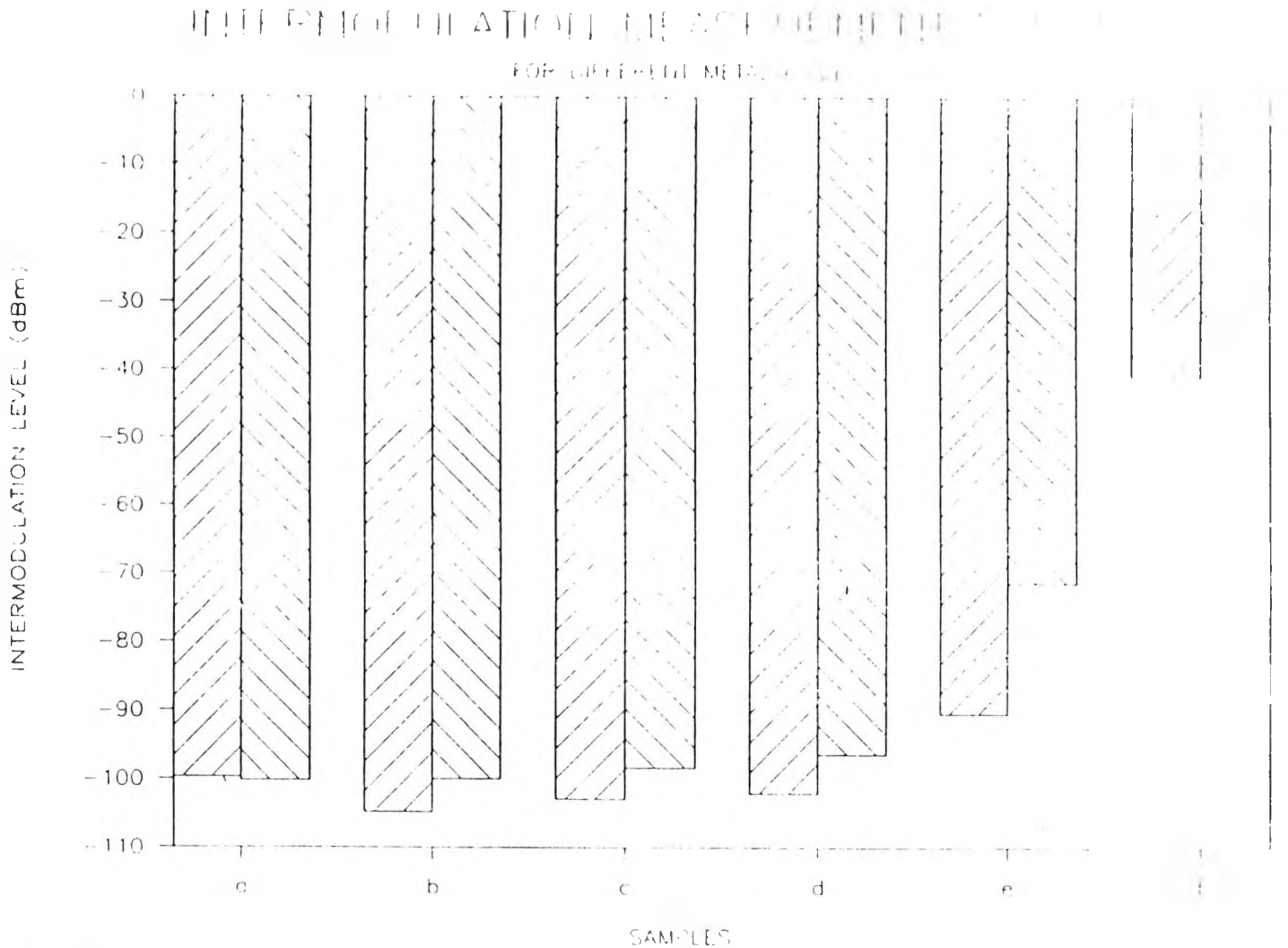

a = background b = gold c = copper d = platinum e = steel f = rusty steel

= before exposed in air = after exposure

FIGURE 6.2 IMI of different metal piece

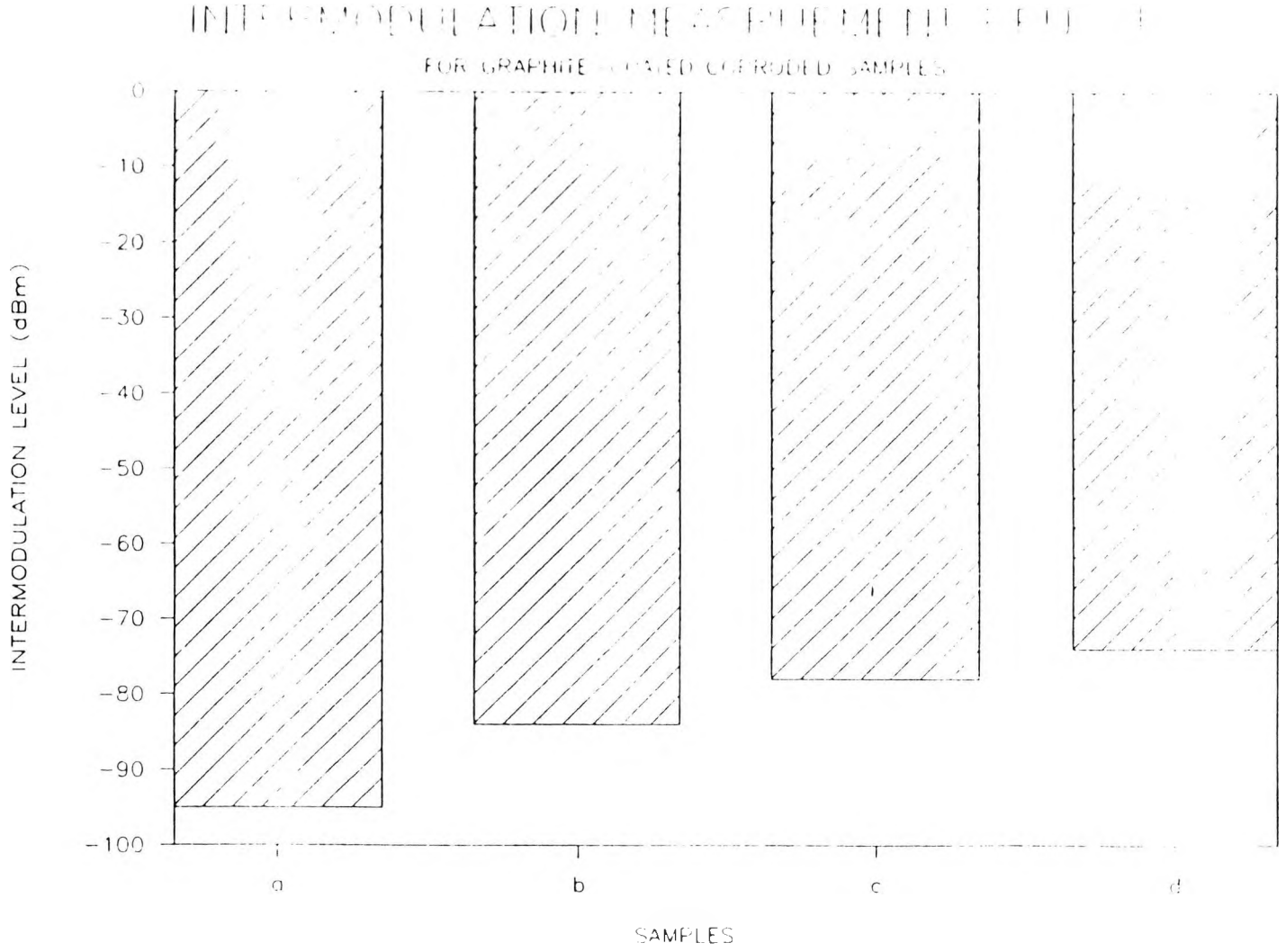

a = background b = graphite-coated clean rod c = graphite-coated corroded (surface) rod
d = corroded (surface only, not ends) rod

FIGURE 6.3 Effect of graphite-based coating on IMI reduction

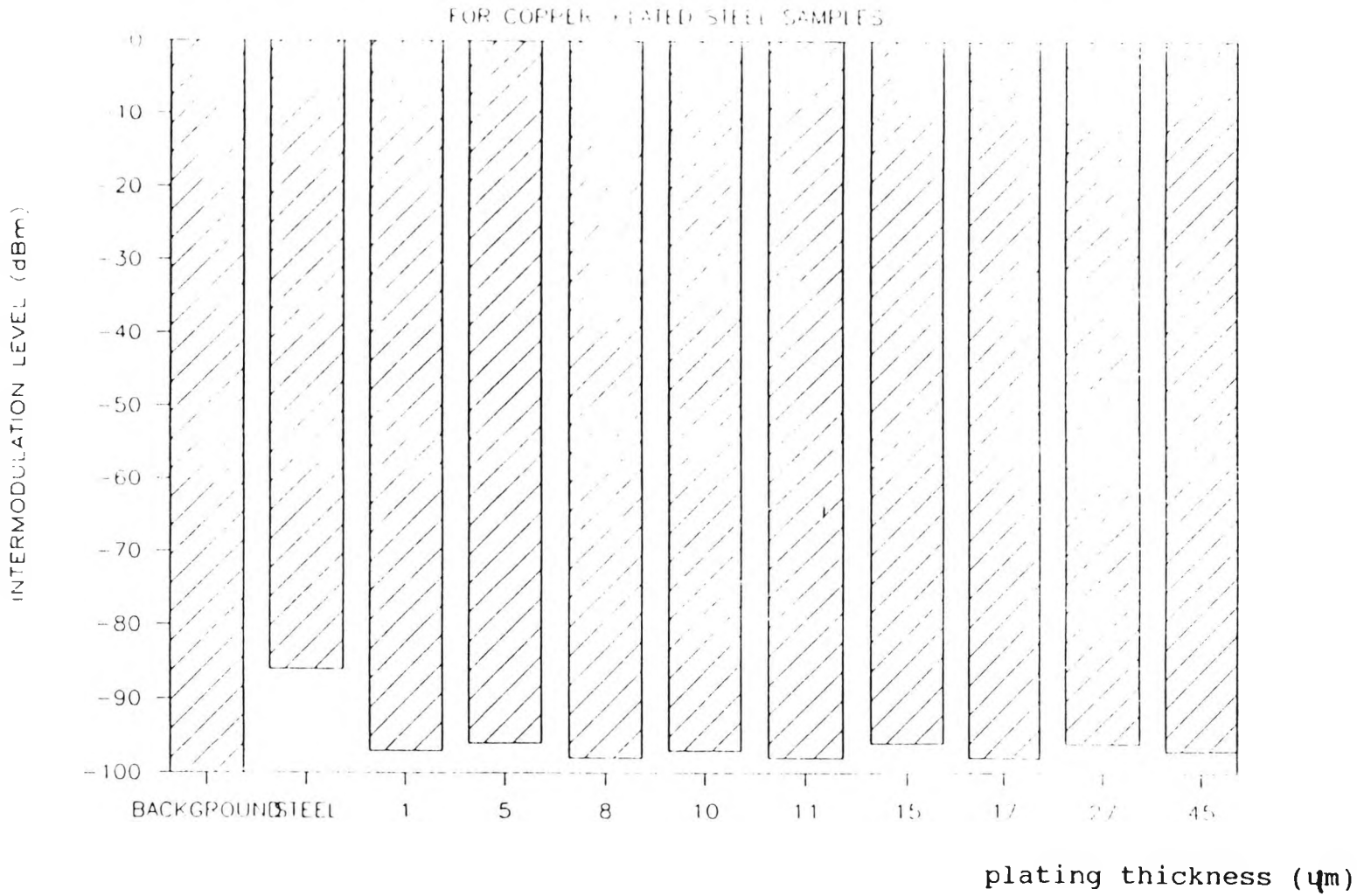

FIGURE 6.4 Effect of copper plating on IMI reduction (various thicknesses)

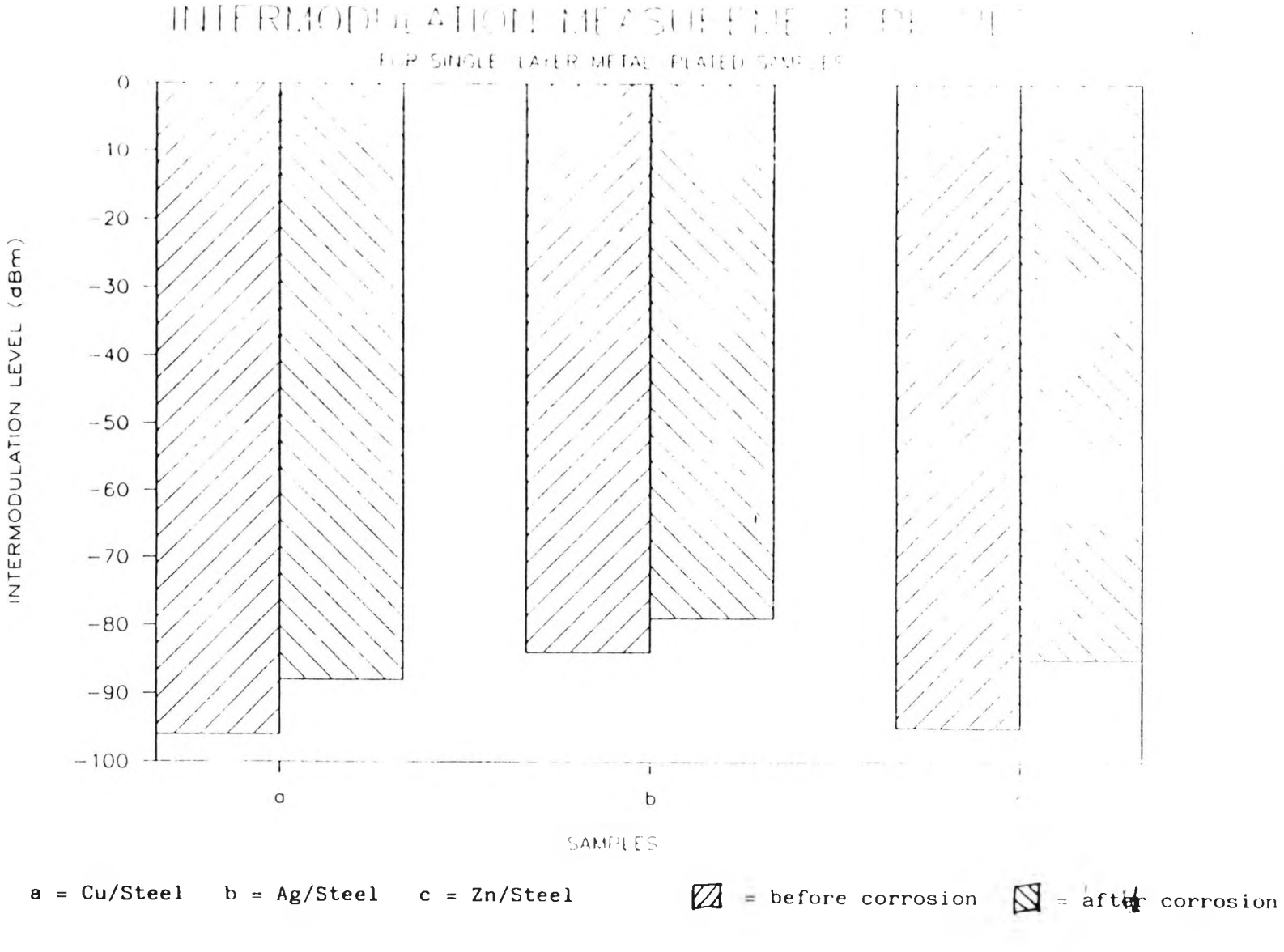

FIGURE 6.5 IMI of single-layer metal-plated samples before and after corrosion

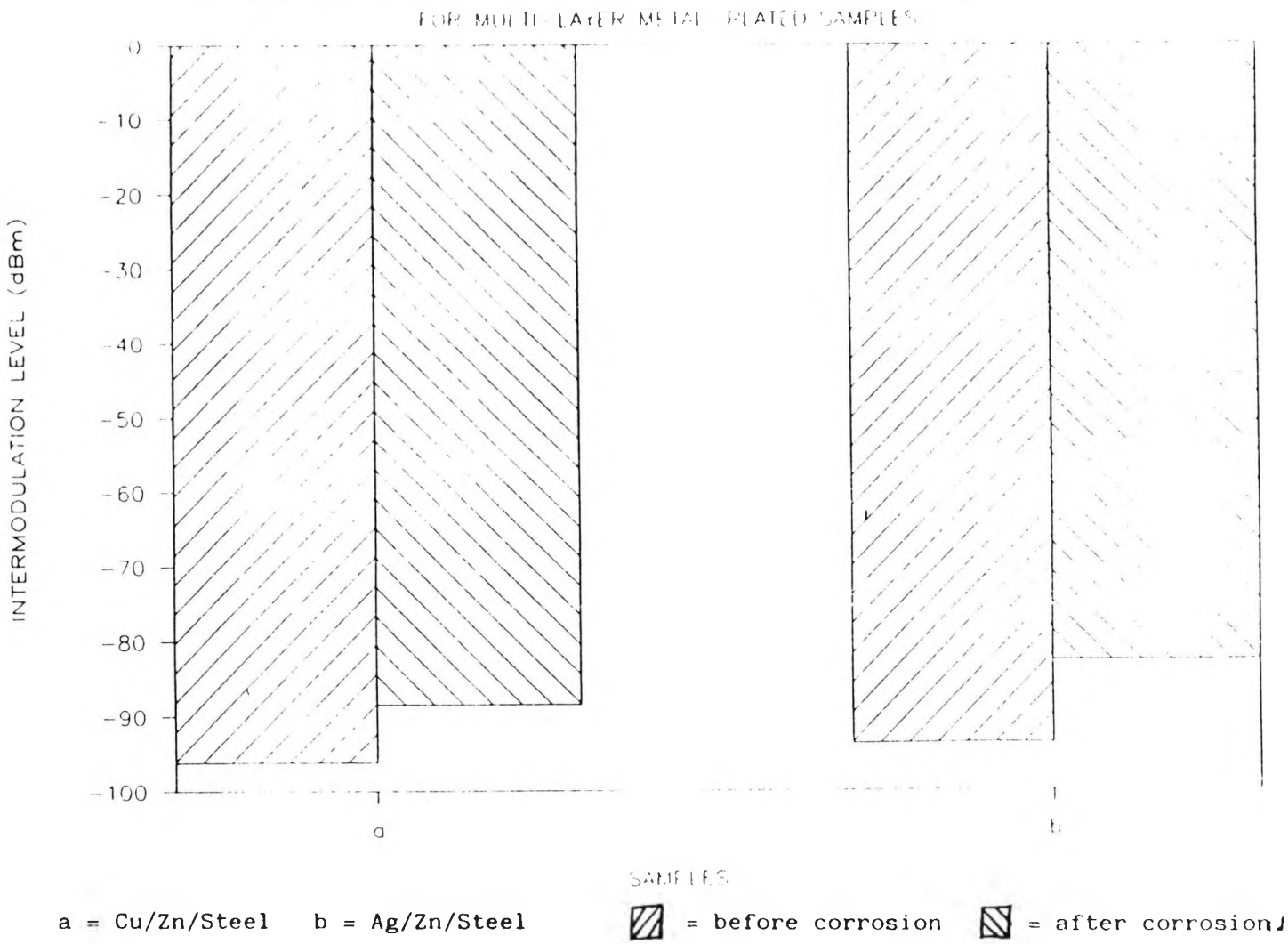

FIGURE 6.6 IMI of multi-layer metal-plated samples before and after corrosion

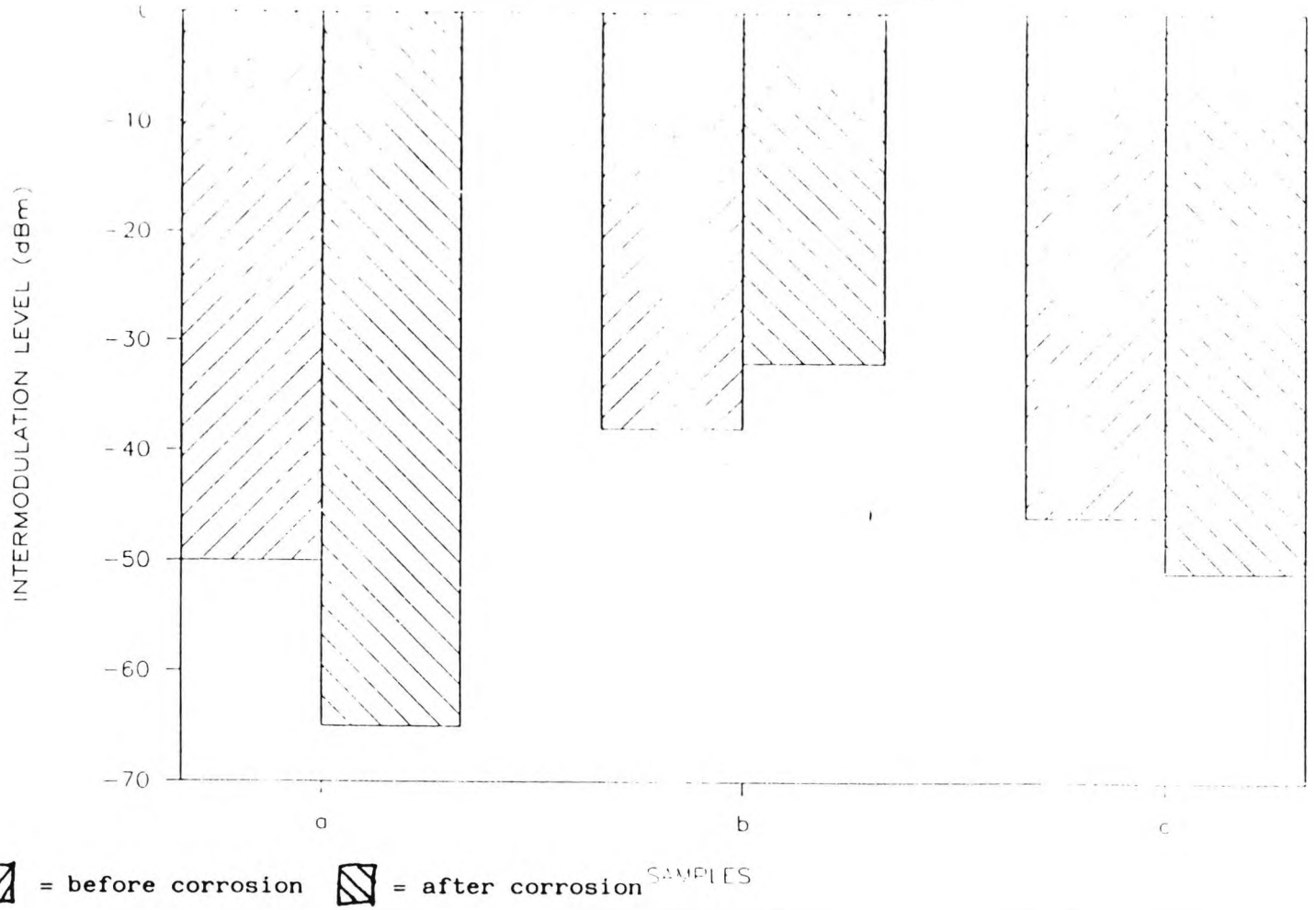

FIGURE 6.7 IMI of corroded joint samples which were silver-plated with different techniques

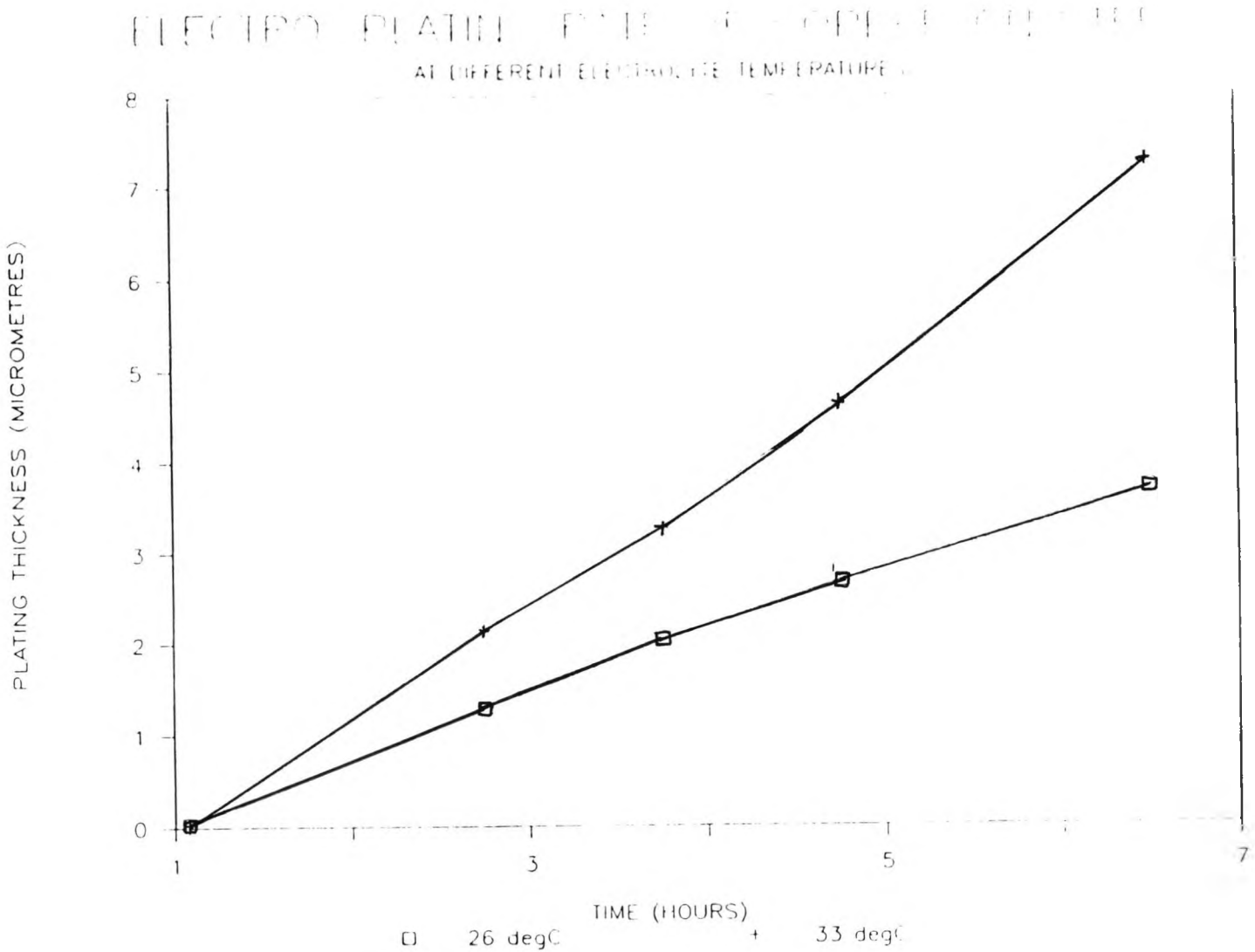

FIGURE 6.8 Plating rates of electroless copper-plating of steel rod samples at different electrolyte temperatures

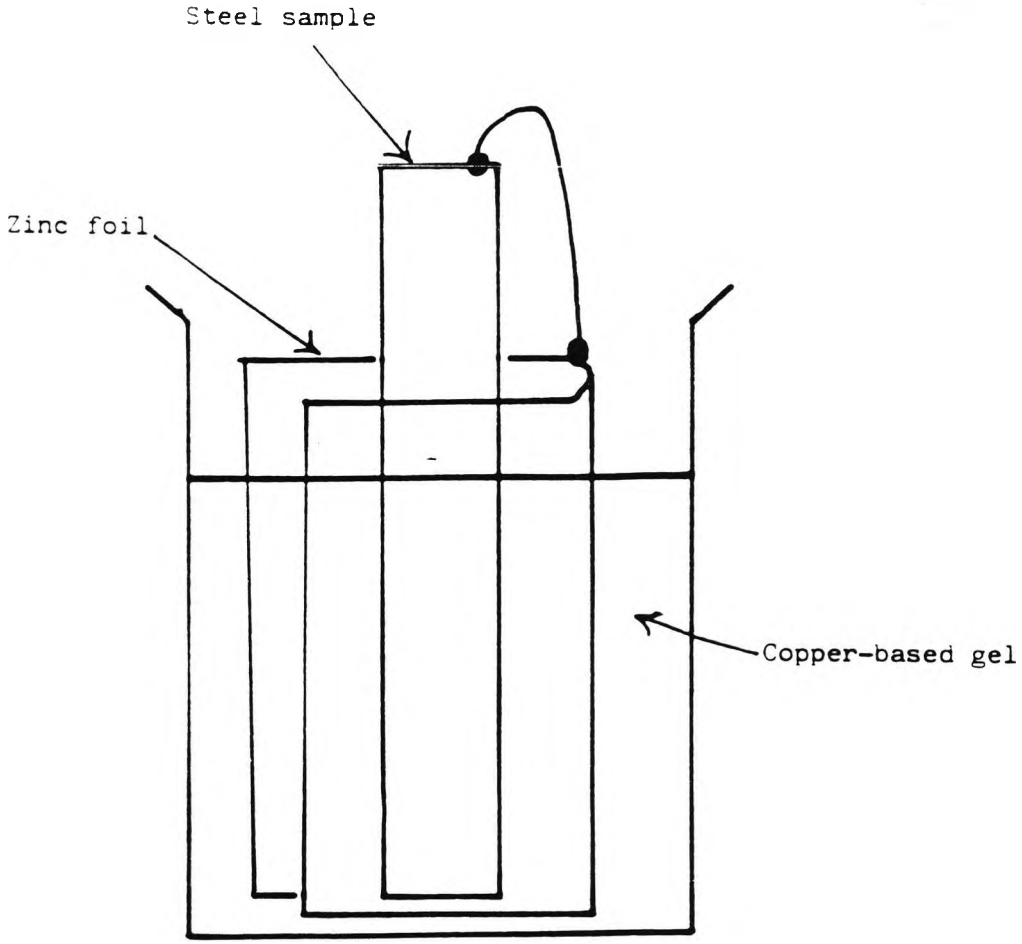

FIGURE 6.9 Sacrificial Zn/Cu Gel plating setup

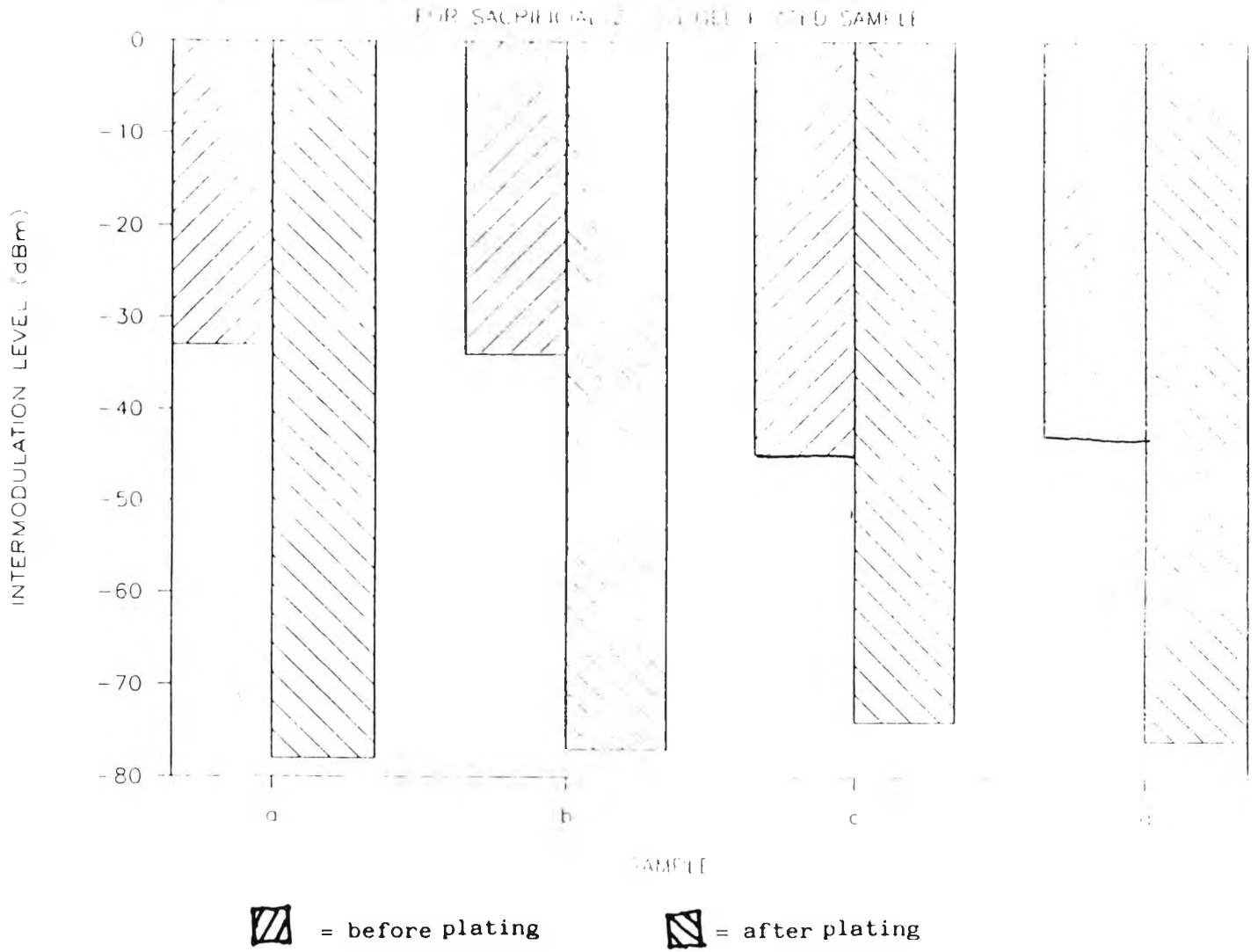

FIGURE 6.10 IMI reduction of sacrificial Zn/Cu Gel plated (previously corroded) joint samples

FIGURE 6.11 IMI of low viscose Gel plated (previously corroded) joint samples

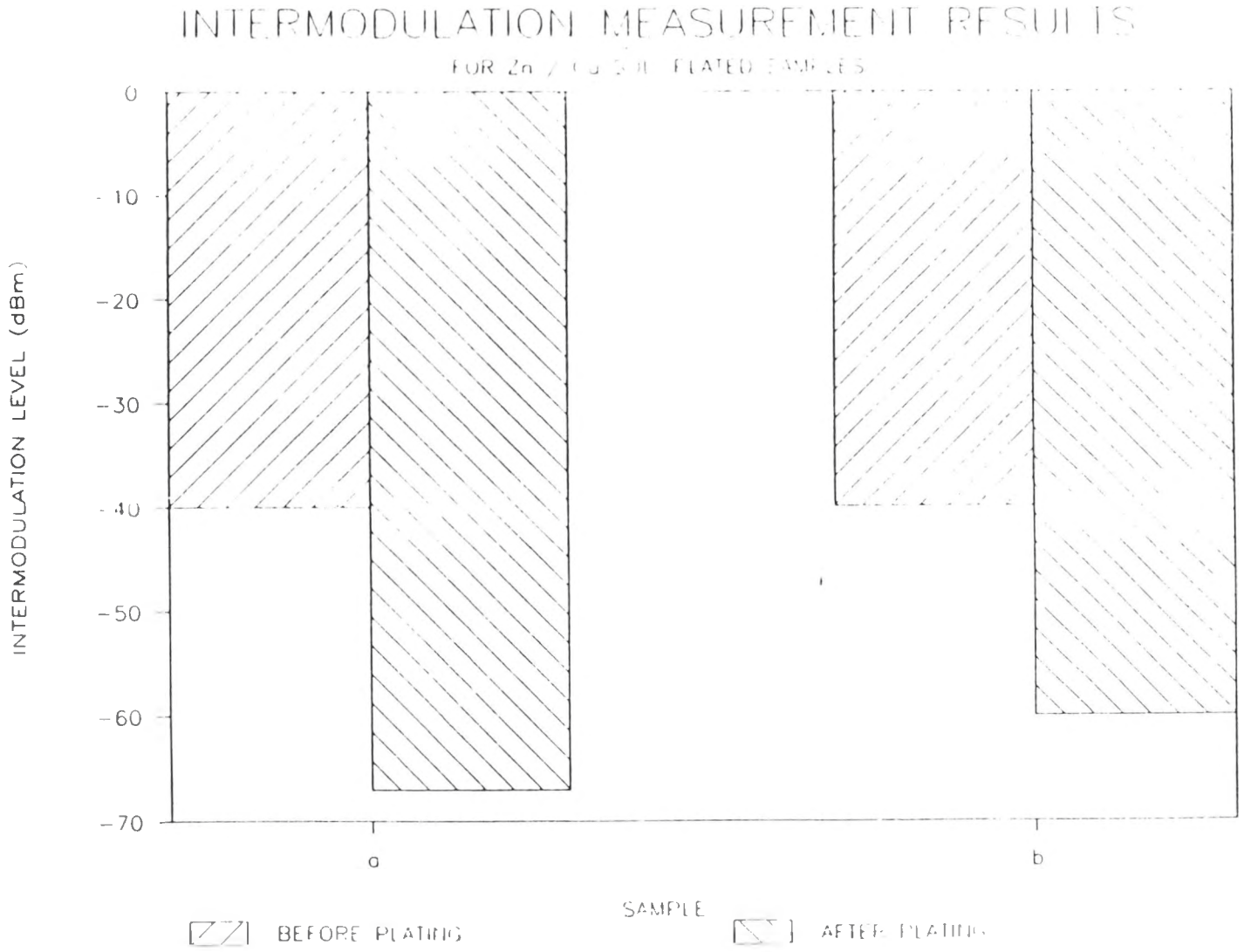

FIGURE 6.12 IMI of low viscose Gel plated (previously corroded) joint samples using sponge to contain the electrolyte

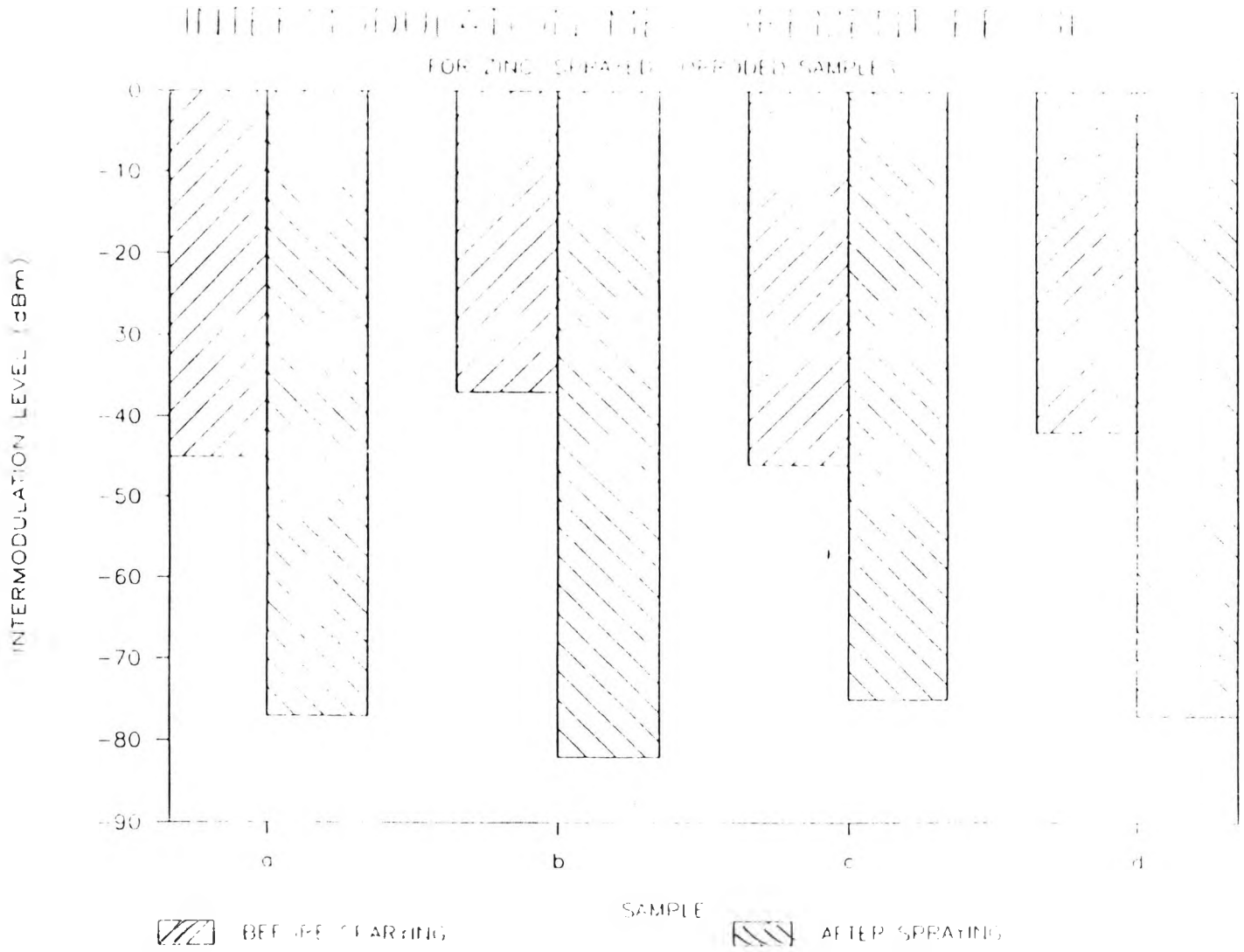

FIGURE 6.13 IMI of zinc sprayed (previously corroded) joint samples

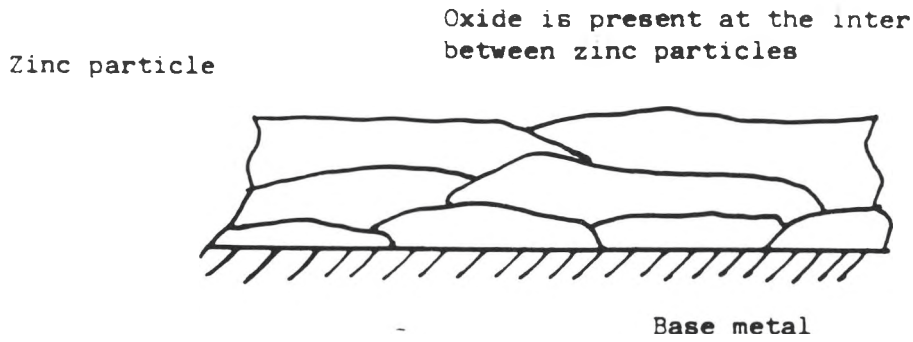

Surface condition of zinc-sprayed sample

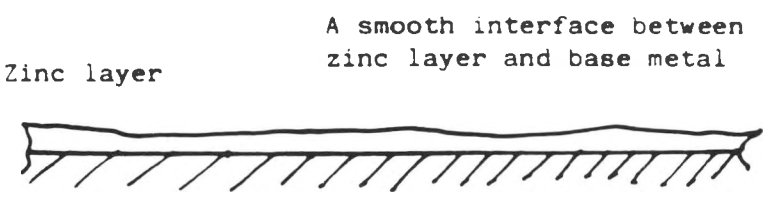

Surface condition of electro-plated sample

FIGURE 6.14 Surface conditions of sprayed zinc and electr
plated zinc

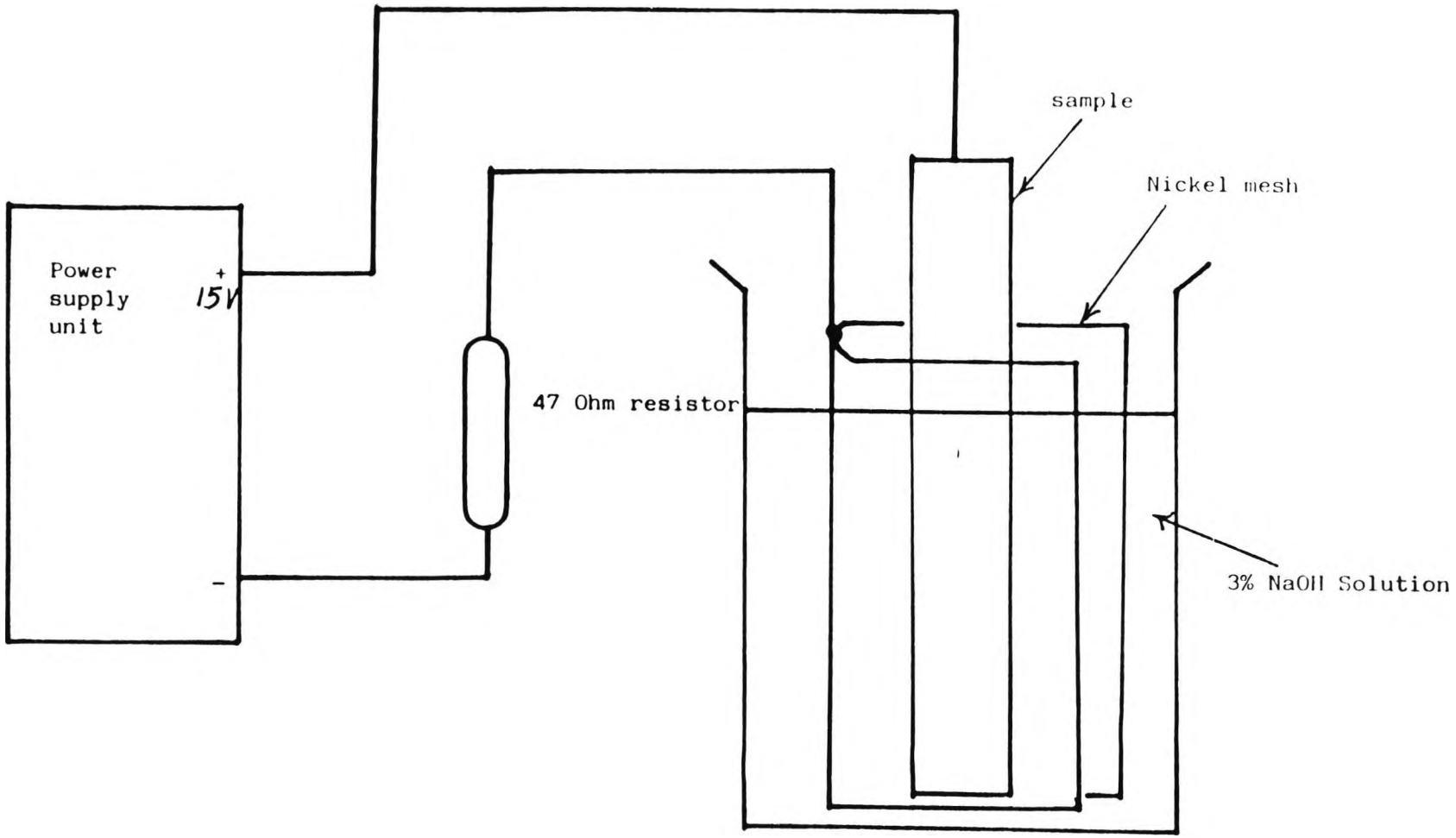

FIGURE 6.15 Setup for accelerated corrosion test

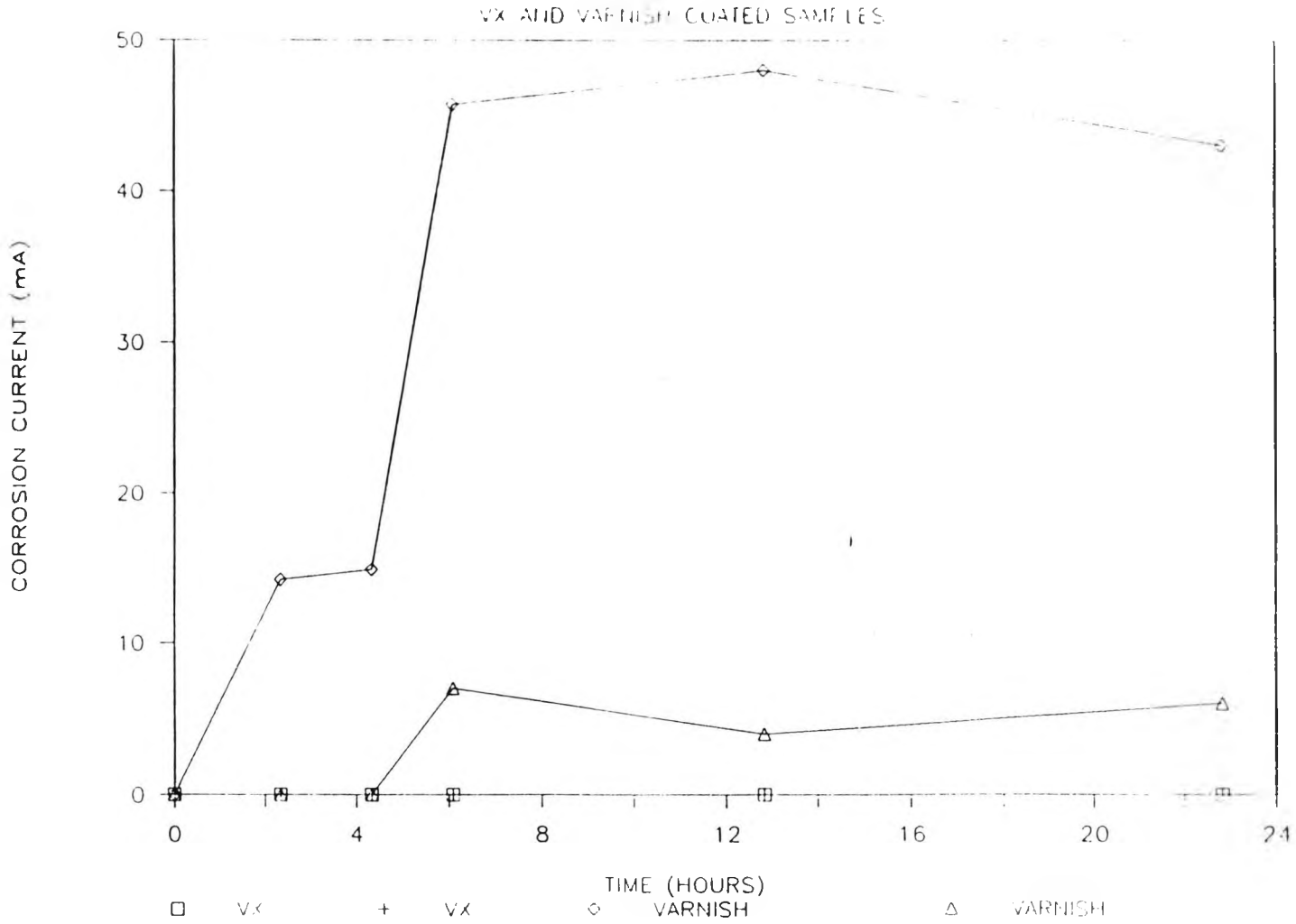

FIGURE 6.16 Corrosion current of test samples vs. time

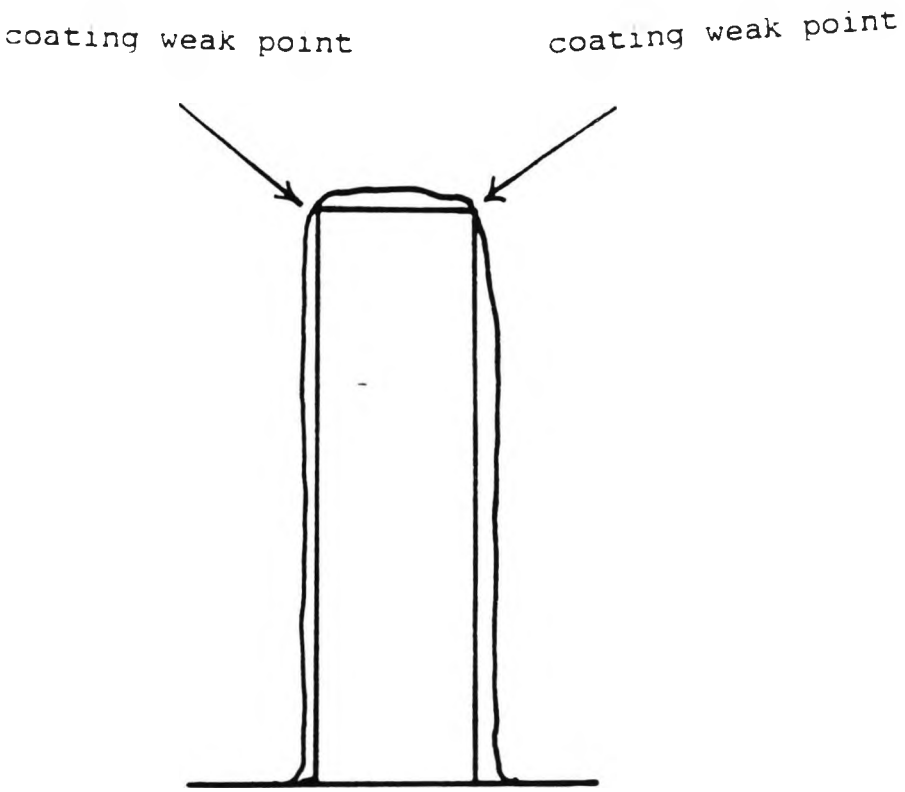

FIGURE 6.17 Weak points of paint-coated samples

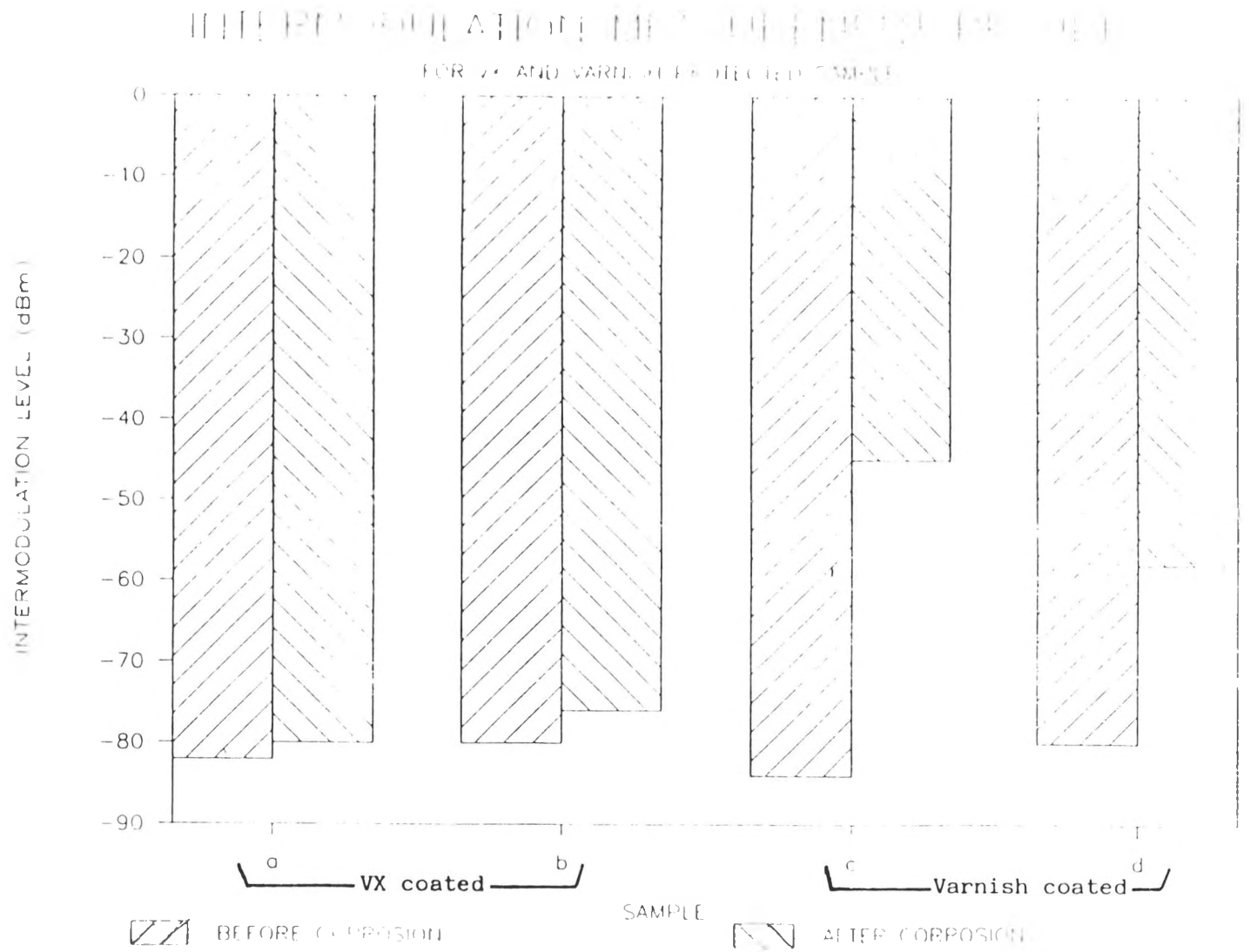

FIGURE 6.18 IMI of test samples after accelerated corrosion test

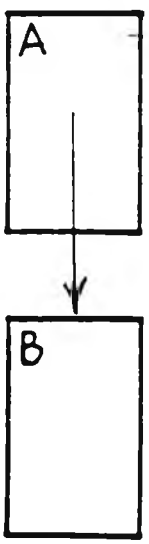

FIGURE 6.19 Cross-sectional area requirements for supporting in a structure

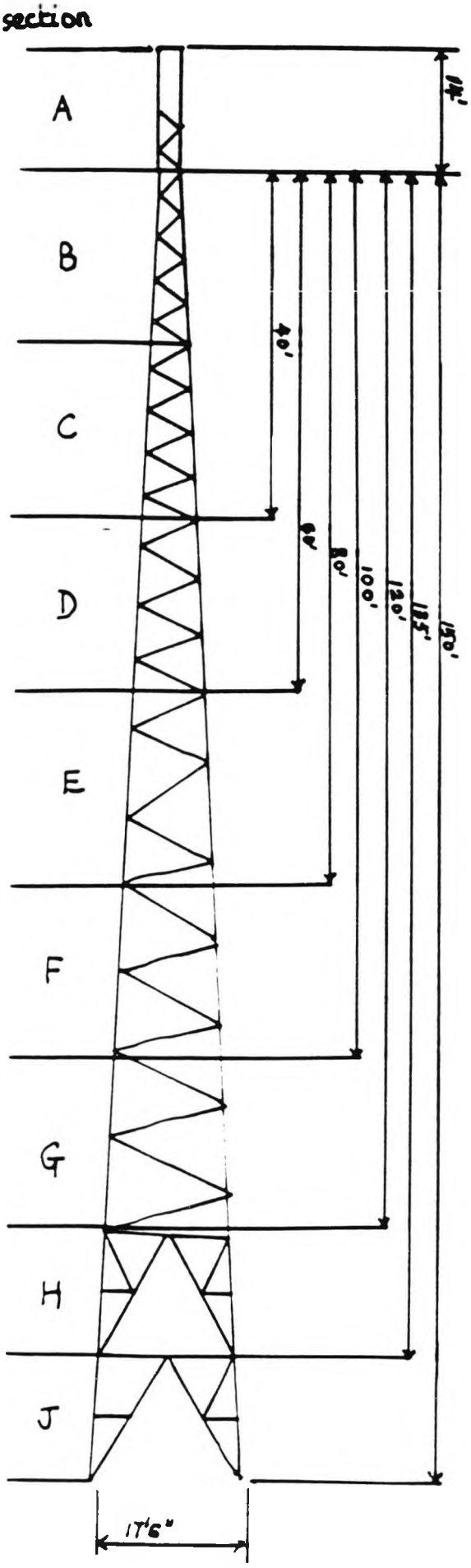

FIGURE 6.20 Cross-section view of a 45 metres lattice tow

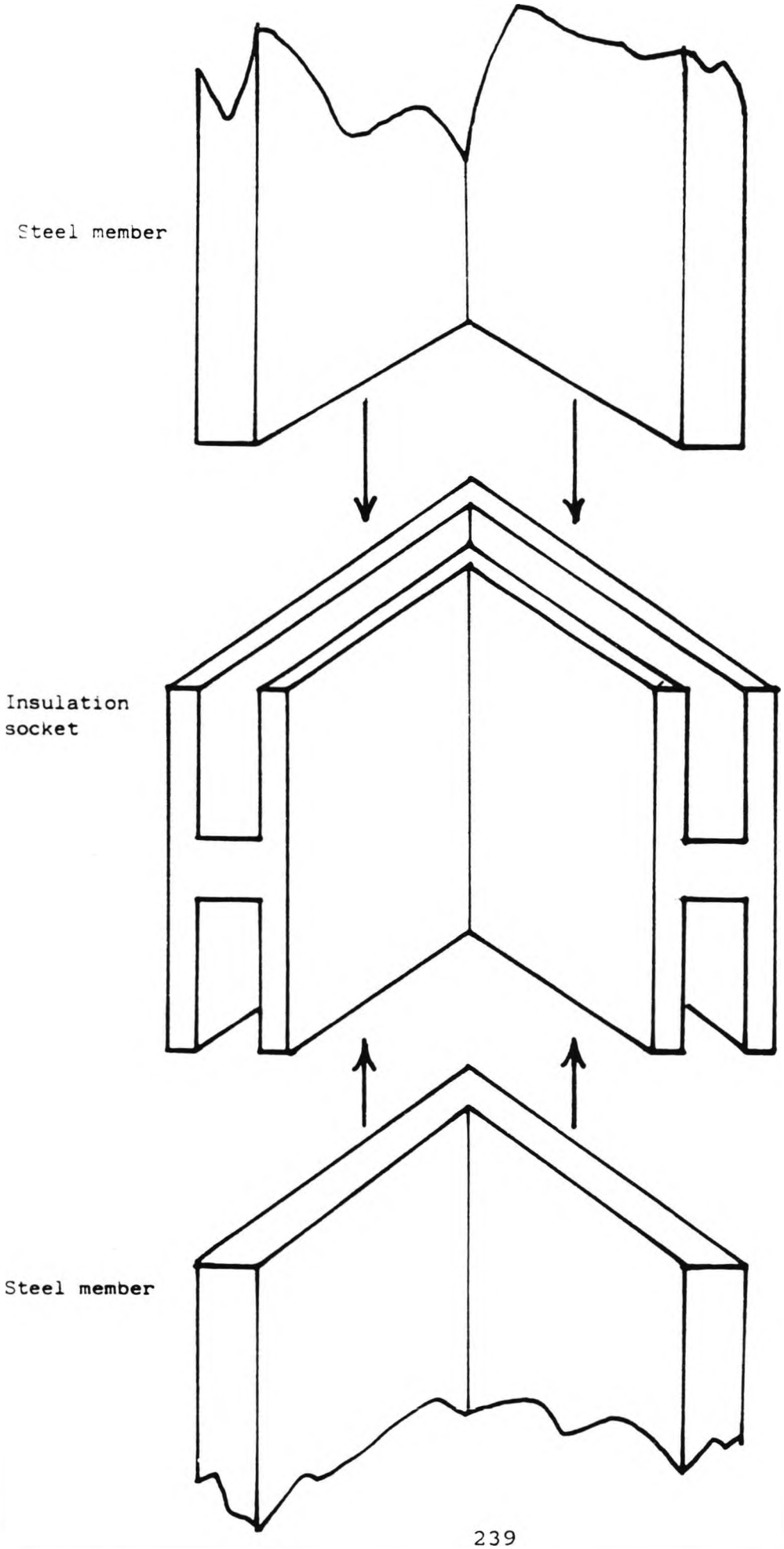

FIGURE 6.21 [illegible] to block the flow of induced radio frequency current

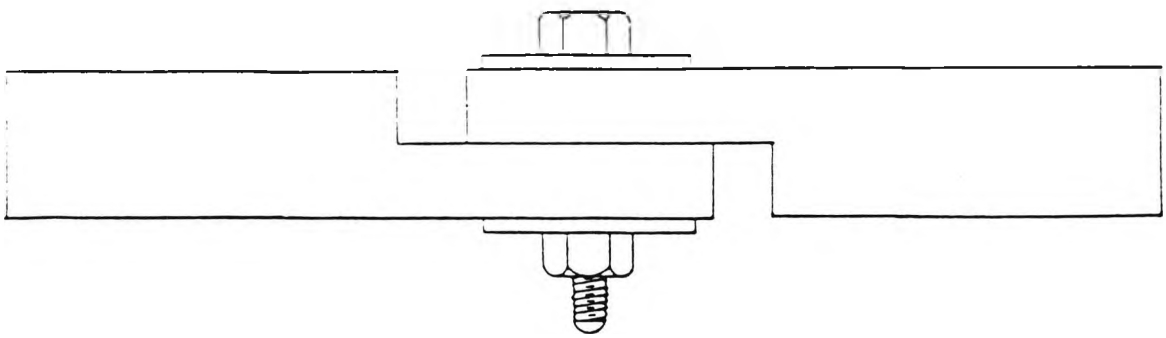

Sample	Metal bolt	Nylon bolt	Insulation at the junction
b		Yes	Yes
c	Yes		Yes
d		Yes	No
e	Yes		No

FIGURE 6.22 Effect of insulating the metallic contacts of a corroded joint sample on IMI

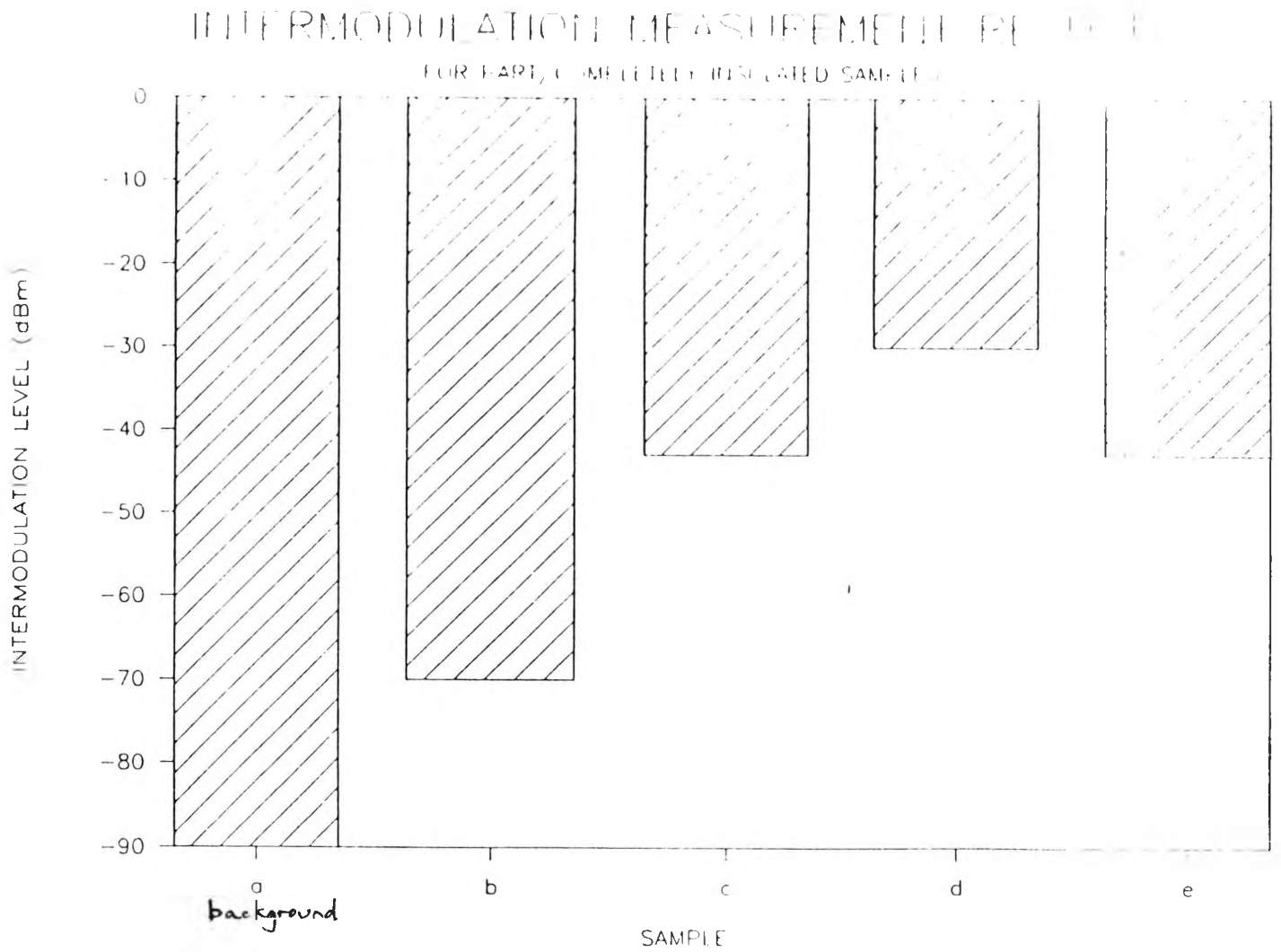

Refer to figure 6.22 for sample details

FIGURE 6.23 IMI measurement results of insulated (previously corroded) joint samples

Chapter 7

Conclusions and Further Work

7.1 General

Intermodulation interference is becoming a severe problem on the efficient use of the electromagnetic spectrum. With the ever-increasing number of cellular mobile radio operators and the associated installations of transmission equipments, the problem of interference will certainly get worse. In recognition of this problem, the governments of the European countries have worked together and is in the process of producing a EC-Directive on Electromagnetic Compatibility (EMC). The directive specifies the limits of spurious radiation from, as well as susceptibility to interference of all electrical, electronic, computing and office equipments. No doubt this will improve the problem of electrical interference generated from electronic equipments. However, this does not apply to interference due to uncontrollable factors, such as structural intermodulation interference due to the electrical environment where communication equipments operate.

7.2 Specific

In this dissertation, it has been shown that corroded metallic joints are capable of generating intermodulation interference. In particular, the non-linearity was found to be due to the rectifying contact effect; whereby, the metallic oxides act as semiconductor in contact with the base metal. The current-voltage non-linearity of a sample depends very much on its surface state, i.e. the severity of corrosion; and in general, the more corroded a sample, the more non-linear is the current-voltage characteristic.

By far, the corroded junction is a much more important source of intermodulation interference than surface corrosion products, or non-linear ferromagnetic effect. The reason is that in the case of a corroded joint, the induced rf current has no alternative current path to bypass the non-linear junction; whereas for surface corrosion, a large portion of the induced rf current would be forced to flow in the bulk of the base metal due to the skin-depth effect, hence a much smaller interference level. It was also found that the capacitance of a corroded joint was nearly constant (within experimental error) over a wide range of applied frequency between 1 MHz and 100 MHz. Interference due to non-linear dielectrics is therefore negligible.

A circuit model was developed for a corroded junction. In essence, the model consists of a non-linear resistance (represents the corrosion products) in parallel with a linear capacitance (represents the junction capacitance).

The non-linear resistance of the corrosion products is represented by its non-linear current-voltage characteristic expressed in a power series. The model was used to predict the intermodulation interference level generated from a test sample. The predicted value is higher than the experimental value; although it was still within the possible observation range of the test equipment.

An investigation on the effects of environmental factors on the background intermodulation level was carried out. From field measurements, it was found that (1) wind-induced vibration in an corroded antenna mast could produce rapid and large changes in the intermodulation level; (2) when it rains, the intermodulation level falls to the floor level of the measurement equipment; and (3) changes in ambient temperature will not cause significant variations in intermodulation level immediately. It was revealed in the experiments that the high permittivity of water is responsible for the immediate reduction in intermodulation level, instead of its conductivity. The effect of wind-induced vibration on the tower member joints was also investigated. It was found that it is possible for a vibrating clean joint to generate low level wide band noise. Since the joints distributed throughout the whole antenna tower, then this could be one of the possible explanations of the observation, by some investigators, that "the whole antenna mast immersed in the sea of intermodulation interference".

Investigations on various methods to reduce intermodulation

interference were also performed. Basically, provision of an alternative linear rf current path is necessary for corroded joints in existing towers; and high corrosion resistant coating and un-corrodible building materials are desirable in constructing new antenna masts. In the first case, it was found that metal plating is the only possible solution which can provide the high enough electrical conductivity for the induced rf current to bypass the corroded junction. In the latter case, a newly-developed coating - Celcote, has shown an excellent corrosion resistance property, suitable for long term outdoor uses. In addition, alternative material, namely, Carbon Fibre Reinforced Plastic (CFRP) and non-conductive polymer, which are virtually un-corrodible were also considered. The cost effectiveness of CFRP was shown to be reasonable if it is used more widely, and new design disciplines are produced for it. Non-conductive polymer is also very useful, but its mechanical properties are not yet up to the necessary construction requirements.

7.3 Further Work

Further work could be carried out along the following paths :

(1) Severity of structural intermodulation interference on other cellular mobile radio frequency band, such as at 900 MHz for Digital European Cellular Network (DECN) and at 1.8 GHz for the Personal Communication Network (PCN) should be investigated, due to the anticipated large number of users.

(2) Since digital communication methods are used extensively nowadays, the effects of intermodulation interference on the quality of speech, data, text and video communication, should also be carried out.

(3) The mechanical properties of the high corrosion resistance coating - Celcote should be evaluated further. It should be able to stand the normal operation requirements, i.e. wind loading, ice loading, ultra violet light exposure ... etc, of an antenna mast; and possible enhancements on its mechanical performance would certainly open a wide market for its applications in both outdoor and marine environment.

(4) More material science research on the properties of CFRP and non-conductive polymers would open a whole new area of mechanically strong and un-corrodible building materials for the construction industry.

Appendix 1

Preparation of Chemical Coatings

The following data relate to those coatings which have been shown to exhibit the physical characteristics required. Other preparations not fulfilling these requirements were discarded.

COATING NO.	DETAILS
A1	2g PVP solution (50g/l aqueous solution) 2g ethylene glycol 0.5g EDTA solution
A2	As A1 with addition of 0.5g HSA carbon black
A3	As A2 " " " " 1g " " "
B1	0.5g $AgNO_3$ solution (2g Ag^+ ion per 100 mls) 2g PVP solution (50 g/l aqueous solution)
B2	As B1 but with 0.25g $AgNO_3$ solution
B3	As B1 but with no $AgNO_3$ solution
C1	2g HSA carbon black 1g PTFE dispersion (containing 60% by weight solid PTFE) 2g PVP solution (50 g/l aqueous solution) 0.5 g EDTA solution (25 g/l aqueous solution)
C2	As C1 but with 1.5g PVP solution
C3	" " " " 1.0g " "
C4	" " " " 0.5g " "
C12	As C1 but with no EDTA solution
C13	" " " " 1.0g "
C14	" " " 2.0g "
D1	2g HSA carbon black 1g PTFE dispersion (containing 60% by weight solid PTFE) 2g PVP solution (50 g/l aqueous solution)
D2	As D1 but with 1.5g PVP solution
D3	" " " 1.0g " "
D4	" " 0.5g " "

E1	2g HSA carbon black 1g PTFE dispersion 2 " adiprene urethane liquid elastomer, added directly to a slurry of first two components. 1g EDTA solution (25 g/l aqueous solution)
E2	As E1 but with 1g adiprene
E3	" " " " 0.5g "
E4	As E1 but with no EDTA
E5	As E2 " " no adiprene

The results shown in this report were obtained using preparation C3. This was selected as it appeared to give a coating which was easily applied by brush and could be cured with a hot air gun to give an even coverage, which was very adherent and resistant to scratching. Applications of C3 were all made from the same bulk batch.

Glossary

PVP	polyvinyl pyrrolidone
EDTA	the sodium salt of ethylenediaminetetraacetic acid
PTFE	polytetrafluoroethylene
HSA	high surface area

Appendix 2

Papers submitted to Conferences

AGARD-CPP-420

AGARD

ADVISORY GROUP FOR AEROSPACE RESEARCH & DEVELOPMENT

7 RUE ANCELLE 92200 NEUILLY SUR SEINE FRANCE

AGARD CONFERENCE PREPRINT No.420

Effects of Electromagnetic Noise and Interference on Performance of Military Radio Commmunication Systems

NORTH ATLANTIC TREATY ORGANIZATION

INTERMODULATION INTERFERENCES IN RADIO SYSTEMS

Mr P.S.W.Ho[1], Dr L.H.Bevan[2], Prof A.C.C.Tseung[2] and Mr W .Wilkinson[1]
Electrical and Electronic Engineering Department[1]/Chemical Energy Research Centre[2]
City University, Northampton Square, London EC1V 0HB, U.K.

Summary: The phenomenon of intermodulation is introduced first. The origins of intermodulation interference in a radio communication systems are considered. Mechanisms responsible for this interference, for example, ferromagnetic nonlinearity and electron tunnelling are considered, and a model based on a metal-semiconductor rectifying junction is suggested. An experimental setup for measuring intermodulation levels of specially treated test samples and the operating procedures are then described. A general principle to overcome the structural intermodulation problem is outlined. Experimental results for some chemical and metallic coatings ,and their merits are presented next. Lastly, the usefulness of monitoring the background intermodulation level of a test site is given. In conclusion, the joint effect is the first order factor in determining the degree of seriousness of the intermodulation problem and the use of high conductivity coating provides the most feasible solution.

1 Introduction

When two or more radio frequency signals f_1, f_2, ... f_n are mixed in a device with non-linear transfer characteristic, spurious frequency components, f_{im}, will be generated and are called Intermodulation Products (IMP).

f_{im} are given by :

$$f_{im} = a_1 f_1 + a_2 f_2 + \ldots\ldots a_n f_n$$

where a_1, a_2,... a_n are either zero or which may be positive or negative integers and ($a_1 + a_2 + \ldots a_n$) is the order of the intermodulation product. In general, the amplitudes of lower order IMPs are larger than the higher order IMPs. However, experimental results [1] have shown that products upto eleventh order or even higher can have adverse effects on the performance of communication systems.

2 Background for investigations

The problems of intermodulation interference in radio communication services are getting more and more serious because of the increasing demands on the available electromagnetic spectrum. As the number of channels increase, the number of IMP increases at a prodigious rate. Intermodulation frequency free planning has been an important and difficult task for communication service planners. Extensive work [2 - 4] have been done on deriving algorithms to calculate the amplitudes and frequency components of the intermodulation products for a given set of input frequencies. The time taken to carry out these calculations are very long for planning a large communication service, such as a cellular mobile radio communication network. The applications of high speed computers or parallel processing computers could reduce the time requirement.

Basically, intermodulation interference (IMI) can be divided into two types. First, those due to active devices in the communication systems, such as the non-linearity of the power amplifiers in the transmitters where common antennas are employed, and overloading of the receiver front-end. The second type is due to the passive components in the communication systems and these include cables, feeders, aerials and the supporting structures.

Effective methods have been found to solve the problems of the active type by careful shielding of equipments, using filters in the transmitter outputs and receiver inputs. However, the passive type is a much more intractable problem, and once generated, cannot be removed by filtering.

3 Causes of Passive Intermodulation Interferences

There are two major causes for the generation of passive intermodulation products, namely non-linear junction effect and B/H non-linearity which is inherent in any ferromagnetic material.

Investigations into the ferromagnetic nonlinearity effects [5,6] have identified that radio frequency connectors with nickel-plating can cause high levels of IMI and are not recommended for use in systems carrying large radio frequency currents and susceptible to intermodulation interference. Betts and Ebenezer [7] found that steel supporting structures for aerials were also a source of problems. However, ferromagnetic non-linearity of a bulk material is only a second order effect. The prime factor is the non-linear junction effect.

The non-linear current/voltage characteristics of a rusty joint (metal-oxide-metal junction) has been assumed by many researchers to be due to electrons tunnelling through the oxide layer. Tunnelling phenomena has been a hot topic among solid state physicists [8-10]. Higa [11] tried to explain the spurious signals generated on large reflector antennas by tunnelling of electrons through aluminium-aluminium oxide-aluminium junctions. Though Quenzer [12] from Naval Research Laboratory, Washington, expressed doubts on Higa's arguments. Woody et al [13] carried out a research program on Metal-Insulator-Metal (MIM) Junctions as a Surface Source of Intermodulation. They found that researchers could not agree to the correct form of the tunnelling equation and more important, the simple electron tunnelling model would not be able to predict IMP levels in real life situations due to their inherent complexities. They adapted an experimental approach and developed an empirical model based on measurements of representative MIM junctions. Their findings also confirmed that MIM junctions can generate IMPs that are much higher that IMPs generated by coaxial cables and connectors. Also they found that many junctions have very unstable IMPs which were neither predictable nor repeatable.

According to quantum theory, the probability of an electron tunnelling through a barrier is inversely proportional to the exponential of the thickness of the insulating layer. An insulating layer of thickness greater than 100 Å is impenetrable for electrons. We are not saying that electron tunnelling cannot be a candidate. For example, aluminium oxide has a film thickness of around 20 Å and tunnelling could be responsible for the observed nonlinear current/voltage characteristic of aluminium-aluminium oxide-aluminium junction.

Structural steel forms various iron oxides when exposed to the atmosphere. The thickness of these oxides are significantly larger than 100 Å. We suspect that in this case the nonlinear current/voltage characteristic might be due to junction effect instead of tunnelling; i.e. rectifying junction effect due to metal-semiconductor contacts. It has been shown that conductivity of transition metal oxides can be very high [14]. For example, at room temperature, the conductivity of FeO is about 20 Sm^{-1}, Fe_3O_4 is nearly metallic, though Fe_2O_3 has a conductivity of order only around 10^{-3} Sm^{-1}. High conductivity is dominated by nonstochiometry of the lattice structure. Conduction in undoped material will have contributions from both donors and acceptors. For cuprous oxide, the conductivity(σ) even has an oxygen pressure(P) dependence of $\sigma \sim P^n$, where n assumes values from 1/7 to 1/8.

4 Experiments

4.1 General

Various techniques have been proposed to overcome the intermodulation problem. They all employed the principle of providing an alternative radio frequency path to the rusty junction. There were particular interests in the chemical approach [15], using high dielectric materials. Their argument is based on modelling the non-linear junction as two back-to-back diodes. Putting high dielectric coating on the joint provides a shunt capacitance across it and at high frequency, this capacitance bypasses most of the induced radio frequency current. However, their results have shown that no significant improvements had been achieved. This might be due to the relatively small ratio of dielectric constants between the coating and air, hence there is always incoming wave transmitted into the corroded metal. There could also be adhesion problem of the coatings as well.

4.2 Measurement techniques and experimental procedure

The block diagram of the test setup is shown in figure(1). The two fundamental frequencies are generated by two synthesized signal generators. Power amplifiers are used to give an output of around 50 Watts for each signal. Harmonics generated in the amplifiers are removed by the high-Q cavity resonant filters connected to the outputs of the amplifiers. These signals are then fed into the combining unit by half-wavelength coaxial cables in order to avoid line resonance effects. Filter unit 3 is tuned to the IMP frequency ($2f_2-f_1$) which rejects any signals at the fundamental frequencies. A dynamic range down to -110 dBm can be measured by the spectrum analyser. The fundamental signals are terminated by 100 metres of RG214 cable which acts a linear dummy load. The intermodulation signal is terminated equally by this linear load and the spectrum analyser. With this setup, a signal to intermodulation level ratio of better than 150 dB can be measured.

Before any experiment is carried out, the test setup has to be calibrated. The filters are tuned to their respective resonant frequency and the power amplifier outputs are fixed at 50 Watts. With a clean cylindrical copper sample in the test cell, the background level of the IMP frequency was measured.

Repeatability is tested by measuring the IMP levels of the same sample for several times. We found that variations in results were normally less than 10 dB. This might be due to change in temperature, microstructures of the contact surfaces etc. However, by doing sufficient number of measurements with each sample, a statistical mean level should be achievable. Samples could then be compared with each other for IMP performance using these mean IMP levels.

5 Results

5.1 Experiment Conditions

All measurements were made under the following conditions :

f_1 = 155.2125 MHz, f_2 = 152.0875 MHz, f_{im} = 148.9625 MHz.

Power level of each input signal is 50 Watts (approximately +47 dBm).
The spectrum analyser reading error is +/- 1 dBm.

Samples were corroded by the electrolysis of artificial sea water, with an anodic potential of around 500 mV (versus hydrogen electrode) for 24 hours, unless stated otherwise.

5.2 Experimental results

Initially, the work at City University was to evaluate the use of a graphite-based coating, since graphite would not form an oxide film when it is corroded. Unfortunately the conductivity of the coating is not good enough to stop radio frequency currents from penetrating into the bulk of steel structures. Results are shown in figure(3).

After suspending the work on the graphite-based coating, we turned our attention to various metal platings. An approach to prevent intermodulation caused by the ferromagnetic nature of steel was to galvanise steel, for initial protection, then plate a layer of a more noble metal such as silver (or copper, tin, etc) on top of the zinc layer. The reason for the top layer was because the corrosion product of zinc could cause some intermodulation product while those of silver did not (or to a lesser extent because they are more conducting).

From figure(4), it can be seen that double-layer plated samples all had an initial intermodulation level of above 90 dBm, i.e. around 10 dBm lower than clean steel sample, and their intermodulation values after corrosion were also around 10 dBm better than corroded steel sample. It appears that the better intermodulation values after corrosion for the double-layer plated samples were due to their better initial-intermodulation values, and the surface corrosion products of copper, zinc, silver and iron all produced similar amount of deterioration in intermodulation performance. However, the surface corrosion product could be eliminated by adding a layer of coating which does not form any solid oxides on the surface of the original high conductivity coatings (see figure(5)).

In order to make comparison with the joint effect, joint samples (see figure(2)) were made and were corroded for intermodulation measurements. By doing this, we were able to convince ourselves that the rusty joint is a first order effect in intermodulation generations (see figure(6)), although the ferromagnetic effects of steel are still important. However, according to the British Standard BS 5493 (protective coating of iron and steel structures against corrosions) and BS 729 (hot-dipping galvanised coating on iron and steel articles), it is required that for steel structures of thickness greater than 5 mm, the zinc coating must have a thickness not less than 86 microns, which is seventeen times the skin-depth for copper at the frequency that we are using.

For a new antenna tower, the structural elements are galvanised. However, the joints between structure elements could lose their initial protection during construction of the tower, and suffer more rapid deterioration giving rise to corrosion due to fretting at the joint. Moreover, a joint will tend to be a moisture trap. Corrosion at these joints can probably be assumed to be the major source of intermodulation.

Our approach to solve the intermodulation problem is to offer an alternative high conductivity path to r.f. current (see figure(7)). An initial experiment involved the covering of a corroded cylindrical steel sample with zinc coating (by electroplating) was done, and the intermodulation level of the sample was very close to the system floor level (see figure(8)).

The problem now is to develop a practical way to carry out the metallic coating of the joints. The methods being considered are metal spraying and electroless plating.

It was also found that metal-based paints would not work because the bulk conductivity of the paint is much less than the metal. An experiment was carried out using silver-based paint with volume resistivity equal to 10^{-5} m. In this case, the intermodulation level dropped from -50 dBm to -65 dBm.

Although the absolute value of -65 dBm is still high, but an improvement of 15 dBm is a convincing argument for intermodulation reduction by covering the rusty joint with a continuous layer of high conductivity material, i.e. metal.

6 Data Acquisition

It is necessary to subject the proposed coating under field trial before a definite judgement of the viability of the coating can be made. Provision has been made to allow remote data logging and data transfer from the remote test site back to the university. Moreover, the data logging system will be used to gather information about the effect of weather conditions on the variations of the background intermodulation level. This is particular useful as it will provide us with an intermodulation signature of the test site. It might even be possible to further develop the techniques and associated statistical software so that the hardware/software system can be transported to any operational site to carry out a site-intermodulation signature analysis, and the feasibility of putting up more services in that site can then be determined.

7 Conclusions

This paper describes the research programme aiming to provide a practical engineering solution of suppressing structural intermodulation interferences. The results will be useful not just to mobile radio communication services, but to satellite communication or any radio installation where intermodulation effects are prevalent due to a multiplicity of systems. A brief survey was done on the mechanism of structural intermodulation. We suggested a more probable mechanism based on metal-semiconductor rectifying effect. Further work will be done to prove it.

8 References

[1] Fudge,R.E., "The re-engineering of the VHF mobile radio services in the UK", PhD thesis, April 1984, The City University.

[2] Debney,C.W., "The measurement and prediction of intermodulation distortion in co-site radio communication systems", PhD thesis, 1983, Southampton University.

[3] Babcock,W.C., "Intermodulation interference in radio systems", The Bell System Tech. Journal, January 1953, pp 63-73.

[4] Gretsch,W.R., "The spectrum of intermodulation generated in a semiconductor diode junction", Proc. IEEE, vol.54, No.11, November 1966, pp 1528-1535.

[5] Young,C.E., "The danger of intermodulation generation by RF connector hardware containing ferromagnetic materials", Proc. 9th Annual Connector Symposium, October 1976.

[6] Bailey,G.C. and Ehrich,A.C., "A study of RF nonlinearities in nickel", Journal of Applied Physics 50, 453 (1979).

[7] Betts,J.A. and Ebenezer,D.E., "Intermodulation interference in mobile multiple transmission communication systems operating at HF (3-30 MHz)", Proceeding of IEE, Vol.120, No.11, November 1973.

[8] Stratton,R., "Volt-current characteristics for tunnelling through insulating films", J.Phy. Chem. Solids, Vol.23, pp 1177-1190, Pergamon Press 1962.

[9] Simmons,J.G., "Generalised formula for the electric tunnelling effect between similar electrodes separated by a thin insulating film", J.of Applied Phys., Vol.34, No.6, June 1963, pp 1793-1803.

[10] Fisher,J.C. and Giaever,I., "Tunnelling through thin insulating layers", J.of Applied Phys., Vol.32, No.6, June 1961, pp 172-178.

[11] Higa,W.H., "Spurious signals generated by electron tunnelling on large reflector antennas", Proc IEEE, Vol.63, No.2, February 1975, pp 306-313.

[12] Guenzer,C.S., comments on ref.[11], IEEE Proc Letters, February 1976, pp283.

[13] Woody et al, "Metal-insulator-metal junctions as surface sources of intermodulation", February 1983, RADC-TR-83-31.

[14] Seitz,F. ed), " Solid state physics", Vol.21, 1968, Academic Press.

[15] Copper,J.C. et al, "Chemically suppressing rusty-bolt intermodulation interference", Proc. IEEE National Symp. on EMC, April 1984, pp 233-240.

9 Acknowledgement

This study is supported jointly by Science & Engineering Research Conucil and the Home Office, UK. The authors are indebted to Mr P.M.Tomlinson and Mr P.Buley of the Directorate of Telecommunications, Home Office; also Dr R.E.Fudge, formely of the Directorate of Telecommunications, Home Office, now with British Telecom and Professor A.C.Davies of City University.

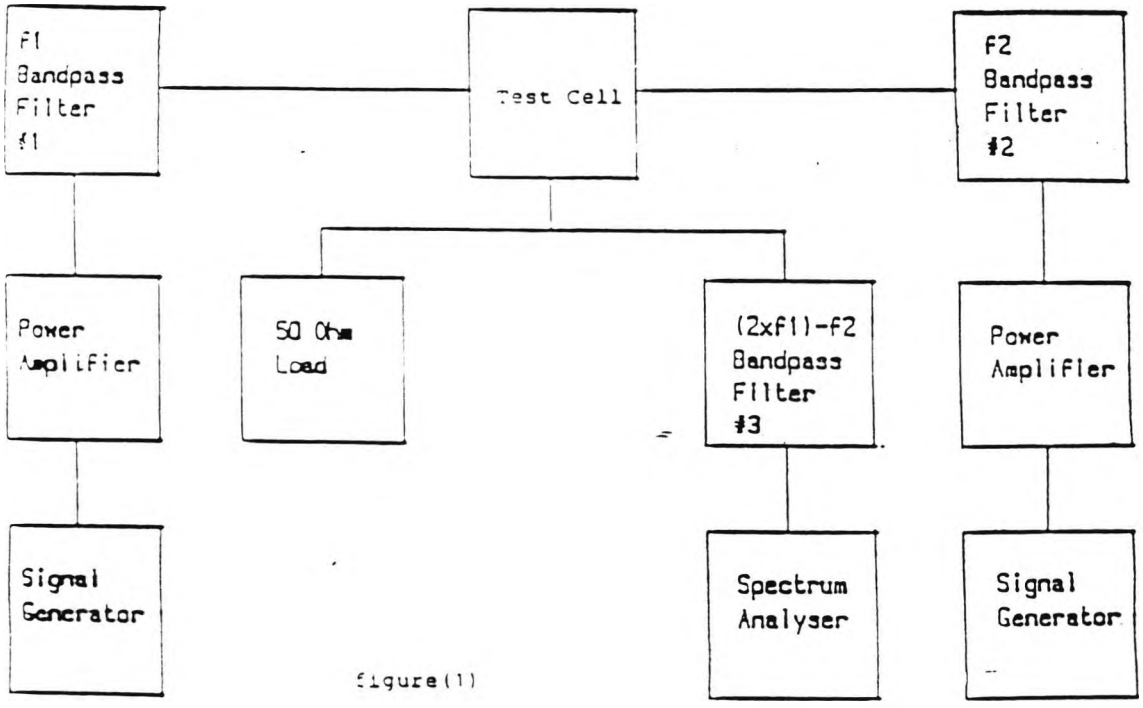

figure(1)

Block Diagram of Test Setup

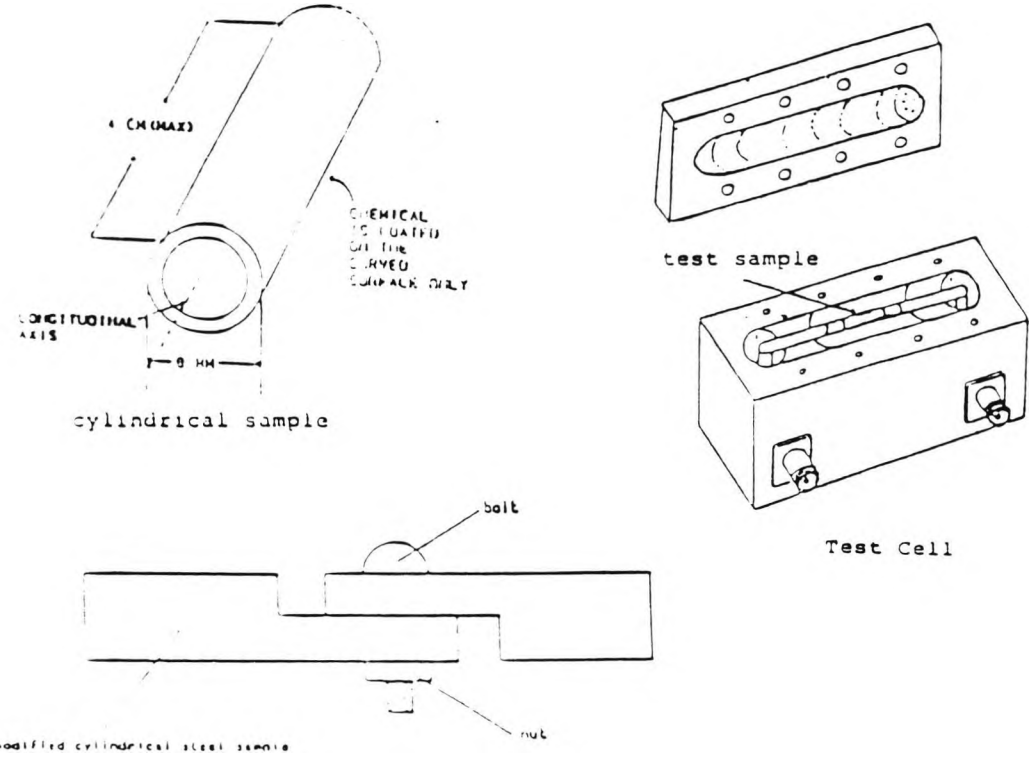

figure(2): Test Cell and Test Samples

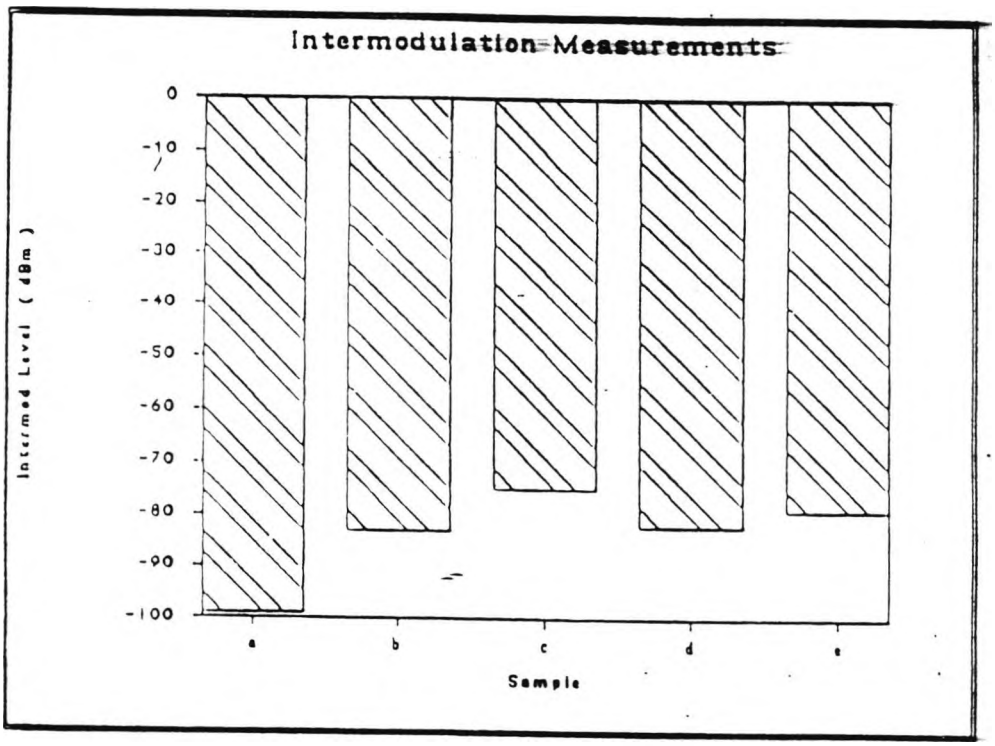

figure(3)

a = background level
b = clean cylindrical steel sample
c = corroded sample of (b)
d = steel sample coated with graphite-based chemical
e = corrodnd steel sample coated with graphite-based chemical

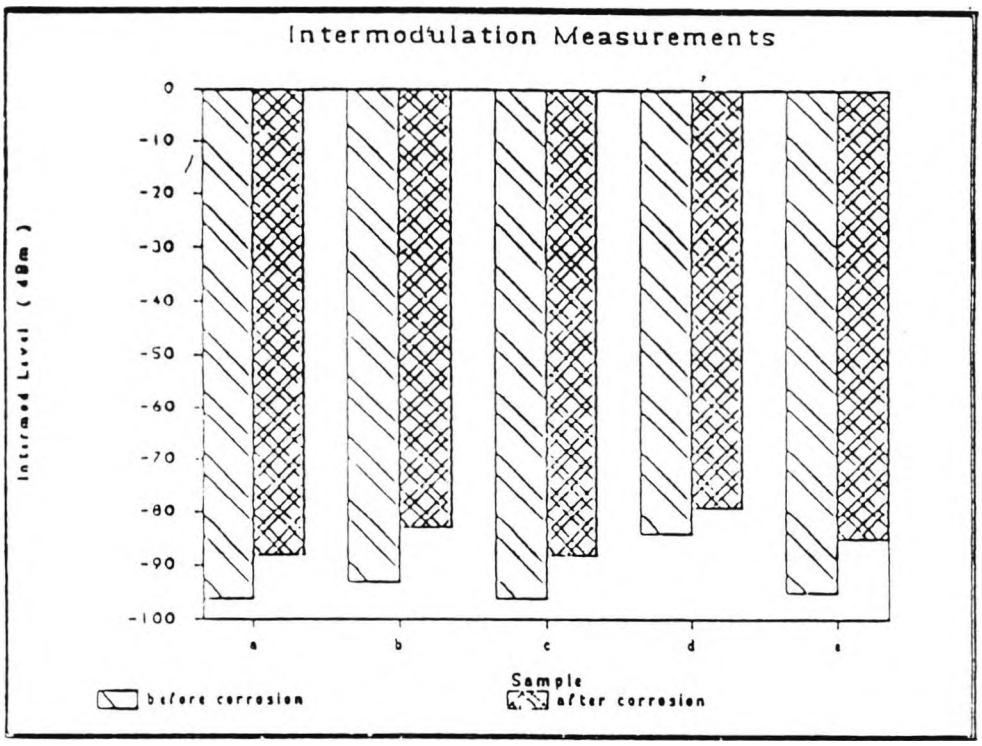

figure(4)

Plated cylindrical steel samples were used in this experiment

Samples (a) and (b) were corroded with concentrated hydrogen-sulphide gas.
Samples (c),(d) and (e) were corroded by the electrolysis of artificial sea water with an anodic potential of around 500 mV (versus standard hydrogen electrode) for 24 hours.

a = copper/zinc/steel
b = silver/zinc/steel
c = zinc/steel
d = silver/copper/zinc/steel
e = silver/steel

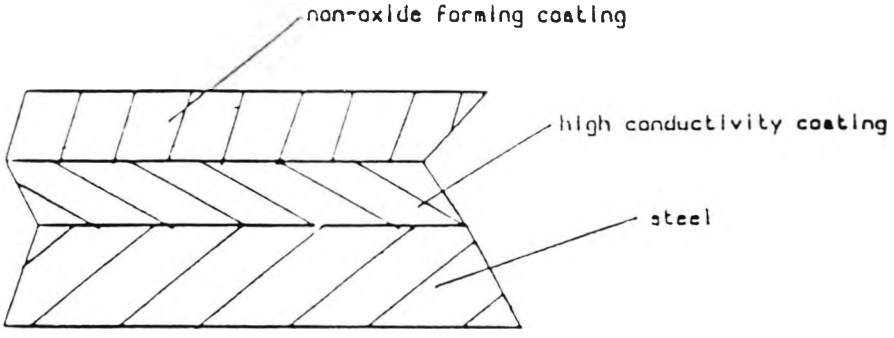

figure(5): double layer coating

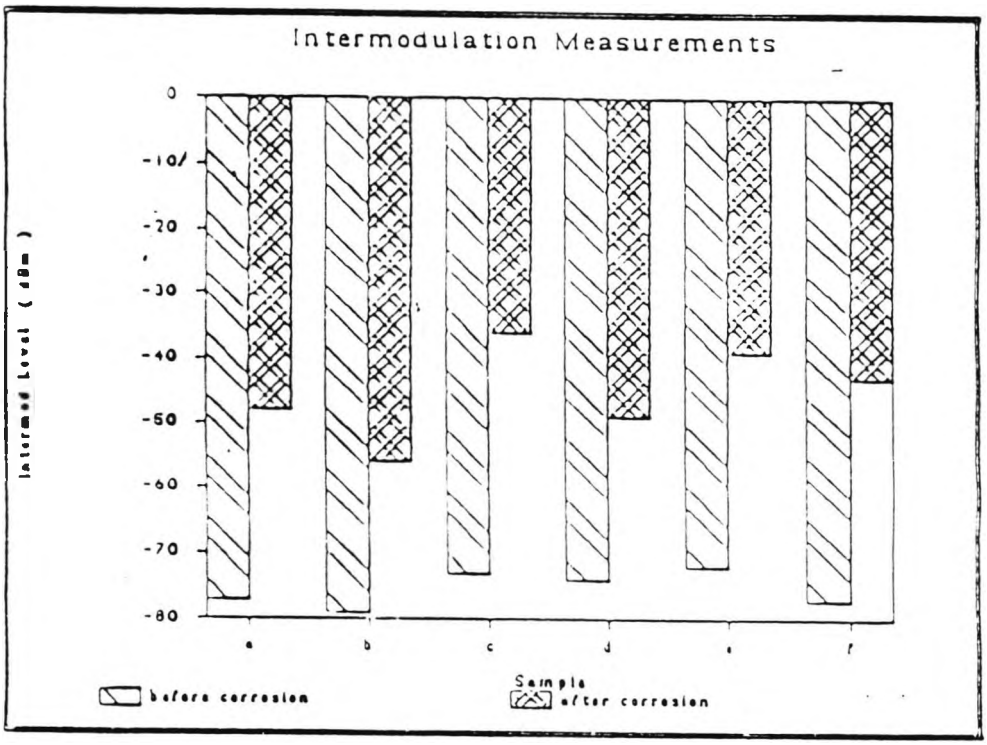

Samples used in this experiment were plain steel joints, adapted from the cylindrical samples used in previous experiments. Six clean samples were used in this experiment. Their intermodulation levels before and after corrosion were measured.

figure(6)

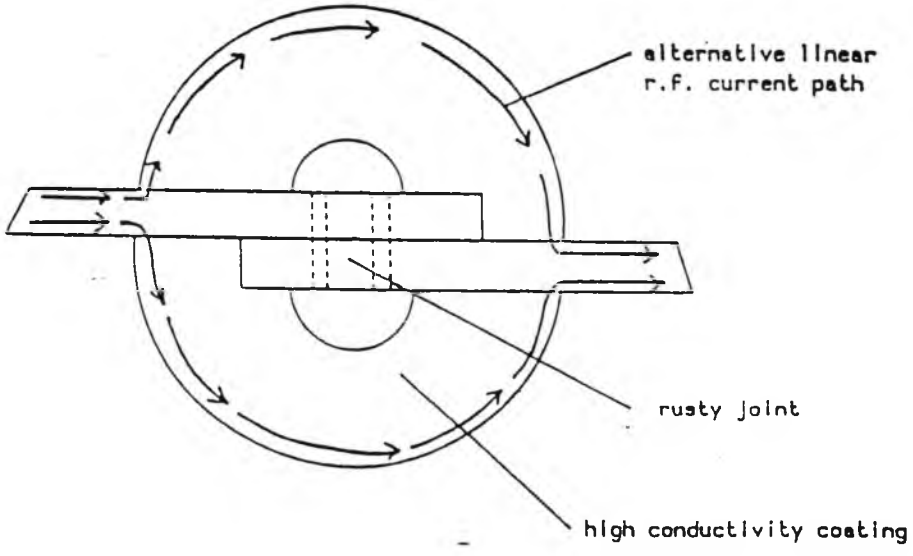

figure(7): Alternative r.f. current path

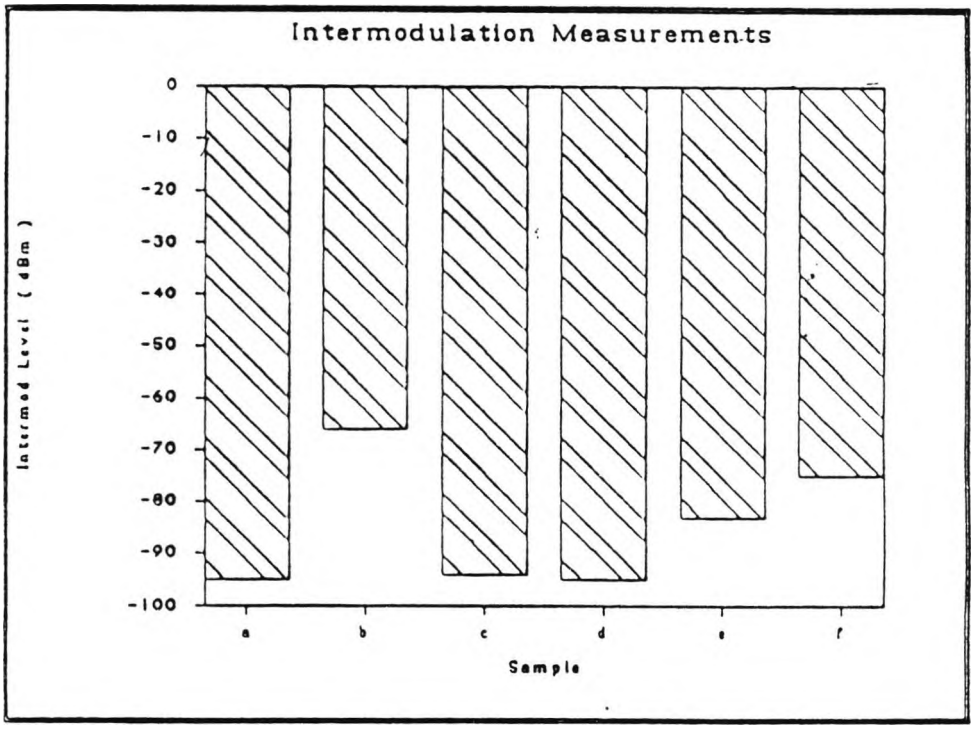

a = copper rod
b = corroded steel (both ends and the surface of the rod were corroded)
c = sample (b) was zinc-electroplated to a thickness of about 1 mm
d = sample (c) was re-corrroded
e = clean steel sample
f = corroded steel sample (just the body, not the ends)

figure(8)

"Suppression of Intermodulation Product Generation in Materials and Sturctures use in Radio Communication"

Proc IERE, Fifth International Conference on Electromagnetic Compatibility, University of York, Oct 1986.

SUPPRESSION OF INTERMODULATION PRODUCT GENERATION IN MATERIALS AND STRUCTURES USED IN RADIO COMMUNICATIONS

H. L. Bevan*, L. G. Frampton*, P. Ho*, A. C. C. Tseung* and W. S. Wilkinson*

SUMMARY

This paper describes work which is being carried out to make a fundamental and detailed investigation into the phenomenon of intermodulation (the so-called "rusty-bolt" effect) arising from non-linear current paths in materials and structures at radio frequencies. An ultimate objective is to develop practical methods whereby problems relating to the co-location of the transmitters and receivers in land mobile radio systems can be overcome. The work is of an inter-disciplinary nature involving the study of the chemistry of surface films and coatings and the measurement of their electrical properties.

The degree of non-linearity is not large but the intermodulation measuring apparatus must be capable of differentiating between large differences of signal level arising from the operational requirements of the radio systems.

Consideration has been given to the problems associated with data acquisition on a continuous basis from field evaluation of experimental treatments applied to antennas, mast structures and surrounding metalwork at radio stations.

1. Introduction

Intermodulation products (IMP) are spurious frequencies generated when two or more signals mix in a device that has a non-linear current-voltage characteristic. With given sinusoidal input components at frequencies f_1, f_2.....f_n the non-linear transfer function, which itself may not be stable, when compounded gives rise to output components both at the input frequencies and at additional frequencies f_{im} given by:

$$f_{im} = a_1 f_1 \pm a_2 f_2 \pm .... \; a_n f_n$$

where a_1, a_2 .... a_n are positive integers and $(a_1 + a_2 + ...a_n)$ is the order of the intermodulation product. Generally the amplitudes of a product fall with increase in order and usually the products of most interest are those of the lowest order which fall near to the input frequencies (f_1 & f_2) of the system, for example, the third-order product $(2f_1 - f_2)$. However, it has been shown [1] that products up to the eleventh order and above can have adverse effects on system performance and spectrum utilisation. Also, as the number of channels increase in a multi-channel system the number of potentially interfering products, particularly of higher order products, increases at a prodigious rate.

2. Background to the Investigations

2.1 General

In general terms, intermodulation generation at communal base station transmitting/receiving sites represent a major obstacle to improved utilisation of the limited radio frequency spectrum available to mobile radio. The generation of unwanted frequencies may be attributed to a number of phenomena, some of which are suppressed by the provision of filters in the transmitter outputs and receiver inputs, and adequate shielding between the component parts

*The City University London

of the system[2]. However, non-linear effects, giving rise to intermodulation, occur in the antennas, mast structures and nearby metal work illuminated by the the transmitter frequencies. Some of the unwanted frequencies which are generated fall into the bands used by the receivers.

The U.K. Emergency Services are moving to new frequency bands as a result of the World Adminstrative Radio Conference (WARC) 1979. The new allocations are not as favourable as the old in respect of interaction and this, together with a decrease in channel spacing to accommodate more traffic, makes the generation of intermodulation products a critical aspect of the engineering of the new network.[1]

2.2 System Requirements

The target figures for equipment to be used in the post-WARC system are as follows:

Receivers:

Minimum received level	- 137 dBW (2 uV emf)
Protection ratio	30 dB
Maximum level of any single, unwanted signal	- 167 dBW (-137 dBm)

Transmitter:

Output power (50W)	+ 17dBW (+47dBm)

The measurement system must be capable, therefore, of detecting an unwanted signal 184 dB below the level of nearby carrier signals, or a ratio of intermodulation power to signal power of 3.98×10^{-19}.

2.3 Previous Work

This has been largely concerned with the implications of intermodulation generation to system design and network planning rather than in the detailed nature of the generating mechanism. The work that has been carried out has dealt with active elements and components, for example, by adding filters when required or adopting solid outer feeder cables instead of braided cables. [2,3]

2.4 Investigation Plan

The aim is to make more fundamental and detailed investigations into the intermodulation arising from non-linear current paths. The authors are of the opinion that an approach to this study whereby a so-called rusty bolt is stimulated by two parallel back-to-back semiconductor diodes, each operating in its forward conducting region, is an over simplification of the problem. We justify this assertion by the fact that our radio frequency measurements are being made in the region of 150MHz in order to satisfy Home Office operational requirements. At this frequency, the skin depths for some common metals are as follows:

Material	Conductivity $\times 10^{7}$ (Sm^{-1})	Skin Depth (μm)
Silver	6.2	5.22
Copper	5.8	5.40
Gold	4.1	6.42
Aluminium	3.7	6.76
Iron	1.1	12.3
Platinum	0.94	13.4

Thus the surface finish in steel, for example, used as a structural element could be a source of intermodulation when illuminated by electromagnetic fields. There is some evidence from field observations that this is actually occurring (1). Also, in addition, these structural elements could be in electrical resonance exacerbating any rusty bolt effects at bolted or rivetted joints.

To complement electrical measurements, carefully-controlled chemical preparation of test samples are being carried out in the study of the physical mechanisms including the effect of climatic conditions and ageing.

3. The Chemical Approach

One method of dealing with the problem of intermodulation in the past has been to identify the troublesome components and electrically by-pass them using straps or plates. Another

approach is to treat the exposed metal parts at the time of installation with a protective film, but clearly this is no solution for existing structures.

The chemical approach which we have adopted has been along two paths:

(1) The oxidation process (corrosion) on the surface of the metal could be reversed by suitable chemical treatment. This involves the application of a film containing a chemical reducing agent capable of reconverting the oxidised species back to the metallic state, usually in a dispersed form, which has the added benefit of restoring surface conductivity. Although possible for metal such as iron, metals such as zinc or aluminium are not amenable to this treatment as chemical means alone are incapable of achieving the reduction.

A range of these preparations has been examined. Mild and strong organic acid reducing agents are combined in varying proportions with liquid urethane elastomers or with polyvinylpyrrolidone (PVP) which has the ability to "mop up" metal ions such as Fe(II) and Fe(III) and facilitate their reduction to metallic iron. The chelating agent ethylenediamine tetraacetic acid (EDTA) or its sodium salt has also been used for similar purposes. In order to achieve control over the necessary viscosity change during application, ethylene glycol, acetone, water and ethanol were used as solvents in the preparations.

Originally, attempts were made to reproduce the results obtained for similar tests carried out by Cooper, Panayappan & Steele [4] in the U.S.A., but it proved difficult, often impossible, to obtain a satisfactory adherent film on the sample using the prescribed proportions of constituents and the approach was considerably modified and augmented in the light of practical experience with the materials. It was also concluded that there would be little to be gained from a comparison of IMP changes when the frequencies employed and sample geometries were quite different in the two laboratory assemblies.

Results obtained for these preparations will be presented at the conference.

(2) An alternative conducting path can be offered which is impervious to atmospheric degradation, and which would reproduce the advantageous properties of a noble metal. The preliminary test results reported here confirm that there is little variance in the intermodulation measured on a sample of a noble metal such as gold or platinum. The surface film of oxide present, because of its conducting nature, continuity, and unchanging character, presents no problem.

Clearly, to construct aerial components from such materials, whilst technically possible, would be economically prohibitive but an equivalent situation could be contrived using the more traditional constructional materials in a number of ways.

This approach makes use of the extensive background of the University's Chemical Energy Research Centre in the fields of electrocatalysis and materials science. The centre has developed a wide range of novel conducting and semiconducting compounds for use as a electrocatalysts in electrochemical systems and has expertise in fabrication techniques and the application of coatings. A number of inexpensive conducting coatings have been formulated and applied to the surface of steel test samples as described in a previous section.

Results obtained from these preparations will be available at the conference.

4. Measurement Techniques

4.1 Work done by other investigators has been directed towards the

intermodulation product (IMP) generation due to nonlinearities in transmission lines, connector and active system elements (reference 5-8). The frequency range from 22 MHz to 425 MHz and from 1GHz were covered in above studies. Betts [9] had investigated intermodulation due to presence of ferromagnetic material in a mast with antennas mounted on it. Suggestions for improving IMP performance were given by these authors and were noted when setting up our test equipment.

The block diagram of the laboratory set up is shown in figure (1). Two synthesized signal generators are employed to provide the two fundamental frequencies at 145 MHz and 150 MHz. The input signals are fed into power amplifiers which can deliver up to 100 Watts output power. High Q-factor filters are used to eliminate any harmonics of the fundamental frequencies. The outputs from the filters are connected to the combining cross by half wavelength lines in order to avoid line resonance effects . Filter unit 3 is tuned to the IMP frequency (i.e. $2f_1 - f_2$) which stops any fundamental signals passing through. Thus the third order intermodulation level can be measured over a wide dynamic range by the spectrum analyser.
The intermodulation signal is terminated equally by the spectrum analyser and a load which consists of 100 metres of cable acting as an infinite line. The fundamental powers are also dissipated in the load.

The test set up was calibrated and both accuracy and repeatability were evaluated. The background intermodulation level was better than -100 dBm at an input power of 50 Watts, i.e. 147 dB below the input.

Repeatability was tested by measuring the IMP levels of the same sample for several times consecutively and day-to-day. We found that variations in results were normally within ±10 dB. This might be due to change in room temperature, humidity etc. However, since our measurement purpose is to eliminate unpromising chemical samples, and by doing sufficient number of measurements with each sample, a statistical mean level should be achievable. Samples could then be compared with each other for IMP performance using these mean IMP levels.

4.2 Experimental Procedure

The samples chosen for our testing purpose were gold, platinum, copper, zinc, steel and corroded steel.

Before any experiment is carried out, the test setup has to be calibrated. Each of the filter units was tuned to its respective resonant frequency. The power output from each signal source into the test-jig was fixed at 50 Watts. Without any sample in the jig, the background intermodulation level was checked.

After calibration, the samples were put in the jig in a sequence as shown in the table, and the corresponding intermodulation levels were recorded when the spectrum analyser reading was stable. This process was repeated for sufficient number of times so that statistical methods can be applied to obtain average intermodulation levels.

From the results in table(1) it was noticed that the inert materials' intermodulation levels show very little difference from the background intermodulation levels. However steel and corroded steel show an appreciable amount of intermodulation product generation.

The samples were exposed to air outside the laboratory for a further period of one week to see the degree of deterioration of the samples due to atmospheric oxidation.

Results are shown in table(2). It was seen that the inert materials' intermodulation levels remained close to their previous values,but steel oxidised significantly and its level increased by about 20dB.

From these results, it is observed

that for steel the intermodulation level increases as the oxide layer grows. Therefore the intermodulation level could be a function of the thickness of the oxide layer.

5 Improvement of Test Sample Preparation Method

The corroded steel sample used in above experiment was prepared in the form as shown in figure(1). This arrangement has two problems. First, the oxide layer might be broken when the specimen is placed in the test jig. Secondly, since the signal frequencies are at around 150 MHz, the RF current flows only close to the surface of the sample due to skin effect. Therefore there is no current flowing in the bulk of the oxide and the intermodulation level might be much less than the true value.

In order to rectify this situation, a new sample preparation method is used and is shown in figure(2). In this method the oxide or any test chemical is coated on the curved surface of the tube where the r.f current flows. The outer ends of the tube are left clean to maintain good electrical contact.

The test-jig has since been modified to hold a test specimen up to a length of 4 cm. Any end-effects due to the discontinuities in the region of the contacts between the sample and test-jig should now be minimized. Results from this new jig will be reported at the conference.

6. Data Acquisition

In order to verify the suitability of laboratory samples chosen in the experiments, they will be tested under real environmental conditions. A test site for this purpose will be provided by the Home Office. It is necessary to collect a sufficiently large amount of data for statistical analysis.

A BBC microcomputer is configured as a remote site data logger. It enables monitoring of essential environmental parameters such as temperature, windspeed, humidity, rainfall and the corresponding intermodulation levels. Appropriate sensors are connected to the BBC microcomputer via a General Purpose Interfacing Bus(GPIB), see figure(2).

Stored data on the BBC microcomputer is transmitted back to an IBM computer in the main site using modems through the public telephone network. Communications software on the BBC microcomputer allows the processes of auto-dialling and data transferrence to be fully automatic.

Acquired data will be processed using statistical methods to 1) obtain average values of data and 2) to reduce the amount of data to be stored.

Statistics software package running on the IBM computer is readily available and by recording the data in an appropriate format, files of data can be used in the software package directly without any modifications.

It is believed that by analysing a sufficient amount of data. At least some confidence will be forthcoming in the most promising of the techniques proposed to overcome the intermodulation problems.

7. Conclusions

The paper reports on work that is in progress to obtain a better understanding of the generation of intermodulation products in radio communication systems. The investigations are directed towards solving problems in a specific mobile radio system but the results will be applicable in any system where transmitter and receivers operate in close proximity, including for example, satellite systems where uplink and downlink signals have very large level differences.

The outcome of the investigations should lead to the development of new techniques in the protection of metals and of surface coatings having improved performance when employed in radio frequency engineering.

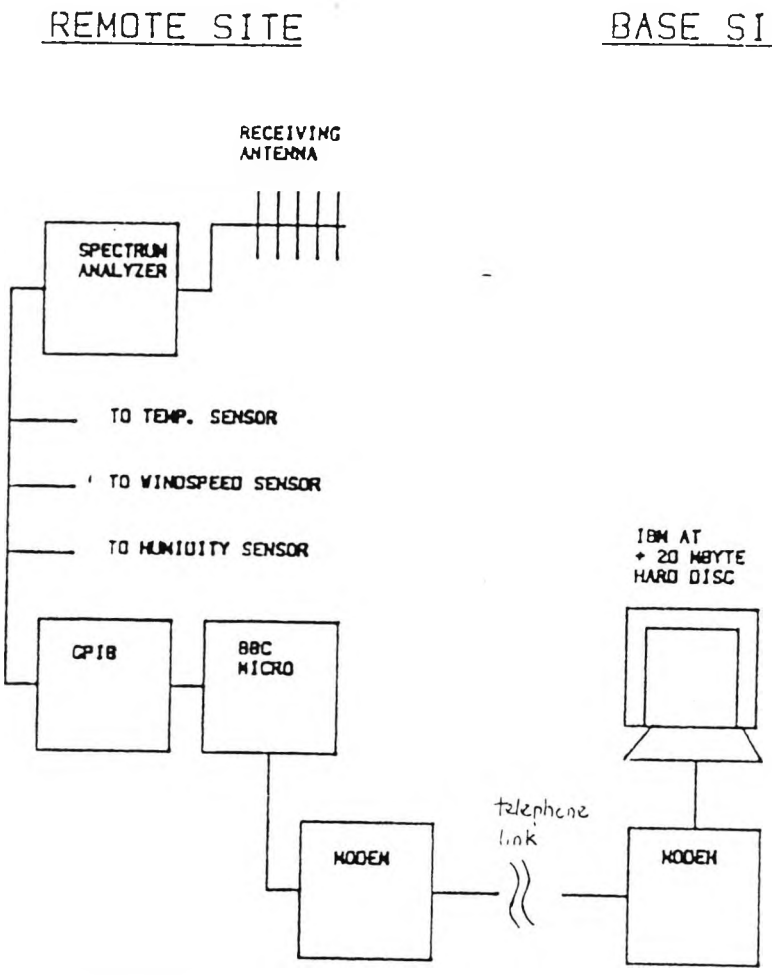

Figure(3) Block diagram of data acquisition system

8. Acknowledgement

This study is supported jointly by Science & Engineering Research Council and the Home Office. The authors are indebted to Mr P M Tomlinson and his colleagues of the Directorate of Telecommunications, Home Office; also Dr R E Fudge, formely of the Directorate of Telecommunications, Home Office, now with British Telecom and Professor A C Davies of the City University.

RESULTS

Measured levels are in dBm
measurement error is +/- 1dBm

SAMPLES	Control	Gold	Platinum	Copper	Zinc	Steel	Corroded steel
test1	-109.00	-102.00	-116.00	-104.00	-105.00	-98.00	-49.00
test2	-112.00	-97.00	-109.00	-109.00	-112.00	-91.00	-43.00
test3	-99.00	-84.00	-112.00	-116.00		-98.00	-38.00
test4	-94.00	-104.00	-105.00	-96.00	-94.00	-84.00	-41.00
test5	-104.00	-101.00	-94.00	-105.00	-103.00	-92.00	-39.00
test6	-97.00	-98.00	-98.00	-98.00	-97.00	-98.00	-40.00
test7	-95.00	-99.00	-98.00	-100.00	-103.00	-90.00	-43.00
test8	-94.00	-99.00	-99.00	-94.00	-96.00	-98.00	-38.00
test9	-97.00	-99.00	-101.00	-100.00	-101.00	-97.00	-34.00
test10	-104.00	-108.00	-105.00	-103.00	-91.00	-91.00	-40.00
AVG	-100.00	-99.70	-94.80	-102.40	-102.00	-90.50	-41.10
STD	6.54	7.19	5.71	5.72	5.01	7.11	3.11
VAR	42.80	4.81	32.56	32.80	5.00	7.65	1.69

TABLE (1)

Samples	Control	Gold	Platinum	Copper	Zinc	Steel	Corroded steel
test1	-96.00	-102.00	-98.00	-106.00	-96.00	-70.00	-40.00
test2	-94.00	-100.00	-96.00	-96.00	-98.00	-78.00	-35.00
test3	-95.00	-99.00	-101.00	-93.00	-88.00	-72.00	-30.00
test4	-97.00	-100.00	-100.00	-99.00	-97.00	-72.00	-31.00
test5	-98.00	-100.00	-103.00	-98.00	-99.00	-73.00	-33.00
AVG	-95.60	-100.20	-100.00	-98.40	-96.40	-71.40	-35.20
STD	1.02	0.98	2.28	4.32	3.50	1.20	0.00

TABLE (2)

References

1. Fudge, R.E. "The re-engineering of the VHF mobile radio services in the UK". PhD. thesis, April 1984, The City University.

2. Gardiner, J.G., Howson, D.P., Baghai, A.A. "Origins an minimization of intermodulation outputs from mobile radio base station multicouplers." Proc. IERE International Conf. on EMC, Sept. 1984. pp.211-216.

3. Betts, J.A. and Debmey, C.W. "Intermodulation measurements on land mobile radio sites", Proc IEE Conf on Radio Transmitter, 1980. pp.52-57.

4. Cooper, J.C. Panayappan, Rm. and Steele, R.C. "Chemically suppressing rusty-bolt intermodulation interference". Proc. IEEE National Symp. on EMC. April 1984, pp.233-240.

5. Cox, R.D. "Measurements of waveguide component and joint mixing products in 6 GHz frequency diversity system". Trans IEEE in communications Technology, Vol. COM-18, No.1., Feb, 1970.

6. Amin, M.B. and Benson, F.A. "Coaxial cables as sources of intermodulation interference at microwave frequencies" Trans, IEEE on EMC, Vol. EMC-20, No.3 Aug. 1978.

7. Bayrek, M. & Benson, F.A. "Intermodulation products from non-linearities in transmission lines & connectors at microwave frequencies". Proc IEE, Vol. 122, No.4, April. 1975.

8. Martin, R.C. "Intermdoualtion generation studies on materials, connectors and structures." Proc. IERE International conf. on Electromagnetic Compatibility. Sept. 1978 .pp. 243-250.

9. Betts, J.A. Ebenezer, D.R. "Intermodualtion interference in mobile multiple transmission communication systems operating at high frequencies (3-30MHz)", Proc IEE, Vol, 120, No.11, Nov. 1973.

REFERENCES

Adler A, "Transition Metal Oxide" : in Frederick Seitz (ed), Solid State Physics, Volume 21, Academic Press, pp 78-83.

Amin M B and Benson F A, "Coaxial Cable as Sources of Intermodulation Interference at Microwave Frequency", IEEE Trans. on EMC, Vol EMC-20, No. 3, 1978, pp 376-384.

Arazm F and Benson F A, "Nonlinearities in Metal Contacts at Microwave Frequencies", IEEE Trans. on EMC, Vol EMC-22, August 1980, pp 142-149.

Babcock W C, "Intermodulation Interference in Radio Systems : Frequency of Occurrence and Control by Channel Selection", The Bell System Technical Journal, January 1953, pp 63-73.

Bailey G C and Ehrlich A C, "A Study of RF Nonlinearities in Nickels", J. Appl. Phys. 50, pp 453, 1979.

Bardeen J and Brattain W H, "Nature of the Forward Current in Germanium Point Contacts", Phys. Rev. 74, 1948, pp 231-232.

Barer R and Peters B F, "Why Metals Fail", Gordon and Breach, 1970.

Barton K (translated by Duncan J R), "Protection Against Atmospheric Corrosion", John Wiley and Sons, 1976.

Bayrak M and Benson F A, "Intermodulation Products from Nonlinearities in Transmission Lines and Connectors at Microwave Frequencies", Proc. IEE, Vol. 122, No. 4, April 1975, pp 361-367.

Bennett W R, "New Results in the Calculation of Modulation Products", Bell System Tech. J., 1933 Vol. 12, pp 228-243.

Betts J A and Ebenezer D R, "Intermodulation Interference in Mobile Multiple Transmission Communication Systems Operating at HF (3-30 MHz)", Proc. IEE, Vol. 120. No. 11, Nov. 1973.

Betts J A and Debney C W, "Intermodulation Measurementsd on Land Mobile Radio Sites", IEE Conf in Radio Transmitter, 1980, pp 52-57.

Bevan H L, Frampton L G, Ho P S W, Tseung A C C, and Wilkinson W S, "Suppression of Intermodulation Product Generation in Materials and Structures used in Radio Communications", Proc IERE, Fifth International Conference on Electromagnetic Compatibility, University of York, Oct 1986.

Bond C D, Guenzer C S and Carosella C A, "Generation of Intermodulation by Electron Tunneling through Aluminium Oxide Film", Naval Research Laboratory Report 8170.

Braun K F, "On the Current Conduction through Metal Sulphides", Ann. Phys. Chem., 153 (1874), pp 556.

Brimblecombe P, "London Air Pollution 1500-1900", Atmos. Environment, 11, 1977, pp 1157-1162.

Cooper J C, Panayappan R M and Steele R C, "Chemically Suppressing Rusty Bolt Intermodulation Interference", IEEE Nat. Symp. on EMC, April 1984, pp 233-240.

Cox R D, "Measurement of Waveguide Component and Joint Mixing Products in 6-GHz Frequency Diversity System", IEEE Trans on Communication Technology, Vol. COM-18, No. 1, Feb 1970.

Debney C W, "The Measurement and Prediction of Intermodulation Distortion in Co-Site Radio Communication Systems", Ph.D thesis, University of Southampton, 1980.

Dryborough D A, "Mobile VHF and UHF Radio Systems in UK", Proc IEE, Vol. 122, No. 10R, Oct 1975, pp 951-975.

Department of Trade and Industry, "Licensing Statistics", DTI, Radio Regulatory Division, June 1986.

Edwards R, Durkin J and Green D H, "Selection of Intermodulation Free Frequencies for Multi-Channal Mobile Radio Systems", Proc. IEE, Vol. 116, No. 8, August 1969.

Fisher J C and Glaever I, "Tunneling through Thin Insulating Layers", Journal of Applied Physics, 1961, Vol.32, No.2, pp 172- 177.

Fontana M G and Greene N D, "Corrosion Engineering", McGraw Hill, 1967.

Fudge R E, "The Re-Engineering of the VHF Mobile Radio Services in the UK", PhD Thesis, City University, 1984.

Gabe D R, "Principles of Metal Surface Treatment and Protection", second edition, Pergamon Press, 1978.

Gardiner J G and Magaza M S A, "Some Alternative Frequency Assignment Procedures for Mobile Radio Systems", J. IERE, Vol. 52, No. 4, pp 193-197, April 1982.

Gardiner J G, Kotsopoulos S A and Heathman A C, "Intermodulation Interference Probilities in the Cellular Radio Frequency Bands", Proc. fourth IERE Int Conf. on EMC, Sept 1984.

Gardiner J G and Kotsopoulos S A, "Relationship between Base Station Transmitters Multicoupling Requirements and Frequency Planning Strategies for Cellular Mobile Radio", IEE Proceedings, Vol. 132, Pt. F, No. 5, August 1985.

Gardiner J G, Hammond D and Heathman A C, "Intermodulation Control Requirement at Cellular Base Stations Sites",

Gardiner J G, Howson D P and Baghai A A, "Origins and Minimisation of Intermodulation Outputs from Mobile Radio Base Station Multicouplers", IERE Int Conf on EMC, Sept 1984, pp 211-216.

Guenzer C S, "Comments on 'Spurious Signals Generated by Electron Tunneling on Large Reflector Antennas' ", Proc. IEEE, Feb 1976, pp 283.

Hallford B R and Ratti J N, "Microwave Receiver Interference Characteristics Measurements", IEEE Trans. on Communication Technology, Vol. COM-14, No.4, pp 455-469.

Hasted J B, "Aqueous Dielectrics"

Higa W H, "Spurious Signals Generated by Electron Tunneling on Large Reflectotr Antennas", Proc. IEEE, Vol. 63, No. 2, Feb 1975, pp 306-313.

Ho P S W, Bevan L H, Tseung A C C, and Wilkinson W S, "Intermodulation Interfernces in Radio Systems", Proc AGARD Conference on Effects of Electromagnetic Noise and Interference on Performance of Military Radio Communication Systems, AGARD-CPP-420, 1987.

Von Hippel A R (ed), "Dielectric Materials and Applications", 1954.

Holbech R J (ed), "Land Mobile Radio Systems", Peter Peregrinus Ltd., 1985.

Howaon D P, "Integrated Site System for VHF/VHF Mobile Communications", Communications International, Feb 1975, pp 16-21.

Jackson G A, "The Early History of Radio Interference", J. IERE, Vol. 57, No. 6, Nov/Dec 1987.

Kellar B S, "Measurement of Intermodulation Products Generated by Corroded or Loose Connections in CATV Systems", NCTA Convention, 1984, pp 23-28.

Knofel Dietbert (translated by Diamant R M E), "Corrosion of Building Materials", Van Nostrand Reinhold Company, 1978.

Kotsopoulos S A, "Minimisation of Intermodulation Interference", IEE Proc. F, 130, (4), 1983, pp 350-355.

Lee J C, "Intermodulation Measurement and Analysis of Some Conducting Materials", IEEE ICC 80, pp 25.6.1-25.6.6. Lee W Y C, "Mobile Communication Engineering", McGraw-Hill, 1982.

Lee W Y C, "Mobile Cellular Telecommunciation Systems", McGraw-Hill, 1989.

Martin R H, "Intermodulation Product Generation Studies on Materials, Connectiors and Structures", IERE Int. Conf. on EMC, 1978, pp 243-250.

Mifsud C J, "Use of a Recursive Formula in Generating Intermodulation Free Frequency Lists", IEEE Trans. on EMC, EMC-16, 1974, pp 50-51.

Nuding E, "Non-Linearities of Flange Connections in Transmission Liens Carrying High RF Power", European Microwave Conf., 1974, pp 613-618.

Parsons J D and Gardiner J G, "Mobile Communication Systems", Blackie and Son Ltd, 1989.

Pannell W M, "Frequency Engineering in Mobile Radio Bands", Granta Technical Editions, 1979.

Pourbaix M (translated by Franklin J A), "Atlas of electrochemical Equilibria in Aqueous Solutions", Pergamon Press, 1966.

Rao C N R and Rao G V S, "Transition Metal Oxides - Crystal Chemistry, Phase Transition and Related Aspects", US Department of Commerce, National Bureau of Standards.

Shands T G and Woody J A, "Metal-Insulator-Metal Junctions as Surface Soruces of Intermodulation", RADC-TR-83-31.

Shands T G, Denny H W and Woody J A, "Intermodulation Interference in Coaxial Cables and Connectors", IEEE Nat. EMC Symp., 1984, pp 293-297.

Simmons J G, "Generalized Formula for the Electric Tunnel effect between Similar Electrodes Spearated by a Thin Insulating Film", Journal of Applied Physics, Vol. 34, No. 6, June 1963, pp 1793-1803.

Smithers B W, "RF Resistivity of Carbon Fibre Composite Materials", IERE Int Conf. EMC, University of Southampton, Sept 1980, pp 183-198.

Steele R and Prabu V K, "High-User-Density Digital Cellular Mobile Radio Systems", Proc IEE, Part F, August 1985.
Steiner J W, "An Analysis fo Radio Frequency Interference Due to Mixer Intermodulation Products", IEEE Trans. on EMC, 1964, pp 62-68.

Stratton R, "Volt-Current Characteristics for Tunneling through Insulating Film", J. Phys. Chem. Solid, Vol. 23, 1962, pp 1177-1190.

Sze S M, "Physics of Semiconductor Devices", second edition, Wiley, 1981.

Tseung A C C, Jiang S P, Shan H and Shan P K, UK Patent, 1990.

Tseung A C C, Private Communication, 1990.

Watson A W D, "The Measurement, Dection, Lcoation, and Suppression of External Non-Lienarities which Affect Radio Systems", IERE Int. Conf. on EMC, 1980, pp 1-10.

Woody J A and Shands T G, "Investigation of Intermodulation Products Generated in Coaxial Cables and Connectors", RADC-TR-82-240, Sept 1982.

Yamamoto S et al, "Electrical Environmental Characteristics for Automotive Electronic Systems", IEEE Trans. on Vehicular Technology, Vol. VT-32, No. 2, May 1983, pp 151-157.

Young C E, "Connector Design Techniques to Avoid RFI" in 11th Annual Connector Symposium, Cherry Hill, NJ, 25-26 Oct 1978.

Van der Zeil, "Solid State Physical Electronics", second edition, Prentice-Hall International, 1968.